THE UNIVERSITY *of* EDINBURGH

Exploration of Brønsted Base Catalysis for Formal C–H Bond Activations

Thesis Submitted in Accordance with the Requirements of the University of Edinburgh for the Degree of Doctor of Philosophy

By

Hanno Kossen

Supervisor: Dr Uwe Schneider

EaStCHEM, School of Chemistry

College of Science and Engineering

The University of Edinburgh

August 2016

DECLARATION

I, Hanno Kossen, hereby declare that, except where specific reference is made to other resources, the work presented in this thesis is the original work of my own research since the start of my PhD degree in September 2012 and any collaboration is clearly indicated. This thesis has been composed by myself and has not been submitted, in whole or part, for any other degree, diploma or other qualification.

Signed: 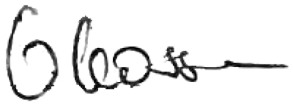

Date:

11/11/2016

Acknowledgements

First of all, I would like to thank my wonderful wife Tomke for her continuous support throughout the duration of my PhD. She made every single Scottish rainy day worthwhile.

I would like to thank Uwe Schneider for giving me the opportunity to carry out the research in his group and for his supervision during my PhD. I also thank the rest of the Schneider group (past and present) for their support and ideas. This also includes all project students that have worked on related projects in the group. Special thanks also go to Andrew Lawrence and his group for great literature meetings. Also thanks to Lorna and Juraj for their help with NMR as well as Alan and Logan for help with MS.

I would also like to thank the Principal's Career Development Scholarship for financial support. Thanks to Peter Kirsop and Michael Seery for their guidance and support regarding teaching. Finally, I would like to thank the School of Chemistry and ScotChem for providing the facilities for the research as well as funding.

Abbreviations

Ac	acetyl
Ar	aryl
atm	atmosphere
aq	aqueous
bp	boiling point
BB	Brønsted base
BHT	butylated hydroxytoluene
Bn	benzyl
Boc	*tert*-butyloxycarbonyl
BOX	bisoxazoline
Bu	butyl
br	broad
cat	catalyst
CDC	carbodicarbene
CDP	carbodiphosphorane
conc	concentration
conv	conversion
Cy	cyclohexyl
d	doublet
DA	di-isopropylamine
DBE	dibenzyl ether
DBU	1,8-diazabicyclo[5.4.0] undec-7-ene
DCM	dichloromethane
DCE	dichloroethane
DFT	density functional theory
Dipp	di-isopropylphenyl
DMAc	dimethylacetamide
DME	dimethoxyethane
DMF	dimethylformamide
DMSO	dimethylsulfoxide
dr	diastereometric ratio
E	electrophile
ee	enantiometric excess
EI	electron ionisation
ESI	electron spray ionisation
Et	ethyl
Et_2O	diethylether
EtOAc	ethyl acetate
equiv	equivalent
FLP	frustrated Lewis pair
HMDS	hexamethyldisilazene
HQ	hydroquinone
HRMS	High resolution mass spectrometry
Hz	Hertz
IMes	1,3-Bis(2,4,6-trimethylphenyl)-1,3-dihydro-2*H*-imidazol-2-ylidene
IPr	1,3-Bis(2,6-diisopropylphenyl)-1,3-dihydro-2*H*-imidazol-2-ylidene
^{i}Pr	isopropyl
IR	infra-red

Abbreviations (continued)

L	ligand
LA	Lewis acid
LB	Lewis base
m	multiplet
MB	mass balance
Me	methyl
MeCN	acetonitrile
Mes	mesityl
MIDA	*N*-methyliminodiacetic acid
MS	molecular sieves
nd	not determined
NHC	*N*-heterocyclic carbene
NMP	*N*-methyl pyrrolidone
NMR	nuclear magnetic resonance
Nu	nucleophile
PA	proton affinity
PC	propylene carbonate
PE	petroleum ether
pin	-pinacolato
Ph	phenyl
PhMe	toluene
PHC	*P*-heterocyclic carbone
PMP	*para*-methoxy phenyl
ppm	parts per million
Pr	propyl
PTLC	preparative thin-layer chromatography
py	pyridine
q	quartet
rt	room temperature
s	singlet
SIMes	1,3-Bis(2,4,6-trimethylphenyl)-4,5-dihydroimidazol-2-ylidene
SIPr	1,3-Bis(2,6-di-isopropyl-phenyl)imidazolidin-2-ylidene
t	triplet
^{t}Bu	*tert*-butyl
TBME	*tert*-butyl methyl ether
TMEDA	tetramethylethylenediamine
THF	tetrahydrofuran
TOF	turnover frequency
TON	turnover number
TMP	tetramethylpiperidine
TMS	tetramethylsilane
Ts	tosyl
9-BBN	borabicyclo[3.3.1]nonane
[DB18]c-6	dibenzo-18-crown-6
[18]c-6	18-crown-6
[15]c-5	15-crown-5
[12]c-4	12-crown-4

Lay summary

The synthesis of complex molecules, such as pharmaceutically active substances or natural products, relies on bond forming reactions of smaller molecular sub-units. These reactions often fail to proceed directly because they require too much activation energy. Therefore, catalysts need to be developed which reduce the activation energy and facilitate the reaction. The catalyst usually acts by activating one or both of the reaction partners either by stabilising naturally occurring transition states or by forming distinct reaction intermediates, resulting in the formation of new bonds.

The presented research focusses on the challenging development of new catalytic methods for the formation of carbon–carbon bonds. Specifically, base catalysts were used for increasing the electron density required for the formation of a new bond with electron accepting species (electrophiles). The first part describes an approach using metal-base complexes in the formation of *homoallylic amines*, which are a versatile structural motif that occurs in complex molecules and their precursors. Importantly, the chosen metal, sodium, is non-toxic, abundant, and environmentally benign. The second part explores the use of metal-free organocatalysts, where challenging carbon–hydrogen (C–H) bonds of small organic molecules were activated. The resulting products contained an amide functional group, which is dominant feature in biological molecules.

Both approaches contribute to the diversity of methodologies available to synthetic organic chemistry. By activating bonds that are common in all organic molecules, these methods are highly applicable and versatile. These new methods may ultimately lead to the development of better and cheaper ways of making complex organic molecules.

Abstract

This PhD project investigates the use of (Lewis or Brønsted) bases in catalysis. While the first chapter explores the use of main group metal amides in C–H bond activation reactions, the second chapter focusses on metal-free organocatalysis using so-called carbones.

In the first chapter, formal allylic C(sp^3)–H bond activations of unfuctionalised alkenes for C–C bond formations with imines were investigated. Alkali metal amides were used as catalysts for these transformations, giving homoallylic amine products. The investigations showed the unique reactivity of the Na-amide catalyst compared to other metal base complexes. The reaction scope and robustness was explored and initial insights into the reaction mechanism were obtained.

A related K-amide catalyst was then developed for the isomerisation of allyl benzenes, as well as functionalised olefins such as allylic silanes, boronic esters, phosphines, amines, ethers, and thioethers. This part explored the use of ligands to increase the catalyst's selectivity. Finally, the metal- or functional group-substituted classes of reagents were used in the functionalised allylation of imines, giving highly complex molecules with a diverse range of applications. Here, unprecedented reactivities were observed for the use of allyl–M reagents, as the allylation involved the activation of C–H bonds rather than C–X bonds. Furthermore, new catalytic formations of heteroatom-substituted homoallylic amines were described.

The following chapter focussed on the use of carbodiphosphoranes (CDPs) in catalysis. These C(0) bases, or carbones, represent a class of heteroallene compounds that exhibit a high electron density on a P(V)-flanked carbon centre. Their potential as either a Lewis or Brønsted base was examined. Different CDPs were synthesised and reacted stoichiometrically with CO_2, boron Lewis acids and metal salts. The generated intermediates were then studied in their reaction behaviour, taking advantage of a potentially available second pair of electrons. The results of these reactions were compared to other carbon bases, such as carbenes or other carbones. Finally, the Brønsted basicity of the CDP was examined in reactions with acidic pro-nucleophiles. The conjugate addition of alkylnitriles to α,β-unsaturated amides was developed using a catalytic amount of CDP. To the best of our knowledge, the first catalytic use of a CDP, as well as the first C–H bond activation of acetonitrile in Michael additions was reported.

Table of Contents

1 General Introduction

Methodological research in the field of organic chemistry is crucial for the development of new routes to important structural motifs. These novel methods may be applied in the synthesis of complex molecules. Bond-forming reactions between two carbon atoms are of great importance for methodological research because C–C bonds are highly stable and among the most dominant features of organic molecules. However, the generation of these bonds may be challenging, hence catalysts are often required in order to accomplish these reactions. This thesis explores the use of metal–base complexes as well as metal-free organocatalysts with respect to their potential in Lewis base (LB) and Brønsted base (BB) catalysis.

Catalysis is a particularly important field of research, as it lends itself to the development of new asymmetric methods in the formation of complex organic molecules. Catalysis is among the most effective methods to ensure a great diversity of routes that may be used to access optically enriched products. The use of naturally occurring chiral substances (chiral pool) allows for a limited amount of transformations to be explored. Using chiral auxiliaries helps to diversify the access to optically enriched molecules, but relies on the stoichiometric use of reagents derived from the chiral pool. Catalysis, in contrast, takes advantage of a large diversity of different methodological approaches and introduces stereodifferentiation by using catalytic amounts of enantiomerically enriched or enantiopure molecules. Therefore, catalytic asymmetric processes are comparatively cost-effective, which accounts for their applications in both industry and academia.

Metal-based catalysis usually introduces asymmetry by using an enantiopure ligand that is bound to the metal centre either through a covalent or a coordinative bond. In this area, it is important that the metal does not catalyse the intended transformation when the enantiopure ligand is unbound; otherwise a racemic background reaction occurs. For organocatalysis, covalent bonds to or non-covalent interactions with the substrates form enantiomerically enriched intermediates, which then translate their chiral information to the final product. Here, a background reaction is unlikely to occur, and enantiodifferentiation takes place through close proximity between the reaction intermediates and the stereogenic element within the catalyst.

The first chapter of this thesis deals with the use of a metal–base complex that is used for the catalytic Brønsted base activation of allylic C(sp^3)–H bonds. The *in situ* generated nucleophilic allylic anion was reacted with suitable electrophiles to generate homoallylic amines in good yields with high selectivities. The used catalyst, a sodium amide, is

commercially available, cheap and can also be prepared in one step from common laboratory reagents. Sodium is non-toxic and among the ten most abundant elements in the Earth's crust.

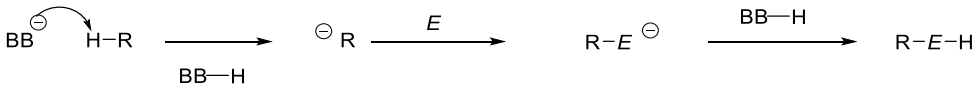

Scheme 1: Brønsted base-catalysed C–C bond formation

The Brønsted base was used for the catalytic deprotonation of an acidic pro-nucleophile, which generated an intermediate with a nucleophilic carbon centre (Scheme 1). Together with an electrophilic carbon centre of another reactant *E*, new C–C bonds were formed. The use of a metal-based catalyst in these reactions stabilised the intermediates' anionic character. The metal ion could also be used for the activation of the Lewis basic electrophile through coordination.

The second part is focussed on catalyst-based research, where one class of potential catalysts was chosen and its chemistry is investigated. This type of research allowed for flexibility regarding substrates and conditions, but its challenge lay in determining the scope and limitations of the new catalytic transformations triggered by this catalyst. Here, the catalytic activity was characterised by the formation of covalent bonds and distinct reactive intermediates that could show a high degree of selectivity for specific substrates.

Next to Brønsted base catalysis, this chapter also included the use of the catalyst as a Lewis base. Lewis bases display an excess of electron density, i.e. a lone pair, which may be used to attack an electrophilic centre A of a pronucleophile (Scheme 2). If a transferable organic rest R is bound to A, the transfer of electron density from this catalyst to the substrate may be exploited further to create a new bond between the organic rest R on A and electrophile *E* (Scheme 2). Now, the electron density on the reacted substrate *E* may be used to displace the initial Lewis base thereby regenerating the catalyst.

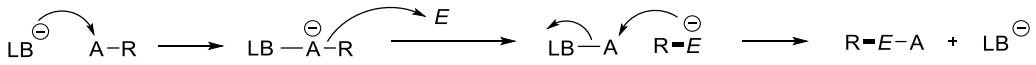

Scheme 2: Generic scheme for Lewis base catalysis

Certain prerequisites have to be fulfilled in order to perform this type of chemistry. Firstly, A–R and *E* have to react as pro-nucleophiles, which means although being intrinsically electrophilic, the attack of an external nucleophile (or Lewis base) renders them nucleophilic. Secondly, the catalyst has to stabilise the intermediates through the formation

of a strong bond with the substrate. At the same time, it has to be easily regenerated in order to ensure high turnover numbers and frequencies (TONs and TOFs).

Carbenes are a common class of reagents used in metal-free organocatalysis. The central carbon atom in the formal +II oxidation state, flanked by two covalently bound nitrogen donor substituents, is the most common structural motif. Extending this principle to phosphorus-flanked carbon bases allows for the introduction of a different type of structures. Next to the P(III) oxidation state, phosphorus can be found in the P(V) oxidation state. Therefore, neutral bases would display a C(0)-character with two lone pairs centred at the carbon atom. These lone pairs may both be used as a very strong base independently, if suitable reaction conditions are chosen.

All in all, this study will investigate different types of carbon bases for their properties and reactivity in organocatalysis as well as metal catalysis.

2 Metal–Base Catalysis

2.1 Introduction

2.1.1 Allylation of Imines using Allyl–M

The allylation of imines furnishes homoallylic amine products, which can be used as a versatile building block for complex molecule synthesis (c.f. leuconicone[1]; Figure 1). Both the amine as well as the alkene can be further functionalised, which allows applications in the synthesis of pharmaceutically and biologically active molecules. They also appear as structural features of natural products (c.f. angustifoline[2]; Figure 1).

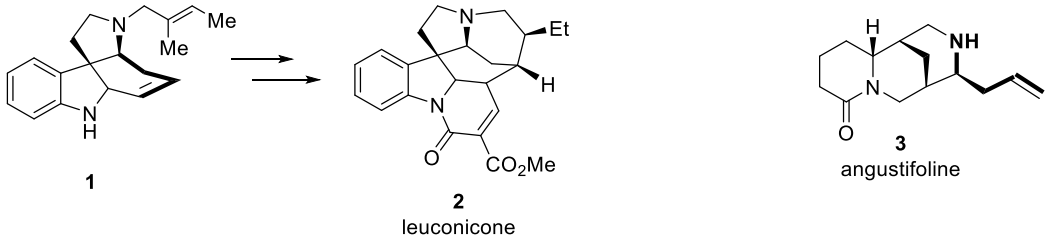

Figure 1: Homoallylic amines in natural products and their precursors

Allylations of electrophiles have been reported for a range of different allyl-containing nucleophiles. The most widely studied ones are the class of allyl-metal reagents, which can be used for the allylations of aldehydes, ketones but also for imines (Scheme 3).[3]

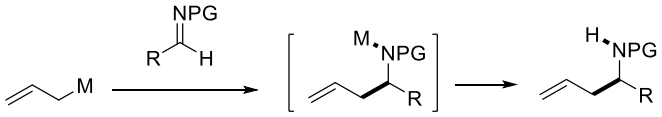

Scheme 3: Allylation of imines

The most reactive allyl-metal reagents are found in groups I, II and XII in the periodic table. These can be prepared by the use of allylic halides (allyl–X) and stoichiometric amounts of elemental metal (Scheme 4).[4] These metals are known to insert into the reactive allyl–X bond in order to generate highly reactive allyl-metal intermediates. The most common examples displaying this type of reactivity are magnesium and zinc, but recently indium has been shown to provide a useful alternative to these metals.[4-5]

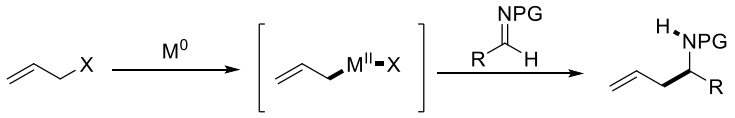

Scheme 4: Barbier-type reactivity

The *in situ* generation of allyl–M, followed by the addition to various electrophiles such as imines can be regarded as a Barbier-type reactivity. Here, control over stereochemical outcome is less likely to be ensured, but reaction intermediates are usually more reactive so otherwise challenging substrates can be activated.

Next to the Barbier-type allylations using allyl-halides, more stable allyl–M can be used directly in the allylations of imines. Allylic silanes, boranes, and stannanes are commonly used reagents that have been used to generate homoallylic amines. Except for the use of highly reactive dialkyl-substituted allylboron reagents (e.g. allyl-9BBN or halogenated semi metals), the reactions with imines generally need to be catalysed a Lewis acid.[4] Here, the imine coordinates to the metal centre, thus increasing its electrophilicity (Scheme 5, top). Alternatively, Lewis base catalysts can be used in these reactions to increase the nucleophilicity of the allyl–M reagent (Scheme 5, bottom). One example for this kind of reactivity has been shown by Friestad.[6] Here, a fluoride catalyst was used for the activation of allyl trimethylsilane, which could then allylate the imine.

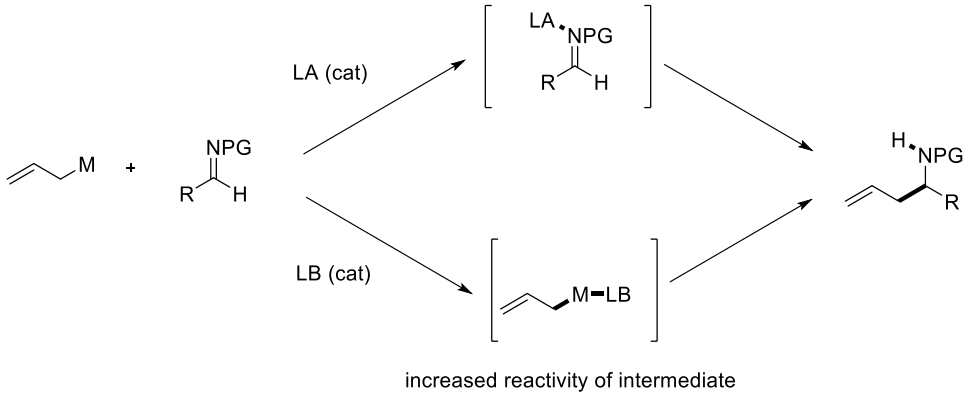

Scheme 5: LA and LB activation modes

The enantioselective allylation of imines to furnish chiral homoallylic amines has been extensively studied and reviewed.[7] Efforts in this field can be classified in two categories: substrate controlled stoichiometric asymmetric induction and enantioselective catalytic allylations using either chiral Lewis acids to activate the electrophile, or chiral Lewis bases to activate to nucleophilic allyl–M.

Compared to the crotylation of aldehydes and ketones, the substituted allylation of imines is much less investigated and no clear classification of different reagents can be made. Leighton reported the diastereoselective crotylation and cinnamylation of imines[8] and hydrazones[9] with substituted chiral silane **4** (Scheme 6). Reagents of this type showed a high selectivity for the formation of products with substituents in *syn*-relationship.

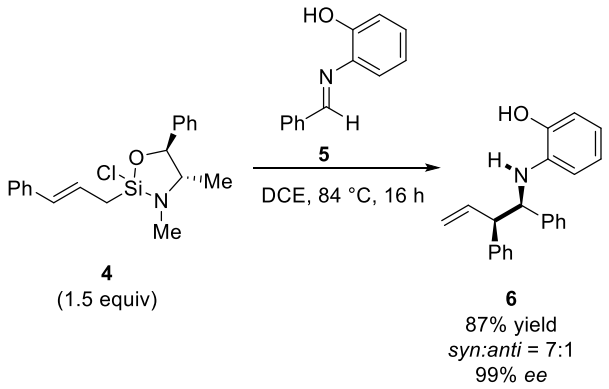

Scheme 6: Diastereoselective cinnamylation of imines

Despite being able to carry out diastereoselective reactions with imines, this method relies on the use of stoichiometric chiral reagents. Chiral catalysts are a much more elegant solution to the formation of chiral homoallylic amines, where only small amounts of chiral reagents are required.

The first catalytic enantioselective allylation was reported in 1998 by Yamamoto.[10] Here allyl–$SnBu_3$ was used as a pro-nucleophile in the reaction with benzyl-protected imine **8** using a chiral palladium catalyst (Scheme 7). Prolonged reaction times at 0 °C furnished homoallylic amine product **9** in good yield and with an enantioselectivity of 90% *ee*. A chiral allyl–Pd species was postulated as an intermediate in this reaction, where the metal acted as a Lewis acid catalyst in the enantioselective allylation.

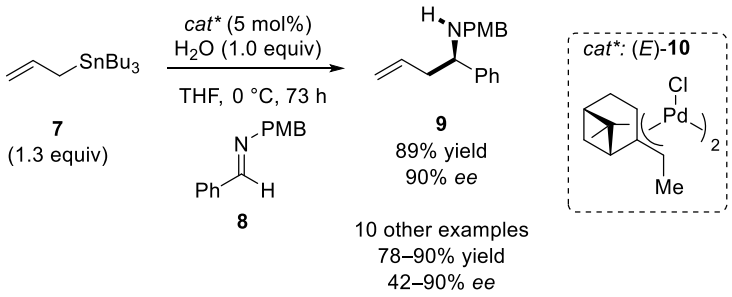

Scheme 7: Asymmetric allylation using Sn

Since then, other Zr[11] and Ag[12] have been developed in the field of transition metal catalysed allylation of imines using allylstannanes.

In 2004, Yamamoto reported an extension of the Pd-catalysed enantioselective imine allylation to allylsilanes.[13] A similar Pd^{II}-catalyst was used with benzyl-protected imines of type **12**. Tetraallylsilane was used as the allylating agent, where a similar allyl–Pd intermediate was postulated to form. Chiral induction of this catalyst was similar to the one used with allyl stannanes. Interestingly, catalytic amounts of fluoride ions were required for the activation of the silane, suggesting that transmetallation could only occur after silicon-ate complex formation. Allylsilanes have also been activated by Cu[14] or Ag[15] catalysts in the enantioselective allylation of imines.

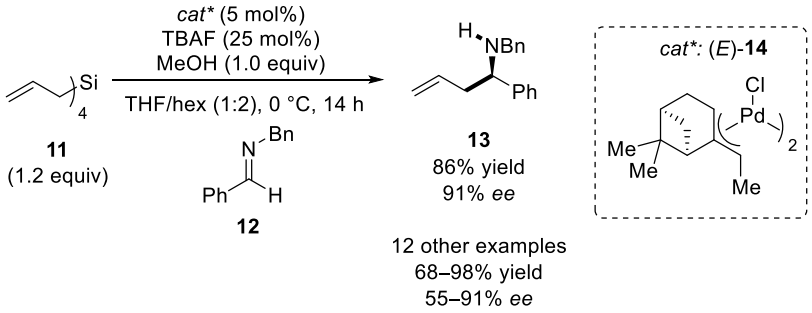

Scheme 8: Asymmetric allylation using Si

Allylboron reagents have originally not received as much attention as the corresponding silanes and stannanes. Shibasaki reported the first use of allyl-boron reagents in the enantioselective allylation of imines using a Cu-catalyst in 2006.[16] In a similar manner to the Pd-catalysed allylations, a chiral copper catalyst was used to generate a reactive allyl–Cu intermediate. A metal alkoxide was used to catalyse the transmetallation from boron to copper in a similar fashion to the fluoride catalyst for allylsilanes. The chiral allyl–Cu reagent was then used for the allylation of ketimines of type **16**, furnishing homoallylic amines like **17** in good yields and good enantioselectivities.

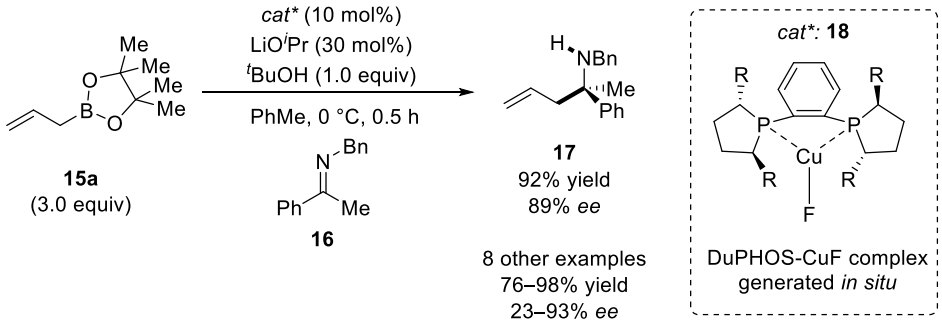

Scheme 9: Asymmetric allylation using B

Alternative NHC-ligands have also been identified in the Cu-catalysed allylation of *N*-phosphoryl imines with the same pro-nucleophile.[17] Potassium allyl trifluoroboron-ates

were identified as useful alternatives to allyl boronic esters due to their high stability. This allylic pro-nucleophile has also been used in the enantioselective allylation of cyclic imines using a Rh-catalyst.[18] The first transition metal-free enantioselective imine allylation was reported in 2007 by Schaus, where an acyclic allylboronic ester was activated by the catalytic use of BINOL.[19] In 2013, the group of Hoveyda published a transition metal-free asymmetric allylation using allylboronic esters (Scheme 10).[20] The work showed the use of a chiral amino phenoxide ligand generated *in situ*. When this ligand underwent transesterification on the boronic acid, a chiral reagent was formed, which underwent allylation through Brønsted base catalysis of the chiral amino group. The use of activated imine **19** allowed for a broad scope of the reaction, furnishing homoallylic amines of type **20** in moderate to excellent yields and with good to excellent enantioselectivities.

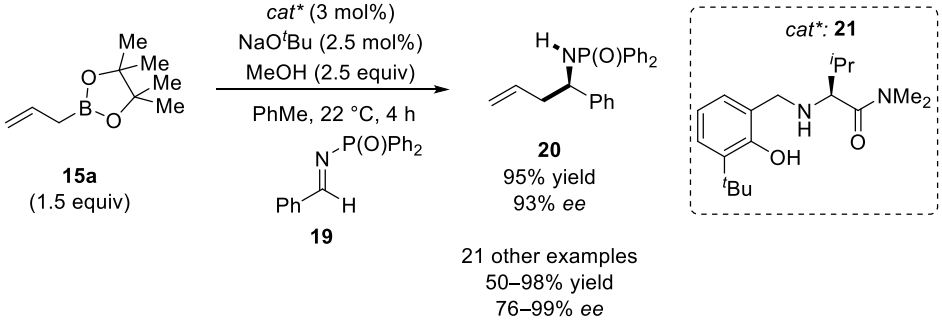

Scheme 10: Organocatalytic asymmetric allylation using B

Other allylations using Pd-allyl species

Jarvo reported the use of allyl–Bpin (**15a**) in the Pd-catalysed allylation of Michael amides **22** (Scheme 11).[21] Due to electron donation from a bidentate carbene/phosphine ligand and the allyl anion fragment, the catalytically active Pd^{II} catalyst is electron-rich. This increased electron density allowed for a nucleophilic allyl transfer in a 1,4-addition to Michael amide **22**. The addition of a basic alkoxide co-catalyst allowed for Lewis base activation of allyl–Bpin by forming a boron-ate complex. Like in Suzuki cross-coupling reactions, a transmetallation of allyl–Bpin with palladium generated a nucleophilic allyl–Pd species.

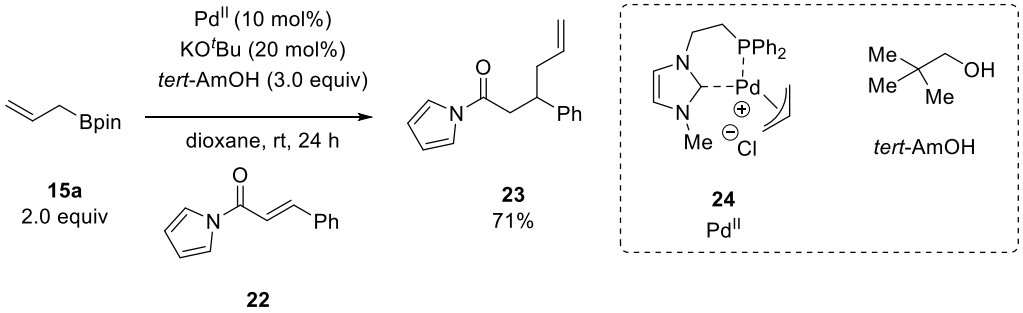

Scheme 11: Nucleophilic allyl–Pd reagents from allyl–Bpin

This example shows the possibility of a *nucleophilic* allyl–Pd generated by using a carbene ligand. The group of Aggarwal reported an orthogonal approach to this chemistry in 2015.[22] Here, an electrophilic π-allyl palladium intermediate **26** was formed from allyl–Bpin **25**, but instead of reacting with an electrophile, oxidative conditions allowed for the formation of an electrophilic Pd^{II}-species, which could be reacted with pro-nucleophiles (Scheme 12).

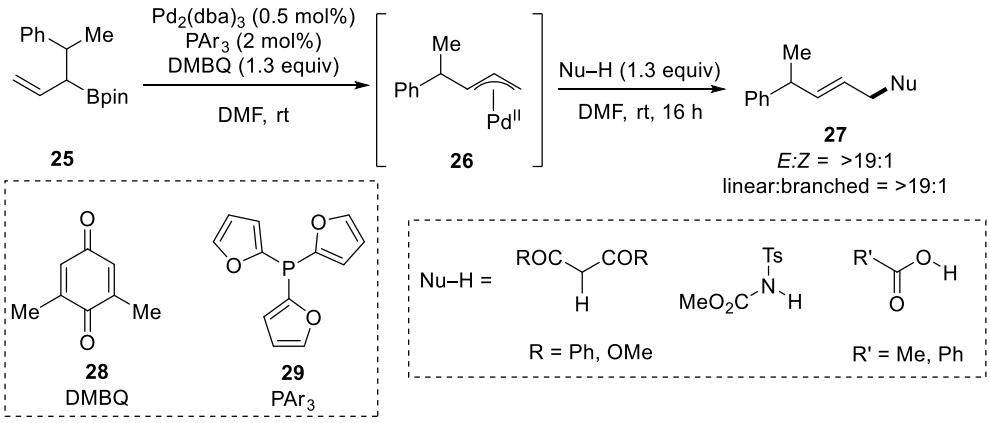

Scheme 12: *Umpolung* of palladium π-allyl

Interestingly, a Pd^0 catalyst was chosen that first needed to be oxidised to a Pd^{II}-species *in situ* before transmetallation could occur. Conditions and substrate scope were closely related to those developed by White for allylic C–H bond activation (*vide infra*).

2.1.2 The Imino-Ene Reaction

All these methods rely on the use of metals in organic chemistry, which constitute the nucleophilic species either directly or *in situ*. These metals are lost upon protonation of the heteroatom, forming stoichiometric metal waste. Therefore, instead of using a C–X bond activation approach, an unfunctionalised approach has been the focus of attention. One example for this is the imino-ene reaction. This reaction provides a different way to prepare homoallylic amines from imines with a much better atom economy.

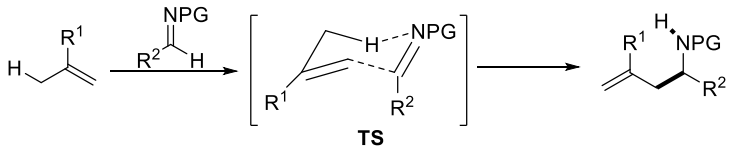

Scheme 13: Imino-ene transition state

This reaction has originally been discovered in 1982, when cyclohexene (**30**) and Ts-protected α-imino ester **31** were heated in neat reaction conditions to give homoallylic amine product **32** (Scheme 14).[23] The activation energy of these reactions is usually very high and prolonged heating was required for obtaining the homoallylic amines.

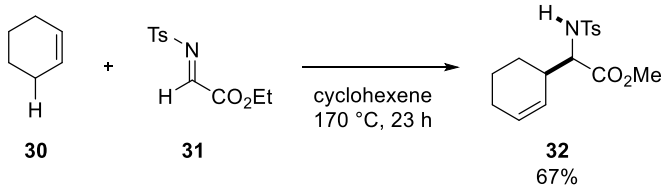

Scheme 14: First example of the imino-ene reaction

Alternatively, Lewis acids were used to reduce the activation energy. Catalytic imino-ene reactions have since been developed with Lewis acidic catalysts such as silanes[24] or metal triflates.[25] In 1998 the Lectka group reported the enantioselective imino-ene reaction, using chiral BINAP-Cu complex **35** (Scheme 15).[26] Both silver and copper salts have been used with a variety of different phosphine ligands to achieve the atom-economic enantioselective allylation of imines.[27]

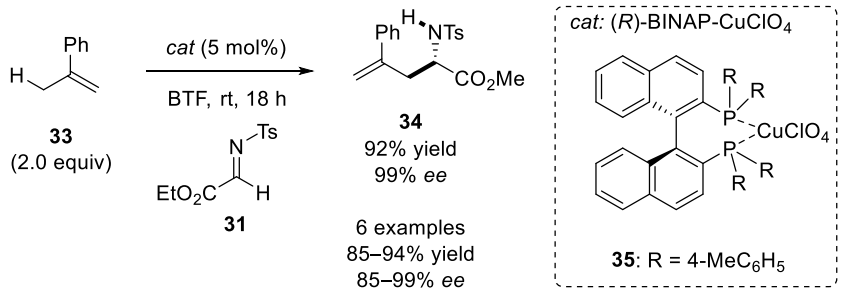

Scheme 15: TM-catalysed imino-ene reactions

The use of allylbenzene as a nucleophile in the imino-ene reaction has also been demonstrated. However, reports are limited and specific imines have been used only. Kresze reported the use of allylbenzene for the imino-ene reaction in 1985 (Scheme 16).[28] The reaction proceeded with activated imines **37** containing a perfluorinated protecting group. Homoallylic amine products **38a** and **38b** were obtained in good yields, while reaction conditions in chloroform at room temperature were mild. Interestingly, neither heating nor the use of Lewis acids was required to obtain the product, which was linked to the fluorinated protecting group showing a significantly increased reactivity towards the addition of nucleophiles.

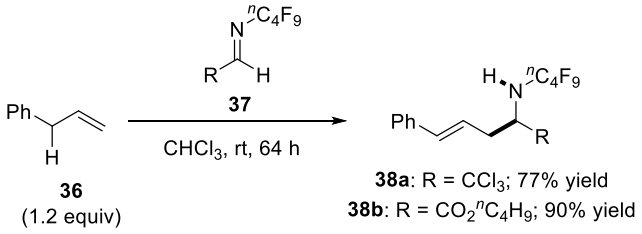

Scheme 16: Imino-ene with allylbenzene I

An alternative imino-ene reaction with allylbenzene was developed by Kumadaki (Scheme 17).[29] Again, a very activated imine was used, but here no fluorinated protecting group was required. Heating allylbenzene and imine **39** in xylene under reflux furnished homoallylic amine **40** in a low yield. This result shows the importance of substrate design in the atom-economic ene reaction between imines and allylic substrates.

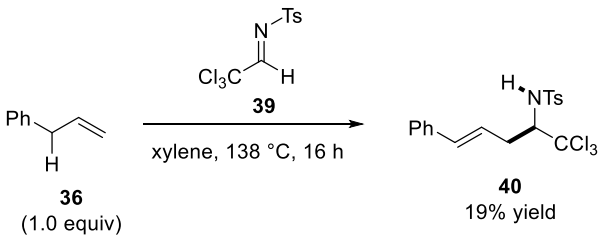

Scheme 17: Imino-ene with allylbenzene II

Generally speaking, the imino-ene reaction provided a good alternative to specific allylation reactions, especially for 1,1-disubstituted alkenes. The use of internal alkenes showed limited applicability and only few α-substituted homoallylic amines could be obtained with good diastereoselectivities. In this area, traditional allyl–M reagents proved to be more reliable. Furthermore, all applications are limited to very reactive electrophiles such as α-imino esters or halogenated imines. More challenging imines have not been used in the imino-ene reaction and therefore further developments in the allylation of imines to furnish homoallylic amines were required. Finally, the use metals as Lewis acid catalysts is not desirable and more environmentally benign methods needed to be developed.

2.1.3 Allylic C(sp^3)–H Bond Activation

An alternative method for the preparation of allylic reagents by C–H activation was provided by the group of White, who reported the activation of allylic C–H bonds for the preparation of linear and branched allylic acetates[30] and carbamates[31] (Scheme 18). Further studies then expanded the nucleophile scope to carbon based pro-nucleophile when using α-nitro esters.[32] The employed Pd^{II}-catalyst was assumed to be able to selectively metallate C–H bonds to form electrophilic palladium species **42**. Coordination of a pro-nucleophile, followed by deprotonation and reductive elimination would give functionalised product **43** and Pd^0. Therefore, stoichiometric amounts of oxidant, such as benzoquinone, were required to regenerate the catalytically active Pd^{II} species.

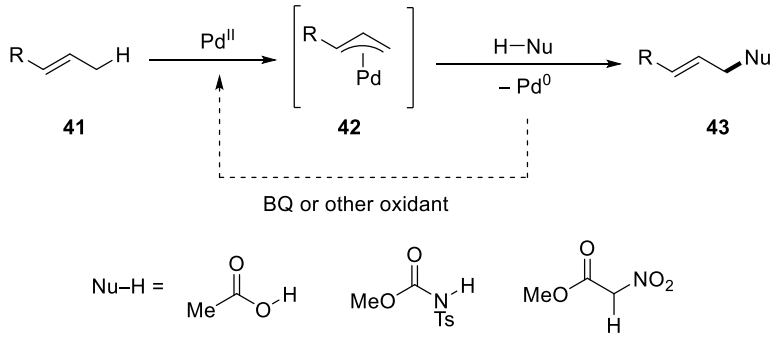

Scheme 18: C–H activation using Pd^{II}

By using an additional chiral Lewis acid, an asymmetric variant of this reaction was also developed.[33] The use of a Cr(III) complex bound to a salen-ligand introduced moderate levels of enantioselectivity (Scheme 19). This way, the activation of unbiased C–H bonds in asymmetric oxidations was achieved.

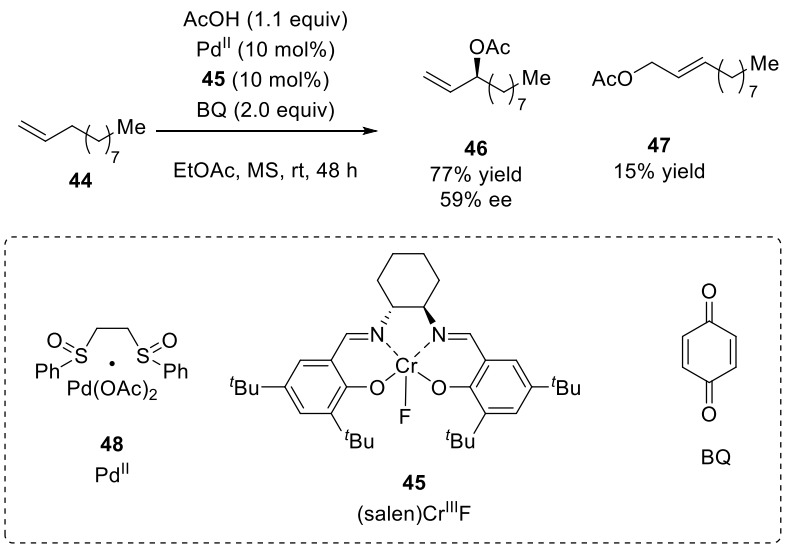

Scheme 19: Asymmetric allylic oxidation using Pd^{II}/Cr^{III}

Trost then extended this field by demonstrating the first enantioselective allylic alkylation using of a 1,3 diketone nucleophile (Scheme 20).[34] Instead of chiral induction arising from a chiral Lewis acid co-catalyst, this work used a chiral and newly developed phosphoramidite ligand (**50**). Again, a benzoquinone oxidant was used to regenerate the active Pd^{II} catalyst.

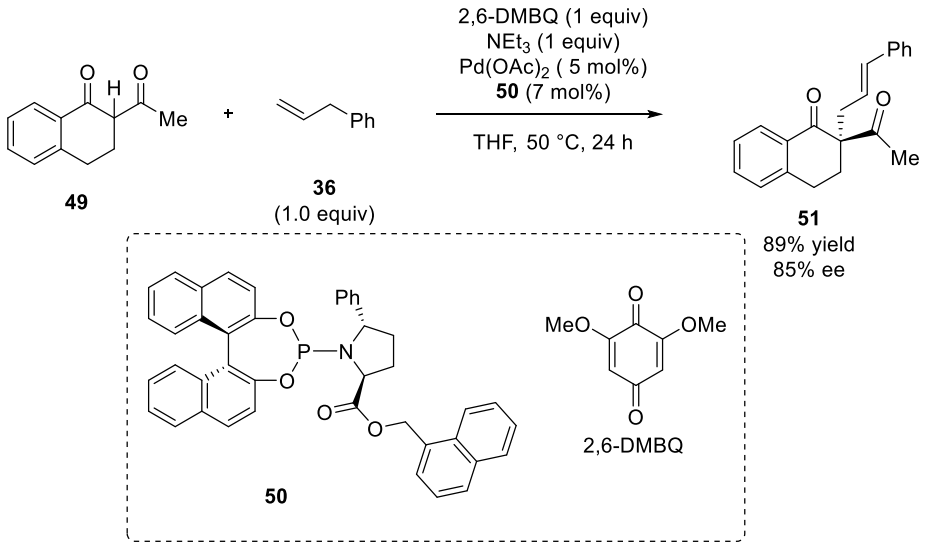

Scheme 20: Asymmetric allylic C–C bond formation using Pd^{II}

The major drawback for this atom economic method was the stoichiometric use of oxidant that was required to regenerate the active Pd^{II} species. Furthermore, the allylic alkylations and oxidations relied on the use of acidic pro-nucleophiles, which were reacted with electrophilic allyl-palladium reagents.

In order to generate a nucleophilic allylic reagent from the allyl–Pd reagent generated *in situ*, an *Umpolung* approach was required that would increase the electron density on the allyl–M reagent. The group of Araki showed that allyl-palladium reagents can be reacted with electrophiles by the conversion of the electrophilic palladium intermediates into nucleophilic indium reagents using In^0 or InI (Scheme 21).[35]

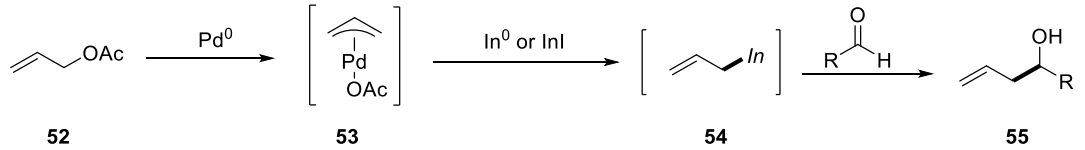

Scheme 21: *Umpolung* of allyl–Pd using indium

The insertion of Pd^0 into allyl acetate **52** generated allyl–Pd^{II} complex **53** *in situ*. This intermediate was analogous to the one generated from C–H activation using Pd^{II}. However, the addition of an electron rich metal allowed for the formation of allyl–In intermediate **54**, which was nucleophilic in nature. This nucleophile was trapped using aldehydes, giving homoallylic alcohols **55** in good to excellent yields. Unfortunately, the same method cannot be applied to the C–H bond activation as this would involve the use of stoichiometric oxidant (benzoquinone) and reductant (indium metal) in the same reaction. Therefore, alternative nucleophilic allyl–Pd species were required.

2.2 Aims

As demonstrated in the introduction, the allylation of imines requires the use of allyl–M reagents as (pro-)nucleophiles.[7c] Except for the imino-ene reaction[36] with limited applicability, electrophilic allylations using C–H bond activations of allylic sp^3-hybridised carbon centres have been reported using transition metal catalysts.[32] An *Umpolung* approach in this field has not been reported. Our goal was to demonstrate the activation of allylic C–H bonds with transition metal-free base catalysts. This approach would allow for the formation of homoallylic amines using unfunctionalised starting materials, taking advantage of the inherent acidity of the allylic C–H bond.

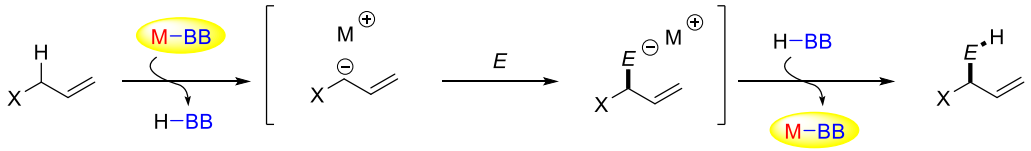

Scheme 22: Allylic C–C using M–BB catalysts

Substituted allylic reagents were considered suitable substrates for the allylation of imines. Depending on the pK_a value of the allylic pro-nucleophile, allylic anions were assumed to be formed upon deprotonation. These nucleophiles could then be reacted with imines to form new C–C bonds, while protonation of the substrate should ensure catalyst turnover. Diversity in this reaction was considered to arise from the variation on the X-group in the pro-nucleophile, or by using alternative nitrogen-containing electrophiles. The use of a chiral catalyst would lead to the development of new methods for the enantioselective preparation of homoallylic amines by C–H bond activation, which has not been reported in the literature to the best of our knowledge.

An alternative route to the allylation of electrophiles using a C–H bond activation approach was the use of transition metal catalysts for the generation of allyl–M species. An *Umpolung* approach that is compatible with redox-active transition metals was therefore required.

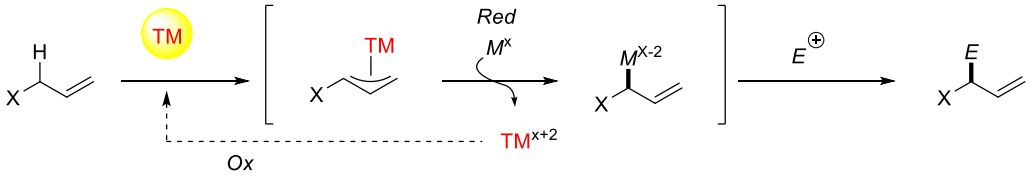

Scheme 23: TM-catalysed C–H bond activation

As many transition metals have been shown to be selective for allylic C–H bond insertion, no activating X-group was assumed to be required for this type of reactivity. However, developing an approach where the reduced transition metals could be oxidised to their catalytically active form in the presence of a reducing agent provided a challenging step.

2.3 Results and Discussion

2.3.1 Formal C(sp^3)–H Bond Activation of Unfunctionalised Alkenes

Functionalisation of C–H bonds using Brønsted base catalysts is challenging and can only be successful with a fine-tuned balance of pK_a values of reaction intermediates. Therefore, different structural motifs were considered before developing novel C–H bond activation reactions. Unsubstituted alkanes have estimated pK_a values of 45–50 (DMSO).[37] The delocalisation effect of an aromatic ring or a conjugated double bond decreases this value to 40–45 (DMSO)[37] for e.g. toluene or propene (Figure 2, left). The combination of two of these anionic stabilising groups decreases the pK_a even further to 30–35 (DMSO).[37] Examples for this kind of substrates are allylbenzene, 1,5-pentadiene and diphenylmethane (Figure 2, centre). For substrates such as cyclopentadiene or indene this effect is even more pronounced because of aromaticity arising upon deprotonation of the substrate (Figure 2, right). Many bases are known for the deprotonation of substrates with pK_a < 30, but accessing C–H bonds that are less acidic is challenging.

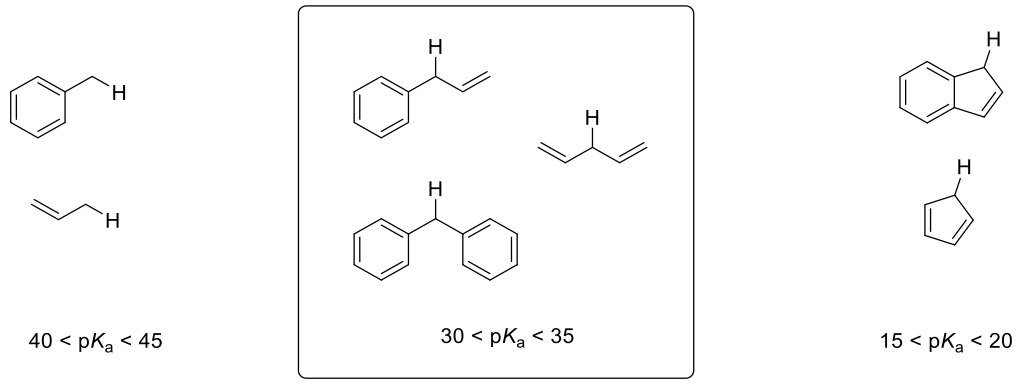

Figure 2: Allylic and benzylic substrates and their pK_a values

In order to activate C–H bonds of the highlighted substrate (Figure 2, centre) with a Brønsted base, the pK_a values of different base catalysts needed to be considered. Commercially available alkyllithium reagents were deemed unsuitable, as these are too basic and are incompatible with many functional groups (Figure 3, left). Furthermore, their conjugate acids are volatile gases, which cannot participate in the reaction after an initiative process. Lithium amides were found to have pK_a values in the range of 30–40 (DMSO)[37] depending on the nature of the amide (Figure 3, centre). Lithium alkoxide bases can also have pK_a values >30 depending on the alkoxide ligand, but these values only apply in DMSO (Figure 3, right).[37] Indeed, due to the strong H-bond donating ability, the pK_a values of metal alkoxides vary significantly with solvent.

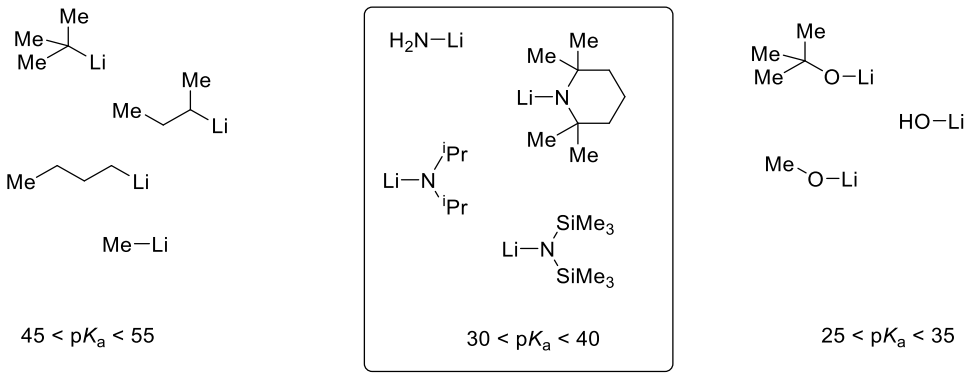

Figure 3: Common lithium bases and their pK_a values

Allylbenzene was chosen as the model substrate in an allylation reaction of electrophiles. In the reaction with *N*-protected imines, different homoallylic amines were expected to form (Scheme 24). Four different isomers were identified, where allylation could occur from either the α- or the γ-position. Both of these can exist as a mixture of isomers: the branched product can have diastereoisomers and the internal double bond of the linear product can exhibit geometrical isomerisation.

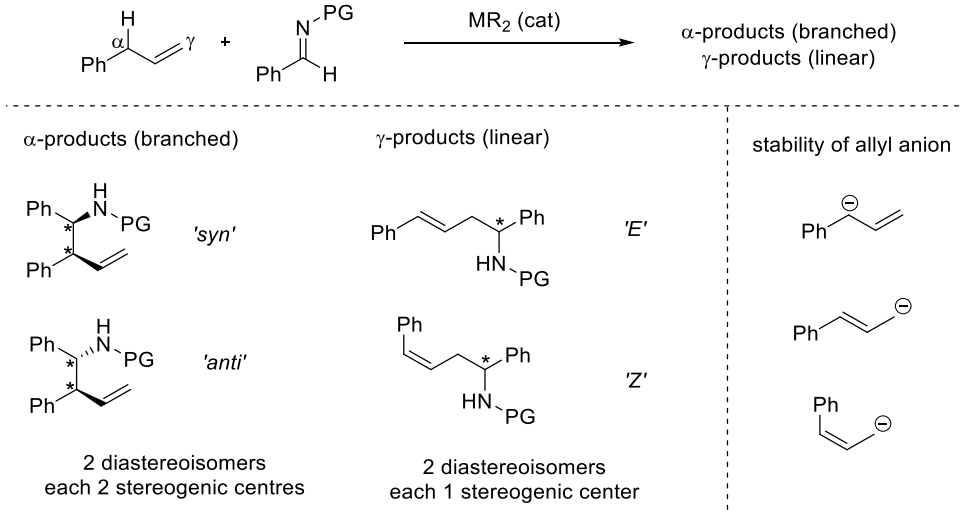

Scheme 24: Possible reaction products from the allylation of imines with allylbenzene

2.3.1.1 Previous work in the group

All experiments in this section were carried out by Wei Bao.

When the reaction of allylbenzene **36** and *N*-Ph-benzaldimine **56a** was carried out using 10 mol% KHMDS in diethyl ether, product **57a** was observed alongside isomerised pro-nucleophile **58**.

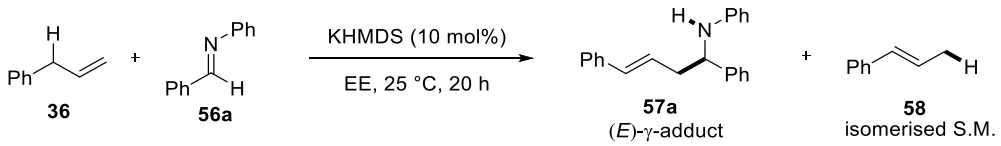

Scheme 25: Reaction outcome of the KHMDS-catalysed allylation reaction

The reaction outcome did not show any α-allylation product, but trace amounts of *Z*-**57a** could be detected in aliquot ^{1}H NMR spectroscopy. An imine screening was performed investigating the scope on the protecting group of the imine (Table 1).

Table 1: Protecting group screening

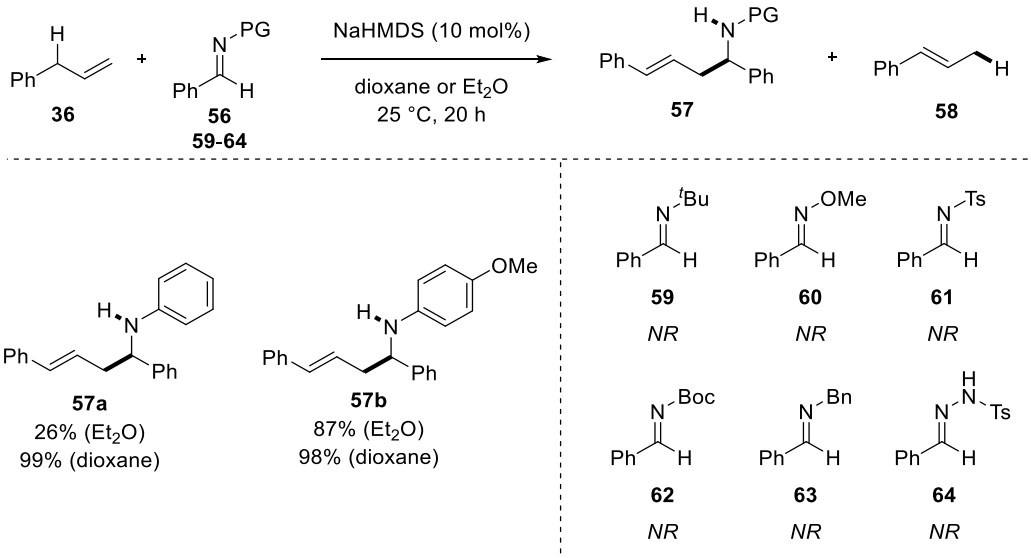

The reaction with different *N*-protected imines showed good reactivity for both the *N*-phenyl- and the *N*-(*para*-methoxy)phenyl (PMP)-imine. All other protecting groups showed no reaction and full recovery of the starting materials. One reason for this observation could the direct reaction of the catalyst with the imine. As none of the reactions show any isomerisation product, it is likely that the allylic anion did not form in the reaction.

An initial optimisation was conducted, investigating the scope of the reaction. To start, a solvent screening was conducted using *N*-PMP-imine and NaHMDS in ethereal solvents

(Table 2). Another solvent screening was then performed with non-ethereal solvents using the same catalyst with the *N*-Ph-imine.

Table 2: Solvent Screening

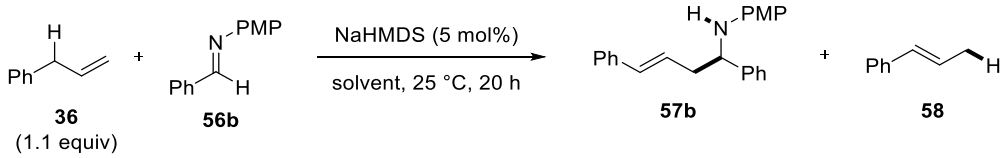

Entry	Solvent (Ɛ)	Yield 57b (%)[a]	58 (%)[a]
1	dioxane (2.3)	98	5
2	TBME (2.6)	68	2
3	Et_2O (4.3)	87	4
4	DME (7.2)	14	28
5	THF (7.5)	17	62

[a] The yield was determined by ^{1}H NMR spectroscopy of a reaction aliquot; internal standard: dibenzyl ether (25 mol%).

The solvent screening in ethereal solvents showed high product yields and low levels of isomerisation for the reactions carried out in dioxane, TBME and Et_2O (entries 1-3). For the reactions carried out in glyme (DME) or THF isomerisation product **58** was observed to be the major product and only 14–17% product were obtained. Screening apolar solvents such as heptane, toluene, trifluorotoluene (BTF), or dichloroethane showed no formation of product **57b**, which could be related to a reaction of the catalyst with the solvent or the catalyst's lack of activity, especially in apolar solvents. The use of DMF showed some product formation, but reaction yields were inferior to the reactions carried out in ethereal solvents.

Further optimisation regarding the reaction temperature, concentration and time were performed. Lowering the reaction temperature to 0–10 °C resulted in a decreased catalytic activity and low product yields were obtained. Increasing the temperature to 30–40 °C increased the level of isomerisation observed. Therefore, all following reactions were performed at 25 °C. Substrate concentrations of 0.4–1.0 M were examined and it was found that higher concentrations resulted in higher reaction yields. Due to the somewhat limited solubility of the imines in dioxane, 0.67 M was chosen as a suitable reaction concentration (300 µL solvent for 0.20 mmol imine). Reaction monitoring over 24 h (NaHMDS, 5 mol% in Et_2O) showed that reaction yields were high only after reaction times >15 h.

2.3.1.2 Specific Literature Precedence

Literature for the formation of linear homoallylic amines of type 57

Product **57**, formed in the reaction shown above, has been previously reported in the literature.[38] Similar products have been reported to be formed through substituted 'classical' allylation or cinnamylation reactions with allyl–M reagents. These require the pre-instalment of functional groups in the allylic pro-nucleophiles.

Hirashita found that homoallylic amines of type **67** can be prepared in a one-pot reaction consisting of an allylation followed by a Pd^0-catalysed cross-coupling reaction (Scheme 26).[38a] In the first step, indium metal was used for the insertion into the allylic C–Br bond. A second equivalent of indium was added to generate a vinyl indium species, which could not react with imine **61**. The *in situ* generated nucleophilic allylic indium reagent was then added to *N*-Ts- or *N*-Ph-protected imines to give intermediates **66**, which contained a vinylic indium iodide species. This vinyl–M was unaffected by the allylation conditions and could be used in a subsequent cross-coupling reaction with phenyl iodide. Moderate to good yields were obtained for homoallylic amine products **67** and **56a**.

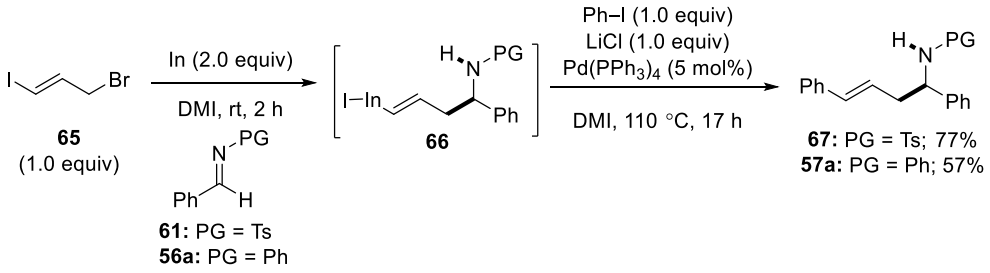

Scheme 26: Two-step Barbier allylation/cross-coupling reaction

In order to avoid the two-step process for the formation of substituted homoallylic amines, cinnamyl bromide **68** was used in the cinnamylation of imines by Szymoniak.[39] The group showed that the insertion of zinc metal into the C–Br bond gave a reactive zinc intermediate, which could be used for the cinnamylation of alkyl ether-protected aldimines **70** (Scheme 27). As both the α- and the γ-addition products could be obtained using this method, a chelating protecting group was chosen that would favour the overall α-addition to the imine, furnishing linear homoallylic amines **71** in moderate to good yields. The imine scope for this reaction included aryl-, cinnamyl-, heteroaryl- and alkyl-imines.

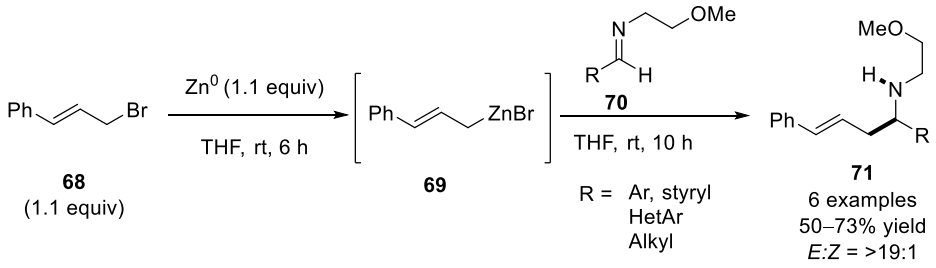

Scheme 27: Barbier-type cinnamylation using Zn

The same pro-nucleophile was used by Taddei in a Cr^{II}-mediated cinnamylation reaction (Scheme 28).[40] PMP-protected imine **56b** was activated by a stoichiometric amount of a boron Lewis acid. This mode of action allowed for the facile addition of a generated allyl–chromium species, giving linear homoallylic amine **57b** in moderate yields. Again, only the α-addition product was observed, which is unusual when using allyl–M intermediates.

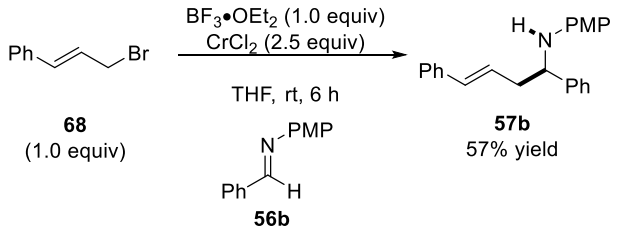

Scheme 28: Barbier-type cinnamylation using Cr

The formation of phenyl-substituted homoallylic amines is not limited to the *in situ* formation of allyl–M reagents. Allylsilanes have also been successfully used in the formation of products **57a**. Hou reported the use of cinnamyl silane **72** in the fluoride-catalysed reaction with imine **56a** (Scheme 29).[38b] Here, the catalyst acted as a Lewis base for the silane. By forming a reactive silicon-ate complex, the nucleophilicity of the allylic reagent was increased enough to react with the unactivated imine. Product **57a** formed with exclusive α-selectivity in a good yield.

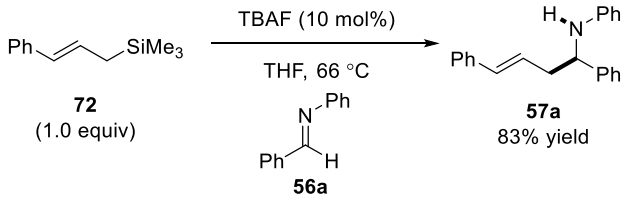

Scheme 29: LB-cat allylation using γ-substituted allylsilane

In contrast to silicon-substituted styrenyl compound **72**, Lectka reported the use of silylated allylbenzene **73** for the Hosomi-Sakurai reaction with activated imine **31** (Scheme 30).[41] A chiral copper catalyst was used as a Lewis acidic activator for the imine, giving product **74** in

a good yield. In contrast to all other reports, this reaction proceeded with exclusive γ-selectivity. Thanks to the absence of an uncatalysed background reaction with allylsilanes, chiral induction was achieved and product **74** was obtained with 75% *ee*.

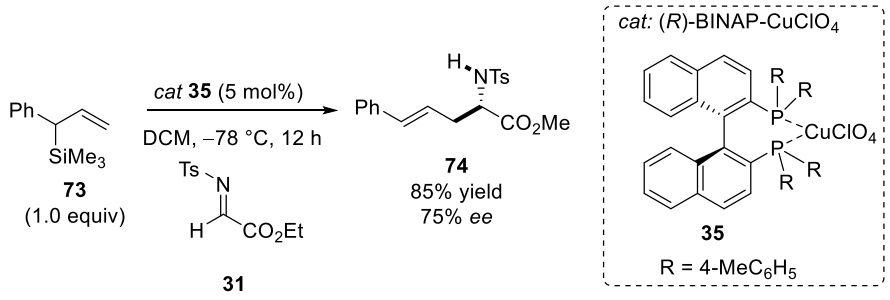

Scheme 30: LA-cat allylation using α-substituted allylsilane

One example in the literature relies on C–H activation instead of C–X activation in the formation of linear substituted homoallylic amines. Unsubstituted allylbenzene **36** was used for the addition to diamine **76** by Savoia (Scheme 31).[42] Here, stoichiometric amounts of BuLi were used for the generation of a reactive allyl–Li reagent. The use of TMEDA allowed for the selective γ-addition of this nucleophile to diamine **76**, giving rise to diallylated diamines **77**. Despite being able to use unfunctionalised starting materials in this reaction, the use of super-stoichiometric amounts of strong base limits the applications of this method.

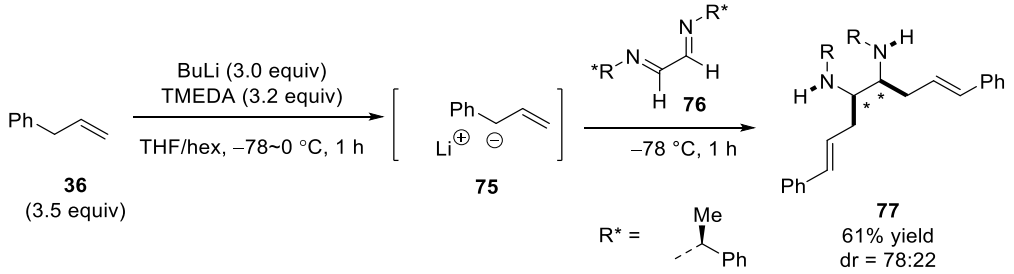

Scheme 31: Stoichiometric cinnamylation using allylbenzene

*No catalytic example of C–H activation has been reported in the literature. Homoallylic amine products of type **57** can only be generated using functionalised allyl–M reagents or stoichiometric amounts of base.*

Stoichiometric reactions with alkali metal amides

Alkali metal amides were used as a catalyst in the reaction between allylbenzene **36** and imine **56**. These bases are commonly used stoichiometrically in organic synthesis. Their basicity is lower than that of alkyllithium reagents and therefore the amides are often used as a milder alternative to BuLi. Of all metal amides, lithium diisopropylamide (LDA) is probably the most common base. It is commercially available as a solid or in ethereal solutions, but can be easily prepared by the reaction of diisopropylamine with BuLi or Li metal, generating Bu–H or H–H respectively. LDA is used for the selective deprotonation of C–H bonds in α-position to carbonyl compounds (Scheme 32). Its large steric bulk prevents the base from acting as a nucleophile and increases the base's selectivity for the deprotonation of the least hindered position. At –78 °C, substituted cyclohexanone **78** is deprotonated by LDA to give lithium enolate **79**, which represents the kinetic enolate because the less substituted alkene is formed. This enolate reacts with electrophiles such as MeI to give **80**.[3]

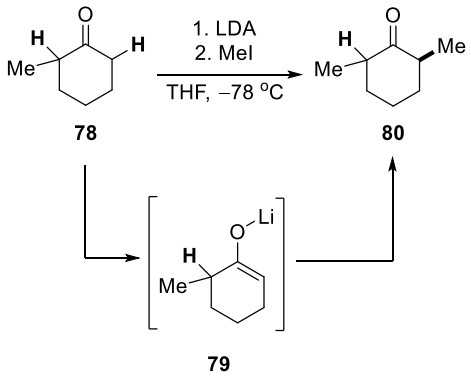

Scheme 32: Use as stoichiometric BB

Other alkali metal amides are also commercially available. The reaction of BuLi with hexamethyldisilazane or tetramethylpiperidine results in the formation of LHMDS and LTMP, which are other commercially available lithium amides. Metal amides of the heavier alkali metals are limited to the preparation from the corresponding metal, as no BuLi analogues for the heavier alkali metals are readily available. Due to their relatively simple preparation, NaHMDS and KHMDS can be obtained commercially, while the corresponding –DA and –TMP complexes are not commercially available. NaHMDS and KHMDS are often used as alternatives to LDA because - like LDA - they are very hindered bases. However, due to the Si-substitution, the amide's basicity is slightly reduced, while the use of heavier elements increases the base's kinetic reactivity.

Despite their decreased nucleophilicity, MHMDS can react as a Lewis base with very reactive electrophiles. One example is the substitution reaction of allyl halides, giving allylic amines (**82**; Scheme 33).[43] As the substrate allows for an S_N2' substitution mechanism, the effect of the base's steric hindrance is attenuated. For this reaction to proceed with allyl chlorides, a Pd^0 catalyst was required.[44]

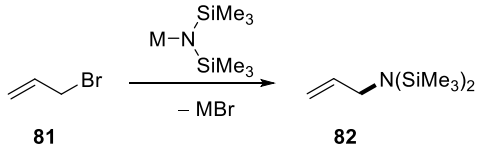

Scheme 33: Use as stoichiometric LB – nucleophilic substitution

Another example of the stoichiometric use of MHMDS as a Lewis base is the formation of *N*-TMS-protected imines (Scheme 34). The nucleophilic attack of secondary alkali metal amides to reactive aldehydes furnishes hemiaminal intermediate **84**. By desilylating the amine, TMS-protected imine **85** and siloxane **86** are generated.[45]

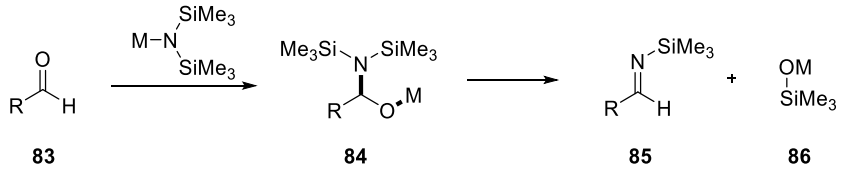

Scheme 34: Use as stoichiometric LB – imine formation

Finally, alkali metal amides are used in transmetallation reactions, generating metal amides of other main group and transition metals (Scheme 35). This method provides access to alkaline earth,[46] zinc,[47] silver,[48] and copper,[49] amides, as well as lanthanide[50] and actinide[51] metal amides.

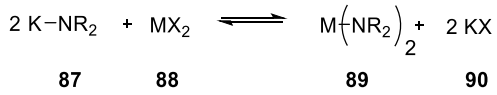

Scheme 35: Stoichiometric use in transmetallation reactions

The structural properties of the three different lithium amides LHMDS, LDA and LTMP were recently compared by Mulvey and Robertson.[52] Their solid state and solution occurrence, as well as their metal–nitrogen bonds were reported. As these bases are encountered in solution only when used in organic synthesis, their structural features were of great importance (Table 3). In general, non-coordinating apolar solvents allowed for the formation of dimeric or oligomeric structures to be stable in solution. For LHMDS, dimers were the only observed species in solution, while LDA and LTMP had significant

proportions of undefined oligomeric structures. Therefore, LHMDS can be assumed to be easily solubilised in toluene, which may not be the case for LDA and LTMP. Ethereal solvents such as THF can break up the aggregates by complexation to the metal centres. When substoichiometric amounts of THF were added to LHMDS, the dominant species in solution was the disolvated dimer (Table 3, bottom). Increasing the concentration of THF then allowed for the coordination of more solvent molecules that lead to the formation of monomeric structures with various degrees of solvation. For LDA no monomeric structures were found even in THF solution and the dominant species was found to be the disolvated dimer. Despite displaying the highest degree of oligomerisation in non-coordinating solvents, LTMP showed a significant proportion of monomeric species even at low THF concentrations. This monomeric species increased with increasing amounts of THF, showing that the aggregates were broken up much faster than for LDA.

Table 3: Structures of lithium amides in solution

Solvent/amide	LHMDS	LDA	LTMP
toluene/ hexane	dimer	trimer/ oligomer	oligomer
THF (<1 equiv)	disolvated dimer	mono and disolvated dimer	monomer and dimer
THF (>1 equiv)	monomer (di- tri- or tetramer)	disolvated dimer	monomer and dimer

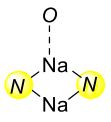

monosolvated Na amide dimer

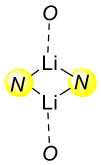

disolvated Li amide dimer

N = NR_2

O = ethereal solvent

When comparing the M–N bond lengths of the different alkali metal amides, a general increase was expected with increased atomic radius for the different metals. Indeed, all amides displayed similar bond lengths when comparing the same metals. The Li–N bonds were ca 2.01 Å, the Na–N 2.40–2.45 Å and the K–N around 2.71 Å. This increase reflects the increase of ionic radii between Li^+ (~ 70 pm), Na^+ (~100 pm) and K^+ (~ 135 pm).[3]

2.3.1.3 Catalyst Screening

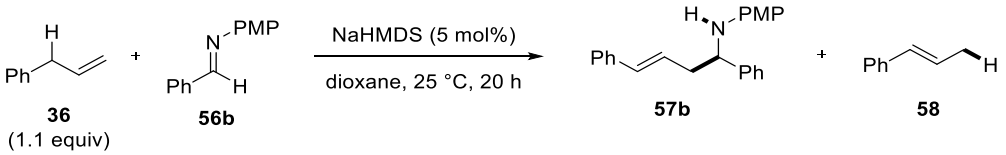

Scheme 36: Alkali metal amide-catalysed cinnamylation

In order to investigate if the reaction of **36** with **56** was specific to alkali metal–HMDS catalysts, a catalyst screening was required. Aspects that needed to be considered were (1) the nature of the amide, (2) the nature of the metal, (3) the use of other metal bases, and (4) metal-free catalysts. *Duplicate catalyst screenings were carried out in parallel by Wei Bao in order to confirm reaction yields, which are stated as the average of two concordant reaction outcomes.*

(1) Different amide ligands for alkali metals were commercially available and their reactivity could be tested directly in different solvents. Here, different substitution patterns on the amide's nitrogen atom are possible (Figure 4). Unsubstituted metal amides (**91**; R = H) are very basic with a pK_a value for the conjugate acid (NH_3) of ca. 41 (DMSO).[37] For tetramethylpiperidine (**92**) and diisopropylamine (**93**), the amide is alkyl substituted, and pK_a values of ca. 37 (DMSO)[37] and 36 (THF) were found respectively. The Si-substituted HMDS (**94**) is significantly less basic with a pK_a value of only ca. 30 (DMSO).[37] This lowered value is related to the ability of the Si atom to stabilise α-anions.

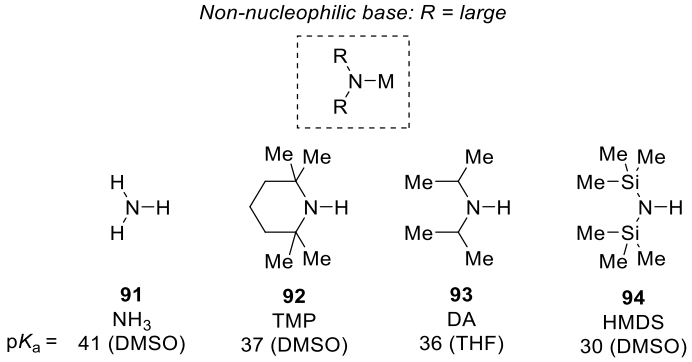

Figure 4: Secondary amines and their pK_as

(2) Besides the alkali metal amides, some other metal–HMDS complexes were commercially available and could be used directly. To compare their reactivity with related alkaline earth metal HMDS complexes, these had to be prepared and purified in order to be examined for their ability to catalyse the cinnamylation of imines with allylbenzene. While the magnesium complex is commercially available and can be prepared using Grignard reagents, the same does not apply to the heavier group II analogues. Two methods for their preparation have

been reported in the literature. The first one uses alkali metal–HMDS complexes and alkaline earth metal iodide salts in a metathesis reaction (Scheme 37).[46] The alkali metal iodide, that formed as a by-product, is more stable than the alkaline earth metal iodide, which shifts this equilibrium to the right. As the reaction was carried out in toluene, a dimeric structure **95** was formed where two amide ligands were bridging the two Ca ions.

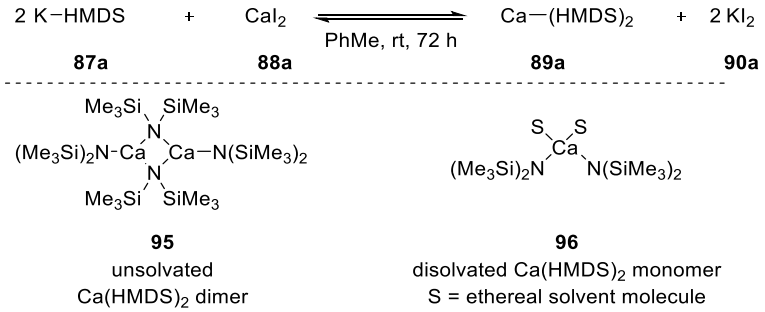

Scheme 37: Preparation of $Ca(HMDS)_2$ from CaI_2

Despite the low solubility of the potassium salt in PhMe and removal by filtration, this method is known to form products that are poisoned with potassium iodide. Even repeated crystallisation of the alkaline earth metal amides cannot completely remove these impurities. An alternative preparation method was provided by Westerhausen.[53] Here, $Sn(HMDS)_2$ (**97**) was used as the amide source and reactions were carried out with elemental alkaline earth metals in a redox transmetallation reaction (Scheme 38).

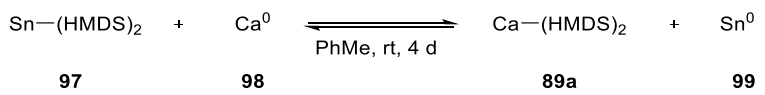

Scheme 38: Preparation of $Ca(HMDS)_2$ from Ca^0

Metallic tin (**99**) was formed as the by-product, which is not soluble in organic solvents and can be removed entirely by filtration. Furthermore, excess Sn(HMDS) can be removed by recrystallisation of the alkaline earth metal amide, as Sn(HMDS) is a liquid at room temperature. One drawback of this reaction was the long reaction time, which was even longer (7 d) for the Sr and Ba analogues. However, the amides were obtained using this method and recrystallisation at –20 °C allowed for the purification of these catalysts as shown by ^{1}H and ^{13}C NMR at room temperature, showing distinct signals for the bridging and the terminal amide ligands of **95**.

(3) Other bases also needed to be tested in this reaction to verify the importance of amide ligands for the deprotonation. This would ultimately give insights into some mechanistic features of the reaction. The metallated product, or product base (**101**), can deprotonate

either the catalyst's conjugate acid (BB–H, formed upon deprotonation of allylbenzene) or allylbenzene directly (Scheme 39).

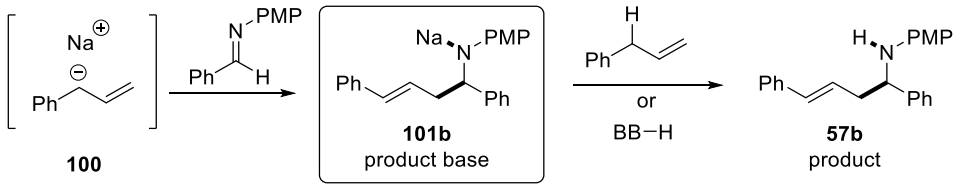

Scheme 39: Product base mechanisms

(4) Finally, the use of metal-free conditions needed to be investigated in order to explore the role of a metal in this reaction. It is possible that an allylic anion can only be stable in the presence of a coordinating metal cation. However, the use of organobases in the isomerisation reaction have shown that the deprotonation of allylbenzene using metal-free conditions is possible.[54] However, the metal ion may also be required for the activation of the electrophile, where C–C bond formations provide an additional challenge to the activation of allylbenzenes.

To start the catalyst screenings, the three commercially available lithium amides, as well as the sodium–HMDS and potassium–HMDS complexes were used in dioxane and THF to compare the different reactivities. Allylbenzene (**36**) was used in a slight excess (1.1 equiv) with respect to imine **56b**, in order to account for any loss of pro-nucleophile to isomerised product **58** (Table 4). Yields were recorded using ^{1}H NMR spectroscopy (e.g. Chart 1), where integration of the alkenyl, benzylic and allylic proton shifts provided reliable data for product **57b** yields [δ = 6.5 and 6.2 ppm (J_{trans} = 15.8 Hz), δ = 4.4 ppm, δ = 2.7 and 2.6 ppm respectively]. Further signals for the PMP-group (δ = 6.7 and 6.5 ppm) and for the N–H (δ = 4.1 ppm) could be detected. Isomerised product **58** was quantified by integration of ^{1}H NMR spectrum signals in the alkenyl region (δ = 6.2 ppm) when the allylic region (δ = 1.9 ppm) overlapped with solvent signals (e.g. THF).

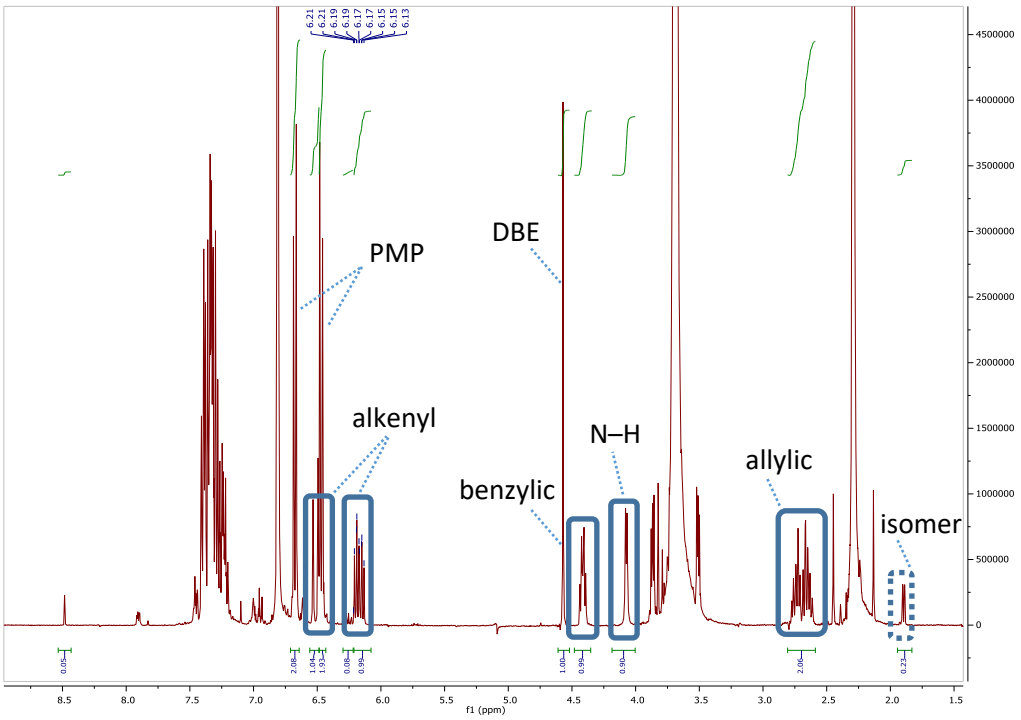

Chart 1: Aliquot ^{1}H NMR spectrum of reaction between 36 and 56b in dioxane

Table 4: Catalyst screening - metal amides in dioxane

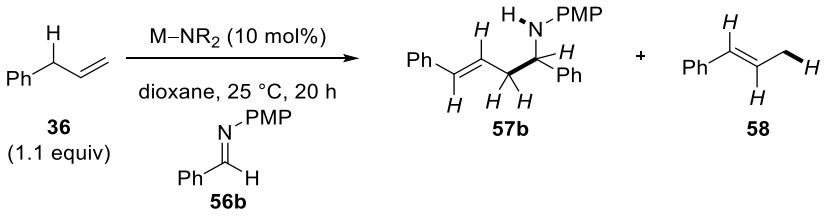

Entry	Catalyst (x mol%)	Yield 57b (%)[a]	58 (%)[a]
1	LTMP	*NR*[b]	-
2	LDA	*NR*[b]	-
3	LHMDS	*NR*[b]	-
4	NaHMDS	98	5
5	KHMDS	23	44

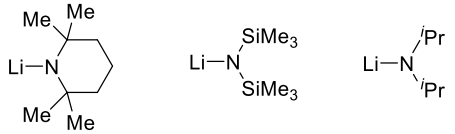

[a] The yield was determined by ^{1}H NMR spectroscopy of a reaction aliquot and represents the average of at least two identical reaction outcomes; internal standard: dibenzyl ether (25 mol%). [b] NR = no reaction; the desired product was not detectable, only starting materials were detected (^{1}H NMR analysis of a reaction aliquot).

In dioxane, none of the lithium amide catalysts showed any reactivity at room temperature (entries 1-3). This was somewhat surprising as the activation of allylbenzene was thought to be mostly dependent on the amide base and less on the nature of the metal. However, excellent results were obtained using NaHMDS, which showed a good balance between activity and selectivity for product **57b** (entry 4). The use of KHMDS was less successful, because much increased levels of isomer product **58** were observed (entry 5).

As different reaction outcomes have been observed for the reaction of NaHMDS in THF, this solvent was also used for a catalyst screening using otherwise unchanged conditions (Table 5).

Table 5: Catalyst screening - metal amides in THF

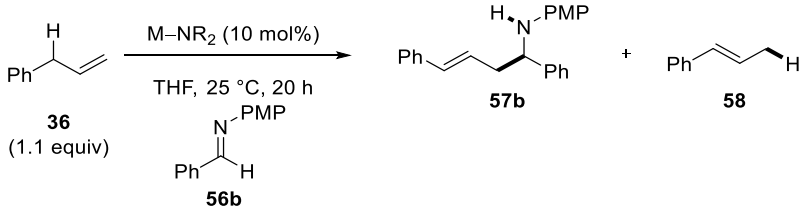

Entry	Catalyst (x mol%)	Yield 57b (%)[a]	58 (%)[a]
1	LTMP	32	2
2	LDA	56	13
3	LHMDS	42	4
4	NaHMDS	17	62
5	KHMDS	0	37

[a] The yield was determined by ^{1}H NMR spectroscopy of a reaction aliquot and represents the average of at least two identical reaction outcomes; internal standard: dibenzyl ether (25 mol%).

In contrast to the results in dioxane, the use of lithium amide catalysts in THF was successful and product yields of 32–56% were obtained (entries 1-3). Both LTMP and LHMDS showed low levels of isomerisation, but product yields did not reach those for NaHMDS in dioxane. NaHMDS and KHMDS both showed similar activity to the lithium amides, but selectivities were favouring the isomerised product **58** and 0–17% yield was observed for product **57b** (entries 4 and 5).

One alternative to using ethereal solvents was DMF, which had proven to be tolerated in the NaHMDS-catalysed cinnamylation reaction. This solvent was also used in a catalyst screening with all commercially available alkali metal amides (Table 6).

Table 6: Catalyst screening - metal amides in DMF

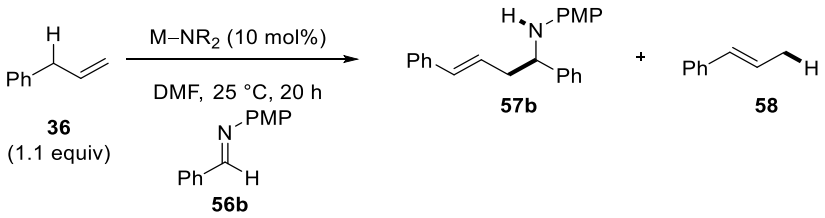

Entry	Catalyst	Yield 57b (%)[a]	58 (%)[a]
1	LDA	10	0
2	LTMP	2	0
3	LHMDS	55	35
4	NaHMDS	13	42
5	KHMDS	26	56

[a] The yield was determined by ^{1}H NMR spectroscopy of a reaction aliquot and represents the average of at least two identical reaction outcomes; internal standard: dibenzyl ether (25 mol%).

The catalyst screening in DMF showed that none of the catalysts gave good reaction yields for product **57b**, as isomerisation of pro-nucleophile **36** remained a major challenge in this polar coordinating solvent. Interestingly, reactions using lithium amide bases showed some activity, with LHMDS giving the best result (55% **57b**) compared to all other catalysts (entry 3). Like in THF, both NaHMDS and KHMDS gave more **58** than **57b** showing that conditions for the C–C bond formations were too basic in this solvent (entries 4 and 5).

In order to compare these results with different metal amides, the alkaline earth metal amides, as well as other commercially available metal hexamethyldisilazides were tested for their ability to catalyse the cinnamylation of imine **56b** in dioxane (Scheme 40).

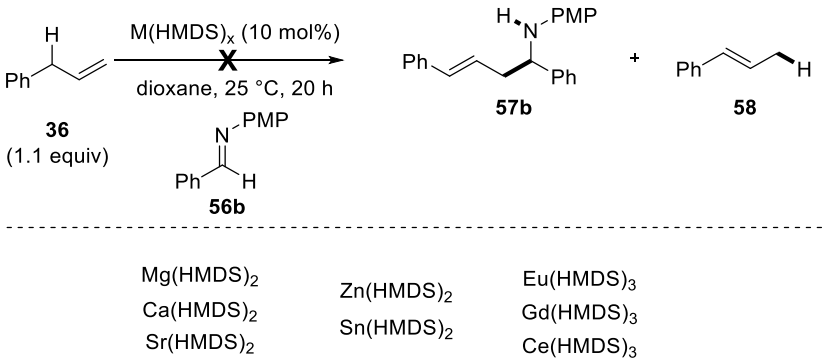

Scheme 40: Catalyst screening – other metal amides

Next to the alkali metals, none of the other metal amides was able to catalyse the reaction between **36** and **57b**. Furthermore, no isomerisation was observed in these reactions, suggesting that the deprotonation of allylbenzene was not achieved. This lack of reactivity for other metals makes the cinnamylation reaction exclusive to alkali metal amides, which

are the cheapest and most accessible catalysts among those used. However, the development of other areas of this research might be dependent on other metals, which allow for stronger coordination than alkali metals, particularly in the field of asymmetric catalysis.

To investigate the choice of base in the reactions of allylbenzene with imine **56b**, strong alkali metal bases were chosen as an alternative. To start, alkali metal hydrides were chosen as strong hydride bases. These salts display a low solubility in organic solvents, which could influence the catalyst's reactivity. Therefore, increased catalyst loadings (10–50 mol%) were used in dioxane, THF and DMF for comparison. None of the employed conditions showed any product formation. Despite their strong basicity and identical metal counterions, the hydride salts did not appear to activate allylbenzene. The absence of any products was somewhat surprising, as at least stoichiometric amounts of either product **57b** or product **58** were expected to be observed.

Therefore, reactions with alkyllithium reagents as even stronger bases were conducted. Catalytic amounts (10 mol%) of methyllithium and butyllithium were studied for the cinnamylation of imine **56b** (Table 7). THF was chosen as an additional solvent to dioxane, as Li bases showed no reactivity in dioxane when using alkali metal amides.

Table 7: Catalyst screening - alkyllithium catalysts

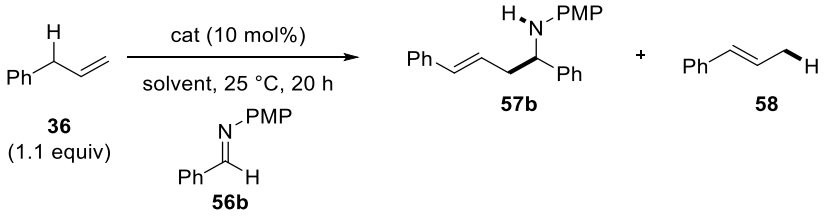

Entry	Cat	Solvent	Yield 57b (%)[a]	58 (%)[a]
1	LiMe	dioxane	14	2
2	Li^{n}Bu	dioxane	10	0
3	LiMe	THF	62	22
4	Li^{n}Bu	THF	74	18

[a] The yield was determined by ^{1}H NMR spectroscopy of a reaction aliquot; internal standard: dibenzyl ether (25 mol%).

For the reactions carried out in dioxane, low reaction yields of 10–14% were obtained (entries 1 and 2). These yields suggested the stoichiometric generation of an allylic intermediate, which then added to imine **56b** selectively. However, when the same reactions were performed in THF, yields of 62–74% for product **57b** were observed, alongside isomerised pro-nucleophile **58** in 18–22% yield (entries 3 and 4). As the catalyst's conjugate acids (Me–H or Bu–H) have a pK_a value >45 (DMSO), they were not considered to be

deprotonated by the product base. Furthermore, these conjugate acids are both gaseous at room temperature and were therefore expected to be removed from the reaction after an initial deprotonation step. Thus, this reaction showed that an initiative pathway for the cinnamylation of imine **56b** with allylbenzene (**36**) was possible. The generation of product **57b** in yields greater than the catalyst loading showed that the lithiated product was likely to be the active catalytic species, which deprotonated further pro-nucleophile to ensure catalyst turnover. Further mechanistic studies were required to test whether this observation could be applied to the alkali metal amide catalysts (cf. Preliminary Mechanistic Investigations, p 60)

Finally, the reactions with strong organosuperbases were conducted, which gave insights into the importance of the metal in the cinnamylation reaction (Table 8). These bases were chosen because the Verkade bases have been reported to be able to activate allylbenzene in acetonitrile (cf. Scheme 63, p 73).[54] The commercially available Schwesinger bases display an even greater structural variety than the Verkade bases and both have been shown to have very high basicities, depending on substitution.[55] Reactions of allylbenzene (**36**) with imine **56b** were carried out in dioxane at room temperature using 5–10 mol% of the Schwesinger or Verkade bases.

Table 8: Catalyst Screening - organobases

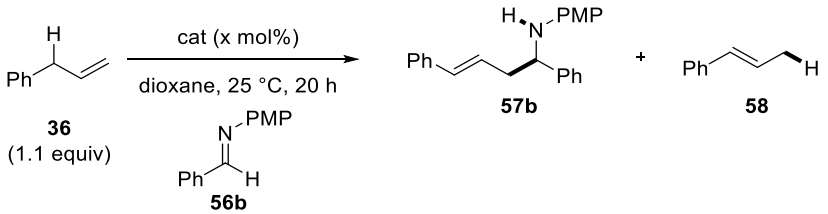

Entry	Cat (x mol%)	Yield 57b (%)[a]	58 (%)[a]
1	**102a** (5)	*NR*[b]	
2	**102b** (5)	*NR*[b]	
3	**103b** (5)	*NR*[b]	
4	**103a** (5)	0	69
5	**104** (5)	0	64
6	**105a** (10)	*NR*[b]	
7	**105b** (10)	*NR*[b]	
8	**105c** (10)	*NR*[b]	

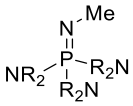

102
Me-P_1
Schwesinger
102a: R = Me
102b: R = pyrr

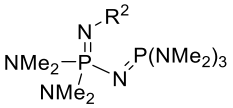

103
R^2-P_2
Schwesinger
103a: R^2 = Et
103b: R^2 = ^{t}Bu

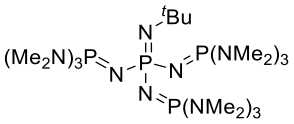

104
^{t}Bu-P_4
Schwesinger

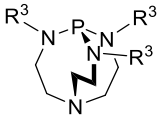

105
^{R3}Verkade
105a: R^3 = Me
105b: R^3 = ^{i}Pr
105c: R^3 = ^{t}Bu

[a] The yield was determined by ^{1}H NMR spectroscopy of a reaction aliquot; internal standard: dibenzyl ether (25 mol%). [b] NR = no reaction; the desired product was not detectable, only starting materials were detected (^{1}H NMR analysis of a reaction aliquot).

Of the Schwesinger bases used, no reaction was observed for the any of the P_1 bases (**102**) or the ^{t}Bu-P_2 base (**103a**) (entries 1-3). However, both the Et-P_2 (**103a**) as well as the ^{t}Bu-P_4 (**104**) bases were able to activate allylbenzene, but only isomerisation product **58** was formed (entries 4 and 5). No C–C bond formation was observed in these reactions, suggesting a lack of imine reactivity after successful deprotonation of allylbenzene. Despite having shown activity in MeCN in the literature,[54] none of the Verkade bases (**105**) was able to activate allylbenzene and no reaction was observed in all cases (entries 6-8). The same reactions were repeated in Et_2O as the solvent, showing identical results. The exclusive isomerisation showed that a metal ion was required not only for the stabilisation of the allylic anion, but also for the activation of the imine. Coordination of the imine to the metal after deprotonation was considered most likely where a hypothesised closed transition state would account for the exlusive γ-addition encountered in this reaction (Scheme 41).

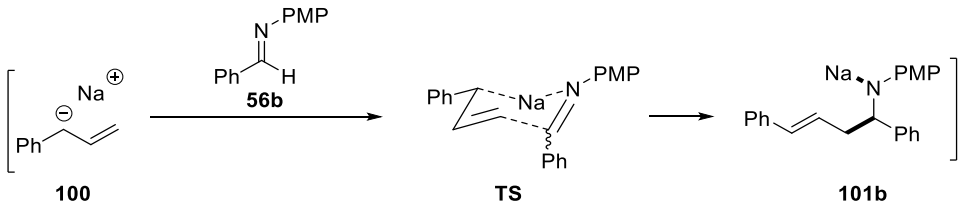

Scheme 41: Possible transition state for the cinnamylation of imines

The interaction between the imine and the metal ion did not have to occur in a a cyclic transition state. An acyclic transition state would also be possible, where multiple metal ions would be involved.

2.3.1.4 Literature for Alkali Metal Amides in Catalysis

Alkali metal amides have been reported in catalysis for different kinds of transformations. Most of these reactions rely on an initiative mechanism, where the amide base was used to deprotonate an acidic substrate that was then reacted with an electrophile to give a product base in a similar fashion to the cinnamylation described above. Several examples are known for C–X bond formation,[56] but reports for C–C bond formations are limited.

C–X bond formation example: hydroaminations

Next to the alkali metal amides, many other catalysts have been identified to catalyse the hydroamination reaction of primary or secondary amines with alkenes and alkynes.[57] Extensive reviews demonstrated the utility and applicability of different catalysts regarding substrate scope and asymmetric variants of the hydroamination reaction.[57a, 57b] Different mechanisms are reported for the catalytic hydroamination. One pathway involves the initiative deprotonation of the amine to form a metal amide, which is used as a nucleophile to generate an alkyl–M intermediate (Figure 5). This intermediate can then be protonated by the amine, regenerating the metal amide to close the catalytic cycle. Regardless of the catalyst used, the intermediate species would always be a metal amide, which is the true catalyst in this reaction.

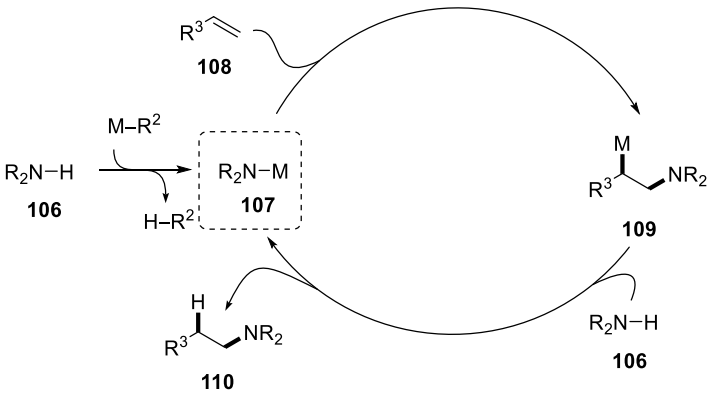

Figure 5: Catalytic cycle for the hydroamination reaction

C–C bond formations

Alkali metal amides have not been extensively studied with respect to their catalytic activity in C–C bond formations. To the best of our knowledge, only five examples of such reactions have been reported in the literature.

The addition of terminal alkynes to carbodiimides has been catalysed using MHMDS catalysts by Richeson (Scheme 42).[58] Here, the lithium amide was assumed to act as an initiator, which allowed for the deprotonation of the terminal alkyne **111** (pK_a ~ 29).[37] The alkyne anion could then add to the carbodiimide to furnish amidine products **113** in high yields.

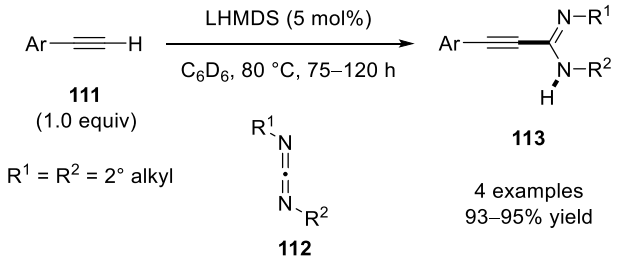

Scheme 42: Alkyne C–H bond activation

Dixon reported the use of KHMDS in a C–C bond formation cascade, including cyclisation and isomerisation to give product **116** (Scheme 43).[59] Unexpectedly, product **116** was found to be formed even when using substoichiometric amounts of base, suggesting a catalytic activity of the metal amide for both the Michael addition, as well as the carbocyclisation. Indeed, proposed enolate intermediate **115** or analogues could deprotonate **114** due to the low pK_a value of the staring material C–H bond (ca. 18, DMSO).[37] Like in the previous example, the metal amide was not considered a true catalyst in the reaction as the deprotonation of the metal amide required a very strong product base intermediate. Again an initiative mechanism was deemed likely, where the alkali metal enolate acted as the catalyst for both C–C bond-forming reactions.

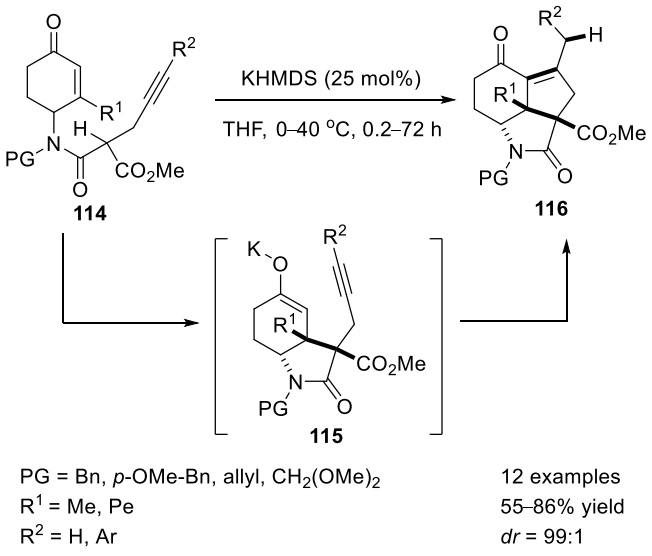

Scheme 43: Dicarbonyl α-C–H activation

During the course of our investigation, Kobayashi published the asymmetric Michael addition of esters and amides to α,β-unsaturated amides (Scheme 44).[60] Here the metal amide was used together with an enantiopure crown ether ligand to provide a chiral metal environment. This complex was used to deprotonate the ester or amide substrates. The potassium enolates were then added to Michael acceptor **118a** with moderate diastereoselectivity and excellent enantioselectivity for the ester pro-nucleophile. In the case of the amide pro-nucleophile, both the diastereoselectivity as well as the enantioselectivity were excellent and 1,5-diamine compounds **119** were obtained in up to 99% yield with 98% *ee*.

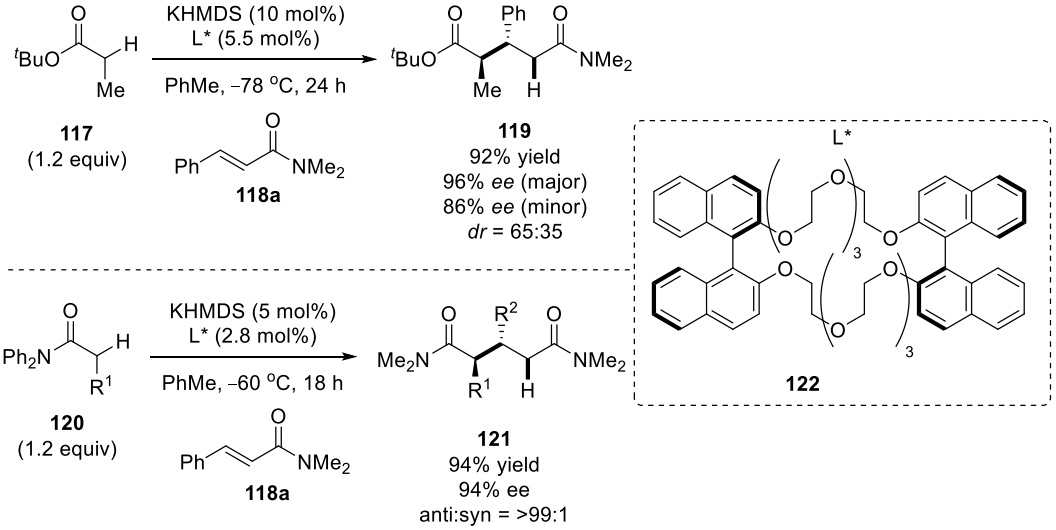

Scheme 44: Ester and Amide C–H activation

Further studies in the group allowed for the Michael addition of alkylnitrile **123** to amide **118a** using the same catalytic system (Scheme 45).[61] Again, yields were high but the asymmetric induction only reached up to 70% *ee*, suggesting less efficient binding of the deprotonated pro-nucleophile to the chiral metal centre. In all cases, the substrate's pK_a value was assumed to be >30; a mechanistic investigation was not reported.

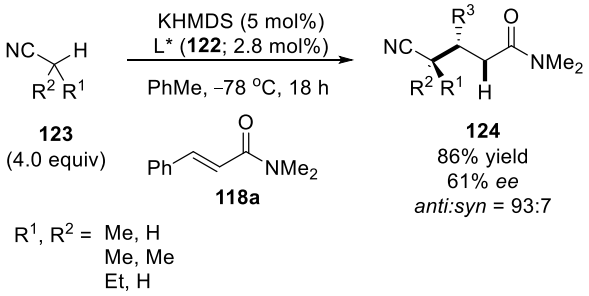

Scheme 45: Alkylnitrile C–H activation

Finally, the group of Lloyd-Jones reported an intriguing catalytic activity of KHMDS in the insertion reaction of carbene **128** into the C–H bond of toluene (Scheme 46).[62] Products of type **127** were observed as side-products in the formation of carbene **128** from pre-carbene **125** and KHMDS in d_8-toluene. It was found that carbene **128** can insert into the C–H bond of toluene (pK_a ~ 43)[37] and that the mechanism for this reaction shows signs of a deprotonative pathway. It was further found that this insertion was catalysed in the presence of NHC–KHMDS (**128**–KHMDS).

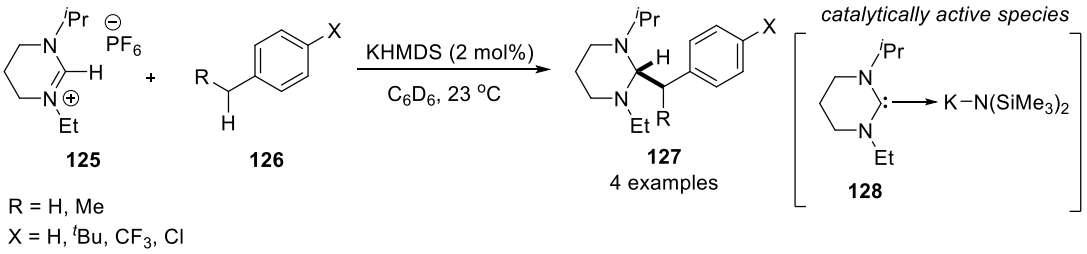

Scheme 46: Benzylic C–H activation

2.3.1.5 Applicability and Robustness

After having demonstrated the possibility of forming product **57b** selectively from allylbenzene (**36**) and imine **56b** using a sodium amide catalyst, the applicability and robustness of this process was investigated. First, the model reaction was stopped after 5 h and the reaction yield for product **57b** was recorded. Reactions using 5–20 mol% NaHMDS were compared in dioxane at 25 °C (Table 9).

Table 9: Catalyst concentration screening

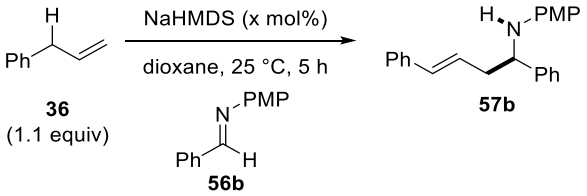

Entry	x (mol%)	Cat Conc (mM)	Yield (%)[a]	TON / TOF (h^{-1})
1	20	133	96	4.8 / 1.0
2	15	100	90	6.0 / 1.2
3	10	67	83	8.3 / 1.7
4	5	50	83	17 / 3.3

[a] The yield was determined by ^{1}H NMR spectroscopy of a reaction aliquot; internal standard: dibenzyl ether (25 mol%).

After only 5 h, the reaction using 20 mol% showed almost complete conversion to product **57b** (entry 1). By successively decreasing the catalyst loading by 5 mol% increments, the yield decreased slightly to 83% when using 10 mol% (entries 2 and 3). These results show that a decreased catalyst concentration lead to a decrease in reaction rate. By using 5 mol% catalyst, a good yield could be obtained after 5 h (83%), giving a high turnover number (17) with a turnover frequency of 3.3 h^{-1} (entry 4). This frequency is the highest one observed for this process and shows a major limitation to this method. However, base-catalysed reactions often cannot compete with transition metal-catalysed reactions, where turnover frequencies are multiple orders of magnitude higher.[63]

Next, even lower catalyst loadings were used in the model reaction (Table 10). For this set of experiments, the substrate scale had to be adapted from 0.20 mmol (>40 mg imine, 5–10 mol% NaHMDS) to 2.50 mmol (>500 mg imine, 0.5 mol% NaHMDS) in order to be able to weigh the catalyst precisely. Catalyst stock solutions could not be used in this reaction as the catalyst's solution behaviour in dioxane was not entirely predictable. Loadings of 0.5–10 mol% NaHMDS were used and reaction time as well as substrate concentrations were adjusted to maximise the product yield.

Table 10: Catalyst loading screening

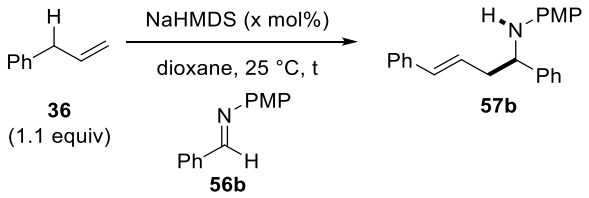

Entry	x (mol%)	Substrate Conc (M)	Cat Conc (mM)	t (h)	Yield (%)[a]	TON / TOF (h^{-1})
1	10	0.67	67	20	99	10 / 0.5
2	5.0	1.00	50	20	99	20 / 1.0
3	2.5	2.00	50	20	78	31 / 1.5
4	2.0	2.50	50	20	76	38 / 1.9
5	1.5	2.50	38	48	71	47 / 1.0
6	1.0	2.50	25	20	5	5 / 0.3
7	0.5	3.33	17	48	*NR*[b]	0 / 0

[a] The yield was determined by ^{1}H NMR spectroscopy of a reaction aliquot; internal standard: dibenzyl ether (25 mol%). [b] NR = no reaction; the desired product was not detectable, only starting materials were detected (^{1}H NMR analysis of a reaction aliquot).

As expected, the reactions carried out with 5–10 mol% catalyst loading gave high yields after 20 h (entries 1 and 2), with increasing turnover numbers (10–20) and frequencies (0.5–1 h^{-1}). For catalyst loadings of 2.0–2.5 mol% the catalyst concentration was kept at 50 mM, but reaction yields decreased to 76–78% (entries 3 and 4). For the reaction using 1.5 mol%, the reaction time was increased to 48 h, as further increasing the substrate concentration was not possible, due to limited imine solubility. A yield of 71% was recorded for product **57b**, giving the highest turnover number for this reaction (47, entry 5). Further decrease of the catalyst loading to 1.0–0.5 mol% resulted in low or no reactivity. This could be due to trace impurities in either solvent, imine or pro-nucleophile.

By lowering the catalyst loading, turnover numbers as high as 47 could be obtained, while reaction rates were generally slow (TON up to 3.3 h^{-1}). The cheap availability of this catalyst (ca. £3 g^{-1} or £0.5 $mmol^{-1}$ as a solid or ethereal solution), which can also be prepared in one step using Na^0 and HMDS amine, balances the fact that catalyst loadings <1 mol% were not tolerated, like they often are when using expensive transition metal catalysts (e.g. $Pd(PPh_3)_4$ >£20 g^{-1} or >£20 $mmol^{-1}$).

Before investigating the substrate scope for this reaction, a robustness screening as suggested by the group of Glorius was performed.[64] Instead of synthesising many analogues of the imine, functional group tolerance was examined by the addition of equimolar amounts of additives containing the functional group in question. Furthermore, competition reactions

could be performed in this way, where the selectivity of a particular group over another could be tested.

The reactions using additives were conducted so that the additive **129**-**142**, the alkali metal amide and imine **56b** were in solution before the addition of allylbenzene (Table 11). In this way, any potential reaction of the catalyst with the additive could take place before the catalyst could interact with the pro-nucleophile. Reactions were then carried out using standard reaction conditions for 20 h.

Table 11: Robustness screening

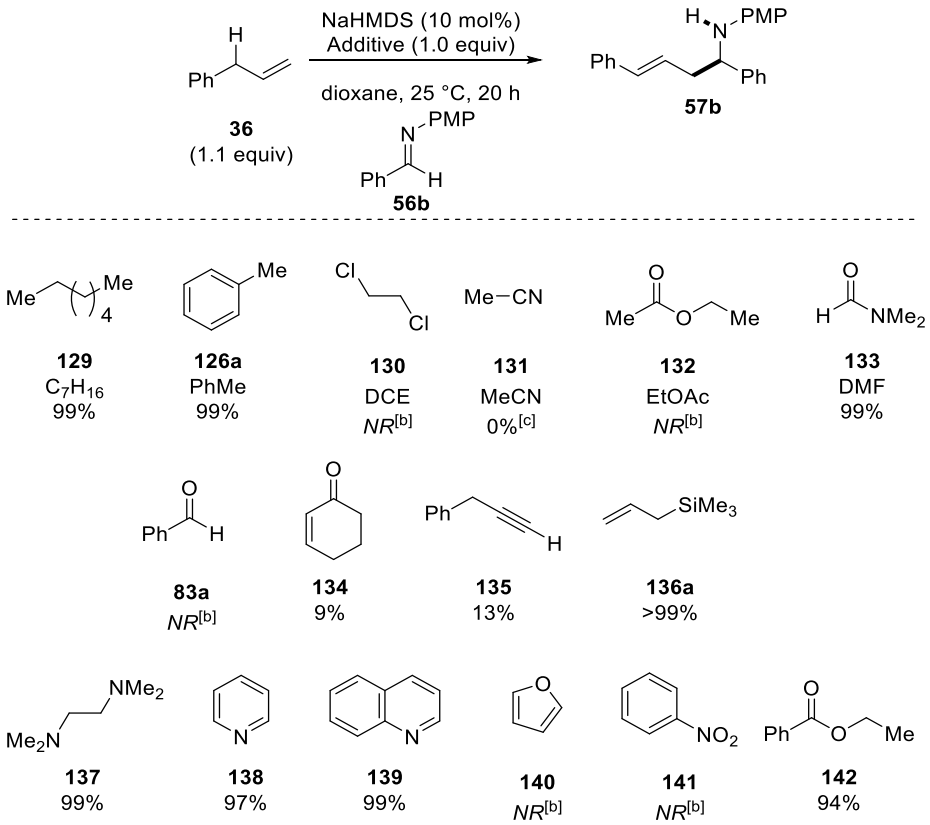

[a] The yield was determined by ^{1}H NMR spectroscopy of a reaction aliquot; internal standard: dibenzyl ether (25 mol%). [b] NR = no reaction; the desired product was not detectable, only starting materials were detected (^{1}H NMR analysis of a reaction aliquot). [c] Acetonitrile activation observed (^{1}H NMR analysis of a reaction aliquot).

First, common organic solvents were tested as dried and purified compounds were readily available in the group. In contrast to the reaction outcome in toluene or heptane as the solvent (which have shown no reaction), these apolar substrates were tolerated in equimolar amounts. The addition of DCE resulted no products being formed, suggesting a reaction between the catalyst and the amide. Indeed, substitution and elimination reactions are both plausible pathways that lead to the formation of NaCl, thus removing the metal from

solution. The reaction with acetonitrile and ethyl acetate resulted in no products being observed. Both substrates can be deprotonated by NaHMDS as they display similar acidity to allylbenzene. While no reaction was observed using the ester, acetonitrile appeared to react with the imine forming new products that could be assigned to the 1,2-addition of the acetonitrile anion (**143b**; Scheme 47).

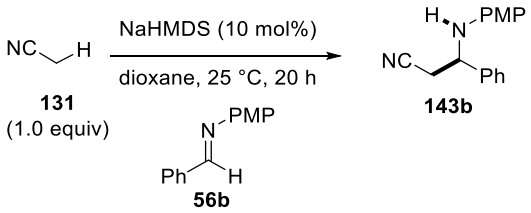

Scheme 47: C–H bond activation of acetonitrile

Other additives had to be dried over MS (4 Å, 2 d) either neat or as solutions in Et_2O, which were subsequently removed *in vacuo*. Benzaldehyde (**83a**) and cyclohexenone (**134**) addition showed no or low product formation. As mentioned, the stoichiometric reaction of NaHMDS with aldehydes is known to give TMS-protected imines,[45] while the conjugate addition of amides is reported for Michael acceptors.[65] Alternative pro-nucleophiles such as alkyne **135** or allylsilane **136a** were also tested. Here, the terminal proton of the alkyne provided an acidic C–H bond leading to a decreased product yield, presumably through partial catalyst deactivation. Allylsilane, however, did not appear to compete with allylbenzene in the cinnamylation reaction and was tolerated by the reaction giving high yields.

Coordinating substrates such as TMEDA, pyridine and quinoline (**137-139**) were all tolerated in the reaction and high yields of 97–99% were obtained. However, other heterocycles, such as furan (**140**), were not tolerated and no products were obtained. The same was true when nitrobenzene (**141**) was used as an additive. In marked contrast to ethyl acetate, ethyl benzoate (**142**) was tolerated in this reaction, giving **57b** in an almost unaffected yield of 94%. This suggested that the ester functional group was tolerated as long as it did not contain acidic α-protons.

2.3.1.6 Scope

The robustness screening provided some initial information on functional group tolerance. Based on this information, different imines were synthesised, purified by recrystallisation and dried as solutions over MS. These imines were then subjected to the optimised conditions from previous reactions, using *N*-PMP-protected benzaldimine **56b**. To start, different aryl aldimines were tested, including alkyl- and halogen-substituted substrates (Table 12).

Table 12: Imine scope – substitution and steric effects

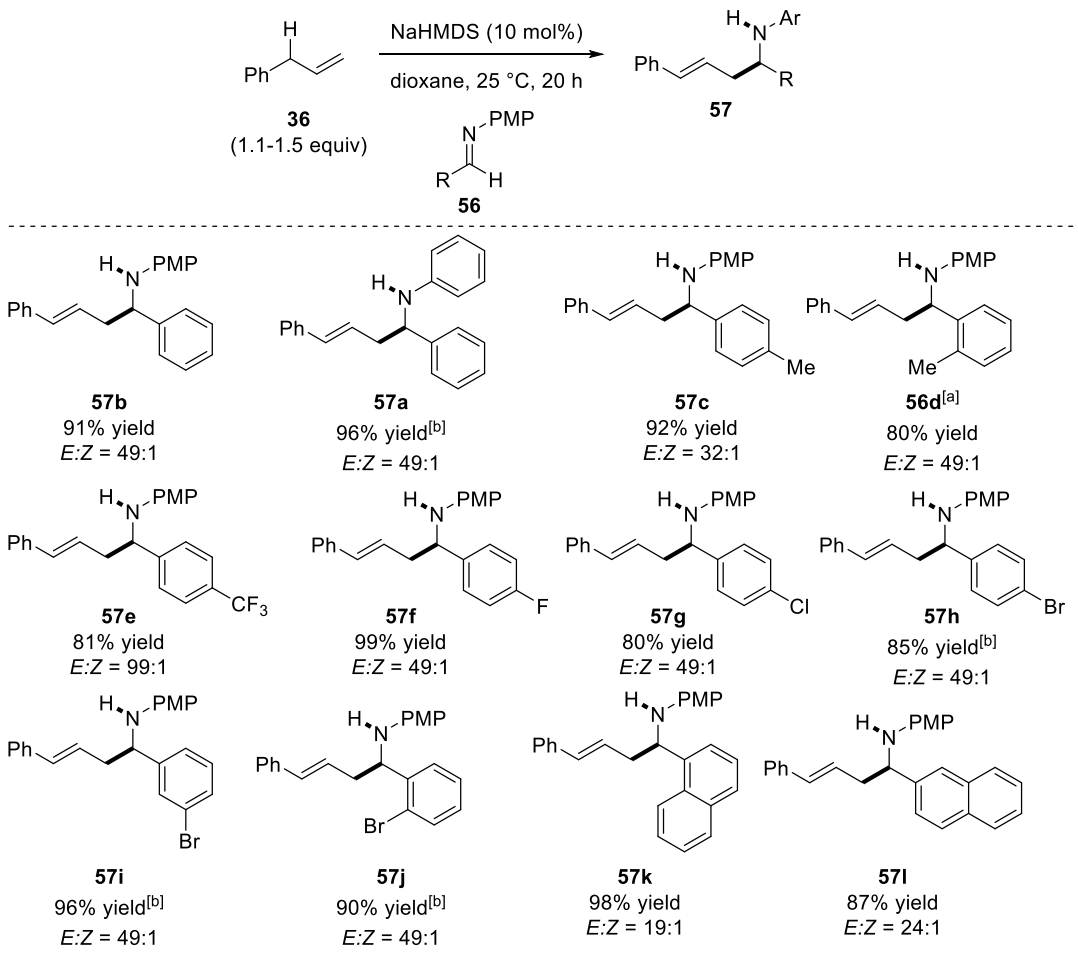

The yield refers to the isolated yield after PTLC purification. *E:Z*-ratios were determined after isolations based on ^{1}H NMR spectroscopy of the purified products. [a] The reaction was carried out by Wei Bao. [b] The isolation was carried out by Wei Bao.

Both the model substrate product **57b**, as well as the previously shown *N*-Ph-protected benzaldimine product **57a** were isolated in good to excellent yields. Substitution of a methyl group in the *ortho*- or *para*-position of the imine was tolerated and gave good yields for products **57d** and **57c**. Substitution of a trifluoromethyl group as well as halogens (F, Cl, Br)

in the *para*-position resulted in the formation of products **57e**-**h** in good to excellent yields. For the bromide-substituted imines, substitution in *ortho*-, *meta*- or *para*-positions was tolerated and no erosion of selectivity regarding the geometrical isomers was observed. For the 1- and 2-naphthyl-substituted products **57k** and **57l**, good to excellent yields were obtained but *E:Z* ratios were significantly decreased to ca 20:1. The reason for this decreased selectivity was unknown. Next, the electronic substitution effects on the imine were tested using different electron-donating and -withdrawing groups (Table 13).

Table 13: Imine scope – substitution and electronic effects

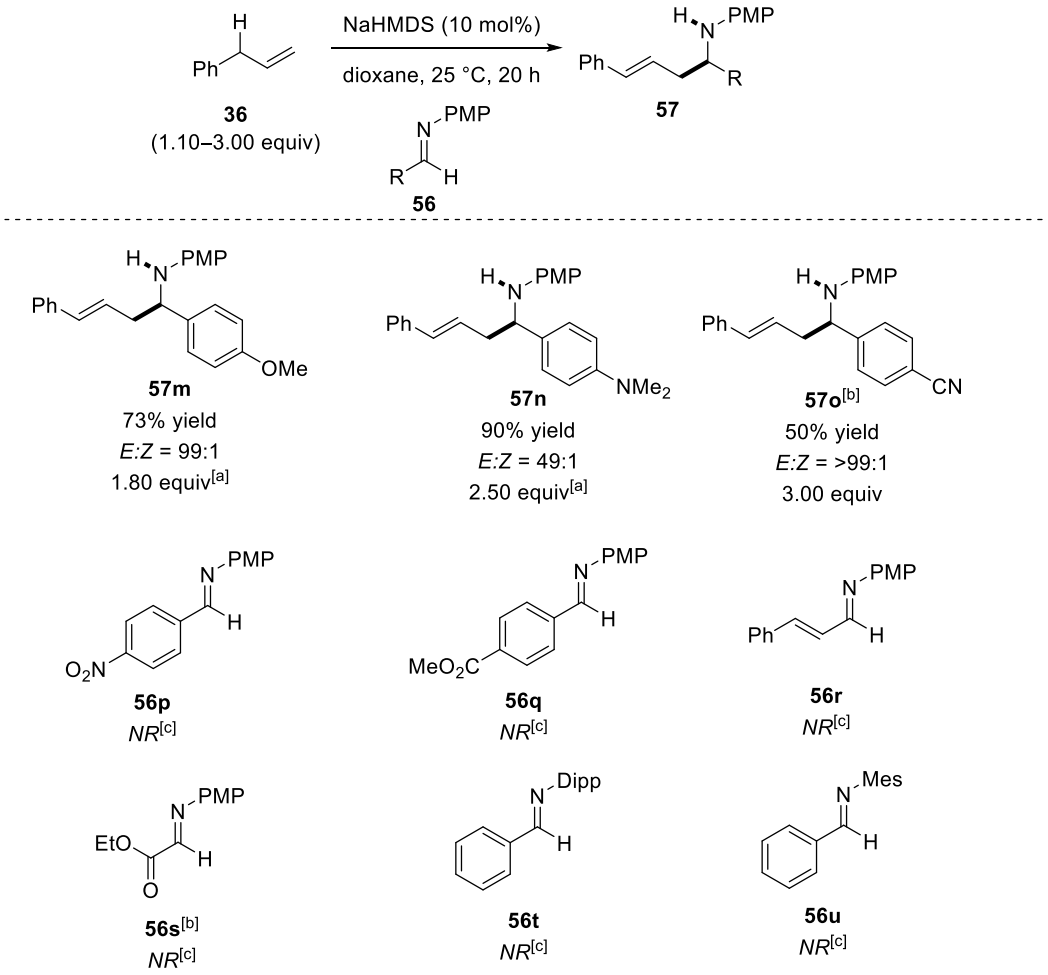

The yield refers to the isolated yield after PTLC purification. *E:Z*-ratios were determined after isolations based on ^{1}H NMR spectroscopy of the purified products. [a] Allylbenzene was added successively in three portions over 20 h. [b] The reaction was carried out by Wei Bao. [c] NR = no reaction; the desired product was not detectable, only starting materials were detected (^{1}H NMR analysis of a reaction aliquot).

When electron-donating groups such as *p*-OMe or *p*-NMe_2 were substituted, the reaction proceeded with high levels of isomerisation, leading to decreased yields. In order to increase the yield for products **57m** and **57n**, additional pro-nucleophile was added to the reaction

mixture successively in portions. This method ensured the use of minimal required amounts of allylbenzene while keeping the concentration of allylbenzene low. The increased electron density was assumed to reduce the imine's electrophilicity. The intermediate allylbenzene anion generated *in situ* was therefore more likely to form isomerised product **58**. Interestingly, the *p*-CN-substituted imine also required a larger excess of pro-nucleophile, and a yield for product **57o** of only 50% could be obtained. However, the nitrile functional group is very versatile and its tolerance to alkali metal amides showed a good applicability of the catalyst. As suggested by the robustness screening, nitro-substituted imine **56p** did not show any reactivity in the reaction with allylbenzene. Surprisingly, also ester-substituted imine **56q** could not be activated. This result contrasted the observation from the robustness screening, where ethyl benzoate was tolerated in the reaction. Further imines such as cinnamyl imine **56r** and glyoxal-derived imine **56s** were tested without success. Finally, other aromatic protecting groups were also tested with imines **56t** and **56u**, but a reaction was not observed for these substrates.

Next, heterocyclic imines as well as an aliphatic aldimine were used (Table 14). Both pyridine and quinolone have been shown to be tolerated in the robustness screening. In the presence of furan, in contrast, no product formation was observed.

Table 14: Imine scope – Heteroaryl- and alkyl-substitution

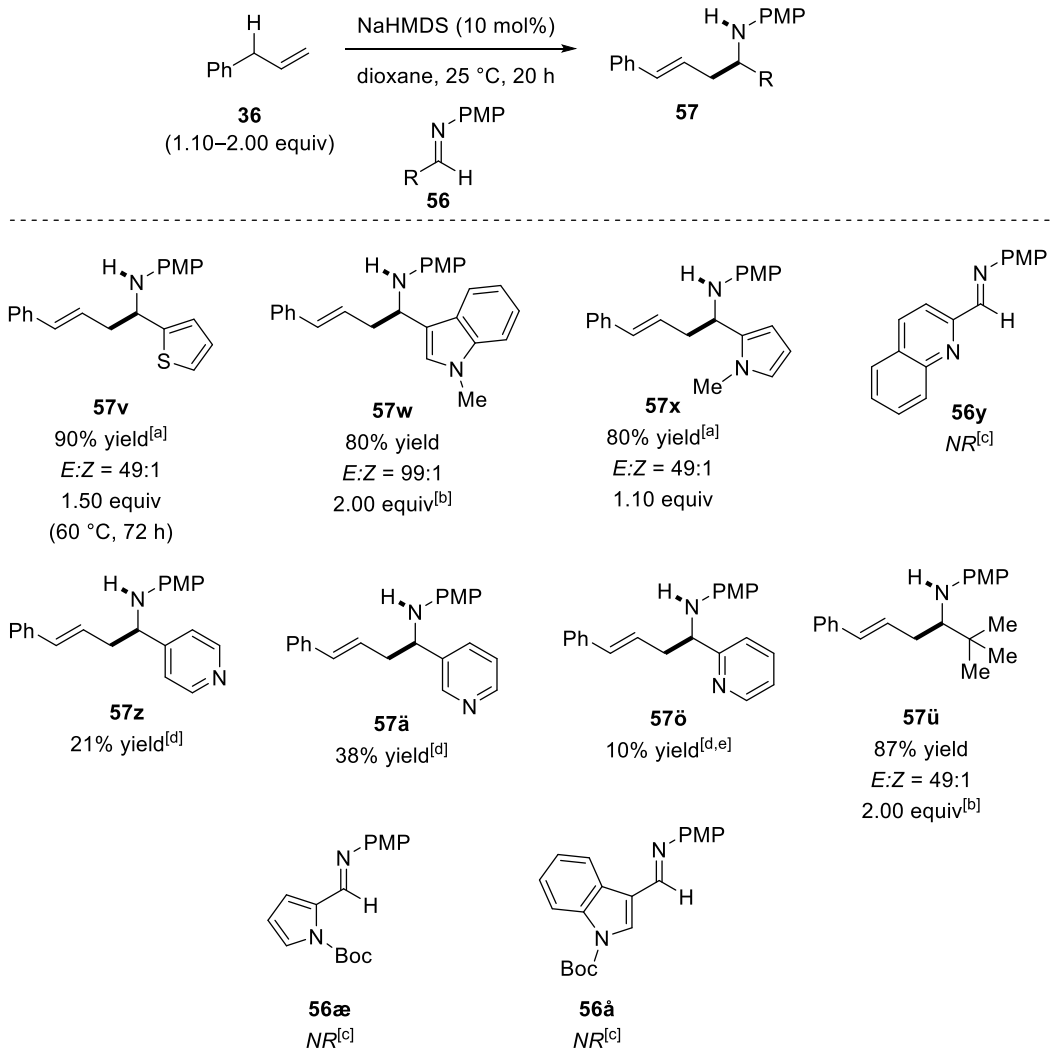

The yield refers to the isolated yield after PTLC purification. *E:Z*-ratios were determined after isolations based on ^{1}H NMR spectroscopy of the purified products. [a] The isolation was carried out by Wei Bao. [b] **36** was added successively in three portions over 20 h. [c] NR = no reaction; the desired product was not detectable, only starting materials were detected (^{1}H NMR analysis of a reaction aliquot). [d] The yield was determined by ^{1}H NMR spectroscopy of a reaction aliquot; internal standard: dibenzyl ether (25 mol%). [e] The reaction was carried out by Wei Bao.

The heterocyclic products **57v-x** were obtained in good yields, although some reaction conditions had to be modified. Thienyl product **57v** was obtained in a high yield only after heating to 60 °C for 72 h. Low levels of isomerisation allowed for this reaction to be heated for prolonged periods of time without significant loss of pro-nucleophile to its isomer. Indole product **57w** was obtained in a similar manner to the electron-rich imine products, where successive addition of the pro-nucleophile allowed for high yields to be obtained. Surprisingly, quinoline-substituted imine **56y** did not show any product formation. Pyridyl substitution on the imine gave poor conversions to products **57z**, **57ä** and **57ö** indicated by

^{1}H NMR spectroscopy of a reaction aliquot. Both quinoline and pyridine were tolerated as an additive in the robustness screening so the low yields could not be directly correlated with functional group intolerance. Finally, *tert*-butyl substituted product **57ü** could be obtained with a yield of 87%. This example showed that this method could be applied to aliphatic imines, provided that the imine did not contain any protons in α-position. Interestingly, reactions with *N*-Boc-protected pyrrole and indole imines **56æ** and **56å** gave no reaction and complete recovery of starting materials based on ^{1}H NMR spectroscopy. Compared to the good results obtained for the alkyl-substituted analogues, the carbamate group was assumed to cause this lack of reactivity. The 2-furyl *N*-PMP-protected aldimine substrate was also synthesised despite the negative effect of furan in the robustness screening (Table 11, p 45). It was hypothesised that impurities in the furan used could have caused a deactivation of the catalyst. However, reactions of the furyl-containing imine with allylbenzene under standard reaction conditions were unsuccessful and a reaction product was not observed.

In order to expand the scope beyond aldimines, different ketimines were also tested in the cinnamylation reaction (Table 15). Different structural motifs were considered in order to furnish homoallylic amine products of type **145**.

Table 15: Imine scope – Ketimines

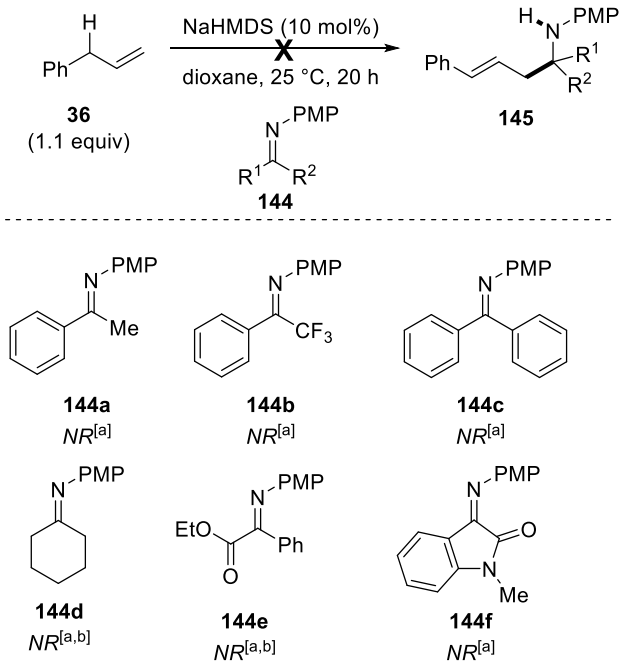

[a] NR = no reaction; the desired product was not detectable, only starting materials were detected (^{1}H NMR analysis of a reaction aliquot). [b] The reaction was carried out by Wei Bao.

Unfortunately, none of the employed ketimines gave products of type **145**. Where the imine contained acidic protons in α-position (**144a** and **144d**), this lack of reactivity was assigned to a deactivation of the catalyst by protonation. For other non-acidic substrates, different reasons needed to be considered. Steric effects could account for the lack of reactivity of some substrates, while 1,2 dicarbonyl-derived ketimine **144f** could have deactivated the catalyst by 1,2-addition of the amide to the imine's C=N double bond.

Next to the imine scope, the allylbenzene scope was also considered. Different commercially available allylbenzenes (substituted on the aromatic ring), were used in the cinnamylation of imine **56b** (Table 16).

Table 16: Allylbenzene scope

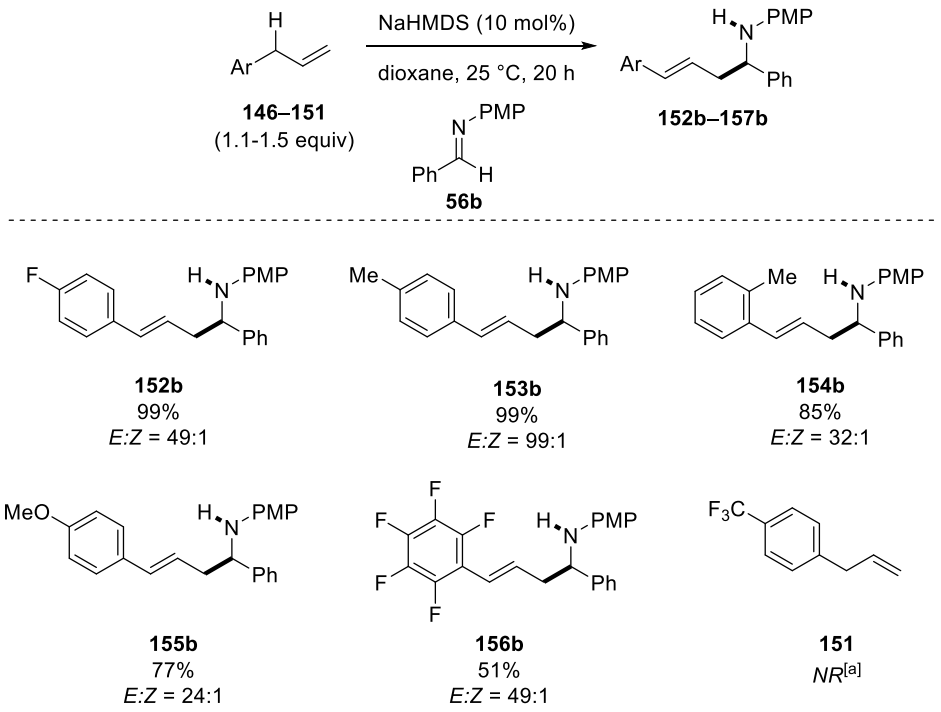

The yield refers to the isolated yield after PTLC purification. *E:Z*-ratios were determined after isolations based on ^{1}H NMR spectroscopy of the purified products. [a] The yield was determined by ^{1}H NMR spectroscopy of a reaction aliquot; internal standard: dibenzyl ether (25 mol%).

Substitution of different functional groups, including fluorine, methyl, and methoxy groups, resulted in the formation of products **152-155** in good to excellent yields. Interestingly, *E:Z* selectivities were much more affected by substitution on the allylbenzene than these were for substitution on the imine. When changing the methyl-substitution from *para* to *ortho*, a decrease in selectivity from 99:1 to 32:1 was observed. Due to the proximity of the methyl group in the *ortho*-position to the double bond in product **154b**, is was assumed that the additional substitution influenced the configuration of a reaction intermediate. Also

methoxy-substituted product **155b** showed a lower *E:Z* selectivity of 24:1. Here, steric interactions were unlikely, hence the nature of this decreased selectivity may be electronic. The perfluorinated product **156b** was not isolated, as yields of only up to 51% were observed in ^{1}H NMR spectroscopy. It was originally assumed that this substrate would stabilise an allylic anion better than allylbenzene, thereby leading to low levels of isomerisation. However, the decreased electron density of the allylic anion could also reduce the nucleophile's reactivity, leading to low yields.

Allylpyridine **158** was used as a highly interesting pro-nucleophile, which allowed for the introduction of a further heterocycle into the homoallylic amine products. This substrate reacted in a slightly unusual way, because often high levels of isomerised pro-nucleophile were observed. Furthermore, the presence of another heteroatom in the product lead to further possible coordination to the catalyst. In order to show the utility of this method for the formation of electron-rich and electron-poor heterocycle-containing products, heterocyclic imines were used in the reaction with 3-allylpyridine (**158**; Table 17).

Table 17: Allylpyridine Scope

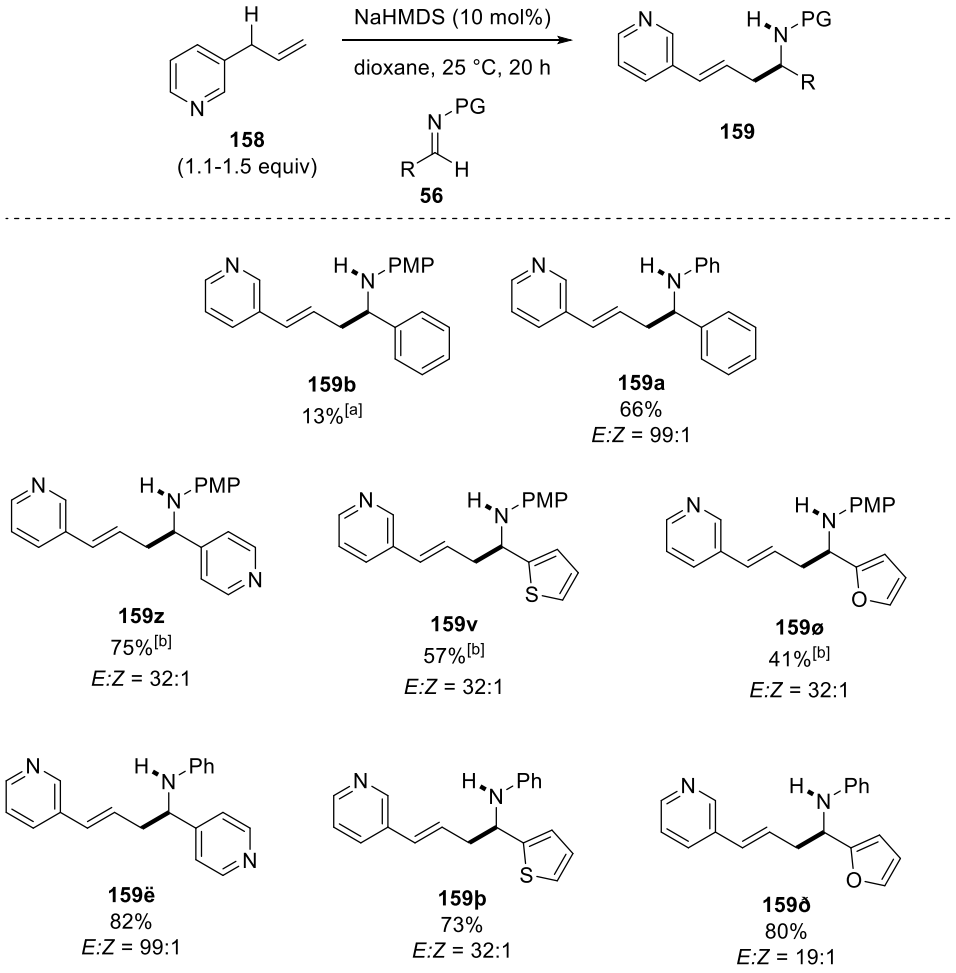

The yield refers to the isolated yield after PTLC purification. *E:Z*-ratios were determined after isolations based on ^{1}H NMR spectroscopy of the purified products. [a] The yield was determined by ^{1}H NMR spectroscopy of a reaction aliquot; internal standard: dibenzyl ether (25 mol%). [b] The isolation was carried out by Wei Bao.

Interestingly, product yields of only up to 13% were observed when *N*-PMP-protected benzaldimine was used in the reaction with 3-allylpyridine. A significantly increased yield of 66% was observed for *N*-Ph-protected product **159a**. The yields for heterocyclic PMP-protected products **159z, 159v** and **159ø**, containing pyridyl, thienyl, or furyl groups, were found to be 41–75%. When the same substrates were tried with *N*-phenyl-protection, compounds **159ë**, **159þ** and **159ð** could be isolated in much improved yields of 73–82%. *E:Z* selectivities varied between 32:1 to 99:1, reflecting the same spectrum of selectivities that had previously been found for allylbenzene.

One final step in the pro-nucleophile scope was to test other substrates similar to allylbenzene. As mentioned at the start of the chapter, both diphenylmethane and 1,5-

pentadiene have pK_a values similar to allylbenzene. In the reactions with 1,5-pentadiene (**160**), 3-methyl-1,5-pentadiene (**161**) and diphenylmethane (**162**), products were found for both diene substrates, but no reaction occurred when using diphenylmethane (Table 18). This lack of reactivity supported the hypothesis of a cyclic transition state, where diphenylmethane does not allow for γ-addition to occur.

Table 18: Other pro-nucleophiles

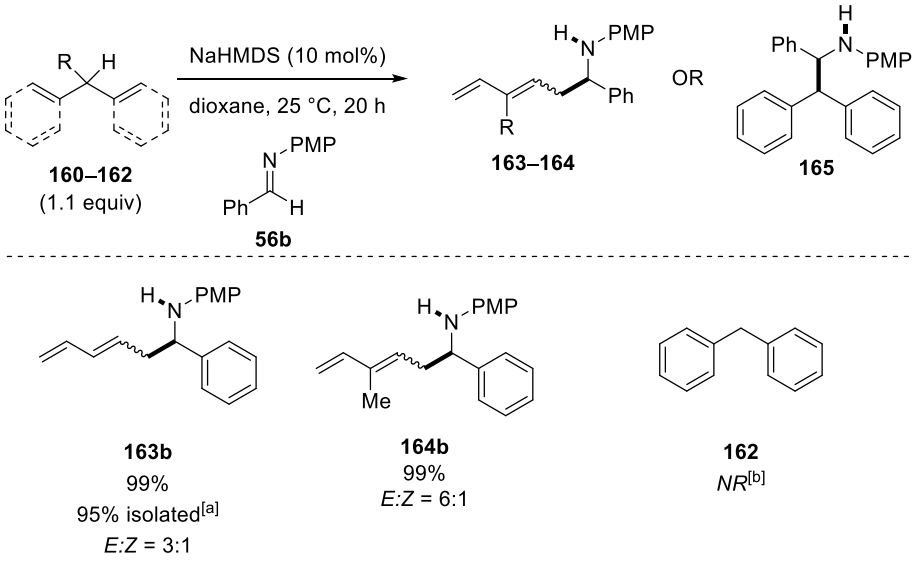

The yield was determined by ^{1}H NMR spectroscopy of a reaction aliquot; internal standard: dibenzyl ether (25 mol%). [a] The isolation was carried out by Wei Bao. [b] NR = no reaction; the desired product was not detectable, only starting materials were detected (^{1}H NMR analysis of a reaction aliquot).

Unfortunately, *E:Z* selectivities were poor in the case of diene pro-nucleophiles and values of 3:1 were observed for unsubstituted product **163b**, while an increased selectivity of 6:1 was noted for the methyl-substituted product **164b**. Despite this method showing a clear preference for *E*-**164b**, the geometric isomers could not be separated using standard chromatographic methods (silica gel flash column chromatography or PTLC), which limited its application. However, an imine scope was developed for this method, in order to investigate the substitution effects, as all imines were readily available in the group (Table 19-20).

Table 19: Pentadiene imine scope I

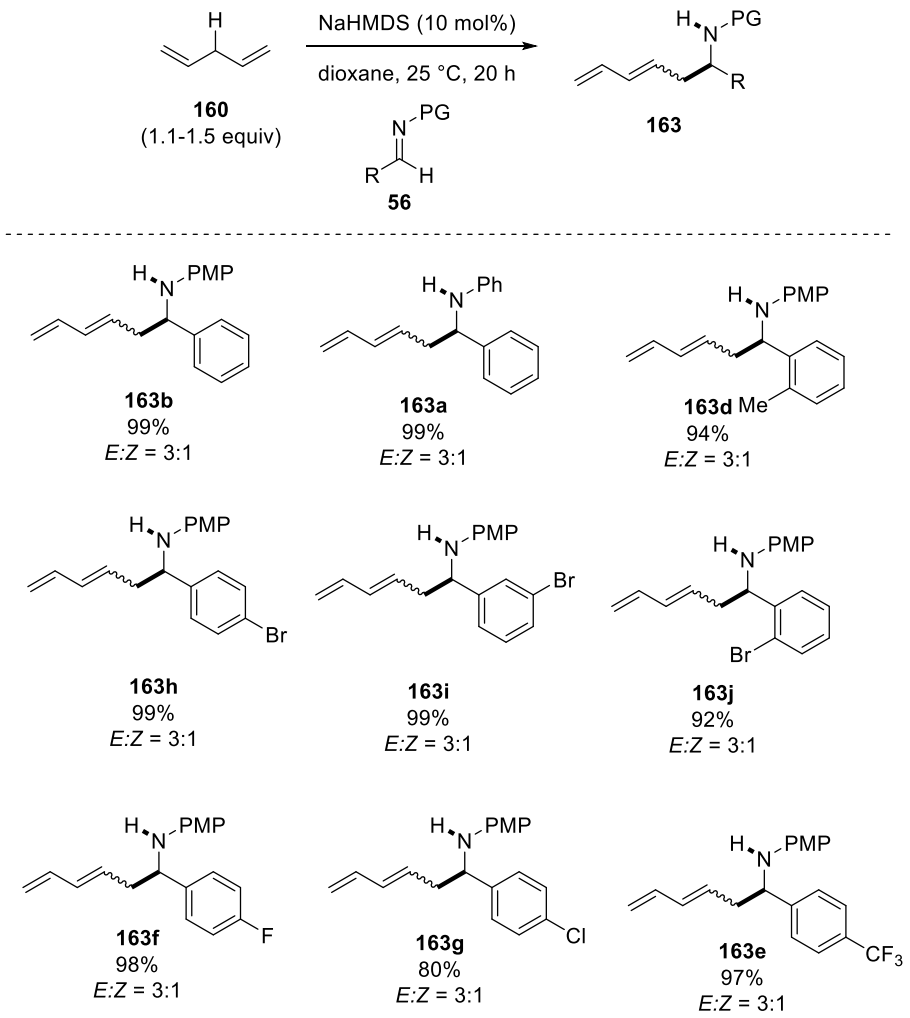

The yield and *E*:*Z*-ratios was determined by ^{1}H NMR spectroscopy of a reaction aliquot; internal standard: dibenzyl ether (25 mol%).

Unsubstituted imine products **163b** and **163a** were obtained in excellent yields and *E*:*Z* selectivities of 3:1. Methyl-substitution, as well as bromide-substitution in all positions gave products **163d-j** in good to excellent yields. Furthermore, fluoride, chloride and trifluoromethyl substitution was shown to be tolerated, giving products **163f-e** in 80–98% yield with similar selectivities.

Table 20: Pentadiene imine scope II

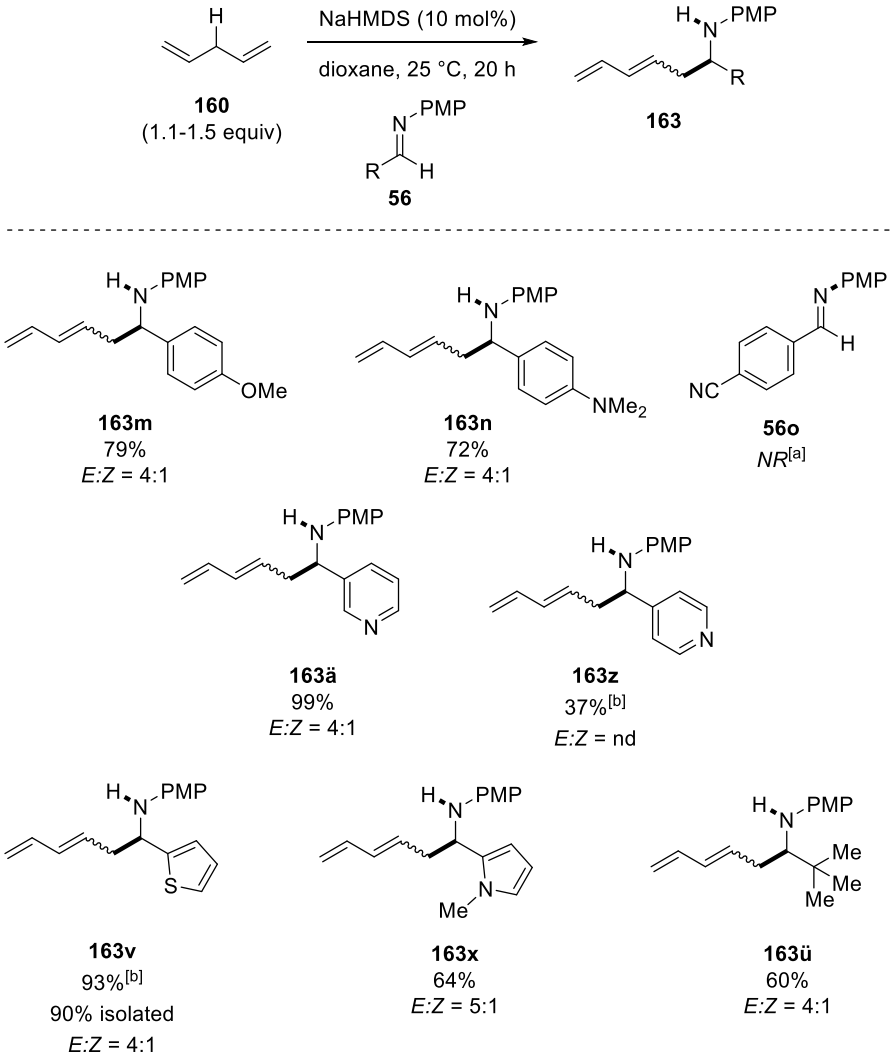

The yield was determined by ^{1}H NMR spectroscopy of a reaction aliquot; internal standard: dibenzyl ether (25 mol%). [a] NR = no reaction; the desired product was not detectable, only starting materials were detected (^{1}H NMR analysis of a reaction aliquot). [b] The reaction was carried out by Wei Bao.

Like in the case of allylbenzene, imine substitution with electron rich substituents was tolerated and products **163m** and **163n** were obtained in 72–79% yield. *E:Z* selectivities were slightly increased to ca. 4:1. Cyano-substitution did not result in any product to be formed in the reaction and only starting materials were observed in ^{1}H NMR spectroscopy. The use of heterocyclic imines was possible and allylated 4-pyridyl-containing product **163ä** was obtained with an excellent yield, while its 3-pyridyl analogue gave a yield of only 37%. Both thienyl and pyrrolyl-substitution was tolerated and products **163v** and **163x** were found with a yield of 64–93%. Finally, this pro-nucleophile was also reacted with the aliphatic imine, giving *tert*-butyl-substituted product **163ü** in a moderate yield and an *E:Z* selectivity of 4:1.

Other pro-nucleophiles

The formation of β-Me styrene (**58**) in the cinnamylation of imines using allylbenzene suggested that 'irreversible' isomerisation occurred under the catalytic conditions. Indeed, **58** contains a double bond conjugated to the aromatic system, which provides a high thermodynamic stability for this product. However, the allyl–Na intermediate that was generated from the deprotonation of allylbenzene was assumed to be similar to the intermediate generated from the deprotonation of β-methyl styrene. Assuming that the allyl–Na exhibited a fast equilibrium to a π-allyl species, the intermediates would indeed be identical. However, once formed, the styrene side-product did not appear to be available for C–H bond activation in the catalytic system. Therefore, reactions with β-methyl styrene (**58**) were conducted with imine **56b** as the electrophile. Unsurprisingly, the reaction under unchanged catalyst conditions (NaHMDS in dioxane) at mild temperatures (25–60 °C) did not proceed and no reaction was observed. Therefore, different catalytic systems were investigated and the influence of ligands was studied (Table 21).

Table 21: Activation of β-methylstyrene

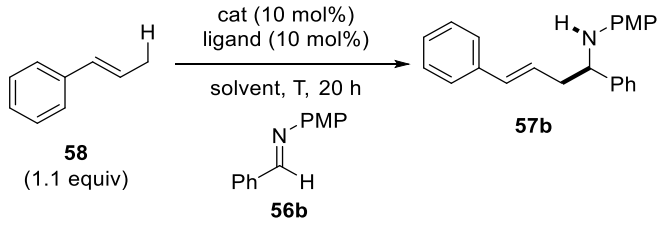

Entry	Cat	Ligand	Solvent	T (°C)	Yield[a] (%)
1	NaHMDS	-	dioxane	25-60	*NR*[b]
2	KHMDS	-	dioxane	25-40	*NR*[b]
3	NaHMDS	[18]c-6	dioxane	25	*NR*[b]
4	NaHMDS	[18]c-6	THF	25	*NR*[b]
5	NaHMDS	IPr	dioxane	60	20
6	NaHMDS	^{t}Bu-BOX*	dioxane	60	10
7	NaHMDS	-	DMF	25	23

[a] The yield was determined by ^{1}H NMR spectroscopy of a reaction aliquot; internal standard: dibenzyl ether (25 mol%). [b] NR = no reaction; the desired product was not detectable, only starting materials were detected (^{1}H NMR analysis of a reaction aliquot).

Heating the NaHMDS- or KHMDS-catalysed reaction up to 60 °C in dioxane did not result in the formation of any products and only starting materials were observed in ^{1}H NMR spectroscopy (entries 1 and 2). The addition of a crown ether ligand also did not show the desired product to form in either dioxane or THF (entries 3 and 4). However, the use of carbene or bisoxazoline ligands at 60 °C furnished product **57b** in 10–20% yield. The best

yield for this transformation was obtained when carrying out the reaction in DMF, a strongly coordinating solvent. Here, the reaction could be carried out at 25 °C giving product **57b** in 23% yield (entry 7). The analogous Li- and K-catalysed reactions also showed conversions, but yields were generally lower. These results showed that the activation of styrene was possible, but required harsher reaction conditions or coordinating solvents to proceed. Furthermore, no branched product was observed in this reaction, suggesting that the reaction took place by deprotonation followed by isomerisation to the same allyl–M intermediate that was generated from allylbenzene. As the product yields were generally low, allylbenzene showed a much better reactivity in the allylation of imines.

Instead of using β-substituted methyl styrene, α-substituted styrene was also investigated with respect to the C–C bond forming reaction using imine **56b**. This substrate was not considered to be activated easily by deprotonation, as the allylic anion did not experience the same stabilisation from the aryl group as the allylbenzene anion. However, this styrene product has been previously activated in imino-ene reactions, so its reaction with imine **56b** had to be tested (Scheme 48). The uncatalysed thermal reaction in dioxane and THF at up to 60 °C did not show any formation of homoallylic amine product **166**.

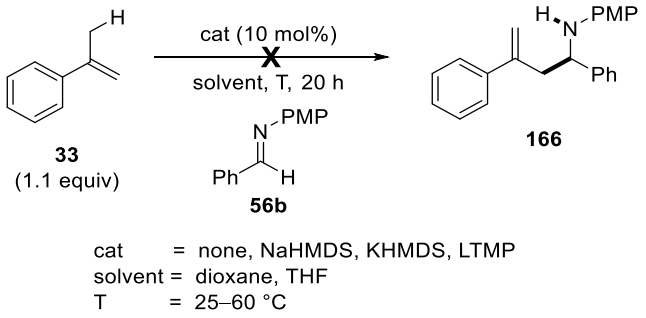

Scheme 48: Activation of α-methylstyrene

None of the used catalytic conditions furnished allylic amine **166**. NaHMDS, KHMDS or LTMP were employed in either THF or dioxane and reactions were heated up to 60 °C. This suggested that the imino-ene reaction with imine **56b** required a high activation energy to proceed. Considering the low reactivity of this imine compared to the α-imino esters, which have usually been used in the imino-ene reaction, this result was not unexpected. Furthermore, none of the alkali metals were considered a good Lewis acid catalyst, which are usually required for the imino-ene reaction to proceed under mild conditions.

2.3.1.7 Preliminary Mechanistic Investigations

In order to improve reaction conditions as well as developing asymmetric variants of the cinnamylation of imines using metal amide catalysis, understanding the reaction mechanism was crucial. One aspect of this was the careful consideration of reaction side-products and possible side-reactions. Many of these have been mentioned before, giving first indications of reaction intermediates. The formation of β-methylstyrene suggested the formation of an allylbenzene anion reactive intermediate, which could react with electrophiles (H^+ or imines) from the γ-position. The lack of β-methylstyrene reactivity in C–C bond forming processes showed that once formed, this side-product could not re-enter the catalytic cycle and pro-nucleophile was lost. This meant, isomerisation could be classified as a catalytic 'decomposition' of starting material (Scheme 49).

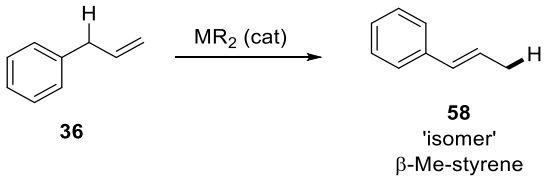

Scheme 49: Isomerisation side-reaction

Alternative off-cycle pathways include possible reversible stoichiometric reactions of the catalyst with the substrates. One example for this would be the attack of the amide to the imine directly, giving rise to an amide that would resemble the product base (Scheme 50). **167** could be a different catalytically active species, or an off cycle reaction, which cannot be detected easily due to the reversibility of the process.

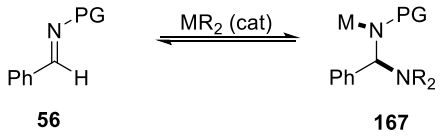

Scheme 50: LB attack of catalyst to imine

Another off-cycle pathway would be the catalytic decomposition of products. The dehydroamination reaction is an example for this kind of reactivity, where the metal amide was assumed to catalyse the elimination reaction (Scheme 51). By providing either a base or a Lewis acid catalyst, the activation energy of the dehydroamination was lowered and aniline and diene product **168a** were formed.

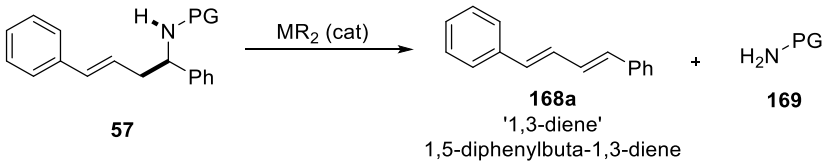

Scheme 51: Dehydroamination side-reaction

Neither of these processes was considered in the initial suggested pathways, which included simplified scenarios for either an initiative or a catalytic reaction mechanism (Figure 6).

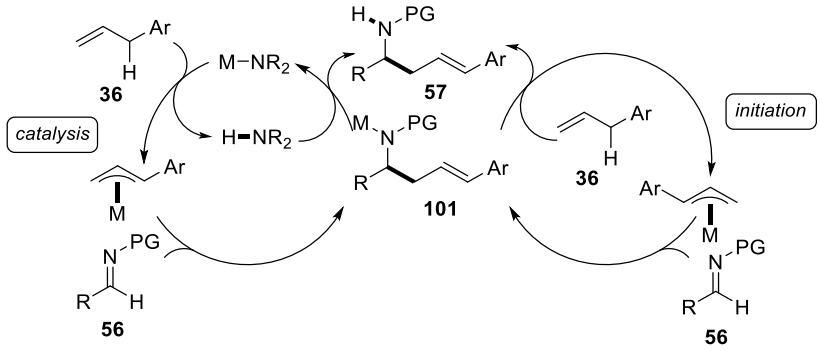

Figure 6: Proposed mechanisms

In the catalytic cycle, allylbenzene was deprotonated by the metal amide, resulting in a secondary amine and an allyl–metal intermediate. This nucleophile could add to imines to give product base **101**, a key intermediate in any mechanism, which would then deprotonate the amine to regenerate the catalyst. Alternatively, an initiative pathway was considered, where product base **101** would deprotonate further allylbenzene to give product **57** and regenerate the reactive allyl-metal intermediate. Both pathways were considered likely and a possible mixture of both pathways simultaneously was also considered. One major source of information was provided by the use of catalytic amounts of alkyllithium reagents, giving product **57** in >60% yield. As mentioned, no catalytic pathway was possible for these bases, as the deprotonation of the catalyst's conjugate acid (R–H) was not possible. This result showed that an initiative pathway was possible. For the development of an asymmetric cinnamylation reaction using allylbenzene (**36**), it was therefore concluded that asymmetric induction from a metal centre was more promising than from the amide, as the metallated species were dominant in at least one possible reaction intermediate involved in the stereodetermining step. Chiral metal environments are usually achieved by coordination with asymmetric donor ligands, which was the focus of the development of the asymmetric cinnamylation of imines (Scheme 59, p 70). In order to attempt to differentiate between the two reaction pathways, preliminary initial rates were monitored. It was assumed that the initiative pathway would display a very distinct reaction profile compared to the catalytic

reaction. To this end, reactions were initially performed at varying catalyst loadings and monitored at specific time intervals over 2-5 h (Table 22). The same experiments were then carried out in the presence of either HMDS amine **94** or reaction product **57m** additive (10-100 mol%) for comparison. Product yields (**57b**) were recorded after 4 h in order to compare results from different reactions at a specific time point.

Table 22: Additive effect on yield

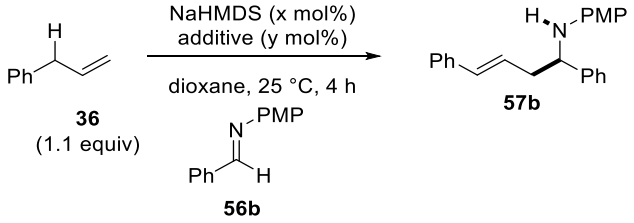

Entry	x (mol%)	Additive (y mol%)	Conv (4 h, %)
1	20	/	78
2	10	/	33
3	5	/	10
4	10	Product **57m** (10)	42
5	10	HMDS (10)	22
6	10	HMDS (100)	6

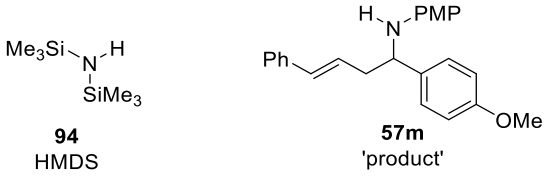

[a] The yield was determined by ^{1}H NMR spectroscopy of a reaction aliquot; internal standard: dibenzyl ether (25 mol%). [b] NR = no reaction; the desired product was not detectable, only starting materials were detected (^{1}H NMR analysis of a reaction aliquot).

The reaction yield after 4 h decreased with decreased catalyst loadings (and hence catalyst concentrations). These reactions showed the relevance of at least one element of the catalyst to the overall rate of the reaction (entries 1-3). The addition of either HMDS (**94**) or product **57m** at the start of the reaction lead to a change on product yield after 4 h in all cases (entries 4-6). In the presence of 10 mol% product **57m** (1 equiv w.r.t. the catalyst), the reaction yield increased from 33% to 42%. The addition of the same amount of HMDS amine lead to a decrease of product yield to 22%. This effect was even stronger when using 100 mol% amine (10 equiv with respect to the catalyst), where only 6% yield was obtained.

When looking at the initial rates of the reaction within the first 5 h of the reaction, more detailed reaction profiles could be analysed (Chart 2). The reaction using 20 mol% NaHMDS showed a steep rise of product yield from the first collected data point. For the

reactions using lower catalyst loadings, a more complicated picture was drawn, where the rate increased over the course of time and a steep rise was only observed after an initial induction period. This induction period was removed when product **57m** was added to the reaction mixture and new product was formed quickly after the start of the reaction. Interestingly, the rate of product formation was similar to the rate observed after the induction period for the additive-free reaction. In the presence of HMDS amine, the rate was considerably decreased when using 100 mol% additive, but the effect was already visible when using only 10 mol% amine.

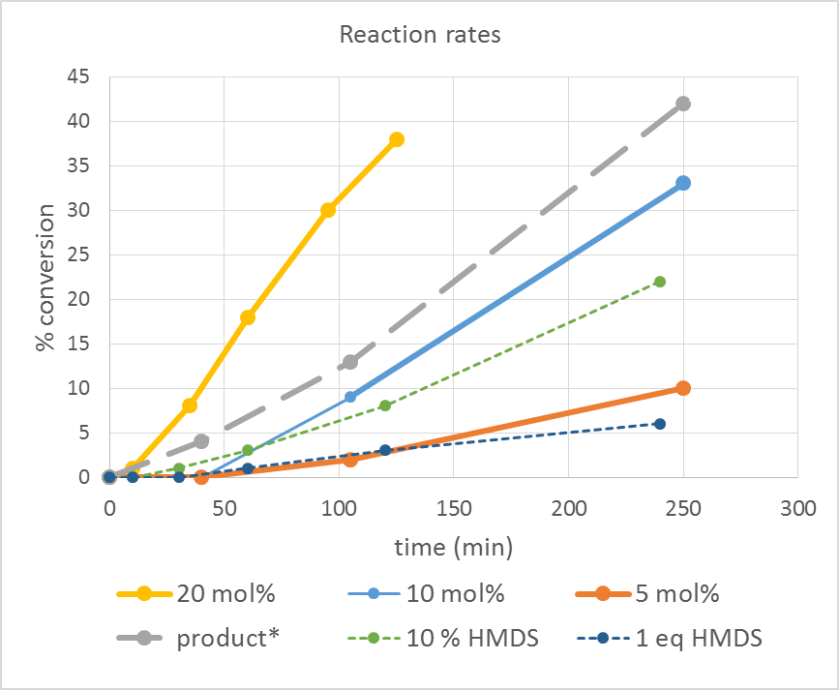

Chart 2: Initial rates of different catalyst loadings (top) or using 10 mol% catalyst together with the specified additives (bottom)

* 10 mol% of product **57m** was used as an additive

The presence of an induction period supported the possibility of an initiative pathway, where the product base formed slowly at the start of the reaction, but as its concentration increased over time, the reaction rate to give product **57b** increased. The presence of HMDS amine decreased the rate of allylbenzene deprotonation as the rate of allylbenzene reprotonation was increased. When product **57m** was added to the reaction, the concentration of product base was assumed to be high from the start of the reaction, leading to a shorter induction period. However, this removal of induction period depended on the efficiency of product **57m** deprotonation by the catalyst. As mentioned before, other off-cycle mechanisms could also lead to the observation of an induction period, such as a possible required attack of the metal amide to the imine, generating the catalytically active amide adduct.

In order to investigate the possibility of a deprotonation of the product by the catalyst, stoichiometric deprotonations were carried out between MHMDS and product **57m** (Scheme 52). Due to the lack of pK_a value data for the product amine, no precise prediction could be made about the relative acidity of amine **57m** and HMDS. Comparing the HMDS pK_a value (~ 30, DMSO)[37] to aniline (~30.6, DMSO),[37] it was assumed that alkylated anisidine should be less acidic than HMDS and therefore the equilibrium of the deprotonation of product **57m** with NaHMDS should lie on the left hand side. Here, the forward reaction mimicked the reaction for the use of product **57m** as an additive, while the reverse reaction represented the catalyst regeneration step in the *catalysis* cycle.

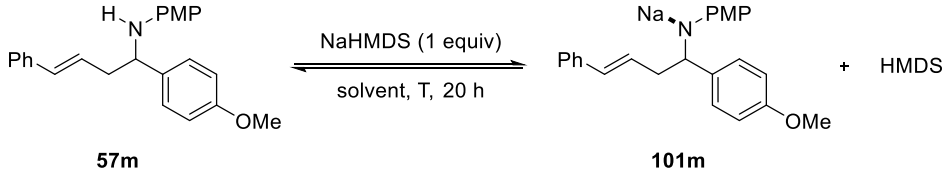

57m **101m**

Scheme 52: Product deprotonation

Of course, the nature of the equilibrium was affected by other factors such as temperature and solvent. Therefore, reactions were carried out in different polar aprotic solvents and ^{1}H NMR spectroscopy in C_6D_6 was used for the detection of potential reaction products (Table 23). Surprisingly, instead of finding evidence for metallated species **101m**, different signals were found. These signals corresponded to previously identified products β-methylstyrene (**58**), imine **56m** and dehydroamination product **168m**.

Table 23: Product deprotonation

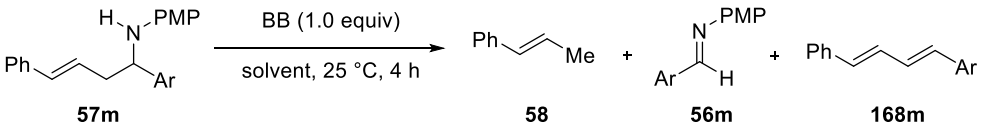

57m **58** **56m** **168m**

Ar = 4-C_6H_4OMe

Entry	BB	Solvent	Conv 58 and 56m(%)[a]	Conv 168m (%)[a]
1	NaHMDS	dioxane	50	0
2		THF	25	75
3		DMF	10	90
4		MeCN	*NR*[b]	-
5	NaH	THF	10	0
6		DMF	100	0

[a] The conversion was determined by ^{1}H NMR spectroscopy of a reaction aliquot; internal standard: dibenzyl ether (25 mol%). [b] NR = no reaction; the desired product was not detectable, only starting materials were detected (^{1}H NMR analysis of a reaction aliquot).

In dioxane, a 50% conversion to products **58** and **56m** was observed, while dehydroamination product **168m** was not observed (entry 1). This outcome changed when the reaction was carried out in THF, where a full conversion was observed in a ratio of 1:4 in favour of dehydroamination product **168m** (entry 2). This selectivity was further increased to 1:9 for product **168m** when the reaction was conducted in DMF. In MeCN, a reaction was not observed, suggesting that deprotonation of acetonitrile lead to the formation of unreactive intermediates.

As these reactions showed a different outcome than expected, deprotonations were also carried out using sodium hydride. This base did not show any dehydroamination occurring in either THF or DMF, but showed selective formation of products **58** and **56m** (entries 4 and 5). The reaction mechanism for the BB activation of product **57m** was assumed to occur via the product base that formed in the equilibrium with the BB. This equilibrium was then shifted towards the right by the decomposition of the product base to imine **56m** and allyl-metal intermediate **100**, which is known to undergo protonation at the γ-position, giving styrene product **58** (Scheme 53). It was therefore found that the retro-allylation was also mediated by the addition of NaHMDS. Indeed, reactions of allylbenzene (**36**) with imine **56b** catalysed by increased loadings (50-100 mol%) of NaHMDS gave significantly lower product yields and increased levels of isomerisation.

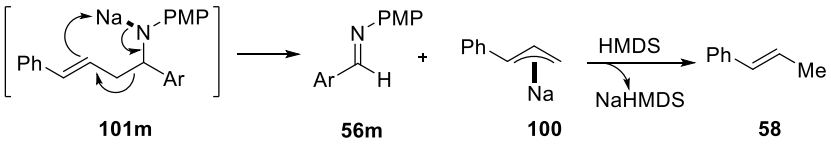

Scheme 53: Proposed mechanism for retro C–C

In contrast to the retro-allylation, the dehydroamination product formed different reaction products that had not been observed in the NaHMDS-catalysed cinnamylation reaction. However, a plausible reaction mechanism would suggest the base-catalysed elimination of anilide **170** that formed anisidine (**169b**) while regenerating the metal amide (Scheme 54).

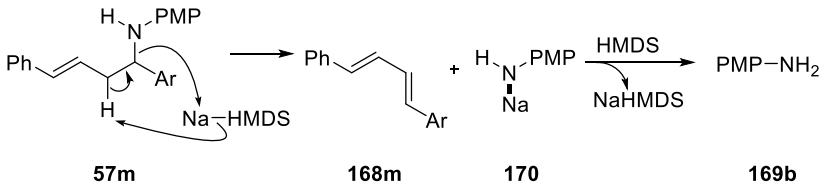

Scheme 54: Proposed mechanism for dehydroamination

In order to test the deprotonation of product **57m** with NaHMDS without the possibility of decomposition reactions of the product base, the use of a product analogue was considered.

The retro-allylation reaction was favoured by the relatively high stability of the allylic anion (**100**). Furthermore, the presence of acidic protons β-position to the amine allowed for the dehydroamination to occur. Both of these pathways were assumed to be blocked by the removal of the allyl group, giving secondary amines substituted by one aryl and one benzyl group. These products could be easily accessed in a one-step reduction of the corresponding benzaldimines using $NaBH_4$ (Scheme 55).

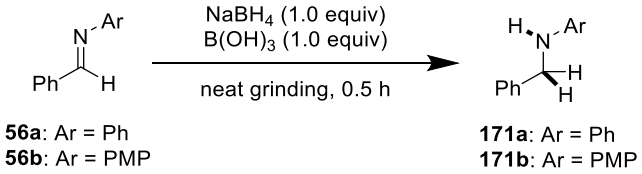

Scheme 55: Reduction of imines to secondary amines

The products of the reduction of *N*-PMP- and *N*-Ph-protected imines **56b** and **56a** gave amines **171b** and **171a**. These amines were used for the deprotonation with NaHMDS as well as NaH for comparison (Scheme 56).

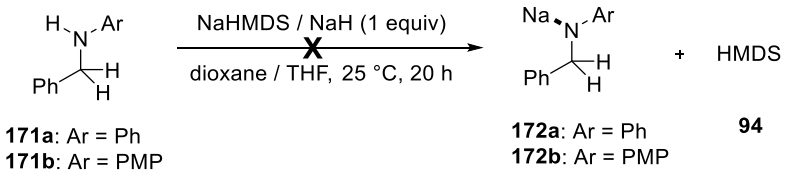

Scheme 56: Secondary aniline deprotonation

Neither of the two substrates showed any decomposition by ^1H NMR spectroscopy ($CDCl_3$). The reactions were then monitored in C_6D_6, but no change in either ^1H or ^{13}C NMR suggested the formation of metallated species **172a-b** or protonated HMDS (**94**). This meant that the product mimics **171a-b** were less acidic than HMDS and that the equilibrium of the reaction of **171a-b** with NaHMDS would lie on the left hand side. Therefore, a pKa value of >30 was assumed not only for amines **171a-b**, but also for product **57**.

With the product mimics **171a-b** in hand, further reactions were carried out where different amines were added to the NaHMDS-catalysed reaction between allylbenzene (**36**) and imine **57m** as additives (10-30 mol%; Table 24). Besides the secondary anilines, substituted primary anilines were also investigated, as some of their pK_a values were found to be in the same area of HMDS.

Table 24: Addition of anilines

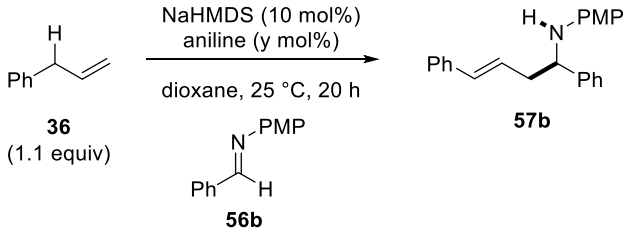

Entry	Aniline (y mol%)	Conv (%)
1	-	98
2	**171a** (10)	91
3	**171b** (30)	88
4	**169b** (10–30)	83–90
5	**169a** (10)	62
6	**173** (30)	60
7	**174** (30)	10
8	**175** (30)	*NR*[b]
9	**176** (30)	*NR*[b]

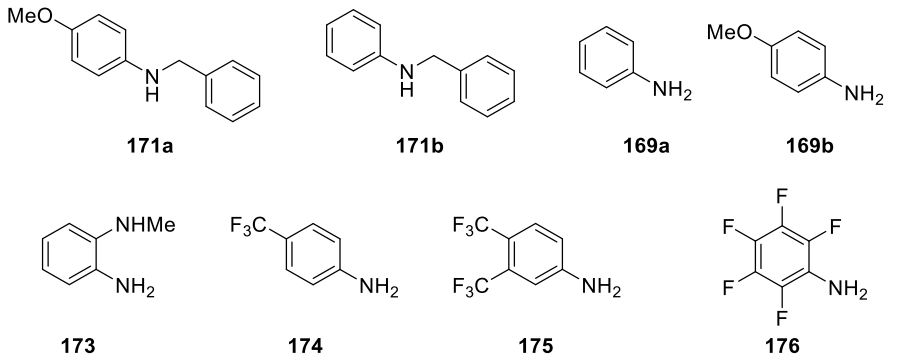

[a] The conversion was determined by ^{1}H NMR spectroscopy of a reaction aliquot; internal standard: dibenzyl ether (25 mol%). [b] NR = no reaction; the desired product was not detectable, only starting materials were detected (^{1}H NMR analysis of a reaction aliquot).

The addition of secondary amines **171a** or **171b** showed little effect on the reactivity compared to the additive-free reaction (98%, entry 1), and product yields of 88–91% were obtained (entries 2 and 3). When anisidine (**169b**; PMP-substituted aniline) was used, a similar observation was made and product yields of 83–90% were observed (entry 4). Using unsubstituted aniline (**169a**) as an additive gave a moderate product yield (62%), suggesting an interaction between the catalyst and the additive (entry 5). Similar conclusions were drawn for the 2-NHMe-substituted aniline (**173**), where a yield of 60% was observed (entry 6). When moving to electron-poor anilines, the effect on the yield was even more pronounced. 4-CF_3-substituted aniline **174** showed a product yield of only 10%, while 3,4-di-CF_3-substituted aniline **175**, as well as perfluorinated aniline **176** showed no reactivity. This trend in reactivity can be rationalised by looking at the pK_a values of the different

anilines (Figure 7). While aniline was found to have a pK_a value of ca. 30.6 (DMSO),[37] substitution effects of electron-withdrawing groups showed significantly lower pK_a values. Substitution effect with electron-donating groups has not been reported except for 2-MeO-substitution, giving a very similar pK_a value to aniline (30.5, DMSO).[37] In this substrate, the electron donating properties were assumed to be balanced by the inductive withdrawal from the oxygen atom in *ortho*-position. Also, H-bonding effects had to be considered. Therefore, it was assumed that *p*-anisidine had a much increased pK_a value compared to aniline. For all anilines with a pK_a value equal to or lower than aniline, a lack of product formation was observed in the cinnamylation reaction, suggesting a catalyst deactivation by formation of an unreactive sodium anilide species. The fact that *p*-anisidine was tolerated in this reaction suggested that no deprotonation of this aniline derivative was possible and therefore the reaction with allylbenzene could proceed in the expected fashion.

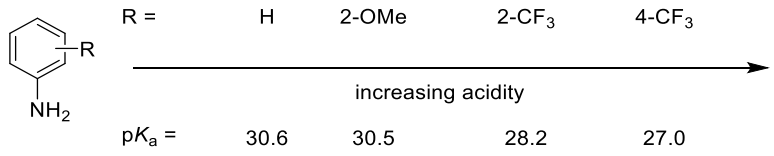

Figure 7: pK_a values of different anilines

These observations lead to the assumption that catalysis with alkali metal anilides could also be possible. As their pK_a values are highly dependent on the substitution pattern, these compounds would be versatile in their application. Alkali metal anilides have been prepared and studied with regards to their structures.[66] More recently, the catalytic use of this class of amides has beem reported in a hydroamination-carbocyclisation cascade reaction.[67] However, further catalytic applications in C–C bond formations have not been explored.

One interesting observation in the reaction with 30 mol% aniline was made, where a different homoallylic amine product was found in small quantities. Upon careful comparison of product ^{1}H NMR spectra of the isolated products, this homoallylic amine product was identified as **57a**, arising from the cinnamylation of *N*-Ph-protected iminie **56a** (Scheme 57).

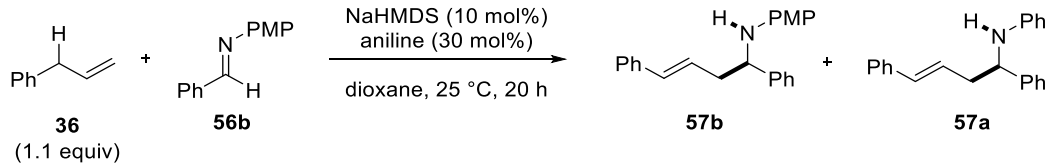

Scheme 57: Side-product formation for the reaction with aniline

Based on the examination of pK_a values for aniline and HMDS, it was assumed that product **57a** did not form upon dehydroamination of *p*-anisidine, followed by hydroamination of

aniline. Instead, the cinnamylation of *in situ* generated *N*-Ph-protected benzaldimine was postulated (Scheme 58). As suggested by the pK_a of NaHMDS and aniline, the catalyst first deprotonated aniline **169a** to give Na-anilide **170a** and HMDS amine. This anilide then reacted with PMP-imine **56b** in a transimination reaction, giving *N*-Ph-imine **56a** and PMP-anilide **170b** as products. Despite the PMP-anilide being a poorer leaving group than the Ph-anilide, the equilibrium is shifted by the fast protonation of PMP-anilide **170b** with HMDS, which is more acidic based on pK_a values. Thus, the catalyst was regenerated and used to catalyse the reaction between the *N*-Ph-imine, as well as the remaining *N*-PMP-imine, that did not undergo transimination. As shown previously, the presence of *p*-anisidine (**169b**) in this process did not interfere with the cinnamylation reaction.

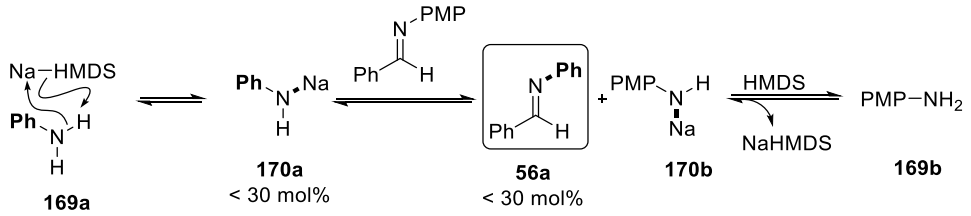

Scheme 58: Proposed mechanisms for side-product formation

The use of strong bases as catalysts in the cinnamylation of imine **56**, as well as preliminary data on the reaction rates suggest that an initiative pathway is accessible when forming product **57**. Stoichiometric deprotonations using a product mimic showed that the *in situ* generated product bases should be more basic than the catalyst's conjugate acids, suggesting that a catalytic pathway would be favoured. Retro-allylation as well as the dehydroamination were found to be mediated by NaHMDS. This result demonstrated the advantage of the catalytic use of alkali metal amides that displayed improved conditions to the stoichiometric variant of this reaction. Finally, the addition of anilines to the reaction mixture gave insights into the basicity of the product base, which was found to lie between aniline and *p*-ansidine (pKa >30.6). Due to their high basicity, reaction intermediates could not be detected using ^{1}H NMR or mass spectroscopy. This detection would be of high value for the elucidation of vital intermediates that could then be used to develop asymmetric cinnamylation of imines using enantiopure alkali metal amide catalysts.

2.3.1.8 Other Work in the Group

*During the course of the investigation, an asymmetric variant of the reaction between allylbenzene and imine **56j** was developed in the group by Wei Bao*. In order to investigate the effect of a chiral ligand on the alkali metal amide catalyst, a ligand screening was performed. This screening showed that crown ethers, carbene ligands as well as bisoxazoline ligands all had an accelerating effect on the formation of product **57**. All of these ligands were available in the group in their enantiomerically enriched forms so a screening of these ligands was next performed in dioxane. Yields were generally good, but induction of enantioselectivity was poor in all of these reactions. It was assumed that the coordination of the chiral ligand was competing with solvent coordination to the metal centre, which lead to insufficient enantiodifferentiation. Therefore, the reaction was performed in apolar solvents which have previously shown no reaction of allylbenzene with imine **57**. Reactions carried out in apolar aromatic solvents resulted in much better enantioselectivities. After optimisation on the imine (providing better separation by analytical chiral HPLC), product **57j** was isolated with an optical enrichment of 46% *ee*. when using a chiral bisoxazoline ligand in *m*-xylene (Scheme 59).

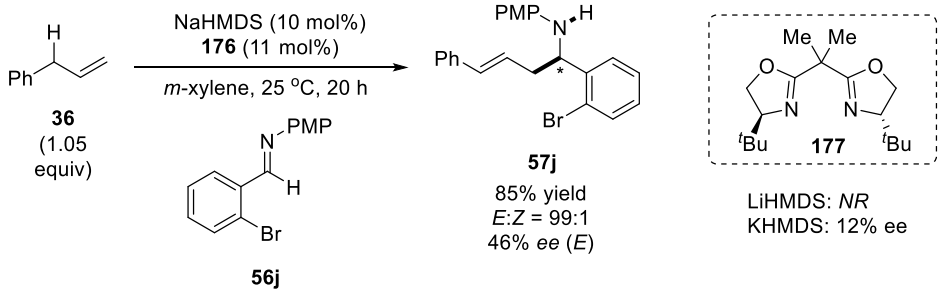

Scheme 59: Enantioselective cinnamylation using a BOX* ligand

No product formed when the same reaction was carried out using LHMDS as the catalyst. For the use of KHMDS, the yield was slightly reduced and the enantioselectivity was only 12% *ee*, showing that the sodium catalyst again proved to be the most effective catalyst among the alkali metal amides. Further studies using the alkaline earth metal amides showed a lack of reactivity for all catalysts as suggested by the initial catalyst screening. These catalysts were assumed to be more suitable for asymmetric induction as coordination to these metals was assumed to be more efficient. Further studies in this field, or by using different enantiopure ligands, are required for obtaining synthetically useful results in the enantioselective cinnamylation of imines with allylbenzenes using Brønsted base catalysts.

2.3.2 Isomerisation

As mentioned before, when conducting the C–C bond formation between allylbenzene (**36**) and aldimines **56**, β-methylstyrene (**58**) was formed as a side-product resulting from isomerisation of allylbenzene (Scheme 60). For this newly developed catalytic method discussed in the previous chapter, the isomerisation was undesired, because once formed, the styrene product **58** could not be activated for C–C bond formation under the employed conditions. Therefore, an excess of pro-nucleophile was usually used to ensure complete consumption of the imine. Also, the catalytic system was optimised so that the rate of the C–C bond formation was enhanced and the rate of the isomerisation was decreased. It is worth noting, however, that the styrene side-product should not be considered as a waste product because this type of compound may be used in many different bond-transforming processes. In addition, the development of a method for the catalytic isomerisation of allylbenzenes is non-trivial.

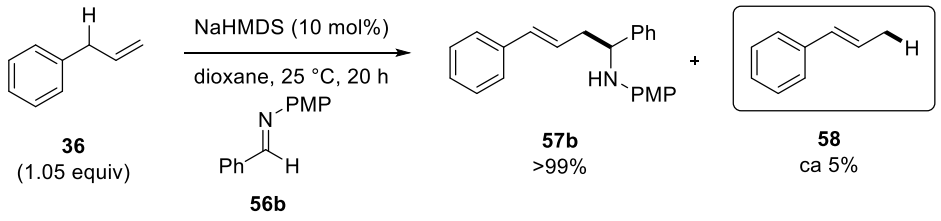

36 (1.05 equiv)

56b

57b >99%

58 ca 5%

Scheme 60: Isomerisation as side-reaction in C–C bond formations

One way to demonstrate the purpose of the isomerisation is to compare the commercial prices for allylbenzene and the two geometric isomers of the corresponding styrene products (Scheme 61). Allylbenzene is commercially available from Sigma-Aldrich in large quantities (100 mL) and high purity (>98%). (*E*)-β-methylstyrene can also be purchased from Sigma-Aldrich, but the cost per gram is almost 10 times higher than allylbenzene. This may seem counterintuitive, because the double bond in the isomerised product is conjugated to the aromatic ring and is therefore thermodynamically more stable. One aspect that needs to be considered here is that β-methylstyrene exists as a mixture of *E*-and *Z*-isomers and the purification of these isomers can be costly.

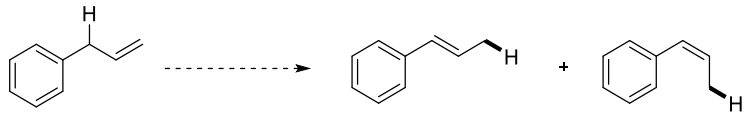

36
allylbenzene
sigma: 1.21 £g^{-1}
TCI: 2.06 $g^{-1}

(*E*)-**58**
E-β-Me-styrene
sigma: 13.8 £g^{-1}
TCI: 17.23 $g^{-1}

(*Z*)-**58**
Z-β-Me-styrene
sigma: NA
TCI: 26.32 $g^{-1}

Scheme 61: Price comparison between allylbenzene and styrene produtcs

This aspect becomes even more relevant when looking at (*Z*)-β-methylstyrene. This compound cannot be obtained from usual suppliers in the UK, but a comparison of the prices from TCI shows that this isomer is 50% more expensive than its *E*-isomer. Generally speaking, allylbenzenes are cheaper because they are easier to purify. Indeed, they do not exhibit geometric isomers and are less likely to undergo oligo- or polymerisation reactions, which also simplifies storage. For all these reasons, many processes have been developed in the field of isomerisation of allylbenzenes and other terminal olefins in general.[68]

With its relatively low pK_a value of ca. 34 (DMSO), allylbenzene has been shown to be isomerised using base catalysts (Scheme 62).[68-69] Both metal hydroxides and alkoxides have been identified as catalysts for this transformation.[70] However, several drawbacks for these processes have been identified. When using inorganic bases, such as metal hydroxides, their low solubility in organic solvents poses a challenge. Efforts have been made to develop phase-transfer-catalysed reactions at high temperatures using water as a co-solvent.[71] However, large amounts of a base were typically required and *E:Z* selectivities of the obtained styrene products were around 19:1.

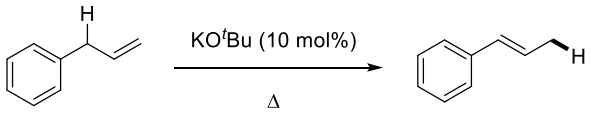

36 **58**

Scheme 62: Base-catalysed isomerisation of allylbenzene

Further developments in the organocatalytic isomerisation of double bonds have been achieved, where the use of a Verkade base has successfully isomerised activated allylic substrates with good to excellent *E:Z* selectivities (Scheme 63).[72]

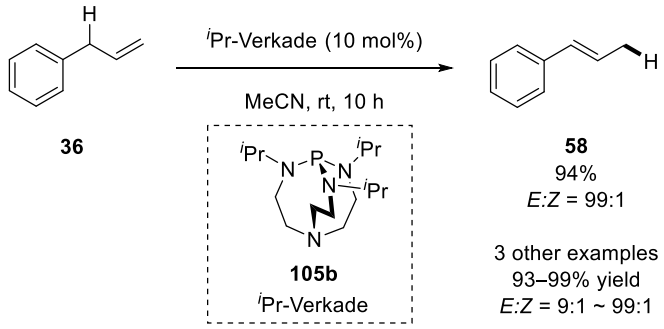

Scheme 63: Organocatalytic isomerisation of allylbenzene

Alternative methods for the formation of styrenes are provided by the use of transition metal catalysts (Scheme 64).[68] These are often very selective processes and their scope outperforms base-catalysed processes. In addition, even unactivated alkenes were succesfully isomerised. Classic examples for these methods include palladium[73], rhodium[74], platinum[75] and ruthenium[76] catalysis. However, the use of expensive and/or toxic metal catalysts that often require expensive ligands may be undesired and more environmentally benign processes are of interest. Recently, iron-catalysed isomerisation reactions have received attention, where the transition metal catalyst was readily available and non-toxic.[77]

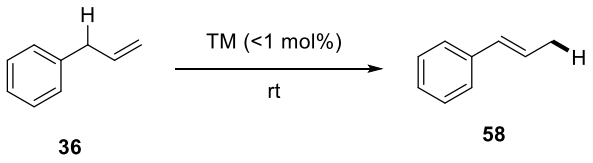

Scheme 64: TM-catalysed isomerisation of allylbenzene

In our system, **58** was observed as a side-product in a C–C bond formation, suggesting that the same metal amide could also act as a catalyst for the isomerisation reaction. This concept was investigated when carrying out the experiment in the absence of an electrophile. When allylbenzene was reacted with a catalytic amount of NaHMDS in dioxane at 25 °C for 20 h, a mixture of *E*-and Z-styrenes was obtained (Scheme 65).

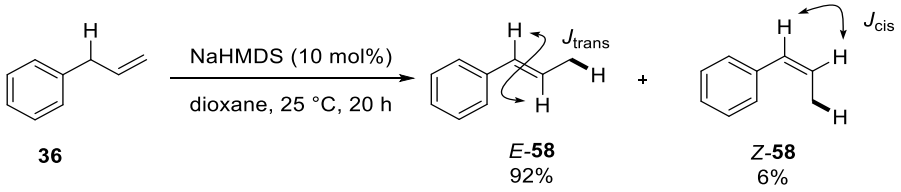

Scheme 65: Metal amide-catalysed isomerisation of allylbenzene

The ^{1}H NMR spectrum of the reaction aliquot showed clear signals for *E*-**58** of the internal alkene (δ = 6.4 and 6.2 ppm, 1H each, dq, J_{trans} = 15.8 Hz).[77a] *Z*-**58** could also be detected and quantified by integration of the β-H (δ = 5.8 ppm, 1H, dq, J_{cis} = 11.5 Hz). None of these signals overlapped with any of the signals from the starting material (**36**) (internal alkenyl signal at δ = 6.0 ppm). Thus this method was used for the analysis of all following isomerisation results. Dibenzylether was added as an internal standard to ensure conservation of the mass balance of the reaction. When product isolations were attempted, the use of this internal standard was omitted.

2.3.2.1 Unfunctionalised Isomerisation - Optimisation

In contrast to the previous C–C bond forming reaction, the major challenge regarding the selectivity in this reaction was posed by the two geometric isomers that formed during the isomerisation. Optimisations regarding the catalyst and the solvent, as well as the temperature and ligands were required. With the confirmation of the catalytic activity of the metal amides in hand, a catalyst screening of all available metal amides was performed in both dioxane and THF, which had previously shown higher levels of isomerisation in the C–C bond formation study (Table 25).

Table 25: Metal amide catalyst screening for the isomerisation of allylbenzene

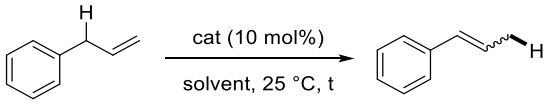

36 **58**

Entry	Catalyst	Solvent	t (h)	Yield (%)[a]	*E:Z* ratio
1	LDA	dioxane	1	25	*nd*
2	LHMDS	dioxane	1	*NR*[b]	-
3	NaHMDS	dioxane	1	16	*nd*
4	KHMDS	dioxane	1	99	15:1
5	LDA	THF	1	28	15:1
6	LHMDS	THF	1	4	*nd*
7	NaHMDS	THF	1.5	16	24:1
8	KHMDS	THF	1	99	15:1

[a] The yield was determined by ^{1}H NMR spectroscopy of a reaction aliquot; internal standard: dibenzyl ether (25 mol%). [b] NR = no reaction; the desired product was not detectable, only starting materials were detected (^{1}H NMR analysis of a reaction aliquot). *nd* = not determined due to unreliable integration of the *Z*-signals.

The reaction time for the isomerisation was decreased to 1 h in most cases in order to be able to better quantify the reactivity differences among the corresponding catalysts. In dioxane,

all lithium and sodium amides showed low or no reactivity for the isomerisation of allylbenzene (entries 1-3). The potassium salt was the only catalyst that showed very high activity, displaying a complete conversion to the product with an *E:Z* ratio of 15:1 (entry 4). Similar results were obtained in THF, where none of the lithium or sodium amides were particularly active after short reaction times (entries 5-7). Like in dioxane, KHMDS was able to isomerise allylbenzene in THF quantitatively with the same geometric selectivity (entry 8). This selectivity is comparable to other organocatalytic processes, but does not compare well to transition metal catalysts where selectivities of 99:1 are often achieved.[76c, 77b]

Other strong bases were also used for the isomerisation of allylbenzene in dioxane and THF. Both metal hydrides and alkyllithium reagents were used in catalytic amounts for the isomerisation reaction (Table 26).

Table 26: Metal hydrides and alkyllithiums in the isomerisation of allylbenzene

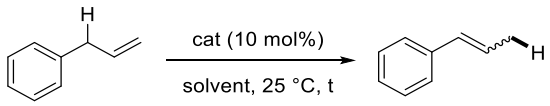

36 **58**

Entry	Catalyst	Solvent	t (h)	Yield (%)[a]	*E:Z* ratio
1	LiH	dioxane	20	*NR*[b]	-
2	NaH	dioxane	18	*NR*[b]	-
3	KH	dioxane	1	88	9:1
4	LiH	THF	20	*NR*[b]	-
5	NaH	THF	18	22	9:1
6	KH	THF	1	99	9:1
7	LiMe (1.6M in Et_2O)	THF	20	13	9:1
8	LiBu (1.6M in hexanes)	THF	24	3	*nd*
9	LiBu (2.5M in hexanes)	THF	24	9	*nd*

[a] The yield was determined by ^{1}H NMR spectroscopy of a reaction aliquot; internal standard: dibenzyl ether (25 mol%). [b] NR = no reaction; the desired product was not detectable, only starting materials were detected (^{1}H NMR analysis of a reaction aliquot).

Metal hydrides are usually commercially available as stabilised suspensions in paraffin oil to prevent hydrolysis through moisture in the air. However, the use of non-stabilised metal hydrides is possible in an inert atmosphere. The three available alkali metal hydrides (Li, Na, K) were used as catalysts in dioxane (entries 1-3). No products could be detected for the reaction with LiH and NaH, but the use of KH provided the desired product in 88% NMR yield, albeit with a lower *E:Z* ratio (9:1) compared with KHMDS (15:1). The same reactions carried out in THF showed slightly increased reactivities for both NaH and KH, but no reaction for LiH (entries 4-6). Also in this solvent, selectivities proved to be lower than those for KHMDS. Finally, alkyllithium reagents were screened in THF (entries 7-9). Both MeLi

and BuLi furnished the styrene product, but only in low yields with no improvement in geometric selectivity. Interestingly, these results already gave a first insight into the mechanistic features of this isomerisation as the conjugate acids of the employed catalysts (H–H or R–H) are not expected to be involved after initial allylic deprotonation of the substrate. This data suggested that an initiative pathway was conceivable for the isomerisation of allylbenzenes.

In order to compare the results of the metal amide catalysis to the reported organocatalysis,[72] a final catalyst screening was performed (Table 27). Here, different organobases and organosuperbases were used in the isomerisation of allylbenzene in THF at 25 °C for 24 h.

Table 27: Organocatalytic isomerisation of allylbenzene

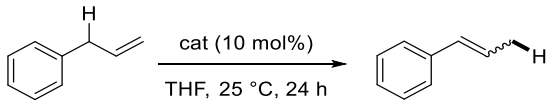

36 **58**

Entry	Catalyst	Yield (%)[a]	*E*:*Z* ratio
1	KHMDS	99	15:1
2	**102a**	*NR*[b]	-
3	**103a**	*NR*[b]	-
4	**104**	65	19:1
5	**105a**	*NR*[b]	-
6	**105b**	*NR*[b]	-
7	**105c**	*NR*[b]	-
8	DBU	*NR*[b]	-
9	**179**	*NR*[b]	-

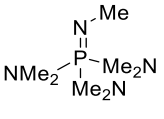

102a
Me-P_1
Schwesinger

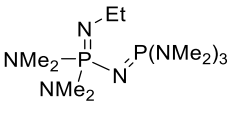

103a
Et-P_2
Schwesinger

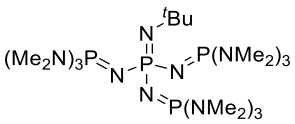

104
^{t}Bu-P_4
Schwesinger

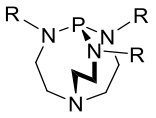

105a: R = Me
105b: R = ^{i}Pr
105c: R = ^{i}Bu
R-Verkade

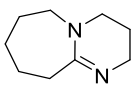

178

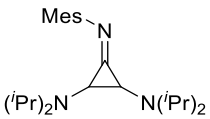

179
BAC-NMes

[a] The yield was determined by ^{1}H NMR spectroscopy of a reaction aliquot; internal standard: dibenzyl ether (25 mol%). [b] NR = no reaction; the desired product was not detectable, only starting materials were detected (^{1}H NMR analysis of a reaction aliquot).

Among the different organocatalysts, only one base proved to isomerise allylbenzene (65% NMR yield, *E:Z* = 19:1, entry 4). The Schwesinger organosuperbases[55a] are known to be highly basic, but here only the P_4-base was able to catalyse this transformation with an *E:Z* selectivity of 19:1. The poor performance of the Verkade bases was surprising (entries 5-7), as these catalysts have been demonstrated to be active in acetonitrile.[72] When the same catalysts were used in MeCN instead of THF, both the ^{i}Pr- and the ^{i}Bu-derivatives showed a high activity for the formation of styrene product **58**. This is in agreement with the proposed mode of action, where the organosuperbase **105** would first deprotonate acetonitrile (Scheme 66). The 'naked' acetonitrile anion would then be basic enough to deprotonate the allylic substrates. In the reactions performed in THF, this process was not possible, leading to a lack of reactivity for these bases.

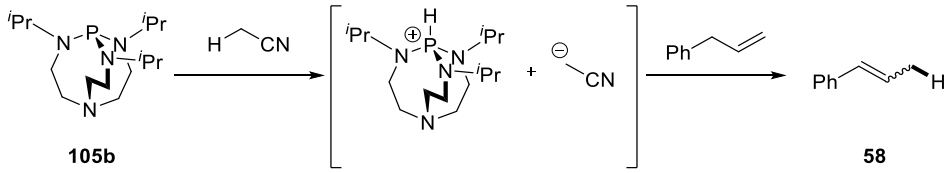

Scheme 66: Verkade base-catalysed isomerization of allylbenzene in MeCN

Overall, the different catalyst screenings provided insightful information for the optimisation of the isomerisation reaction. The most active catalyst for this reaction was shown to be KHMDS, which was significantly more reactive than other metal amides or organobases and provided high *E:Z* ratios. THF was identified as a good solvent because it showed high reactivities and selectivities.

Catalyst Loading

Next, the catalyst loading was optimised for the KHMDS-catalysed isomerisation of allylbenzene (Table 28). THF was chosen as the solvent as reactions proved to be generally faster. Experiments were carried out at 25 °C, providing the mildest and most applicable conditions. Catalyst loadings of 10-0.1 mol% were used to isomerise the terminal double bond of **36**.

Table 28: Catalyst loading for the isomerisation of allylbenzene

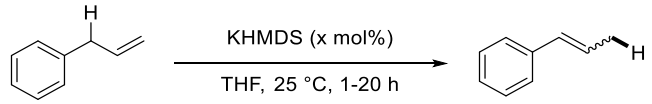

36 **58**

Entry	x mol%	t (h)	Yield (%)[a]	*E:Z* ratio	TON	TOF (h^{-1})
1	10	0.5	99	15:1	10	20
2	10	20	99	15:1	10	0.5
3	5	0.5	99	13:1	20	40
4	2	0.5	94	13:1	47	94
5	1	0.5	85	13:1	85	170
6	0.5	0.5	14	10:1	28	56
7	0.1	0.5	*NR*[b]	-	-	-

[a] The yield was determined by ^{1}H NMR spectroscopy of a reaction aliquot; internal standard: dibenzyl ether (25 mol%). [b] NR = no reaction; the desired product was not detectable, only starting materials were detected (^{1}H NMR analysis of a reaction aliquot).

First, the effect of the reaction time on the *E:Z* selectivity was investigated (entries 1 and 2). These reactions showed that no erosion of selectivity occurred even at prolonged reaction times. For the reaction using 10 mol%, a turnover number of 10 and a turnover frequency of up to 20 $h^{-1}$was obtained (entry 1). Next, the catalyst loading was successively decreased and yields were recorded after only 30 min (entries 3-7). The substrate concentration was kept constant across these experiments, which meant that the catalyst concentration was decreased accordingly. Therefore, a decrease in the reaction rate was expected when lowering the catalyst loading, leading to lower yields after a given reaction time. Indeed, a lower yield was observed when the catalyst loading was decreased to 1 mol% where <90% yield was recorded (entry 5). This reaction showed the highest turnover number (85) and turnover frequency (170 h^{-1}). When the loading was further decreased, the yield dropped significantly and at 0.1 mol% catalyst loading, no reaction was observed after 30 min (entry 7).

In order to be able to control the geometrical outcome of the double bond, the different allylic binding modes needed to be analysed. Upon deprotonation of the allylic C–H bond, an allyl metal intermediate may form, which can exist in different isomeric forms (Scheme 67). These binding modes can all be summarised as the allyl–M complex, but the equilibrium between the different species governs the geometric outcome of the olefin.

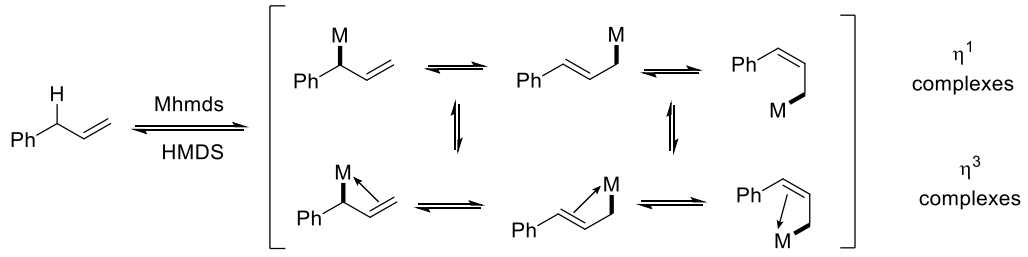

Scheme 67: Binding modes for metallated allylbenzene

The η^1 and the η^3 complexes may both exist as either the *E*- or the *Z*-isomer of the styrenyl product. If protonation occurs in α-position to the metal, the respective amount of the styrenyl–M *Z*-isomer dictates the final amount of protonated *Z*-isomer present. If protonation occurs in the γ-position, the amount of *Z*-isomer present depends on the relative positions of the proton source and the metal in the benzylic position. All other pathways generate the starting material as the product (Figure 8).

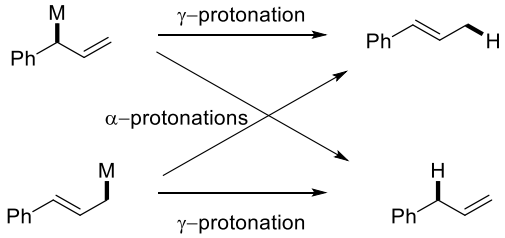

Figure 8: Protonation of different intermediates

Changing the nature of the allyl metal intermediate was assumed to be the best way to increase the *E*-selectivity. Changing the nature of the metal has not proven to be successful in the catalyst screenings. As an alternative, a ligand may be used for the coordination to the metal centre (Scheme 68). For alkali metals, crown ethers have been known to have large binding affinities, depending on the cavity size. Of course, ethereal solvents may also act as a ligand to the metal centre as shown in the trisolvated potassium ion in dioxane (**181**, right).

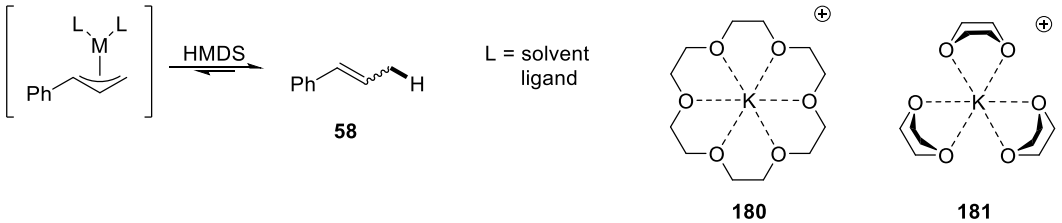

Scheme 68: (Crown-) ether ligation to alkali metals

Ligand Screening

When performing the ligand screening, several factors needed to be considered. Generally speaking, most carbene or diimine based ligands require *in situ* deprotonation of the corresponding precursor before being able to ligate a metal centre. Therefore, two equivalents of base with respect to the ligand were added to the reaction. Different types of ligands were screened in THF and dioxane under the optimised conditions (Table 29).

Table 29: Ligand screening for the alkali metal amide catalyzed isomerisation

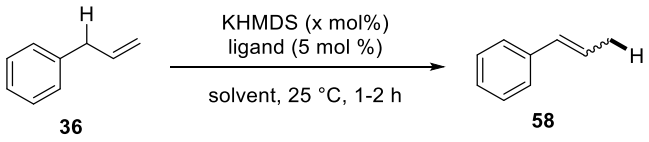

36 **58**

Entry	x mol%	Solvent	Ligand	Yield (%)[a]	*E:Z* ratio
1	5	THF	-	99	15:1
2	10	THF	IMes–HCl	98	24:1
3	10	THF	IPr–HCl	99	19:1
4	10	THF	**184**	96	19:1
5	10	THF	**185**	97	24:1
6	10	THF	Ph-BOX*	95	24:1
7	5	THF	[15]c-5	95	49:1
8	5	THF	[18]c-6	92	99:1
9	5	THF	[DB18]c-6	95	49:1
10	5	dioxane	[15]c-5	91	99:1
11	5	dioxane	[18]c-6	91	99:1
12	5	dioxane	[DB18]c-6	96	19:1

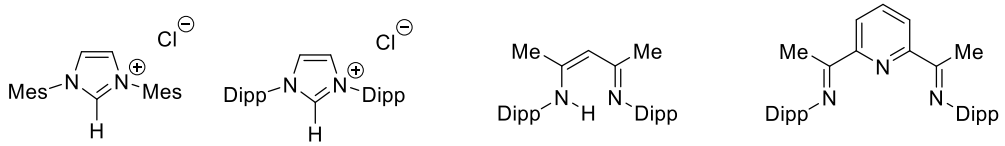

182 IMes–HCl

183 IPr–HCl

184 (Dipp)nacnac–H

185 py-(Dipp)nacnac

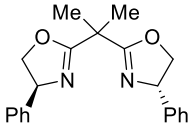

186 Ph-BOX*

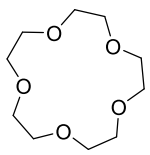

187 [15]c-5

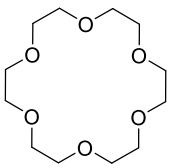

188 [18]c-6

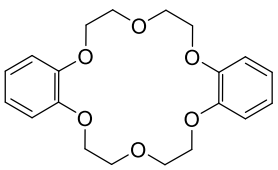

189 [DB18]c-6

[a] The yield was determined by ^{1}H NMR spectroscopy of a reaction aliquot; internal standard: dibenzyl ether (25 mol%). [b] NR = no reaction; the desired product was not detectable, only starting materials were detected (^{1}H NMR analysis of a reaction aliquot).

Two carbene, two diimine and a chiral bisoxazoline ligand were screened in THF (entries 2-6). Here, the base (10 mol%) and the ligand (5 mol%) were pre-stirred in THF for 10 min before the addition of the alkene. All of these reactions gave the styrene product after 2 h in high yields. Unfortunately, only small changes in selectivity could be observed. One problem in these cases could be the incomplete coordination of the ligand to the metal. This could arise from the fact that after deprotonation of the precursor, the free ligand, protonated HMDS and a potassium complex formed. This potassium complex could compete with the relevant allyl–M species for coordination. Therefore, reactions with these protic ligands were not investigated further and attention was directed towards the crown ethers (entries 7-12). Depending on their size, these ligands have different binding affinities for the different alkali metals. Using a 1:1 molar ratio of ligand and KHMDS, reactions were carried out after a short pre-stir time (5 min, entries 7-9). Again, the styrene product was obtained in high yields; gratifyingly, the *E:Z* ratio was significantly improved by the addition of the ligands. For all three crown ethers, selectivies increased and an *E:Z* ratio of up to 99:1 was observed. However, the displayed reaction yields also reflect the mass balance of the reaction, indicating that a small amount of unwanted side-reaction must have been occurring. These side-products could not be detected by ^{1}H NMR spectroscopy. When the same ligands were tested in dioxane as the solvent, similar results were obtained (entries 10-12). While selectivities reached up to 99:1, yields were slightly diminished, but >90% in general. The use of [18]crown-6 proved to be the most effective ligand for the KHMDS-catalysed isomerisation of allylbenzene, but because different metals could have higher affinities for other ligands, different combinations of metals and ligands had to be tested to identify the best catalyst system.

To this end, NaHMDS was chosen as an alternative candidate for the isomerisation of allylbenzene. Reactions were carried out using [18]crown-6 and [15]-crown-5 in both THF and dioxane (Table 30).

Table 30: Different catalyst systems for the isomerisation of allylbenzene

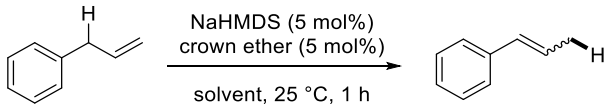

36 **58**

Entry	Crown ether	Solvent	Yield (%)[a]	*E:Z* ratio
1	–	THF	20	24:1
2	[15]c-5	THF	99	32:1
3	[18]c-6	THF	99	49:1
4	–	dioxane	7	n.d.
5	[15]c-5	dioxane	91	24:1
6	[18]c-6	dioxane	91	19:1

[a] The yield was determined by ^{1}H NMR spectroscopy of a reaction aliquot; internal standard: dibenzyl ether (25 mol%).

For NaHMDS, a significant enhancement of the reactivity was observed when crown ethers were used in both dioxane and THF. The reaction without ligand in THF proceeded with a low yield and an E:Z selectivity of 24:1 (entry 1). When crown ethers were added, quantitative results were obtained and selectivies were improved (up to 49:1, entries 2 and 3). However, the selectivity obtained with KHMDS (99:1) was not achieved. Similar conclusions can be drawn from the reactions in dioxane, where much higher yields were observed for the reactions with ligand (entries 5 and 6) compared to the unligated catalyst (entry 4). Despite selectivities having also improved, the *E:Z* ratio was still inferior to the KHMDS/[18]crown-6 system.

Based on the observation that the crown ethers activated the catalyst, it was assumed that reactions using this catalyst system could be performed in a variety of solvents. A solvent screening was performed using solvents ranging from apolar to polar for the isomerisation reaction using KHMDS and [18]crown-6 in a 1:1 molar ratio (Table 31).

Table 31: Solvent Screening for the KHMDS/[18]c-6 catalytic system

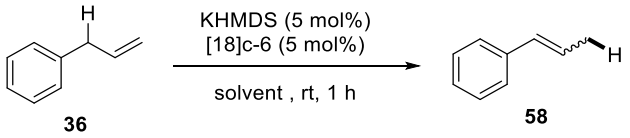

36 58

Entry	Solvent (Ɛ)	Yield (%)[a]	*E*:*Z* ratio
1	Heptane (1.9)	95	99:1
2	PhMe (2.4)	94	49:1
3	Dioxane (2.3)	91	99:1
4	TBME (2.6)	90	49:1
5	Et_2O (4.3)	91	49:1
6	DME (7.2)	88	99:1
7	THF (7.5)	92	99:1
8	EtOAc (6.0)	85	15:1
9	MeCN (37.5)	64	15:1
10	DMF (38.0)	87	99:1

[a] The yield was determined by ^{1}H NMR spectroscopy of a reaction aliquot; internal standard: dibenzyl ether (25 mol%).

As expected, all aprotic solvents used tolerated the reaction conditions and gave the styrene product in good to excellent yields (entries 1-10). Apolar hydrocarbon solvents, as well as all ethereal solvents gave good selectivities of at least 49:1 in favour of the *E*-isomer (entries 1-7). When moving to more polar solvents, the selectivity decreased significantly for ethyl acetate and acetonitrile, but increased again for DMF (entires 8-10). This observation suggested that the selectivity did not depend primarily on the polarity of the solvent. Other factors that needed to be considered were the solvent's ability to coordinate to the metal and their potential C–H acidity. Indeed, ethyl acetate (pK_a ~ 30) and acetonitrile (pK_a ~ 31) are both more acidic than allylbenzene and are therefore more likely to be deprotonated first to form the corresponding potassium enolates, which may act as a catalyst or initiator. Therefore the isomerisation mechanism in these cases may be different, leading to poorer selectivities than for all other solvents.

2.3.2.2 Unfunctionalised Isomerisation - Scope

Finally, the scope of the isomerisation of allylbenzenes was investigated (Table 32). Substitution effects on the aryl ring were studied using electron-donating and -withdrawing groups.

Table 32: Scope for the isomerisation of allylbenzenes

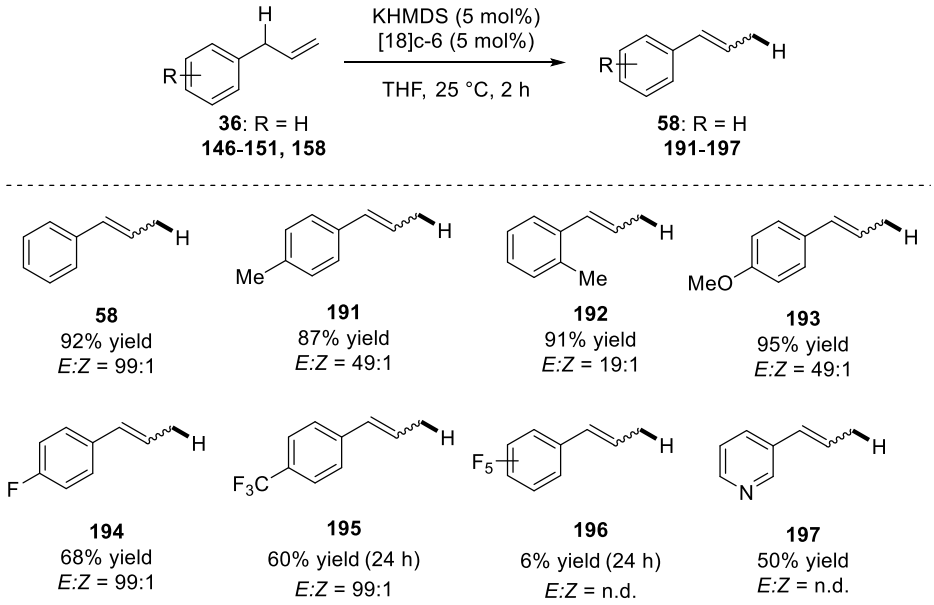

The yield was determined by ^{1}H NMR spectroscopy of a reaction aliquot; internal standard: dibenzyl ether (25 mol%).

^{1}H NMR spectroscopic analysis was performed for the quantification of the results. Spectral data were found to be identical to literature-reported values. [73b, 77a, 78] Methyl-substitution in the *para*- and *ortho*-positions was tolerated and gave good yields. For the *ortho*-methyl-substituted styrene, the selectivity did not reach the previously observed levels, suggesting an interference of the methyl group with the allyl–metal intermediate. The introduction of a methoxy group in the *para*-position increased the reactivity further and gave product **193** with a selectivity of 49:1. For the electron-poor allylbenzenes, yields were diminished to 6–68% were obtained for the products obtained from *para*-fluoro-allylbenzene, *para*-trifluoromethyl-allylbenzene, and 3-allylpyridine. The perfluorinated allylbenzene showed no reaction after 2 h, and even after prolonged reaction times, syrenyl product **196** was only obtained in 6% yield.

Alkene-substituted allylbenzenes were not commercially available and had to be prepared. Preparation of the olefins using Wittig chemistry was identified as the simplest route to a variety of different compounds as these can be prepared from a common phosphosium precursor (Scheme 69).

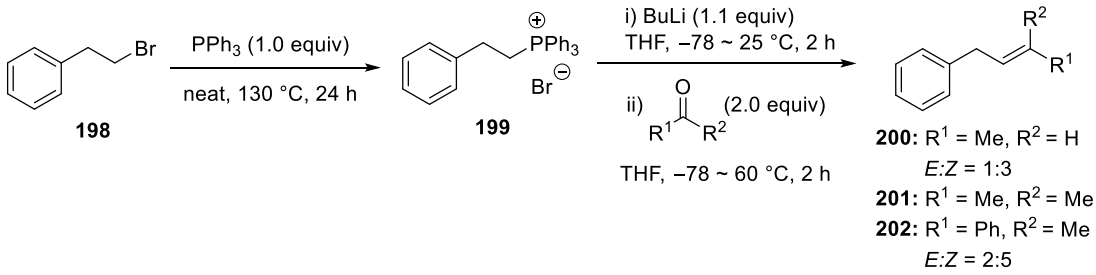

Scheme 69: Preparation of substituted allylbenzenes

The phosphonium salt was prepared in quantitative yields from the corresponding bromide **198** and triphenylphosphine, and used without purification after ^{31}P NMR spectroscopy confirmed the presence of a single ^{31}P NMR environment. The Wittig precursor was then deprotonated using BuLi at –78 °C, followed by the addition of the corresponding ketone or aldehyde at –78 °C and subsequent heating to 60 °C. The mono- and disubstituted olefins (**200**-**202**) were purified by flash column chromatography on silica gel and dried over molecular sieves (4Å) before use. The allylbenzenes with terminal alkene substituents were then used in the isomerisation reaction using the optimised reaction conditions (Table 33).

Table 33: Scope for the isomerisation of substituted allylbenzenes

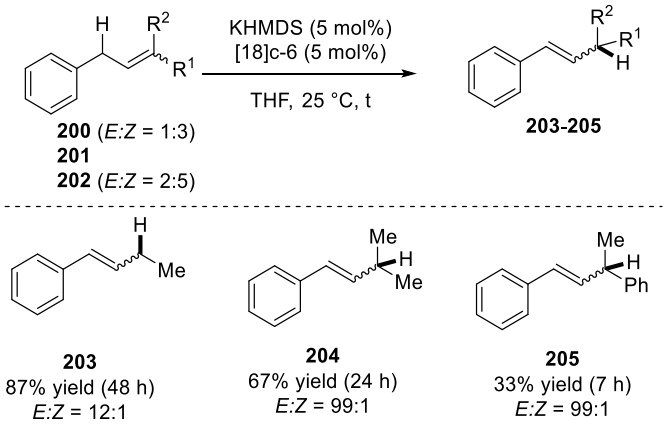

[a] The yield was determined by ^{1}H NMR spectroscopy of a reaction aliquot; internal standard: dibenzyl ether (25 mol%).

Substitution on the olefin was generally tolerated and both the methyl as well as the dimethyl substitution allowed for good yields to be obtained. As the starting material for the monomethylated product **200** was used as a 1:3 mixture of *E/Z* geometric isomers, the resulting *E:Z* selectivity of 12:1 was acceptable. The aryl-substituted substrate **202** showed low conversions to the styrenyl product **205**, because the product contained an equally reactive proton in the benzylic position. The less substituted alkene **205** was not as stabilised as the starting material, so as expected, more starting material than product was obtained.

The isolation of the allylbenzenes is described in the literature for many substances but proved to be challenging.[77a] Chromatography on silica gel can allow to separate the product from the catalyst and other impurities. However, separation from the starting material may be difficult and the different geometric isomers are too similar in size and polarity for sufficient separation. Additionally, the storage of these products in the absence of solvents may lead to oligomerisation products. Hydroquinone (HQ) or butylated hydroxytoluene (BHT) are known to inhibit some of these unwanted decomposition reactions, but depending on the substitution these could not be prevented entirely. To prove the principle, several compounds were purified by flash column chromatography on silica gel and the solvents were removed using a weak vacuum for short periods of time.

The scope could also be extended to 1,4-diene substrates, which have previously been activated in C–C bond-forming reactions with imines. When subjecting these substrates to the developed conditions, the corresponding 1,4-dienes formed in high yields (Table 34).

Table 34: Scope for the isomerisation of 1,5-dienes

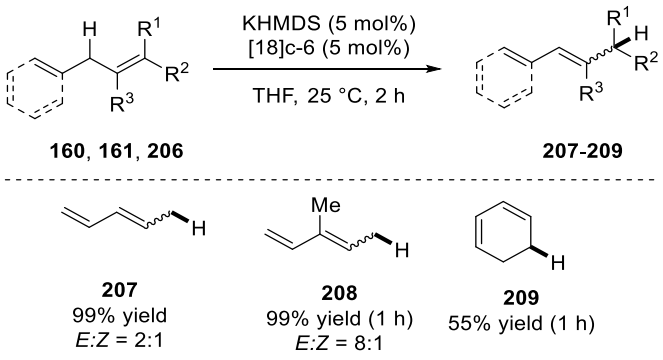

207
99% yield
E:*Z* = 2:1

208
99% yield (1 h)
E:*Z* = 8:1

209
55% yield (1 h)

[a] The yield was determined by ^{1}H NMR spectroscopy of a reaction aliquot; internal standard: dibenzyl ether (25 mol%). [b] *NR* = no reaction; the desired product was not detectable, only starting materials were detected (^{1}H NMR analysis of a reaction aliquot).

1,3-pentadiene and the methyl-substituted products **207** and **208** were obtained as ca. 8:1 mixtures of *E*- and *Z*-isomers. This poor selectivity may arise from a smaller difference in size between the different substituents. However, good yields were obtained for these volatile substrates proving the general applicability of this process. In the case of 1,4-cyclohexadiene, issues with double bond geometries were not encountered. However, the product underwent a disproportionation reaction to give cyclohexene and benzene (Scheme 70). This reaction accounted for the remaining mass balance in the reaction and a yield of only 55% could be observed.

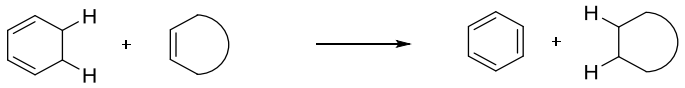

209 210

Scheme 70: Disproportionation of 1,3-cyclohexadiene

2.3.2.3 Functionalised Isomerisation – Use of Allyl–M

As the developed catalytic system for the simple isomerisation was applicable to allylbenzenes and 1,4-pentadienes, more complex allylic motifs were investigated. Allylsilane was assumed to be a suitable substrate for the isomerisation in the presence of a functional group. The α-silicon effect has been reported to stabilise anions in α-position to a silicon atom.[79] Combined with the stabilising effect of the allyl group, the aciditiy of allylsilane was expected to be significantly lower than its carbon analogue, 4,4-dimethylpent-1-ene **211** (pK_a value >40, Scheme 71). By using an appropriate Brønsted base, allylsilane would be deprotonated in α-position, giving rise to a potentially basic silylated carbanion.

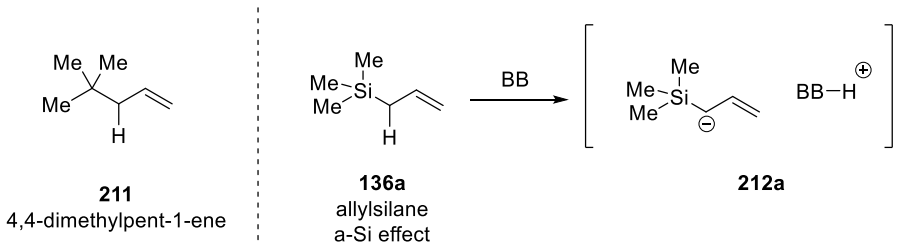

211
4,4-dimethylpent-1-ene

136a
allylsilane
a-Si effect

212a

Scheme 71: The α-Si effect

However, compared to allylbenzene, allyl silane **136a** poses an additional challenge as it contains both a Brønsted and a Lewis acidic site (Scheme 72). Indeed, the base catalyst used for the deprotonation could also attack the silicon Lewis acid and form a pentavalent silicon–ate species.

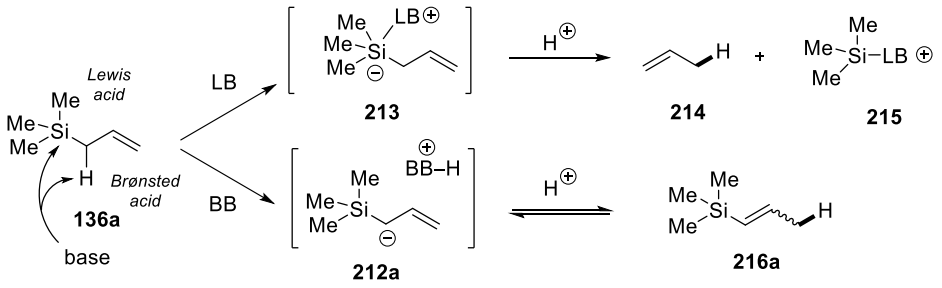

Scheme 72: Selectivity for base-activated allyl–Si

Both pathways lead to charged intermediates that can react with a proton to give corresponding olefinic products. However, if the base catalyst reacted as a nucleophile to activate the silicon centre, protonation would occur with loss of the silane group giving propene **214** as a product. Only the chemoselective deprotonation and reprotonation in γ-position would lead to the intended isomerised vinyl silane product **216a**.

Allylsilanes and siloxanes have been isomerised in the literature using stoichiometric amounts of strong Brønsted base[80] or transition metal catayst.[81] Good *E:Z* selectivities have been observed in both processes. The same BB cat principle was hoped to be applicable to other semimetals including boron and tin, for which only transition metal-catalysed isomerisations have been reported.[82] The α-boron effect has been described previously,[83] but no such effect has been discovered for tin. By using different catalysts and substitution, a method was attempted to be developed for the catalytic isomerisation of allyl–M compounds (Scheme 73).

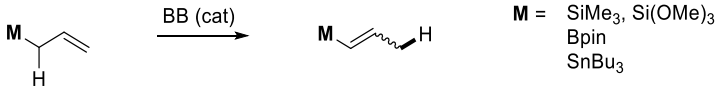

Scheme 73: BB catalysed cinnamylation of allyl–M

Scope

All allylic substrates were subjected to the previously developed conditions using a catalytic amount of KHMDS in the presence of [18]crown-6 as a ligand in THF at 25 ºC. Not all allyl–M reagents were equally reactive and some methods had to be optimised in order to achieve good yields (Table 35). Results were quantified using ^{1}H NMR spectroscopy by integration of the new alkenyl signals with respect to DBE as the internal standard. The formation of propene as a side-product was not detected in any of the reactions and mass balances suggested that other side-products were not formed either.

Table 35: Scope for the isomerisation of allyl-metal reagents

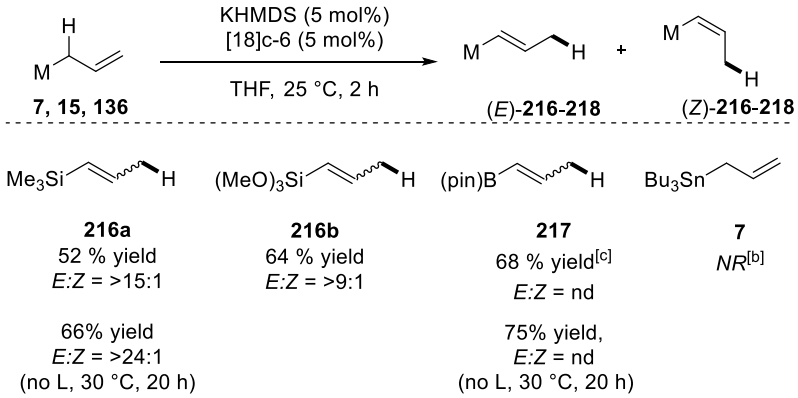

[a] The yield was determined by ^{1}H NMR spectroscopy of the reaction mixture; internal standard: dibenzyl ether (25 mol%). [b] NR = no reaction; the desired product was not detectable, only starting materials were detected (^{1}H NMR analysis of the reaction mixture). [c] Reaction time was 24 h. [d] Decomposition of starting material.

Allyl trimethylsilane reacted smoothly under the employed conditions to give the corresponding vinyl silane **216a** in acceptable yields. The major product was identified as the *E*-isomer (δ = 6.1 ppm, J_{trans} = 18.4 Hz), and the *Z*-isomer formed as a minor product (δ = 6.4 ppm, J_{cis} = 13.9 Hz) giving an *E:Z* selectivity of 15:1 (spectral information in line with reported literature). [84] This reactivity was decreased when conducting the reaction in the absence of the ligand, but increasing the temperature and the reaction time improved both the yield to 66% and the *E:Z* selectivity to 24:1.

Siloxanes are more stable analogues of silanes, because the oxygen substituents can potentially donate electron density towards the Lewis acidic metal centre. The isomerisation reaction with siloxanes gave slightly higher yields than for the silanes using the standard conditions. While the yield for styryl siloxane **216b** was improved, the selectivity of this transformation decreased; the *E*-isomer (δ = 6.5 ppm, J_{trans} = 18.8 Hz) was only favoured over the *Z*-isomer (δ = 6.7 ppm, J_{cis} = 14.0 Hz) with a ratio of 9:1 (spectral information in line with reported literature).[85] Because of its slightly higher activity, metal alkoxides were also tested in this reaction. These bases were reported to catalyse the isomerisation of allyl–Si compounds in DMSO. Here, they were tested in DMF as an alternative polar aprotic solvent. Some reactivity was found using sodium or potassium *tert*-butoxides, but reactivities were genereally low. Furthermore, sodium and potassium hydroxides could also be used as catalysts in DMF but again, yields did not exceed the reactivity of the metal amide catalysts.

By changing the metal to boron, a more challenging reaction was attempted. The pinacol-derived allyl boronic ester was chosen as a model substrate, because protection of the Lewis acidic centre with oxygen-based substituents proved beneficial in the case of silicon. Initial

attempts to isomerise this substrate were successful and good yields of the akenyl boronic ester *E*-**217** (δ = 6.7 ppm, J_{trans} = 17.8 Hz) were obtained. *Z*-**217** could not be quantified due to overlapping signals with the *E*-isomer as reported in the literature.[82a] The isomerised product was obtained in slightly higher yields when the reaction was performed in the absence of the ligand at slightly elevated temperatures, but the effect on the geometric selectivity was not recorded. Like before, no propene was observed as a result from LB activation of the starting material.

For the allyl–Sn species, only the tributyl-substituted substrate was commercially available. This compound showed no reactivity under the developed conditions with or without ligand even at elevated temperatures (up to 60 °C). Also, the use of stronger bases such as LDA or LTMP did not give the isomerised product; only the starting material was detected in all reaction mixtures.

Allyl–M reagents have been shown to be activated by alkali metal amides in the case of silanes, siloxanes and boronic esters. These results suggested a potential application also in C–C bond formation, treated in the next chapter. First, the isomerisation of other functionalised alkenes was investigated.

2.3.2.4 Functionalised Isomerisation – Use of Allyl–FG

Moving on from group XIII (B) and XIV (C, Si), allylic substrates containing other main group elements were also examined for their ability to stabilise anions in α-position. The deprotonation using a Brønsted base, followed by reprotonation in γ-position would give rise to isomerised products containing main group elements in vinylic positions (Scheme 74).

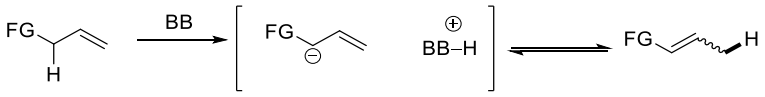

Scheme 74: Deprotonation and isomerisation of allyl–FG

For sulfur and phosphorus, this effect is well-known and different reasons can be attributed to the stabilisation of negative charges in vicinal positions. Originally, it was believed that these elements have accessible vacant d orbitals that can provide a stabilisation effect by withdrawing electron density (Scheme 75).[86] It was also postulated that the σ*-orbital of the corresponding C–X bonds would accommodate for electron density and this effect would be more likely than the access of d orbitals.[87]

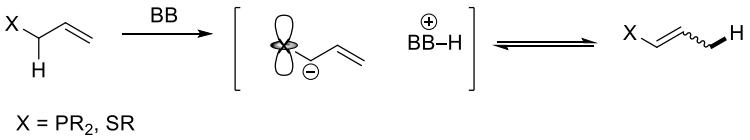

Scheme 75: Stabilisation of α-anions by d-orbitals

Base-catalysed isomerisations of allylic thioethers[88] and phosphines[89] are reported in the literature, where alkali metal *tert*-butoxides or hydroxides were used as catalysts in DMSO for the transposition of the double bond. Further studies showed that with appropriate ligands, KOH can be used as an effective catalyst in the same polar solvent.[88b] Recently, the Verkade base has been used to isomerise allyl thioethers in acetonitrile, albeit with no control over the alkene geometry.[72] Transition metals have also been reported to isomerise these substrates in high yields and much improved selectivities.[90]

For the lighter analogues of sulfur and phosphorus – oxygen and nitrogen – no stabilising effect has been reported. Their accessibility of σ* orbitals is of course highly dependent on the substitution pattern and these substrates are generally more challenging to activate (Scheme 76).

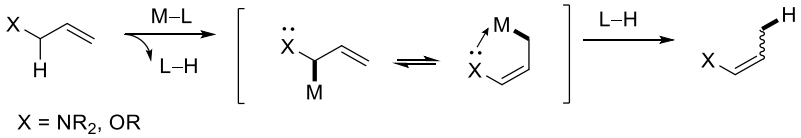

Scheme 76: Stabilisation of γ-anions by coordination

Like their heavier analogues, allyl ethers and amines have been reported to isomerise using catalytic amounts of metal alkoxides in DMSO.[91] Due to a lack of control over the *E:Z* ratios of the double bond, transition-metal-catalysed processes have been developed for both theses substrates.[92] As the resulting enamines and enol ethers are of high synthetic use, the isomerisation reaction has been coupled to other reactions.[89]

Initial isomerisation reactions were attempted using the previously developed conditions of KHMDS/[18]-c-6 in THF at 25ºC (Table 36).

Table 36: Scope for the isomerisation using KHMDS/[18]-c-6

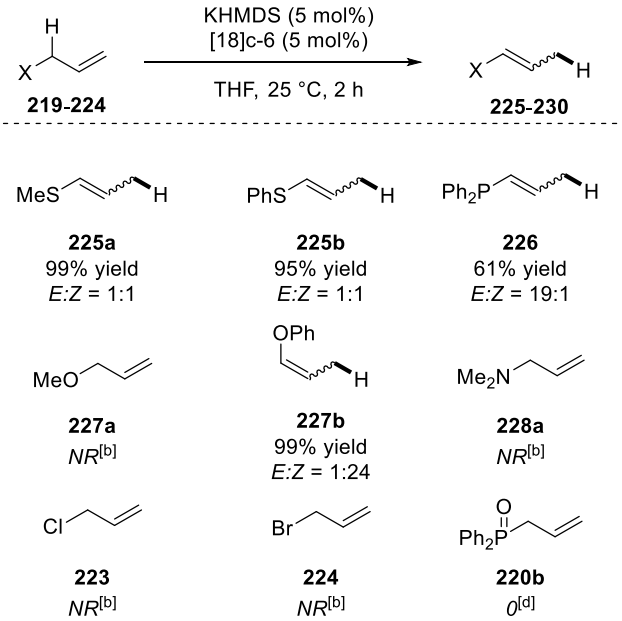

Both allyl sulfides employed gave good conversions to the vinyl sulfides in high yields, but with no differentiation between geometric isomers. Vinyl phosphine product **226** could be obtained in a moderate yield and with a good selectivity using standard conditions. Of the allyl ethers, only the phenyl substituted ether showed reactivity and the selectivity was high. Here, the *Z*-isomer formed as the major product with the minor *E*-isomer present in only small amounts. The amine substrate **228a** showed no reaction under the employed conditions. Also the allylic halides, which were used as a new class of reagents, showed no reactivity under the employed conditions. Allyl phosphonate **220b** showed reactivity, but no isomerised product could be identified. Instead, polymerisation was assumed due to the observation of broad signals in ^{1}H NMR spectroscopy.

Allyl Sulfides

As shown in the initial table, commercially available allyl phenyl thioether **219b** showed good reactivity, but selectivities were poor. Therefore, this substrate was tested in the isomerisation reaction using KHMDS in the presence of a crown ether or a carbene ligand in different solvents (Table 37). Conversions were monitored using ^{1}H NMR spectroscopy by comparison of the starting material alkenyl signal (δ = 5.9 ppm, 1H) to the product signals (δ = 6.1, 6.0 ppm, J_{trans} = 14.8 Hz, 1H each; δ = 6.2, 5.9 ppm, J_{cis} = 9.2 Hz, 1H each).[54]

Table 37: Isomerisation of allylsulfide 219b

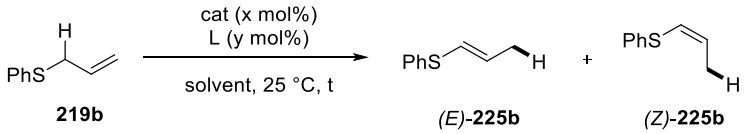

219b *(E)*-**225b** *(Z)*-**225b**

Entry	Cat (x mol%)	Ligand (y mol%)	Solvent	t (h)	Conv (%)[a]	*E:Z* ratio
1	KHMDS (10)	-	THF	4	99	1:1
2	KHMDS (10)	-	PhMe	1	90	1:4
3	KHMDS (10)	-	m-xylene	1	99	1:5
4	KHMDS (10)	[18]c-6 (10)	THF	2	99	1:1
5	KHMDS (10)	[18]c-6 (10)	dioxane	3	99	1:2
6	KHMDS (10)	[18]c-6 (10)	Et_2O	3	99	1:1
7	KHMDS (10)	[18]c-6 (10)	PhMe	3	99	1:1
8	KHMDS (8)	SIPr (10)	PhMe	1	85	1:6
9	KHMDS (8)	SIPr (10)	m-xylene	1	99	1:6

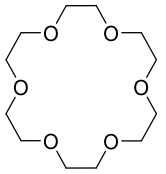

188
[18]c-6

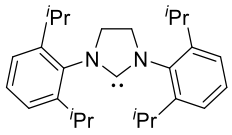

231
SIPr

[a] The conversion was determined by ^{1}H NMR spectroscopy of the reaction mixture without internal standard (based on relative ^{1}H NMR analysis of the starting material and the product)

Allylic thioether **219b** showed good reactivity even when using ligand-free conditions (entries 1-3). Little change in reactivity was observed in different solvents, but the *E:Z* selectivity was influenced by the nature of the solvent. While reactions in Lewis basic ethereal solvents such as THF gave no selectivity, performing the reaction in more apolar aromatic solvents increased the selectivity to up to 5:1. Interestingly, *Z*-**225b** was found to be the major isomer of the vinylic product. In the presence of a crown ether lower selectivities were observed in all solvents (entries 4-7). Even in toluene, no selectivity could be observed for this reaction. The ligand in this case may be seen as a mimic for an ethereal solvent, which has shown low selectivities before. However, the combination of KHMDS and a stonger σ donor ligand, i.e. an NHC, triggered the isomerisation of allyl thioether **219b** to give high yields and improved *E:Z* selectivities that could even slightly improve the results of KHMDS alone in aromatic solvents. This improvement showed that carbene coordination to the metal centre may occur in apolar aromatic and non-basic solvents, leading to a change in the catalyst's activity.

Allyl Phosphines

Based on the previous results, reactions with allyl diphenylphosphine **220** were carried out using a metal–base as the catalyst in the absence of a ligand (Table 38). Yields were recorded for the formation of the vinyl phosphine products *E*-**226** (δ = 6.2–6.3 ppm, 2H) and *Z*-**226** (δ = 6.5–6.6 ppm, 2H).[93]

Table 38: Isomerisation of allyldiphenylphosphine

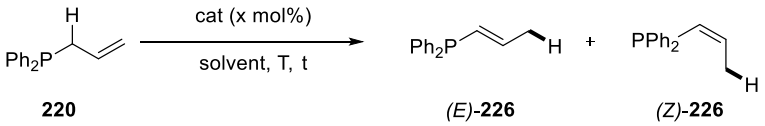

220 *(E)*-**226** *(Z)*-**226**

Entry	Cat (x mol%)	Solvent	t (h)	T (°C)	Yield (%)[a]	*E:Z* ratio
1	KHMDS (10)	THF	4	25	83	19:1
2	LTMP (10)	THF	2	25	51	19:1
3	NaO^{t}Bu (20)	dioxane	24	25	21	5:1
4	NaO^{t}Bu (20)	DMF	3	25	84	5:1

[a] The yield was determined by ^{1}H NMR spectroscopy of the reaction mixture; internal standard: dibenzyl ether (25 mol%).

The reaction catalysed by KHMDS showed that allylphosphine **220** was isomerised quickly under mild conditions (entry 1). The reaction was also successful using LTMP (entry 2); both metal amide catalysts gave an *E:Z* selectivity of 19:1. As this compound was easy to activate, Na^{t}OBu was tested in the isomerisation in dioxane and DMF (entries 3 and 4). Using 20 mol% of the catalyst gave low yields even after 24 h when performed in dioxane, but high yields of product **226** were obtained in DMF after 4 h. This variation of reactivity showed how the basicity of the alkoxide anion varied in different solvents. Interestingly, in both cases, the double bond geometry could not be controlled as well as by using metal amide catalysts.

Allyl Amines

Due to the lack of reactivity of dimethyl allylamine **222a** using KHMDS/[18]c-6 as the catalyst system, a more detailed study of the isomerisation of this substrate was performed. To this end, different catalysts and ligands were used in THF at different temperatures (Table 39). ^{1}H NMR spectroscopy was used for monitoring the reaction without the use of an internal standard. Spectral analysis was compared to the literature reported data for the *E*-**228a** (δ = 5.9, 4.2 ppm, J_{trans} = 13.7 Hz, 1H each) and the *Z*-**228a** (δ = 5.6, 4.3 ppm, J_{cis} = 9.0 Hz).[94]

Table 39: Isomerisation of dimethylallylamine

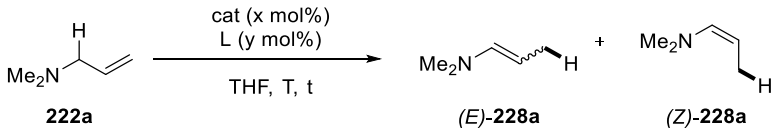

222a *(E)*-**228a** *(Z)*-**228a**

Entry	Cat (x mol%)	Ligand (y mol%)	T (°C)	t (h)	Conv (%)[a]
1	KHMDS (10)	-	25–60	20	*NR*[b]
2	LDA (10)	-	25–60	20	*NR*[b]
3	LTMP (10)	-	25	20	*NR*[b]
4	LTMP (10)	-	60	20	68[c]
5	KHMDS (10)	[18]c-6 (5)	25	6	*NR*[b]
6	KHMDS (10)	[18]c-6 (10)	25–60	20	*NR*[b]
7	LTMP (10)	[18]c-6 (10)	25	20	*NR*[b]

[a] The conversion was determined by ^{1}H NMR spectroscopy of the reaction mixture without internal standard (based on relative ^{1}H NMR analysis of the starting material and the product). [b] NR = no reaction; the desired product was not detectable, only starting materials were detected (^{1}H NMR analysis of the reaction mixture). [c] *E:Z* = 1:1.

No reaction of dimethylallylamine **222a** was observed when different metal amides were used at room temperature (entries 1-3). Only the use of LTMP at 60 °C for 20 h allowed for the formation of the desired enamine in good yields (entry 4). However, no geometric selectivity was obtained. When reactions were carried out in the presence of [18]crown-6 as a ligand at room temperature, no product and only staring material was detected in ^{1}H NMR spectroscopy of a reaction aliquot (entries 5-7). In order to examine another allylic amine in the isomerisation reaction, diphenylallylamine was prepared in one step from allyl bromide and diphenylamine (Scheme 77). This reaction gave the corresponding allyl amine on gram-scale, and the substrate was purified and dried (4 Å MS) before use in catalysis.

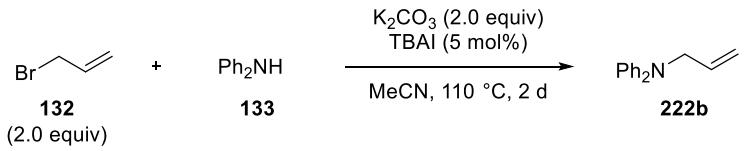

Scheme 77: Preparation of allyldiphenylamine

Like its methyl-substituted analogue, diphenylallylamine was subjected to the KHMDS/[18]crown-6 catalyst conditions at different temperatures (Table 40).

Table 40: Isomerisation of diphenylallylamine

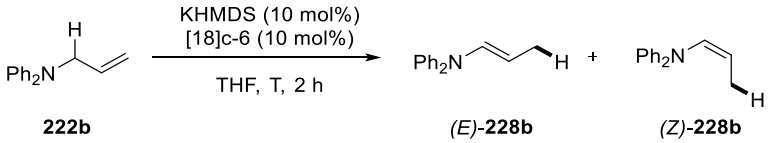

Entry	Temp (°C)	Conv (%)[a]	*E:Z* ratio
1	25	99	1:10
2	40	99	1:10
3	60	99	1:8

[a] The conversion was determined by ^{1}H NMR spectroscopy of the reaction mixture without internal standard (based on relative ^{1}H NMR analysis of the starting material and the product).

This diphenyl amine analogue showed a much improved reactivity profile, and gave the desired enamine in quantitative yields (entries 1-3). No starting material was detected after 2 h and *Z*-**228b** (δ = 6.1, 5.0 ppm, J_{cis} = 8.2 Hz, 1H each) and *E*-**228b** (δ = 6.6, 4.7 ppm, J_{trans} = 13.7 Hz, 1H each) were found as the only products. In contrast to the results for dimethyl allylamine, the selectivity for this mixture of geometric isomers was much greater and the *Z*-alkene was formed as the major isomer in a 10:1 ratio (entries 1 and 2). This ratio was slightly decreased when performing the reaction at elevated temperatures (entry 3).

One way to improve the selectivity of this transformation was the use of a different catalyst. Alkali metal alkoxides have been reported to catalyse the isomerisation of allylamines in DMSO (Scheme 78).[91b]

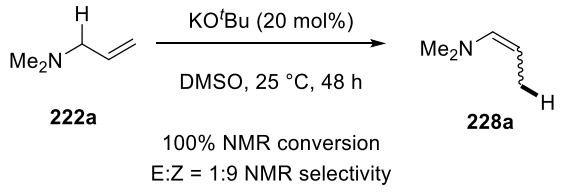

Scheme 78: Literature reported isomerisation of allylamines

In order to compare the results to the metal alkoxide-catalysed isomerisation, allylamine **222b** was reacted with alkali metal alkoxides in DMF and DMSO (Table 41).

Table 41: Metal alkoxides in polar solvents

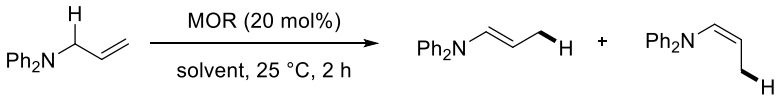

222b *(E)*-**228b** *(Z)*-**228b**

Entry	MOR	Solvent	Yield (%)[a]	*E:Z* ratio
1	LiO^{t}Bu	DMF	*NR*[b]	-
2	NaO^{t}Bu	DMF	39	1:8
3	KO^{t}Bu	DMF	99	1:8
4	KOMe	DMF	80	1:5
5	KOH	DMF	96	1:5
6	LiO^{t}Bu	DMSO	99	1:13
7	NaO^{t}Bu	DMSO	98	1:11
8	KO^{t}Bu	DMSO	99	1:7

[a] The yield was determined by ^{1}H NMR spectroscopy of the reaction mixture; internal standard: dibenzyl ether (25 mol%). [b] NR = no reaction; the desired product was not detectable, only starting materials were detected (^{1}H NMR analysis of the reaction mixture).

While LiO^{t}Bu showed no activity in DMF (entry 1), both the sodium and potassium bases gave **228b** in moderate to excellent yields, albeit with lower selectivity than the KHMDS/[18]crown-6 catalyst system (entries 2-3). Furthermore, potassium methoxide and even hydroxide were able to catalyse the isomerisation reaction in good to excellent yields, but the *E:Z* selectivity was further decreased (entries 4 and 5). When comparing the different *tert*-butoxide salts in DMSO, all catalysts showed excellent activity, but the selectivity decreased from lithium to sodium to potassium.

Z-configuration
amine coordination to M

E-configuration
no coordination possible

Figure 9: Binding modes of metallated enamine 228b

It is likely that the *Z*-isomer was found to be the major product because of a significant stabilisation occurring when the amine functional group coordinated to the metal centre of the allylmetal species, the assumed intermediate (Figure 9). This coordination would only be possible when the intermediate is in a *Z* configuration and subsequent protonation would then occur at the α-position relative to the metal. The higher selectivity arising from the lithium alkoxide supported this hypothesis because amine coordination to the small lithium ion (~ 70 ppm)[95] is more energetically favourable than coordination to larger cations. Here, the thermodynamic stability of *trans*-substituted alkenes favoured the formation of *E*-configurations, leading to a decrease in selectivity.

Other metal alkoxides have also been explored in this field with little success. Both magnesium ethoxide and calcium methoxide showed no reactivity in either DMF or DMSO. Furthermore, the KO^{t}Bu-catalysed isomerisation was also attempted in other solvents, such as THF, dimethylacetamide (DMAc), acetonitrile (MeCN), benzonitrile (PhCN) and propylene carbonate (PC). No reaction occurred in any of these solvents, limiting the applicability of the metal alkoxide catalysis to the use of DMF and DMSO only.

Allyl Ethers

In a similar fashion to the allylamines, allyl ethers were studied in the isomerisation reaction to form enol ethers, an important class of substrates. As shown in the initial screening, no reactivity was observed for the methyl-substituted allyl ether, but the phenyl-substituted analogue gave promising results (Table 36, p 92). Therefore, the phenyl-substituted allyl ether **221b** was subjected to different catalysis conditions and the formation of the corresponding enol ethers was monitored by ^{1}H NMR spectroscopy (Table 42).

The signals for *Z*-**227b** (δ = 6.4 and 4.9 ppm, J_{trans} = 6.0 Hz, 1H each) and *E*-**227b** (δ = 6.4 and 5.4 ppm, J_{cis} = 12.0 Hz, 1H each) were compared to literature-known data.[96] Similar conditions were then applied to the methyl-substituted allyl ether **221a** and the ^{1}H NMR analysis data of *Z*-**227a** (δ = 5.9 and 4.4 ppm, J_{trans} = 6.2 Hz, 1H each) was also compared to literature-known data.[97]

Table 42: Isomerisation of allyl ethers

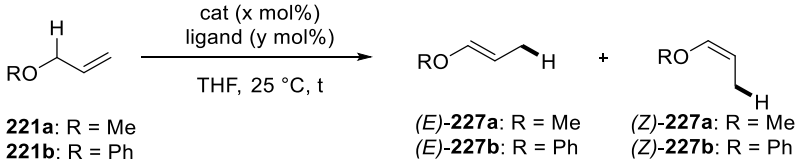

221a: R = Me
221b: R = Ph

(E)-**227a**: R = Me
(E)-**227b**: R = Ph

(Z)-**227a**: R = Me
(Z)-**227b**: R = Ph

Entry	R	Cat (x mol%)	Ligand (y mol%)	t (h)	Yield (%)[a]	*E:Z*
1	Ph	KHMDS (5)	[18]c-6 (5)	4	99	1:24
2	Ph	KHMDS (10)	-	4	(51)	1:24
3	Ph	LDA (10)	-	2	98	1:24
4	Ph	LTMP (10)	-	2	74	1:24
5	Me	KHMDS (10)	[18]c-6 (10)	2	*NR*[b]	-
6	Me	KHMDS (10)	-	4	*NR*[b]	-
7	Me	LTMP (10)	-	2	(99)	1:99

[a] The yield was determined by ^{1}H NMR spectroscopy of the reaction mixture; internal standard: dibenzyl ether (25 mol%). When no internal standard was added, numbers indicated in brackets refer to the conversion based on relative ^{1}H NMR analysis of the starting material and the product. [b] NR = no reaction; the desired product was not detectable, only starting materials were detected (^{1}H NMR analysis of the reaction mixture).

As mentioned, the reaction with KHMDS/[18]crown-6 proceeded quantitatively at room temperature with a selectivity of 24:1, the major isomer bearing *Z*-geometry (entry 1). This selectivity could not be improved when the experiments were run in the absence of a ligand (entry 2) or by using lithium amides (entries 3 and 4). The methyl-substituted analogue was harder to activate and a reaction was not observed using KHMDS either with or without a crown ether ligand (entries 5 and 6). Only the use of LTMP as a strong base allowed for the formation of enol ether **227a** in high yields and with exclusive *Z*-selectivity (entry 7).

As metal alkoxides have been shown to achieve the isomerisation of allylamines in DMF, this system was also used for the isomerisation of allyl phenyl ether **221b** (Table 43). Alkali and alkaline earth metal alkoxides or hydroxides were used in this transformation.

Table 43: Metal alkoxide isomerisation of allyl phenyl ether

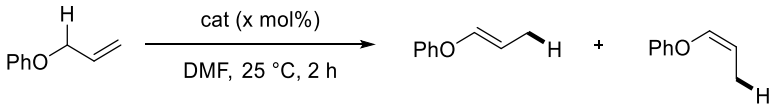

221b *(E)*-**227b** *(Z)*-**227b**

Entry	Cat (x mol%)	Yield (%)[a]	*E:Z*
1	LiO^{t}Bu (20)	45	1:40
2	NaO^{t}Bu (10)	3	1:19
3	KO^{t}Bu (20)	99	1:40
4	KOH (10)	*NR*[b]	-
5	$Ca(OMe)_2$ (20)	*NR*[b]	-

[a] The yield was determined by ^{1}H NMR spectroscopy of the reaction mixture; internal standard: dibenzyl ether (25 mol%). [b] NR = no reaction; the desired product was not detectable, only starting materials were detected (^{1}H NMR analysis of the reaction mixture).

All alkali metal *tert*-butoxides were able to catalyse the isomerisation reaction in DMF, albeit with varying success (entries 1-3). Of these metal alkoxides, KO^{t}Bu performed with the best results regarding both reactivity and selectivity, and even improved previous results using alkali metal amides. Neither potassium hydroxide, nor calcium methoxide were able to isomerise the allyl ether under the indicated reaction conditions (entries 4 and 5)

Overall, it was found that alkali metal amides were able to catalyse the isomerisation of heteroatom-substituted allylic substrates in groups XIII–XVI. In particular, allyl silane and boron reagents were activated, where the metal's ability to stabilise α-anions was exploited. In the case of sulfur and phosphorus, as well as their lighter analogues, oxygen and nitrogen, significant contribution of σ* orbital stabilisation was assumed to aid the isomerisation reactions. These findings were of great importance to the developments of new synthetic methods, not only in the field of C–H bond formations, exemplified in these isomerisation reactions, but also in the field of C–C bond formations, which involve similar reaction intermediates. Indeed, by trapping the substituted allylic anion with a suitable electrophile before reprotonation, novel methods for building up complex structures could be explored, which will be covered in the following chapter.

2.3.3 Functionalised C–C Bond Formation Using Allyl–M

With the knowledge of the isomerisation of metal-substituted allylic substrates in hand, these compounds were also considered as pro-nucleophiles for C–C bond formations. Here, similar challenges as with the isomerisations were faced, where the intended catalytic Brønsted base activation of the pro-nucleophile competed with the unwanted attack of a Lewis base at the Lewis acidic metal site. In the presence of an electrophile other than a proton, each of these two intermediates would then give rise to different products. The attack at the Lewis acidic metal centre would create an 'ate'-complex, which could either be protonated to yield propene, or react with an electrophile, leading to allylated products. In both cases, the metal functional handle would be lost (Scheme 79).

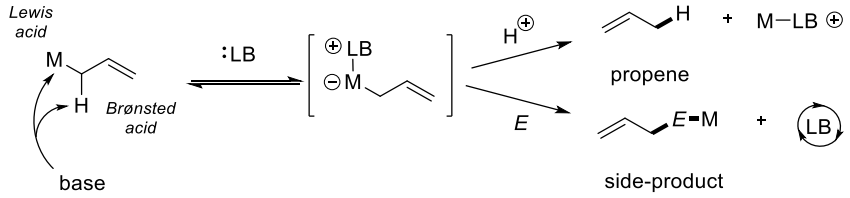

Scheme 79: Conventional catalytic Lewis base activation of allyl–M reagents

Depending on the metal centre and the electrophile, these allylated reaction products can be obtained even in the absence of a Lewis basic catalyst, as described in the introduction. Direct allylations of this kind are known for organometallic reagents such as boron, silicon, and tin, as well Barbier-type reactions from the corresponding allylic halides (Scheme 80).[7b]

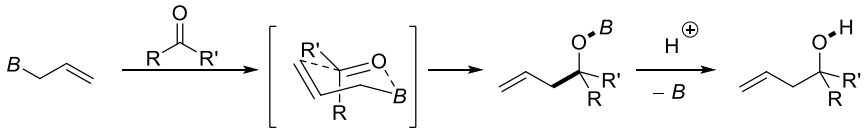

Scheme 80: Example of a ketone allylation with an allyl–*B* reagent (closed TS)

We aimed to form C–C bonds by activating the allylic Brønsted acidic site, next to the metal centre, using a deprotonation pathway. Here, the reactive intermediate would be an allylic anion - including the metal functional handle - that could react with an electrophile (Scheme 81). The reaction with a proton would lead to the isomerised allylic starting material, which has been discussed in the previous chapter. Only the selective reaction with an electrophile would generate the allylated products with incorporation of the metal into the product.

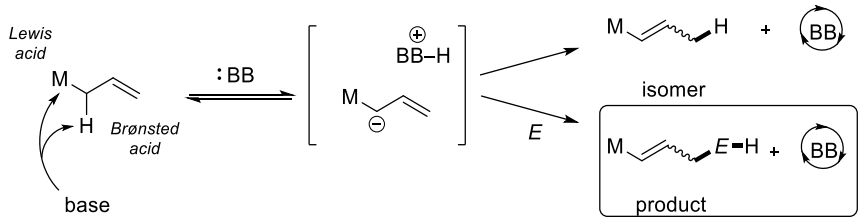

Scheme 81: Unprecedented catalytic Brønsted base activation of allyl–M

Stoichiometric Brønsted base activation of allylsilanes has been achieved in the literature giving silylated products of type **135** (Scheme 82).[42, 98] Here, the allylsilane was metallated using BuLi in the presence of TMEDA as a chelating ligand. The resulting silylated allyllithium complex was then added diastereoselectively to chiral diimine **134** to give bis-allylated product **135** with incorporation of the silyl group.

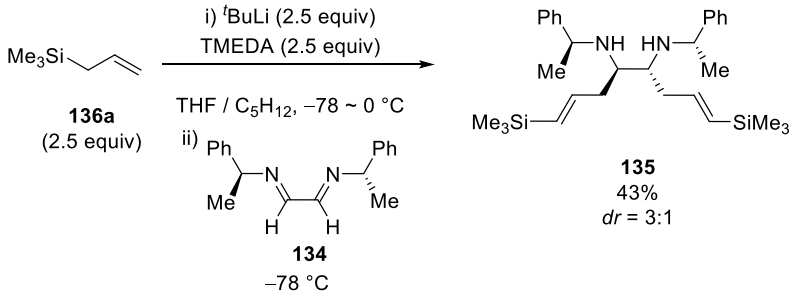

Scheme 82: Functionalised allylation using stoichiometric Brønsted base

From the isomerisation reactions, it was established that the allylic anion can be formed by deprotonation in α-position to the metal centre. By using a strong and bulky base such as alkali metal hexamethyldisilazides, good conversions were obtained for the formation of isomerised products. In this chapter, the allylic anion intermediate was expected to be trapped in the reaction with a suitable electrophile. Imines have previously been shown to be reactive electrophiles in the allylation reactions with allylbenzene. Both carbonyl-contaning electrophiles, as well as aziridines would be suitable alternatives depending on the conditions and the used catalyst (Figure 10).

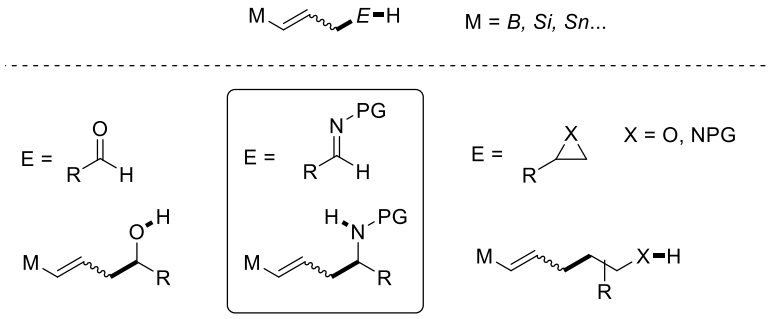

Figure 10: Different electrophiles for functionalized C–C bond formations

In all cases, the products from such a C–C bond formation would retain the functional handle in the form of a vinyl metal that could be used in further transformations. Specifically, the use of Pd-catalysed cross-couplings were thought to be an application that would allow for the formation of highly complex structures. The Suzuki (*B*),[99] Hiyama (*Si*),[100] or Stille (*Sn*)[101] cross-coupling reactions have been well studied and were assumed to be compatible with the reaction conditions developed in the C–C bond formations, leading to one-pot procedures for the bis-functionalisation of allylic substrates (Scheme 83).

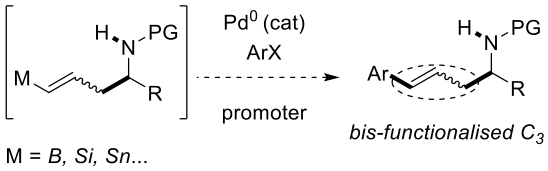

Scheme 83: Pd-catalysed cross coupling reactions

2.3.3.1 Silicon

$SiMe_3$

As the isomerisation of allylsilanes and siloxanes was achieved using alkali metal amides (Table 35, p 89), this class of catalysts was investigated in the functionalised allylation of imines. *N*-PMP-protected benzaldimine **56b** was reacted with allylsilane **136a** in different solvents at 25 °C for 20 h (Table 44).

Table 44: Allylation using allylsilanes

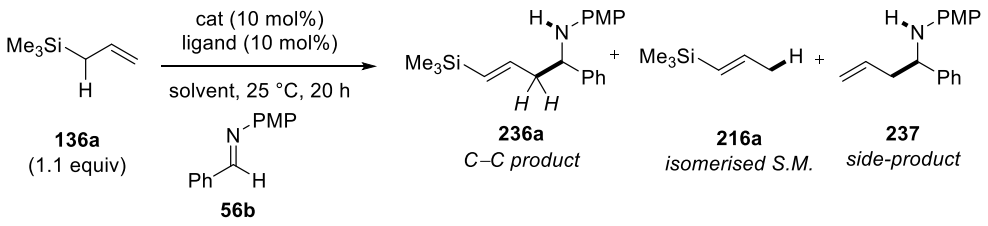

Entry	Cat / Ligand	Ligand	Solvent	Yield 236a (%)[a]	216a (%)[a]	237 (%)[a]
1	NaHMDS	-	dioxane	*NR*[b]	-	-
2	KHMDS	-	dioxane	37	14	0
3	KHMDS	-	THF	10	0	0
4	KHMDS	[18]c-6	dioxane	18	6	30
5	KHMDS	[18]c-6	THF	20	8	50
6	$Ca(HMDS)_2$	[18]c-6	dioxane	*NR*[b]	-	-

[a] The yield was determined by ^{1}H NMR spectroscopy of a reaction aliquot; internal standard: dibenzyl ether (25 mol%). [b] NR = no reaction; the desired product was not detectable, only starting materials were detected (^{1}H NMR analysis of a reaction aliquot).

The use of NaHMDS proved somewhat limited as no reaction occurred in dioxane (entry 1). Therefore, reactions were carried out with KHMDS in both dioxane and THF (entries 2 and 3). Product **236a** was formed in both solvents with slightly better results in dioxane (37%), but isomerised side-product **216a** was also observed in 14% yield (entry 2). ^{1}H NMR spectroscopy allowed for the identification of the different products. The isomerised starting material **216a** was identified by comparison to previous and literature-reported data.[84] Product **236a** is an unknown compound, but characteristic signals in ^{1}H NMR spectroscopy of a reaction aliquot at δ = 2.6 and 2.5 ppm for the allylic protons in **236a** have been identified. By using [18]crown-6 as a ligand for KHMDS in order to increase the catalyst's reactivity and selectivity no improvement in yields could be noted (entries 4 and 5). Instead, new signals in ^{1}H NMR spectroscopy were observed, which could be assigned to the formation of unfunctionalised side-product **237**.[102] This meant that the use of a ligand for the metal centre increased the Lewis basicity of the metal amide, leading to the attack at the metal centre to give product **237**. The use of DMF as a polar aprotic solvent in the reactions catalysed by NaHMDS and KHMDS also proved to be unsuccessful at improving the yields of product **236a**. Finally, a calcium amide catalyst was used with a crown ether ligand to catalyse the C–C bond formation, but no reaction was observed (entry 6). As reactions with allylsilane **136a** showed promising results with allylation yields of up to 37%, other silanes were considered for this type of reaction.

Si(OMe)$_3$

Allylsiloxane **136b** was used as an alternative Si-containing pro-nucleophile. This substrate proved to be easier to activate in isomerisation reactions (Table 35, p 89) and was therefore assumed to be more active in reactions with electrophiles as well. Reactions of siloxane **136b** with imine **56b** were carried out using different metal amide catalysts in dioxane and THF (Table 45).

Table 45: Alkali metal amide catalysts in the allylation of imines using siloxane 136b

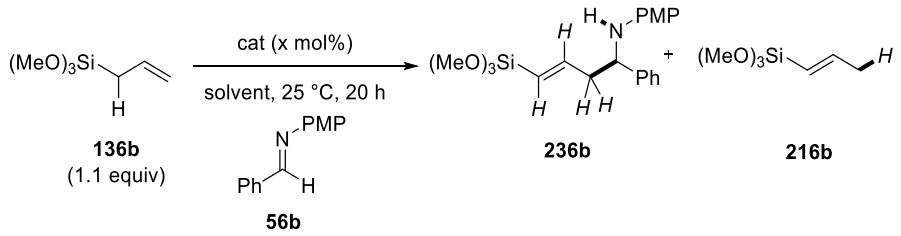

Entry	Cat (x mol%)	Solvent	Yield 236b (%)[a]	216b (%)[a]
1	LHMDS (20)	dioxane	47	0
2	NaHMDS (10)	dioxane	85	7
3	KHMDS (10)	dioxane	40	33
4	LTMP (10)	dioxane	15	0
5	NaHMDS (10)	THF	65	21
6	LDA (10)	THF	*NR*[b]	-
7	LTMP (10)	THF	22	0

[a] The yield was determined by ^{1}H NMR spectroscopy of a reaction aliquot; internal standard: dibenzyl ether (25 mol%). [b] NR = no reaction; the desired product was not detectable, only starting materials were detected (^{1}H NMR analysis of a reaction aliquot).

The use of all alkali metal amide catalysts gave product **236b** selectively over the formation of isomerised starting material **216b** in both dioxane and THF (entries 1-4 and entries 5-7 respectively). Remarkably, in none of these reactions direct allylation products with loss of the siloxane functional group was observed. This selectivity may be related to the shielding effect of the Si-substitutents, which decrease the metal's electrophilicity through donation of electron density. Product **236b** was identified by ^{1}H NMR spectroscopy of a reaction aliquot. Signals were recorded at δ = 6.4 and 5.6 ppm (J_{trans} = 18.9 Hz) for the protons in the alkenyl positions, δ = 4.4 ppm for the benzylic proton, and δ = 2.7 and 2.6 ppm for the two allylic protons. In order to avoid overlap with any alkenyl signals, isomerised side-product **216b** was quantified by integrating the terminal methyl signal at δ = 1.9 ppm (dd, 3H). All integrations were relative to the internal standard (DBE, 0.25 equiv, δ = 4.6 ppm, 4H).

Among the used alkali metal amides, NaHMDS performed best, giving **236b** in 85% yield (entry 2). For both the Li and the K analogues, only modest yields of 40–47% could be obtained (entry 1 and 3). However, different factors caused these yields to be low: In the case of LHMDS, a lower reactivity was observed, whereas the KHMDS-catalysed reaction showed high levels of isomerisation occurring, leading to a 'loss' of pro-nucleophile to generate undesired side-product **216b**, which did not appear to participate in C–C bond formation.

In order to compare the reactivity of this amide catalyst with other metals, a catalyst screening was performed using the corresponding alkaline earth metal amides. These

catalysts were also of interest in light of developing enantioselective reaction conditions: coordination to the more Lewis acidic alkaline earth metal centres by chiral ligands may be more efficient, increasing the potential for stereodifferentiation. Reactions were carried out using 10–20 mol% of the catalyst under otherwise unchanged reaction conditions (Table 46).

Table 46: Alkaline earth metal catalysts in the allylation of imines using siloxane 136b

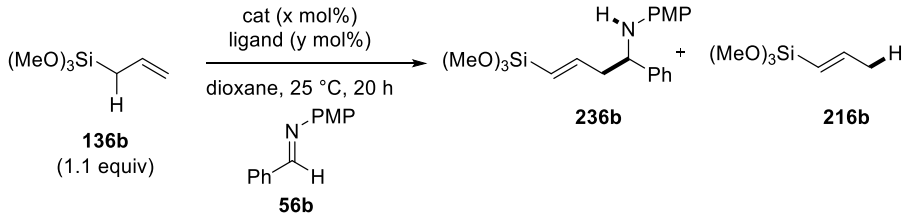

Entry	Cat (x mol%)	Ligand (y mol%)	Yield 236b (%)[a]	216b (%)[a]
1	$Mg(HMDS)_2$ (10)	-	*NR*[b]	-
2	$Ca(HMDS)_2$ (10)	-	*NR*[b]	-
3	$Sr(HMDS)_2$ (10)	-	*NR*[b]	-
4	$Ca(HMDS)_2$ (20)	[18]c-6 (20)	17	2

[a] The yield was determined by ^{1}H NMR spectroscopy of a reaction aliquot; internal standard: dibenzyl ether (25 mol%). [b] NR = no reaction; the desired product was not detectable, only starting materials were detected (^{1}H NMR analysis of a reaction aliquot).

None of the alkaline earth metal hexamethydisilazide catalysts was able to catalyse the reaction between siloxane **136b** and imine **56b** (entries 1-3). Only the addition of a ligand gave the intended product, albeit in only 17% yield (entry 4). Overall, alkaline earth metals were not found to be suitable catalysts in the allylation of imines using allylsiloxanes.

Due to the promising results with NaHMDS in dioxane, an initial imine scope was investigated to probe the applicability of the developed method. Different imines were reacted with a slightly increased excess of siloxane **136b**. Aromatic, heteroaromatic and aliphatic aldimines were used to give products **236** (Table 47).

Table 47: Imine scope of the allylation using allyltrimethylsiloxane

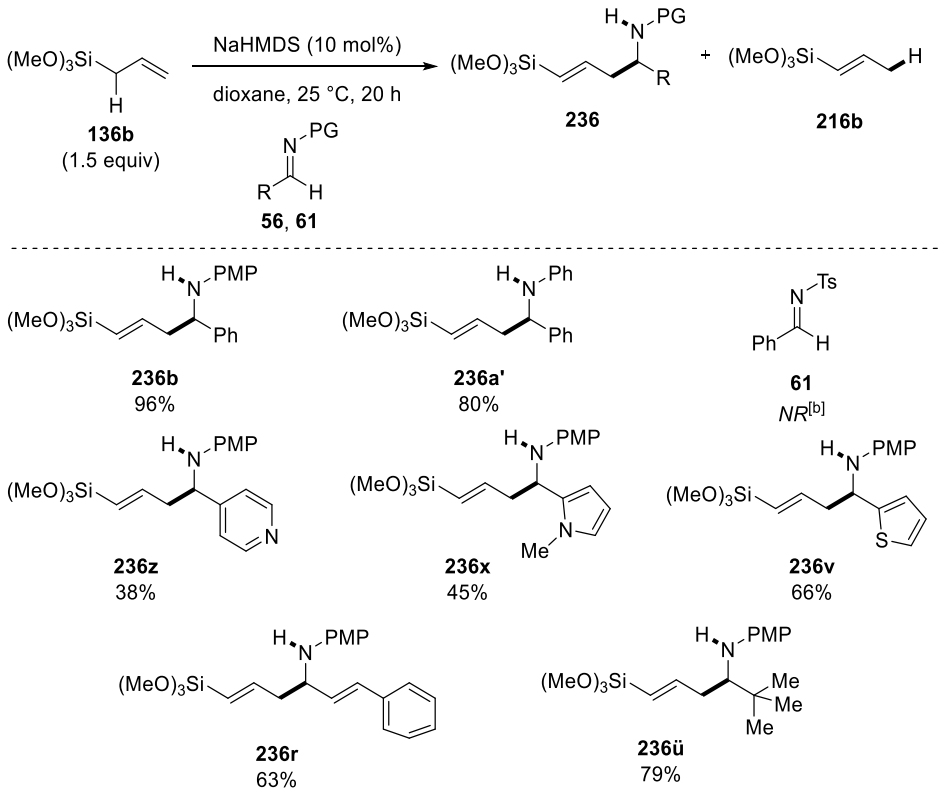

The yield was determined by ^{1}H NMR spectroscopy of a reaction aliquot; internal standard: dibenzyl ether (25 mol%). [b] NR = no reaction; the desired product was not detectable, only starting materials were detected (^{1}H NMR analysis of a reaction aliquot).

Both the *N*-PMP- and the *N*-Ph-protected benzaldimine gave good to excellent yields in the formation of functionalised homoallylic amines **236b** and **236a'**. Like in the case of the cinnamylations with allylbenzene, *N*-Ts-protected aldimine **61** showed no reactivity. Heteroaryl-substituted imines were tolerated under these conditions including pyridyl-, pyrrolyl-, and thienyl-substitution, albeit with decreased yields of 38–66%. Surprisingly, cinnamaldimine product **236r** was obtained in 63% yield, which has been an unsuccessful substrate the case for the unfunctionalised cinnamylation. Finally, alkyl-substituted aldimines were shown to be reactive and product **236ü** was obtained in 79% yield. Like in previous reactions with this imine, a relatively high level of isomerisation was observed (50%).

In summary, the catalytic system that had been developed for the allylations using allylbenzene was directly applicable to the use of allylsiloxane **136b**, and a variety of homoallylic amines containing a vinyl siloxane functional group were obtained in good to excellent yields. To the best of our knowledge, this method is the first Brønsted base activation of allyl–Si reagents for C–C bond formations that allow for the incorporation of the Si functionality into the final compound.

2.3.3.2 Boron

Bpin

Allyl–Bpin (**15a**) was chosen as the most suitable model substrate for C–C bond formations with imines. In isomerisation reactions, it was shown to be activated by a Brønsted base catalyst (Table 35, p 89). Like in previous examples, this pro-nucleophile was also reacted with the PMP-protected aldimine **56b** using alkali metal amides as the catalyst in different solvents (Table 48).

Table 48: Alkali metal amide catalysed allylation using allylboronate 15a

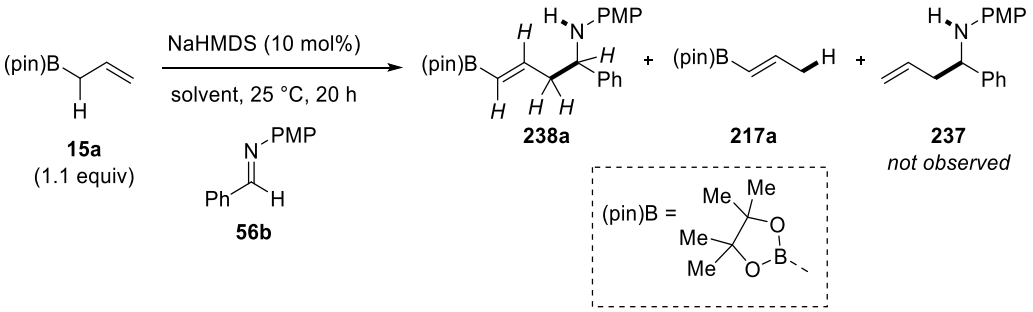

Entry	Cat (x mol%)	Solvent	Yield 238a (%)[a]	217a (%)[a]
1	LHMDS (20)	dioxane	32	0
2	NaHMDS (10)	dioxane	47	0
3	KHMDS (10)	dioxane	14	0
4	NaHMDS (10)	THF	23	7
5	NaHMDS (10)	DMF	72	37
6	NaHMDS (10)	PhCN	5	8

[a] The yield was determined by ^{1}H NMR spectroscopy of a reaction aliquot; internal standard: dibenzyl ether (25 mol%).

^{1}H NMR spectroscopy showed the formation of signals at δ = 5.6 ppm (J_{trans} = 17.8 Hz) for one of the alkenyl signals, δ = 4.8 ppm for the benzylic position, and δ = 2.7 and 2.6 ppm for the two allylic hydrogens. Integration with respect to the internal standard, DBE, showed that **238a** was formed in 14–47% yield in dioxane (entries 1-3). No side-product other than the isomerised starting material **217a** was observed. NaHMDS was chosen as the best alkali metal amide catalyst and was used in THF, DMF, and PhCN respectively (entries 4-6). This solvent screening revealed that the use of both THF and PhCN gave lower yields in both reactions (entries 4 and 6). DMF was a more suitable solvent for the formation of product **238a**; a yield of 73% was obtained (entry 5). However, the selectivity of this reaction remained challenging as the remaining pro-nucleophile isomerised entirely.

In order to investigate if other catalysts displayed a higher selectivity, both stronger lithium and alkaline earth metal amides were used in the allylation of imine **56b** with allyl boronic ester **15a** (Table 49).

Table 49: Catalyst screening for the allylation using allyl boronate 15a

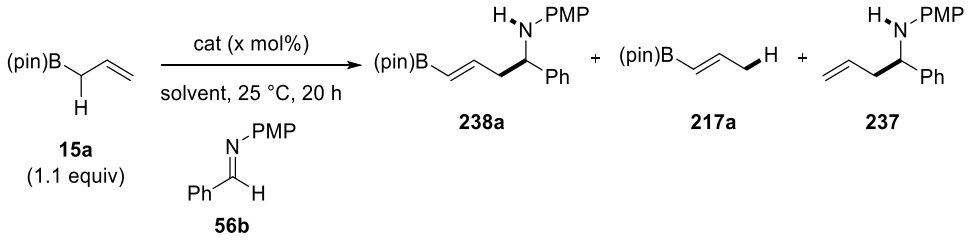

Entry	Catalyst (x mol%)	Solvent	Yield 238a (%)[a]	217a (%)[a]	237 (%)[a]
1	LDA (10)	dioxane	*NR*[b]	-	-
2	LDA (10)	DMF	23	8	5
3	LTMP (10)	dioxane	1	0	2
4	LTMP (10)	DMF	2	0	0
5	$Mg(HMDS)_2$ (20)	dioxane	*NR*[b]	-	-
6	$Ca(HMDS)_2$ (20)	dioxane	0	0	30
7	$Sr(HMDS)_2$ (20)	dioxane	0	0	100

[a] The yield was determined by ^{1}H NMR spectroscopy of a reaction aliquot; internal standard: dibenzyl ether (25 mol%). [b] NR = no reaction; the desired product was not detectable, only starting materials were detected (^{1}H NMR analysis of a reaction aliquot).

No reaction was observed when LDA was used as the catalyst in dioxane (entry 1). In DMF, however, product **238a** was formed in 23% yield; the formation of isomer **217a** (8%) and direct allylation product **237** (5%) was also observed (entry 2). Despite being present in small quantities only, side-product **237** could be identified by comparison with literature reported ^{1}H NMR spectroscopic data.[103] The use of the more basic LTMP resulted in lower product yields in both dioxane and DMF (entries 3 and 4). When looking at the results of the alkaline earth metal amide catalysts, very different reaction outcomes were observed. No reaction was observed for the reaction using magnesium amide even at 20 mol% catalyst loading (entry 5). Both the calcium and the strontium analogues did not give the desired product **238a**, but instead catalysed the formation of side-product **237** (entries 6 and 7). This difference in product selectivity was unexpected because the loss of the boronic ester functional group had not previously been observed in >5% yield. Overall, the results of NaHMDS in DMF could not be improved by changing the catalyst so a yield of 72% remained the best result for the functionalised allylation of imines, which represents the first Brønsted base activation of this substrate in C–C bond formations.

Boranes and Boron-ate Species

Allyl–9BBN (**15b**) could not be used as a pro-nucleophile in this reaction because the background allylation reaction with imine **56b** proceeded smoothly in the absence of a catalyst at room temperature (Scheme 84).[104] Dialkyl-substituted boranes are much more Lewis acidic as indicated by their chemical shift in ^{11}B NMR spectroscopy. While allyl–Bpin shows a signal at δ = 32 ppm, allyl–9BBN appears at δ = 80 ppm. The oxygen-substituents in boronic acids and esters can donate electron density to the vacant π orbital on B. For alkyl-substituents, this effect cannot take place, leading to an increased electrophilicity. The coordination of imine **56b** lead to the formation of a stable transition state, where the allylation occurred with boron transfer to the amine, followed by protonation. For proof of principle, NaHMDS was added to the reaction mixture in catalytic amounts, but no incorporation of the borane into the final product was observed in either dioxane or THF.

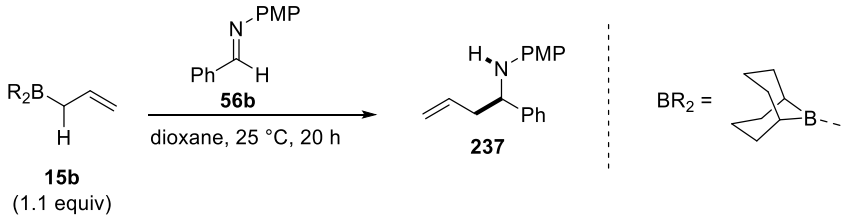

Scheme 84: Uncatalysed allylation of imine 56b

Next, C–C bond formations with MIDA boron-ate and trifluoroboron-ate complexes as pro-nucleophiles were attempted using different catalysts and solvents. First, MIDA boron-ate **15c** was used using sodium and potassium amide catalysts both in the presence and in the absence of a crown ether ligand (Scheme 85).

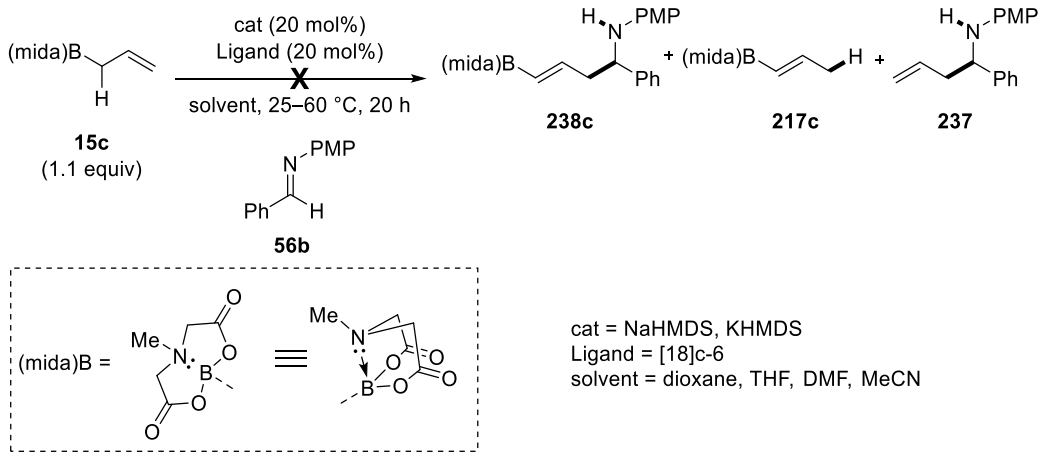

Scheme 85: MIDA-boron-ate allylations

No reaction was observed under any of the employed conditions, even when heating up to 60 °C. Next to dioxane, reactions were carried out in polar aprotic solvents such as THF,

DMF, and MeCN. None of these reactions showed the formation of any products and only starting materials were recovered based on ^{1}H NMR spectroscopy.

Next, potassium trifluoroboron-ate **15d** was examined in the same reaction. Again, different catalyst systems were explored using polar aprotic solvents to ensure maximum solubility. Reaction monitoring was performed by ^{1}H NMR spectroscopy in D_2O due to the low solubility of the pro-nucleophile in $CDCl_3$ (Scheme 86).

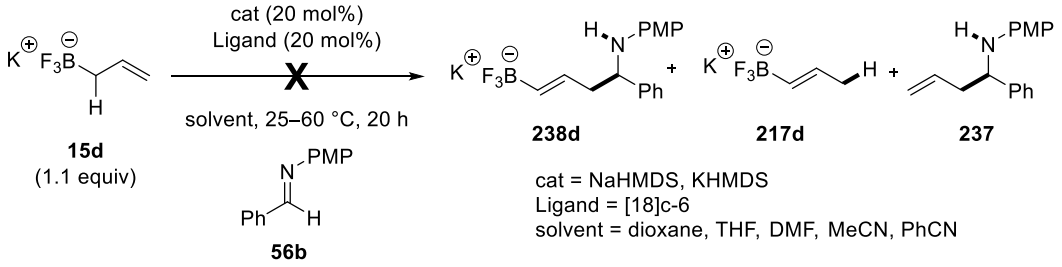

Scheme 86: Allyl–BF_3K allylations

None of the conditions allowed for product **238d** to be obtained. Reactions were carried out in dioxane, THF, DMF, MeCN, and PhCN, but neither the desired product, nor any of the side-products were observed and aliquot ^{1}H NMR spectroscopy only showed signals for the starting materials. For both boron-ate complexes, a high reactivity was expected as the tetravalent boron atoms were much less electrophilic. However, solubilising the corresponding pro-nucleophiles and products in aprotic solvents proved difficult, which may account for their poor reactivity.

2.3.3.3 Tin, Magnesium and Palladium

$SnBu_3$

The third type of allylic metal reagents was the use of tin, which had not been a successful candidate in the isomerisation reaction (Table 35, p 89). Again, different alkali metal amide catalysts were used for C–C bond formations in dioxane and THF (Scheme 87). None of these conditions resulted in the activation of pro-nucleophile **7**; only starting materials were recovered based on ^{1}H NMR spectroscopy. The use of $M(HMDS)_2$ (M = Ca, Sr) also failed to achieve the activation of this substrate, even in the presence of a crown ether ligand.

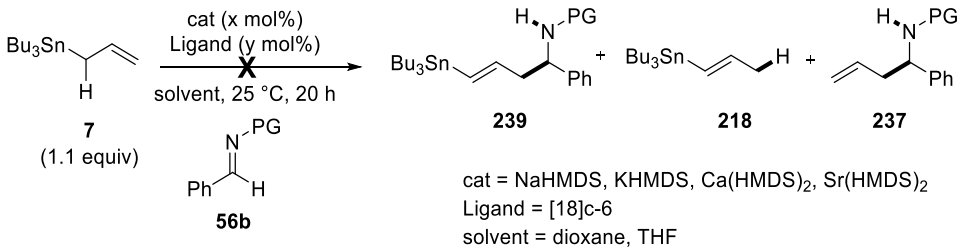

Scheme 87: Allyl-*Sn* in allylation reactions

MgBr

Next, more classical allyl-metal reagents were considered. Commercially available allyl magnesium bromide (**240**) was chosen as a possible pro-nucleophile, but like in the case of allyl–9BBN, the direct reaction with imines posed a challenge. Indeed, allylation of imine **56b** using magnesium reagent **240** was shown to proceed in dioxane and Et_2O at 25 °C or –78 °C respectively (Scheme 88). The addition of NaHMDS to this reaction mixture did not result in any change of reactivity and only unfunctionalised product **237** was obtained regardless of reaction solvent or temperature.

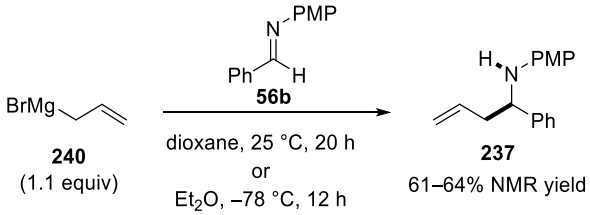

Scheme 88: Allylation of imine 56b using allyl–MgBr

PdCl

As an alternative and less reactive allyl–M reagent, allyl palladium chloride (**241**) was chosen, containing a transition metal in allylic position. This compound is usually encountered as a catalyst or pre-catalyst in cross coupling reactions, but was thought to be a possible reaction partner with potentially high stability of the metallated homoallylic amine product. Palladium complex **241** is commercially available as a dimeric structure, where each palladium centre binds to one η^3 allylic ligand and is bridged by two chloride ions (Figure 11). Due to the highly delocalised nature of the electron density in the allylic ligands, this substrate was considered to be highly challenging to activate. Studies of allyl–Pd species showed a fast interconversion of *E*- and *Z*-isomers of substituted allyl species in the presence of coordinating anions.[105] It was assumed that the coordination to the metal centre would give rise to a faster equilibrium between the *E*- and *Z*-isomer. Previous studies had shown

that this isomerisation was likely to proceed via an η^1-intermediate.[106] Therefore, it was assumed that the addition of coordinating anions could increase the availability of the σ-complex of **241** leading to a higher reactivity for Brønsted base activation.

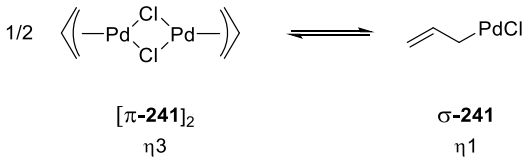

Figure 11: Allyl palladium chloride dimer

No background reaction was observed between allyl palladium chloride **241** and imine **56b**. Metal amides were then screened in different solvents and inorganic additives were added in order to achieve the allylation reaction with allyl–PdCl (Table 50).

Table 50: Allylation reactions using allyl–PdCl

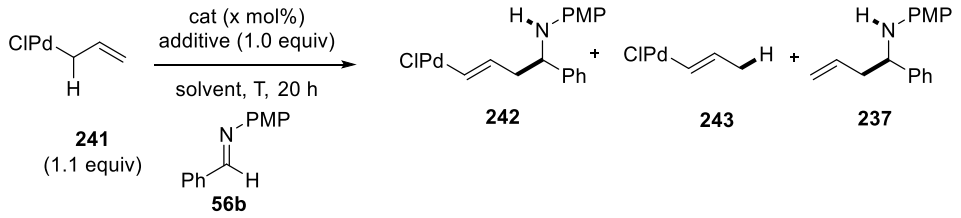

Entry	Cat (x mol%)	Additive	Solvent	T (°C)	Yield 242 (%)[a]
1	NaHMDS (20)	-	dioxane	25-100	*NR*[b]
2	NaHMDS (20)	-	THF	25-100	*NR*[b]
3	$Ca(HMDS)_2$ (10)	-	dioxane	25	*NR*[b]
4	$Sr(HMDS)_2$ (10)	-	dioxane	25	*NR*[b]
5	NaHMDS (10)	KCl	dioxane	25	*NR*[b]
6	NaHMDS (10)	KF	dioxane	25	*NR*[b]
7	NaHMDS (10)	KO^{t}Bu	dioxane	25	*NR*[b]
8	NaHMDS (10)	KCl	DMF	25	*NR*[b]
9	NaHMDS (10)	KF	DMF	25	*NR*[b]
10	NaHMDS (10)	KO^{t}Bu	DMF	25	*NR*[b]

[a] The yield was determined by 1H NMR spectroscopy of a reaction aliquot; internal standard: dibenzyl ether (25 mol%). [b] NR = no reaction; the desired product was not detectable, only starting materials were detected (^{1}H NMR analysis of a reaction aliquot).

No reaction between **241** and **56b** was observed when the alkali or alkaline earth metal amide catalysts (10–20 mol%) were used (entries 1-4). Heating the reaction did not result in any formation of products. Instead, a black reaction colour was observed suggesting partial decomposition of the pro-nucleophile. Dry aliquot conditions in C_6D_6 showed the formation of new allylic species in ^{1}H NMR spectra, but these new signals disappeared when using wet NMR solvents. By adding coordinating anions to the reaction mixture, the equilibrium was attempted to be shifted towards an allyl–Pd σ-complex. The interaction of the Lewis bases

with the Lewis acidic palladium was thought to favour the formation of an η^1 complex that would be more reactive in Brønsted base activation. However, the addition of equimolar amounts of potassium chloride, fluoride, and *tert*-butoxide did not result in the activation of this pro-nucleophile in dioxane (entries 5-7) or DMF (entries 8-10). Unfortunately, the activation of this challenging substrate was not achieved. Further investigations would be required in order to obtain the desired palladium-containing homoallylic amines.

2.3.4 Functionalised C–C Bond Formation Using Allyl–FG

In a similar manner to the allyl–M reagents, the use of a heteroatom-substituted allylic reagents could give rise to novel products containing a vinylic functional group. As introduced in the previous chapter, phosphines and amines, as well as thioethers and ethers have all demonstrated the possibility to be deprotonated using alkali metal amide catalysts. The reaction of the corresponding anionic intermediates with suitable electrophiles would give rise to allylation products that would contain important functional groups, which can be further utilised in subsequent reactions (Scheme 89).

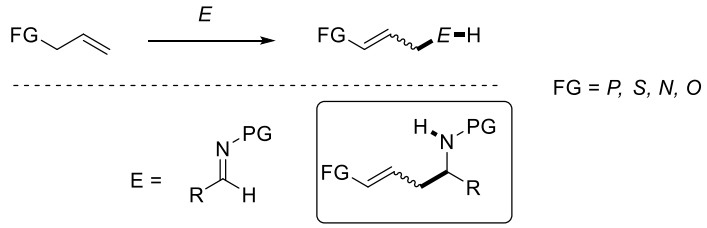

Scheme 89: Allylation of allyl–FG

In all previous reactions, imines have been the most promising electrophiles together with alkali metal amide catalysts. The products of these transformations would contain a functional group in vinylic positions. This structural motif may be exploited for further modifications: For allylic alcohols and amines, the corresponding enol ethers and enamines are nucleophilic in nature and may react with different electrophiles to form molecules of high complexity in only two steps (Scheme 90).

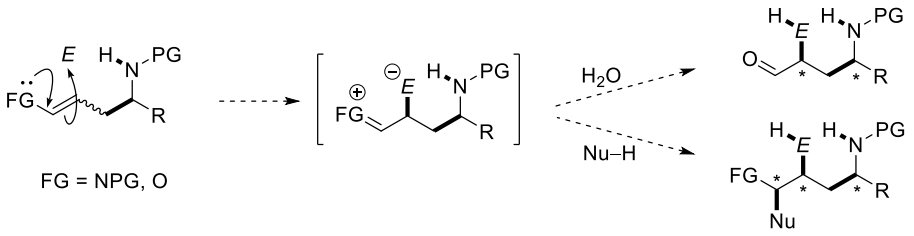

Scheme 90: Applications of enamines and enol ethers

Phosphine-containing products were thought to be useful in the field of ligand synthesis, where the presence of an amine in the same molecule may allow for the formation of bidentate ligands (Scheme 91). To this end, the double bond might need to be reduced in order to achieve a higher degree of flexibility that is required for efficient binding to potential Lewis acids.

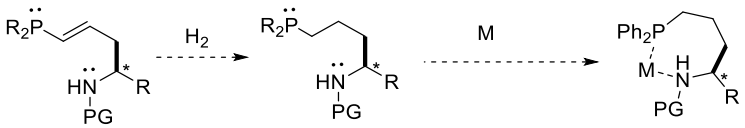

Scheme 91: Applications of vinyl phosphines

In the literature, the deprotonation of these allylic substrates has been performed using stoichiometric amounts of bases, creating allylic anions, usually at low temperatures. Common bases, such as BuLi, but also LDA, have been used for the more reactive substrates (*S*,[107] P,[108] N,[109] O,[110]). The *in situ* generated allyl anions have subsequently been reacted with a range of electrophiles to give the functionalised allylated products of type **246** using aldehydes, ketones, and imines (Scheme 92).[111] However, all methods rely on the stoichiometric use of a Brønsted base, creating waste material and extra costs.

Here, we report the catalytic use of a Brønsted base in allylation reactions using heteroatom-substituted allylic pro-nucleophiles. Reactions were carried out using mild reaction conditions giving linear substituted homoallylic amine products.

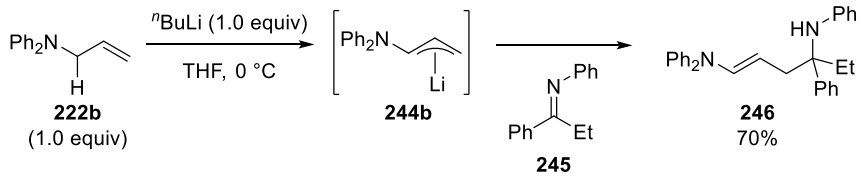

Scheme 92: Stoichiometric deprotonation of allyl–NPh_2

2.3.4.1 Thioethers

First, the possibility of C–C bond formations with heteroatom-substituted allyl reagents was examined using allyl phenyl thioether **219b**. This reagent was reacted with imine **56b** using different alkali metal amides in dioxane and THF (Table 51). Reaction monitoring was carried out using ^{1}H NMR spectroscopy, where product signals were recorded for both the *E*- and the *Z*-isomers of product **247b** as well as isomer **225b**.

Table 51: Metal amide screening for the allylation using allyl phenyl thioether

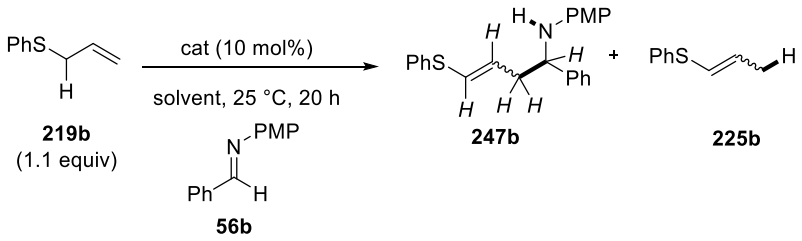

Entry	Cat	Solvent	Yield 247b (%)[a]	*E:Z*	225b (%)[a]
1	LHMDS	dioxane	80	5:1	5
2	NaHMDS	dioxane	91	2:1	16
3	KHMDS	dioxane	42	2:1	66
4	LHMDS	THF	18	4:1	21
5	NaHMDS	THF	64	1:1	44

[a] The yield was determined by ^{1}H NMR spectroscopy of a reaction aliquot; internal standard: dibenzyl ether (25 mol%). [b] NR = no reaction; the desired product was not detectable, only starting materials were detected (^{1}H NMR analysis of a reaction aliquot).

Alkali metal amide catalysts proved to be efficient in the functionalised thio-allylation in dioxane (entries 1-3). The pro-nucleophile was completely consumed in all cases and only product signals for homoallylic amine **247b** or isomerised pro-nucleophile **225b** were visible in the aliquot ^{1}H NMR spectra. Product signals for product *E*-**247b** appeared at δ = 6.2 and 6.0 ppm (J_{trans} = 14.9 Hz) for the alkenyl signals, δ = 4.3 ppm for the benzylic proton, and δ = 2.6 ppm for the two protons in allylic position. Product *Z*-**247b** displayed signals at δ = 6.4 and 5.8 ppm (J_{cis} = 9.6 Hz; alkenyl), δ = 4.4 ppm (benzylic), and δ = 2.8 ppm (allylic). The isomerisation was quantified by integration of the terminal methyl group (*E*-**225b**: δ = 1.9 ppm, 3H, *Z*-**225b**: δ = 1.7 ppm, 3H). Good yields for **247b** were obtained in the LHMDS- and the NaHMDS-catalysed reaction respectively (entries 1 and 2). KHMDS catalysis showed a high degree of isomerisation and consequently lower yields for product **247b** (entry 3). Interestingly, the *E:Z* selectivity varied substantially across these three catalysts: while a clear preference for *E*-**247b** was found when using a lithium amide catalyst (5:1), a decreased selectivity of only 2:1 was observed for both the sodium and the potassium amide. This effect was even more pronounced when the reaction was carried out in THF, where LHMDS catalysed the reaction with a good selectivity, albeit with a low yield (entry 4). The reaction using NaHMDS in THF gave a much better yield, but no geometric selectivity was observed (entry 5).

Next, ligands were screened to develop a more selective method for the formation of product **247b**. During the isomerisation of pro-nucleophile **219b**, it was found that carbene ligands were suitable for improving the *E:Z* selectivity in apolar aromatic solvents (Table 37, p 93). Crown ethers usually had a negative effect on the selectivity of the isomerisation and were

consequently omitted here. Carbenes and a bisoxazoline were chosen for the ligand screening using LHMDS, as this amide has shown the most selective reaction profile (Table 52).

Table 52: Ligand screening for the LHMDS catalysed functionalised allylation

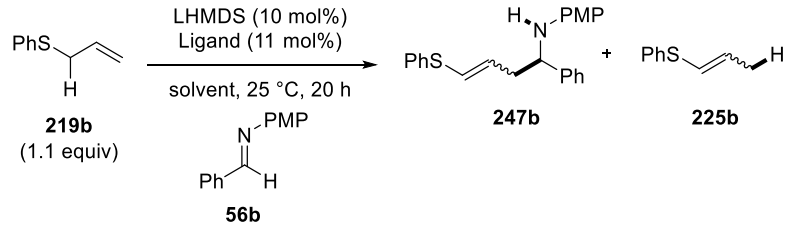

Entry	Ligand	Solvent	Yield 247b (%)[a]	*E:Z*	225b (%)[a]
1	-	dioxane	80	5:1	5
2	SIPr	dioxane	*NR*[b]	-	-
3	SIMes	dioxane	75	1:1	13
4	BOX*	dioxane	13	6:1	0
5	-	PhMe	8	6:1	2
6	SIPr	PhMe	*NR*[b]	-	-
7	SIMes	PhMe	*NR*[b]	-	-
8	BOX*	PhMe	*NR*[b]	-	-

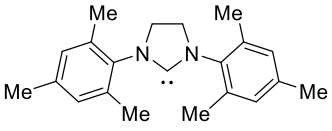

248
SIMes

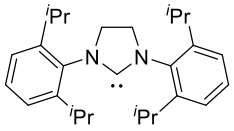

231
SIPr

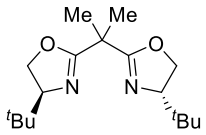

176
BOX*

[a] The yield was determined by ^{1}H NMR spectroscopy of a reaction aliquot; internal standard: dibenzyl ether (25 mol%). [b] NR = no reaction; the desired product was not detectable, only starting materials were detected (^{1}H NMR analysis of a reaction aliquot).

Compared to the reaction with LHMDS in dioxane in the absence of a ligand (entry 1), both carbenes proved to be unsuitable for improving the catalyst's performance (entries 2 and 3). The addition of the SIPr ligand (**231**) resulted in no reaction, whereas the use of SIMes (**248**) gave comparable yields to the unligated catalyst, but no selectivity was obtained. The use of enantiopure BOX ligand **176** slightly improved the selectivity, albeit with only 13% yield (entry 4). In toluene, the reaction catalysed by LHMDS in the absence of a ligand showed a yield of only 8%, but an improved selectivity of 6:1 was observed (entry 5). The use of ligands in this system, however, resulted in a loss of reactivity; no reaction was observed for both carbenes and the bisoxazoline ligands (entries 6-8). As NaHMDS showed the highest overall yield, this catalyst was chosen for another ligand screening (Scheme 93).

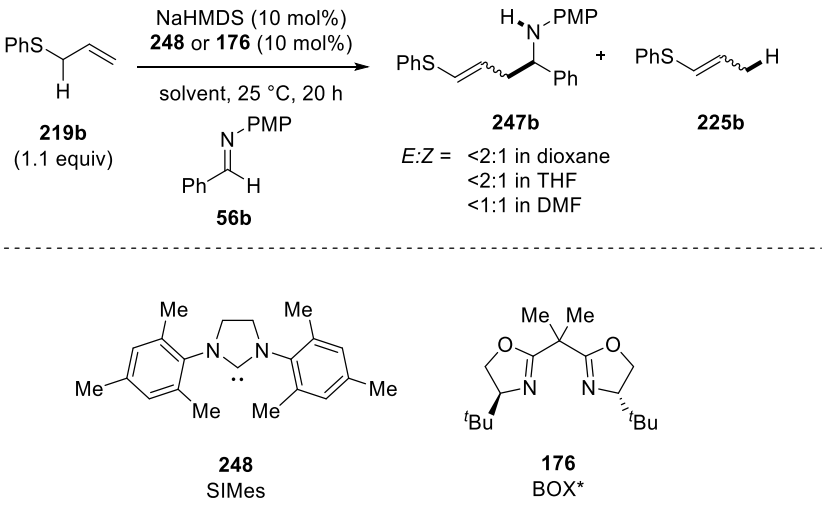

Scheme 93: Ligand screening for the NaHMDS catalysed functionalised allylation

When adding a carbene or a bisoxazoline ligand to the reaction, the *E:Z* ratio of 2:1 was not significantly improved in any coordinating solvent. Reactions carried out in dioxane gave equal or lower selectivities and an increased level of isomerised pro-nucleophile. Reactions in THF showed a slight increase in reactivity compared to the reaction without ligand, as well as a slightly improved *E:Z* selectivity. In DMF, no selectivity was observed, and a 1:1 mixture of geometric isomers was obtained. The most likely cause for this lack of improvement was the choice of solvent: In coordinating solvents, the effect of the ligand binding to the metal amide may be less pronounced as the ligand competes with the solvent for coordination.

Finally, alkaline earth metal amides were also examined with respect to their ability to catalyse the thio-allylation. Magnesium, calcium, and strontium amides were used in dioxane (Scheme 94).

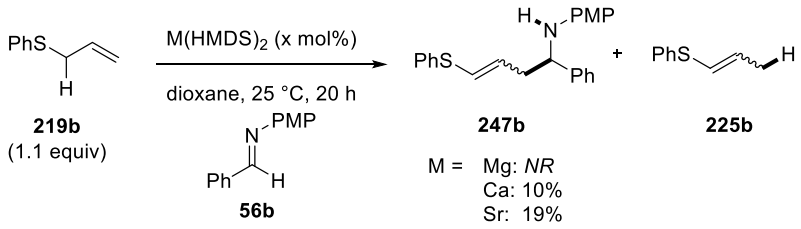

Scheme 94: Alkaline earth metal amide catalysed functional allylation

The magnesium amide gave no reaction; only starting materials were observed in aliquot ^{1}H NMR spectroscopy of the reaction mixture. Both calcium and strontium amide catalysed the reaction in low yields, but the selectivity was not determined. Overall, the best *E:Z* ratio of 6:1 was observed for the use of LHMDS in toluene, although only low yields were recorded. The use of LHMDS in dioxane gave a similar level of selectivity (*E:Z* = 5:1) with a much higher yield of 80%. Generally, certain effects of the carbene and bisoxazoline ligands on the

metal's reactivity and selectivity were found, suggesting that binding of these ligands to alkali metal centres was possible. However, effects were much less pronounced than in the case of crown ethers, which were assumed to bind much more strongly to the alkali metal ions. However, the potential for asymmetric transformations has been shown through these reactions, where the use of chiral ligands can be investigated further in the development of new enantioselective methods for the formation of sulfur-containing homoallylic amines of type **247**.

2.3.4.2 Ethers

Next, the lighter analogue, allyl phenyl ether (**221b**), was investigated. This pro-nucleophile has been shown to be much more difficult to activate in isomerisation reactions (Table 42, p 99). Furthermore, the major isomerised product was found to be the *Z*-isomer, which was originally considered to be thermodynamically less stable. Pro-nucleophile **221b** was found to be active only in the presence of a crown ether-ligated alkali metal amide. However, the use of KHMDS as a catalyst often lead to increased levels of isomerisation in previous allylation reactions. Therefore, the allylation of imine **56b** with allyl ether **221b** was conducted using NaHMDS and a range of ligands in dioxane and THF (Table 53).

Table 53: Ligand screening for the allylation with allyl phenyl ether

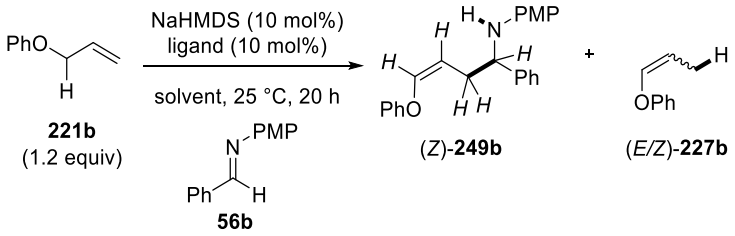

Entry	Ligand	Solvent	Yield 249b (%)[a]	227b (%)[a]
1	-	dioxane	*NR*[b]	-
2	-	THF	*NR*[b]	-
3	[18]c-6	dioxane	26	53
4	[18]c-6	THF	15	99
5	[15]c-5	dioxane	24	33
6	SIPr	dioxane	*NR*[b]	-
7	SIMes	dioxane	*NR*[b]	-

[a] The yield was determined by ^{1}H NMR spectroscopy of a reaction aliquot; internal standard: dibenzyl ether (25 mol%). [b] NR = no reaction; the desired product was not detectable, only starting materials were detected (^{1}H NMR analysis of a reaction aliquot).

In the absence of a ligand, NaHMDS was not able to catalyse the oxy-allylation in either dioxane or THF at 25 ºC (entry 1 and 2). Heating the reaction mixture to 40 °C allowed for

the formation of product **249b** in 14% yield. *Z*-**249b** showed chemical shifts at δ = 6.5 and 4.8 ppm (J_{cis} = 6.1 Hz), δ = 4.3 ppm, and δ = 2.8 and 2.6 ppm in ^{1}H NMR spectroscopy for the alkenyl, benzylic, and allylic positions respectively. Further quantification was facilitated by integration of the product's aromatic PMP-group signals at δ = 6.7 and 6.4 ppm (2H each). The formation of *E*-**249b** could not be observed in any of these reactions. This meant that this C–C bond-forming reaction either proceeded with very high selectivities or that all product peaks for both isomers overlapped. However, considering the difference of the alkene shifts for isomerised pro-nucleophile **227b** in ^{1}H NMR spectroscopy (δ = 4.9 or 5.4 ppm for the *Z*- or *E*-isomer respectively), it was assumed that the lack of additional sets of product signals was caused by the absence of *E*-**249b** in these reactions. Side-product **227b** was quantified by integration of the terminal methyl H signals for the two geometric isomers (distinct signals, both at δ = 1.7 ppm).

The additional use of a crown ether ligand at room temperature gave product **249b** in 15–26% (entries 3-5). The level of isomerisation was relatively high in all these reactions (up to 99% in THF). Carbene ligands were then examined (entries 6 and 7). The use of these ligands did not increase the metal amide's reactivity; a reaction was not observed.

As the catalyst's reactivity was generally low, the potassium amide-catalysed reactions were studied next. Knowing that the pro-nucleophile was prone to isomerisation once activated, two equivalents of this substrate were used (Table 54).

Table 54: KHMDS catalysed allylation with allyl phenyl ether

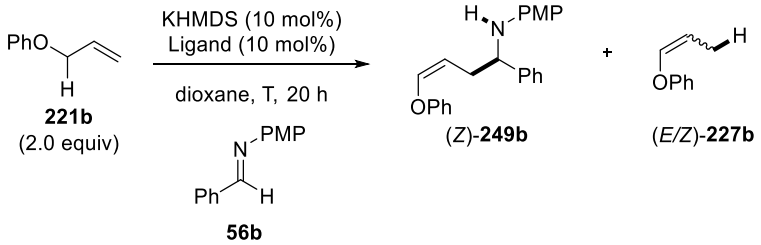

Entry	Ligand	T (°C)	Yield 249b (%)[a]	227b (%)[a]
1	-	25-40	*NR*[b]	-
2	-	60	19	17
3	[18]c-6	25	24	27
4	[18]c-6	60	49	91
5	[18]c-6	80	50	111
6	[15]c-5	25-40	5	13
7	[15]c-5	60	7	31
8	[DB18]c-6	60	*NR*[b]	-

[a] The yield was determined by ^{1}H NMR spectroscopy of a reaction aliquot; internal standard: dibenzyl ether (25 mol%). [b] NR = no reaction; the desired product was not detectable, only starting materials were detected (^{1}H NMR analysis of a reaction aliquot).

The reaction with unligated KHMDS gave no reaction at 25–40 ºC (entry 1), but 19% of product **249b** was obtained when the reaction was conducted at 60 °C (entry 2). The use of [18]crown-6 as a ligand at 25 ºC gave similar results and a yield of 24% was recorded (entry 3). When performing this reaction at 60–80 °C, yields increased to up to 50% (entries 4 and 5). At the same time, the level of isomerisation also increased and around twice the amount of isomer product **227b** was obtained. Other ligands performed much poorer in this oxy-allylation: The use of [15]crown-5 resulted in low yields; no reaction was observed when the more rigid [dibenzo-18]crown-6 ligand was used (entries 6-8).

Reactions with KHMDS were then carried out in other solvents, such as THF, TBME, and DMF both with and without crown ether ligands (Scheme 95). These reactions showed that the use of more polar solvents increased the reactivity of KHMDS, but best results were obtained by using [18]crown-6 as a ligand. In all these reactions, high levels of isomerisation were observed, which were increased compared to the use of dioxane (up to **227b**:**249b** = >4:1). Other reactions with [15]crown-5 or [dibenzo-18]crown-6 showed no improvement for the developed reaction outcomes and usually resulted in increased levels of isomerisation.

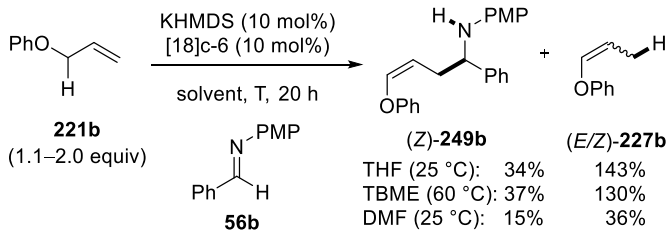

Scheme 95: KHMDS catalysed allylations with allyl phenyl ether

Finally, lithium amide bases were examined for their ability to catalyse the oxy-allylation of imine **56b** with allyl ether **221b**. As both NaHMDS and KHMDS showed high levels of isomerisation when the activation of the pro-nucleophile was achieved, it was hoped that LHMDS would allow for a more selective reaction to proceed. Additionally, LDA and LTMP were used as more basic amides. Unfortunately, all three lithium amides proved to be inactive in dioxane and THF (Scheme 96). The addition of [18]crown-6 to the reaction also did not show any product formation. Heating these reactions to 40 °C or conducting the reactions with LTMP or LDA in DMF also did not give product **249b**.

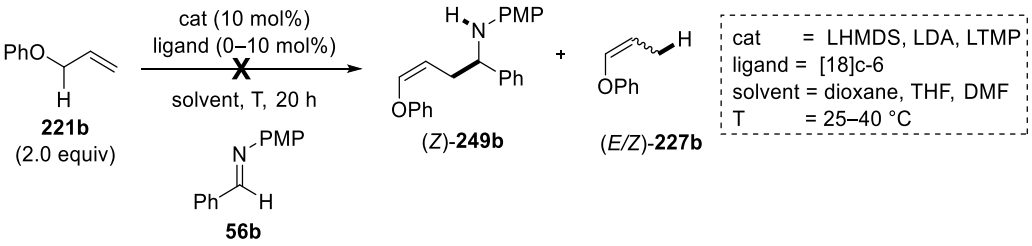

Scheme 96: Lithium amide catalysed allylation reactions

The enol ether-containing homoallylic amine **249b** could be formed in 50% yield by using excess allylic reagent and a strong alkali amide metal base catalyst system (KHMDS/[18]c-6). The selectivity with respect to undesired isomerisation of the pro-nucleophile was poor, regardless of the catalytic system used. However, a catalytic method for the addition of allyl ethers to electrophiles has been demonstrated, providing highly complex structures in a single step.

2.3.4.3 Amines

NMe_2

The use of an allylic amine in C–C bond formations with imines was of particular interest, because the enamine-containing homoallylic amine products of type **250** were thought to be reactive intermediates that may be further functionalised easily. The isomerisation of dimethyl allylamine **222a** was achieved only by using LTMP at 60 °C (Table 39, p 95). In C–C bond formations with imine **56b**, LTMP and other alkali or alkaline earth metal amide catalysts were screened in dioxane, THF, and DMF at temperatures ranging from 25–60 °C (Scheme 97). None of the conditions showed the formation of product **250a** or isomerised starting material **228a**. Furthermore, the addition of crown ether ligands did not increase the desired reactivity.

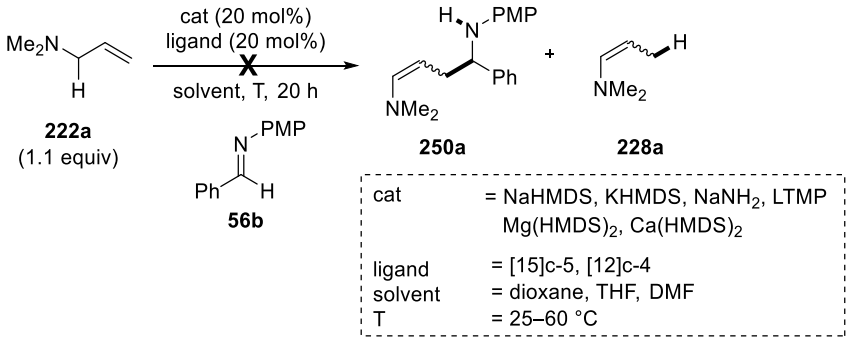

Scheme 97: Allylations using dimethyl allylamine

It was assumed that a stronger base was required to activate the dimethyl-substituted allylic amine. The use of LTMP showed some potential in isomerisation reactions, but its reactivity was not increased with crown ethers. Despite their high basicity, the lithium amides have generally shown milder reaction profiles than their sodium or potassium analogues. However, NaTMP and KTMP are not commercially available. A similar challenge in the case of alkyllithium bases has been addressed by using Schlosser's base: Here, an alkyllithium was mixed with an alkali metal *tert*-butoxide in order to generate a more reactive alkylsodium or alkylpotassium species *in situ*.[112] It was therefore anticipated that a similar method may be applicable to lithium amides, where the strong binding preference of lithium for the alkoxide base would serve as a driving force to generate heavier TMP-complexes (Scheme 98).

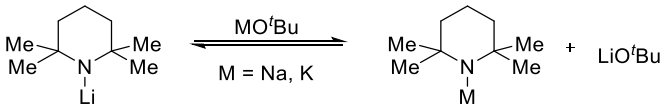

Scheme 98: *In situ* generation of M–TMP complexes

NaO^{t}Bu or KO^{t}Bu (20 mol%) were used in combination with LTMP or LDA (20 mol%) for the *in situ* generation of the corresponding sodium and potassium amides. When tested in the amino-allylation between **222a** and **56b**, no reaction was observed in dioxane and THF. Heating these reactions up to 60 °C did not result in the formation of any products either. As the isomerisation results showed a much increased reactivity of the diphenyl-substituted allylic amine **222b**, our attention was focussed on this pro-nucleophile.

NPh_2

The use of diphenyl allylamine (**222b**) had shown good yields in the isomerisation reaction and required relatively mild reaction conditions for the formation of the corresponding products **228b** (Table 40).

Table 40, p 96). Therefore, the reactions of amine **222b** with imine **56b** were attempted using metal amide catalysts in the absence of a ligand in dioxane and THF. Unfortunately, none of the alkali metal HMDS-complexes displayed any reactivity. Also the use of stronger amides such as LDA and LTMP resulted in no reaction. Therefore, the use of a crown ether ligand was deemed necessary for the reaction to proceed, and a metal screening was conducted in the presence of [18]crown-6 (Table 55).

Table 55: Catalyst screening for the allylation with *N,N*-diphenyl allylamine

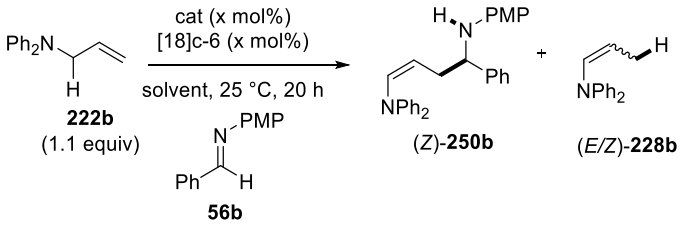

Entry	Cat (x mol%)	Solvent	Yield 250b (%)[a]	228b (%)[a]
1	LHMDS (20)	dioxane	8	7
2	NaHMDS (10)	dioxane	42	21
3	KHMDS (20)	dioxane	37	50
4	NaHMDS (20)	THF	20	89
5	KHMDS (20)	THF	35	66

[a] The yield was determined by ^{1}H NMR spectroscopy of a reaction aliquot; internal standard: dibenzyl ether (25 mol%).

The reactions using the alkali metal amide catalysts in dioxane followed a trend of increased reactivity for the heavier metals. While LHMDS gave product **250b** in 8% yield alongside a similar level of isomerisation (entry 1), NaHMDS showed a much improved reactivity (42%; entry 2). The formation of product *Z*-**250b** was monitored by ^{1}H NMR spectroscopy, where indicative new signals appeared at δ = 6.2 and 4.9 ppm (J_{cis} = 8.2 Hz) for the alkenyl, δ = 4.2 ppm for the benzylic, and δ = 2.2 ppm for the two allylic hydrogen atoms. Further evidence for the new product was provided by new signals appearing in ^{1}H NMR spectra for the aromatic PMP group at δ = 6.7 and 6.4 ppm (*J* = 8.9 Hz, 2H each). Like in the case of the allyl ethers, product *E*-**250b** could not be detected with separate signals. Again, the structurally related isomerised pro-nucleophile product **228b** displayed distinct signals for the *E*- and *Z*-isomers, which were quantified by integration of the allylic signals (δ = 1.7 and 1.3 ppm respectively). The distinct alkenyl signals for *Z*-**228b** (δ = 5.0 ppm) and *E*-**228b** (δ =

4.7 ppm) suggested that C–C bond formation product *E*-**250b** should be identifiable and the lack of the corresponding signals suggested its absence in all reactions.

The reaction with KHMDS gave product **250b** in 37% yield because of an increased level of isomerisation (entry 3). Reactions in THF showed a high activity for both NaHMDS and KHMDS; the ratio between C–C bond formation and isomerisation was better using KHMDS (entries 4 and 5). As the highest product yield was obtained using NaHMDS and [18]crown-6 in dioxane, a ligand screening was performed in this solvent in order to identify any other suitable crown ethers that could activate the catalyst sufficiently. Due to the high levels of isomerisation observed, reactions were carried out using a larger excess of allylamine **222b** (2.0 equiv; Table 56).

Table 56: Ligand screening for the allylation using diphenyl allylamine

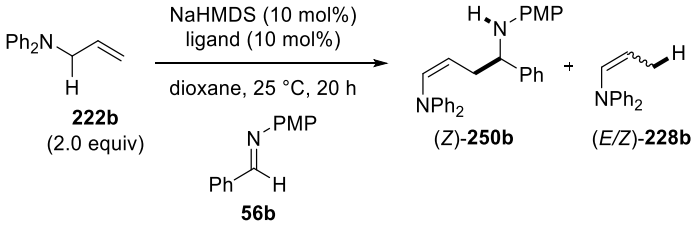

Entry	Ligand	Yield 250b (%)[a]	228b (%)[a]
1	-	*NR*[b]	-
2	[18]c-6	65	134
3	[DB18]c-6	9	10
4	[15]c-5	35	89
5	[12]c-4	*NR*[b]	-

[a] The yield was determined by ^{1}H NMR spectroscopy of a reaction aliquot; internal standard: dibenzyl ether (25 mol%). [b] NR = no reaction; the desired product was not detectable, only starting materials were detected (^{1}H NMR analysis of a reaction aliquot).

As mentioned before, in the absence of a ligand, the reaction did not proceed (entry 1). The use of [18]crown-6 allowed for the formation of **250b** in 65% yield, albeit with a very high level of side-product formation (134%; entry 2). None of the other crown ether ligands was able to improve the catalyst's performance in this reaction, with yields ranging from 0–35% (entries 3-5).

Next, a solvent screening was conducted to identify the most suitable solvent for the amino-allylation (Scheme 99). Diethyl ether, THF, and benzonitrile were chosen as alternative solvents for the reaction catalysed by NaHMDS/[18]c-6, but product **250b** was obtained in only 0–17% yields. To verify these results, the same solvents were also examined with NaHMDS and [15]crown-5 as the ligand. Product yields were found to be slightly higher

than before (0–31%), but none of the solvents gave superior results to the reactions in dioxane.

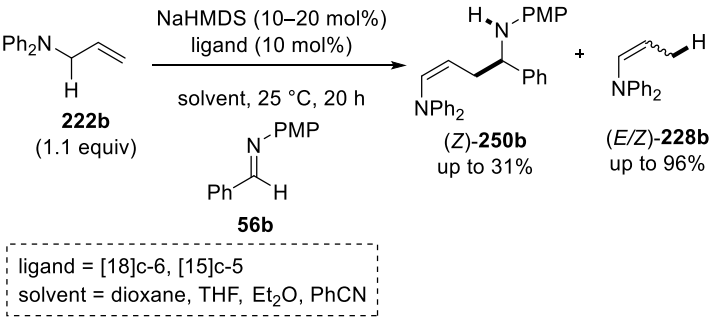

Scheme 99: Solvent screening for the functional allylation with an allylic amine

As none of the developed conditions gave sufficient selectivity for the amino-allylation of imine **56b**, alternative catalyst systems were explored. As KHMDS gave promising results together with [18]crown-6 in dioxane, another solvent screening was performed (Scheme 100). Yields for the reaction with this catalytic system could not compete with the results obtained with NaHMDS. By using 2.0 equiv **222b**, a maximum yield of 43% could be obtained in THF, but the high level of isomerisation (140%) did not allow for this reaction to proceed further.

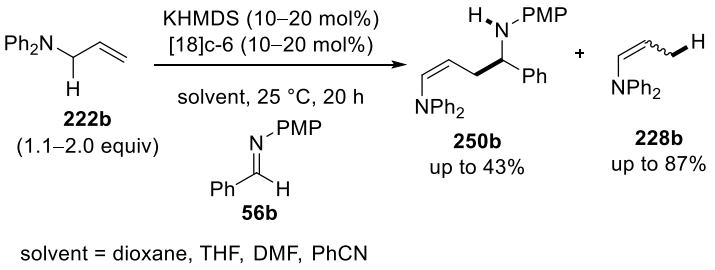

Scheme 100: Solvent screening using KHMDS/[18]c-6

As no change of catalyst system resulted in yields >65%, other methods were attempted in order to increase the product yield. The use of more pro-nucleophile resulted in even higher levels of isomerisation with respect to C–C bond formation. This was linked to an increase of pro-nucleophile concentration resulting in a higher reaction rate for the isomerisation reaction. A successive addition of the pro-nucleophile was attempted, where initially 1.0 equiv was reacted with the imine for 12 h, followed by two consecutive additions of 0.5 equiv after 6 h each. However, no improvement in yield could be observed in these reactions either; aliquot ^{1}H NMR spectroscopy revealed that additional pro-nucleophile added at a later stage was exclusively isomerised to **228b,** and did not participate in any C–C bond formation. A final attempt to improve the reaction yield was attempted by varying the reaction concentration: reactions were carried out with imine molarities ranging from 0.25–

2 M. Unfortunately, initial reactions carried out at 0.5 M concentrations proved to be most successful; increasing or decreasing the concentration did not allow for the improvement of product yield.

Finally, alkali metal alkoxides were tested as catalysts in the reaction of allylamine **222b** with imine **56b**. Solvents such as THF, DMF, and DMSO were tested as the isomerisation using these catalysts had shown that only polar aprotic solvents were able to promote the activation of diphenyl allylamine (Table 57).

Table 57: Metal alkoxides in the functionalised allylation of imines

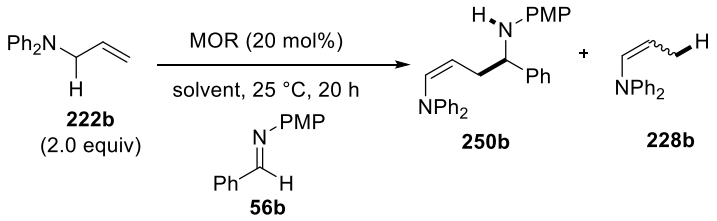

Entry	Base	Solvent	Yield 250b (%)[a]	228b (%)[a]
1	NaO^{t}Bu	THF	*NR*[b]	-
2	KO^{t}Bu	THF	0	87
3	NaO^{t}Bu	DMF	32	85
4	KO^{t}Bu	DMF	28	85
5	KOH	DMF	0	25
6	NaO^{t}Bu	DMSO	10	0

[a] The yield was determined by ^{1}H NMR spectroscopy of a reaction aliquot; internal standard: dibenzyl ether (25 mol%). [b] NR = no reaction; the desired product was not detectable, only starting materials were detected (^{1}H NMR analysis of a reaction aliquot).

The use of NaO^{t}Bu and KO^{t}Bu displayed formation of product **250b**, depending on the reaction conditions. In THF, no reaction was observed for NaO^{t}Bu whereas the use of KO^{t}Bu resulted in exclusive isomerisation (entries 1 and 2). However, the use of DMF as the solvent allowed for the formation of product **250b** in 28–32% yield, albeit with high levels of isomerisation (entries 3 and 4). By using KOH as the catalyst in DMF, only the isomerised substrate was detected (entry 5). The use of DMSO as the solvent also allowed for the exclusive formation of product **250b**, albeit with a low yield of only 10% (entry 6).

As these reaction conditions showed the possibility to use metal alkoxides for the formation of homoallylic amines, it was hypothesised that aldehydes could be more suitable reaction partners, leading to homoallylic alcohol products (Scheme 101). The use of these electrophiles is limited with metal amides catalysts, as these are known to react with aldehydes. This side-reaction is not the case for metal alkoxides and the structural resemblance between the catalyst and the product base suggested a potential reaction.

Unfortunately, initial results with benzaldehyde (**83a**) as the electrophile showed no amino-allylation products.

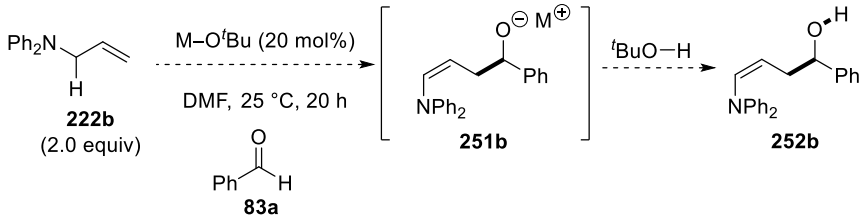

Scheme 101: Allylation of benzaldehyde with diphenyl allylamine

Cyclic urea

In order to expand the scope of the amino-allylation, a different type of amine product was synthesised and examined in the allylation reaction. Allyl urea **253** was used as a commercially available starting material. However, this substrate was unsuitable for Brønsted base catalysis because of its three acidic N–H protons that were expected to be more acidic than the hydrogen in allylic position.[37] Protection of all positions was ensured in a two-step synthesis of compound **222c** (Scheme 102). First, oxalyl chloride was used in order to form cyclic trione product **254**, substituting two of the acidic protons in one step. The urea was subsequently methylated using MeI, giving product **222c** in gram quantities. Purification by recrystallisation, followed by drying (THF solution over 4 Å activated MS, then HV) gave a suitable substrate that could be tested in Brønsted base-activated C–C bond formation.

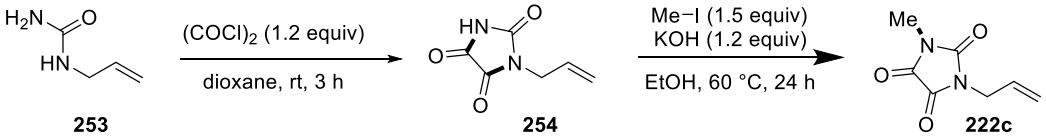

Scheme 102: Protection of allylurea 253

Allylurea **222c** was used in the allylation reaction with imine **56b**, catalysed by alkali metal amides in dioxane or THF (Scheme 103). None of the employed conditions allowed for the activation of this pro-nucleophile. The substitution pattern on the amine functional group was found to be crucial for the ability to activate the pro-nucleophile. As the difference between a dimethyl- and a diphenyl-substituted amine was pronounced, changing the functional group substantially, like in substrate **222c**, was likely to alter the substrate's reactivity. However, other urea substrates may be more reactive.

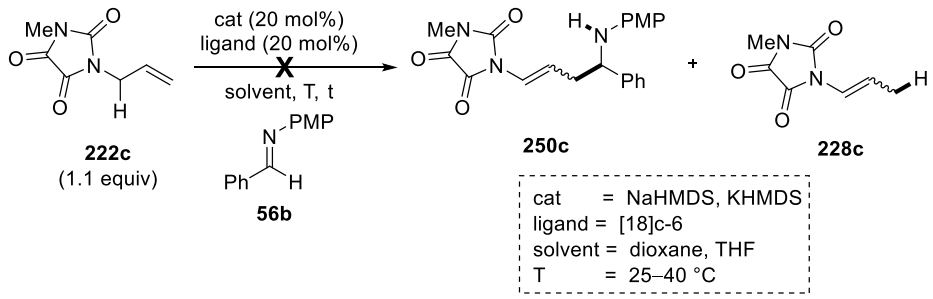

Scheme 103: Allylation with allylurea 222c

2.3.4.4 Phosphines

The heavier analogue of diphenyl allylamine, diphenyl allylphosphine (**220**), was used in the phosphino-allylation with imine **56b**. This substrate was much easier to activate and metal amide catalysts were directly screened in the absence of a crown ether (Table 58).

Table 58: Allylation reactions with diphenyl allylphosphine

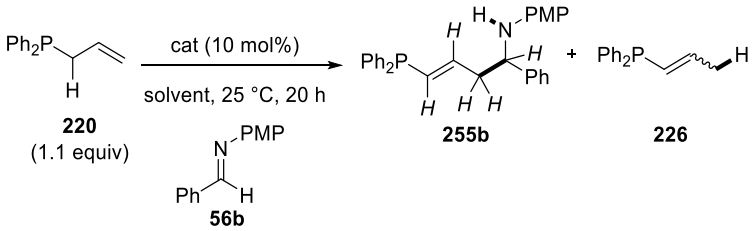

Entry	Cat	Solvent	Yield 255b (%)[a]	226 (%)[a]
1	LHMDS	dioxane	8	7
2	NaHMDS	dioxane	82	25
3	KHMDS	dioxane	14	55
4	NaHMDS	THF	40	59
5	NaHMDS	DMSO	0	100

[a] The yield was determined by ^{1}H NMR spectroscopy of a reaction aliquot; internal standard: dibenzyl ether (25 mol%).

When LHMDS was used as the catalyst for the reaction of allylphosphine **220** with imine **56b** in dioxane, a low product yield of only 8% was observed (entry 1). ^{1}H NMR spectroscopy of reaction aliquots was used for monitoring the reaction. New signals appeared at δ = 6.3 and 6.1 ppm (J_{trans} = 16.5 Hz, alkenyl), δ = 4.4 ppm (benzylic), δ = 2.7 ppm (2H, allylic). ^{1}H NMR signals for the aromatic protons of the PMP group appearing at δ = 6.7 and 6.4 ppm (2H each) could also be used for quantification. Integration of ^{1}H NMR signals at δ = 1.9 and 2.0 ppm allowed for the quantification of isomerised product **226** (*E*-**226** and *Z*-**226** respectively). The formation of *Z*-**255b** was not identified by ^{1}H NMR spectroscopy, as new signals were not detected. However, the absence of distinct signals

does not exclude the formation of *E*-**255b**, as signals might overlap with its geometric isomer.

The NaHMDS-catalysed reaction gave **255b** in 82% yield together with a relatively low level of isomerisation (25%; entry 2). When KHMDS was used as the catalyst, the yield for isomer product **226** increased, while the yield for product **255b** decreased to 14% (entry 3). When NaHMDS was used in THF or DMSO, lower selectivities for product **255b** were observed; most or all of the pro-nucleophile was converted to isomerised product **226** (entries 4 and 5). Therefore, NaHMDS in dioxane was again identified as the best conditions for the phosphino-allylation of imines **56**. In order to increase the yield further, this reaction was carried out for 48 h. The aliquot ^{1}H NMR spectrum of this reaction showed the appearance of new signals that could not be assigned to any of the previously identified products. However, the new signals were assigned to a fully aromatic compound that may form through dehydroamination of product **255b** to give 1,3-diene **256** and *p*-anisidine (**169b**; Scheme 104).[113] Indeed, aromatic signals for *p*-anisidine could be observed as a by-product, confirming the occurrence of an elimination reaction.[114]

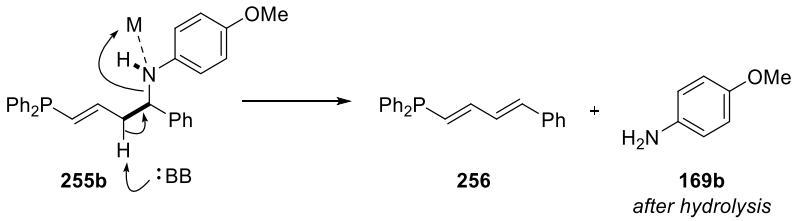

Scheme 104: Dehydroamination of 255b

As reaction conditions were milder, the phosphino-allylation was also attempted using metal alkoxide catalysts. These reactions were conducted in dioxane, DMSO, and DMF (Table 59).

Table 59: Metal alkoxides in the phosphino-allylation

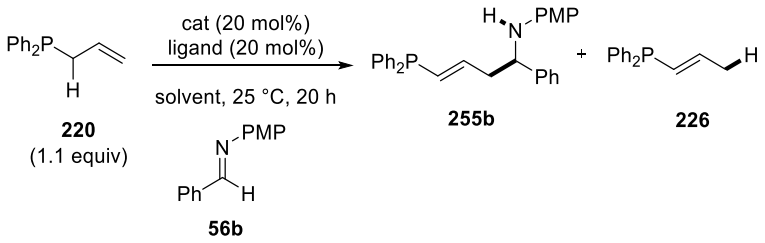

Entry	Cat (Ligand)	Ligand	Solvent	Yield 255b (%)[a]	226 (%)[a]
1	NaO^{t}Bu	-	dioxane	*NR*[b]	-
2	NaO^{t}Bu	[18]c-6	dioxane	12	66
3	NaO^{t}Bu	-	DMSO	0	100
4	NaO^{t}Bu	-	DMF	0	74

[a] The yield was determined by ^{1}H NMR spectroscopy of a reaction aliquot; internal standard: dibenzyl ether (25 mol%). [b] NR = no reaction; the desired product was not detectable, only starting materials were detected (^{1}H NMR analysis of a reaction aliquot).

The reaction of NaO^{t}Bu in dioxane showed no reaction at room temperature (entry 1). In the presence of a crown ether ligand, this catalyst gave product **255b** in 12% yield and a high level of isomerisation (66%; entry 2). When the reaction was carried out in DMSO or DMF in the absence of a crown ether, no C–C bond formation was observed, but most or all of the pro-nucleophile was 'lost' to isomer **226** (entries 3 and 4).

Alternative catalysts were also screened. Sodium hydride was used in dioxane both with and without [18]crown-6 as a ligand, but a reaction was not observed. Like before, reactions carried out in DMSO showed exclusive formation of isomer **226**.

As the best results were obtained using NaHMDS in dioxane, this system was used for screening different imines to investigate the scope of the reaction (Table 60). Due to potential loss of pro-nucleophile to isomerisation, reactions were carried out using 1.5 equivalents allylphosphine **220**.

Table 60: Imine scope for the phosphino-allylation

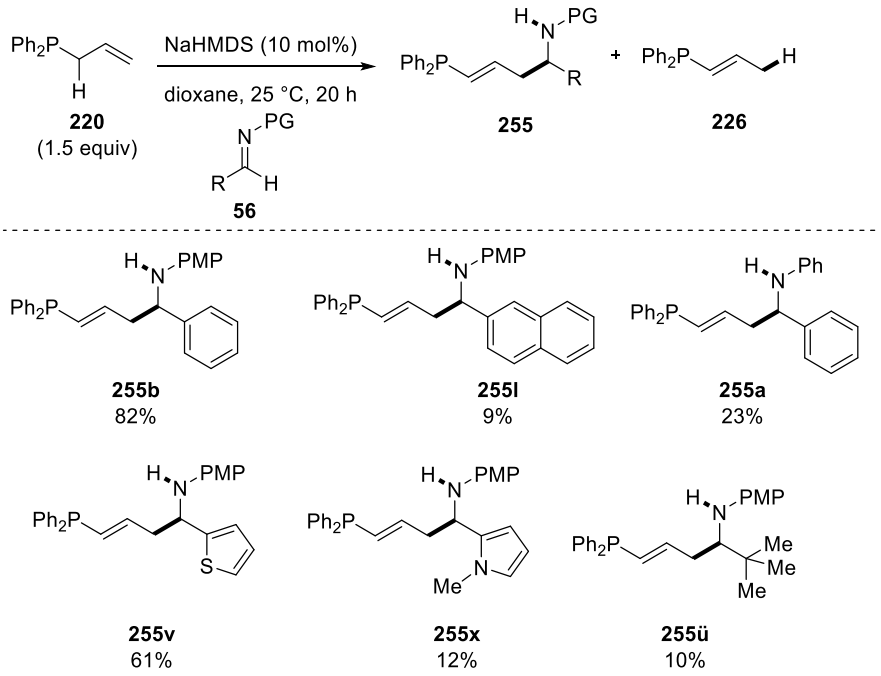

The yield was determined by ^{1}H NMR spectroscopy of a reaction aliquot; internal standard: dibenzyl ether (25 mol%). [b] NR = no reaction; the desired product was not detectable, only starting materials were detected (^{1}H NMR analysis of a reaction aliquot).

Other than the model imine **56b**, most imines performed poorly in the reaction with allylphosphine **220**. The naphthyl-product **255l** as well as pyrrolyl-substituted product **255x** and *tert*-butyl-substituted product **255ü** were all obtained in 9–12% yields. The *N*-Ph-protected imine product **255a** showed a slightly increased yield of 23%, which was still below synthetic use. Only thienyl-substituted product **255v** could be obtained in acceptable yields of 61%. Overall, the allylation using diphenyl allylphosphine was not a very applicable method and will require more development in the future.

2.4 Conclusions and Future Work

The use of a sodium amide catalyst allowed for the activation of allylic C–H bonds and the subsequent addition to imines gave homoallylic amines. The products were obtained with exclusive γ-selectiviy and good to excellent *E:Z* selectivities. This approach was applied to allylbenzene in the first instance, which represented the activation of unfunctionalised olefins in C–C bond formations. Catalyst loadings as low as 1.5 mol%, as well as turnover numbers of >40 have been observed for this reaction. A robustness screening showed the catalyst's intolerance to protic substrates, but a general tolerance of most common functional groups. The scope for both the imine as well as the pro-nucleophile was explored. Substituted aryl-, heteroaryl- and *tert*-alkyl-substituted *N*-PMP-protected aldimines, as well as substituted allylbenzenes and allylpyridine furnished a variety of >30 different linear homoallylic amines. Initial mechanistic investigations demonstrated the presence of an induction period, which suggested an initiative role of the metal amide catalyst. Further experiments with substrate mimics showed that a catalytic pathway was also likely to occur. Further work in this field would require a more detailed look at reaction kinetics, as well as Hammet plots for both the imine and the allylbenzene. Furthermore, mass spectrometric analysis under inert conditions may allow for the detection of highly sensitive reaction intermediates (Figure 12).

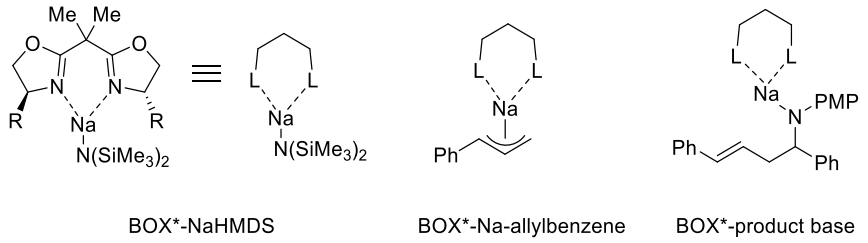

Figure 12: Potential metallated chiral intermediates

The isomerisation of allylbenzene was observed as a side reaction of the C–C bond forming reaction. This formation of styrene products was optimised using a catalyst system composed of KHMDS and a crown ether ligand. Excellent *E:Z* selectivities were obtained for this reaction and a substrate scope showed the applicability of the method to a fairly broad range of substituted allylbenzenes. A robustness screening may elucidate other functional group tolerance in the future. Furthermore, competition reactions may reveal the selectivity of the allylbenzene isomerisation over other alkenes that could be present in a substrate for potential application in more complex syntheses (Scheme 105).

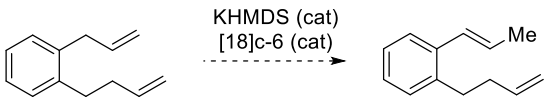

Scheme 105: Predicted selective isomerisation of allylbenzenes

The isomerisation reaction was then applied to allylic substrates, where the phenyl group of allylbenzene was replaced with a metalloid or another functional group. The isomerisation of allylsilanes and boronic esters has been demonstrated, while other metals such as tin did not show any intended reactivity. Allylic phosphines and thioethers, which are both known to stabilise α-anions, were also isomerised using the developed conditions, albeit with a low *E:Z* selectivity for the thioether. This geometric selectivity was improved by changing either the solvent, the metal, or the ligand, showing that a high degree of fine-tuning was possible with these reagents. The isomerisation was also applied to allylic amines and ethers, although more forcing conditions were required for these substrates. The resulting *Z*-enamines and ethers were assumed to be highly versatile in subsequent bond-forming reactions (Scheme 106).

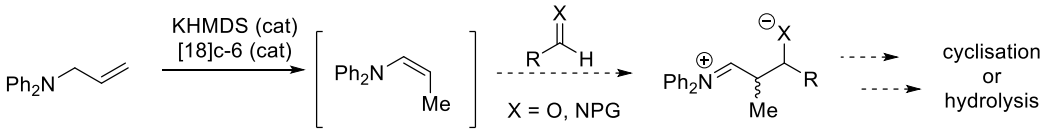

Scheme 106: Predicted reactivity of functionalised enamines

Finally, C–C bond formations between the functionalised olefins and imines were developed. For the allylic metal reagents, the functionalised allylations showed an exclusive Brønsted base activation of the pro-nucleophile, which did not compete with a potential Lewis base attack of the catalyst to the metal centre. Here, metallated homoallylic amines were produced in good yields with excellent γ- and *E*-selectivities. Future work in this area would include the cross coupling of these reaction intermediates to give more stable homoallylic amines (Scheme 107). Ideally, a one-pot method would be developed, where the cross coupling conditions are compatible with the allylation conditions.

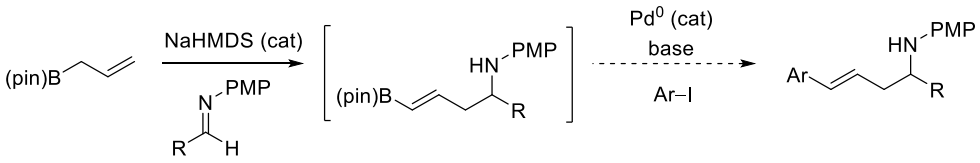

Scheme 107: Predicted reactivity of functionalised vinyl boronic esters

For the heteroatom-substituted pro-nucleophiles, allylations occurred for both the thioether and the phosphine in good yields. Products were obtained with good *E:Z* ratios, which could be improved based on the knowledge obtained in the isomerisation work. However, further investigations are required in order to expand the imine scope. Interestingly, both the allylic amine and ether could be activated in C–C bond formations with imines, giving substituted homoallylic amines with a *Z*-configuration. These products contained enol ethers and enamines, which may be reacted with activated electrophiles to give more complex structures in the future. However, the yields for these allylations were only modest and more work is required in this field in order to optimise the reaction conditions.

Finally, enantioselective reactions need to be developed for the functionalised allylations using allyl–M and allyl–FG. These reactions are particularly challenging, due to the inherent Lewis acidity of the allyl–M reagents, or the Lewis basicity of the allyl–FG pro-nucleophiles. These groups can interfere with the coordination of a ligand to the catalyst, which would decrease the catalyst's ability to induce chiral information to the product. However, the use of a carbene ligand for improving the *E:Z* selectivity of the reaction shows potential in the field of ligand effects, which may be applied to enantioselective allylations in the future.

3 Metal-Free Organocatalysis

3.1 Introduction to Carbodiphosphoranes

3.1.1 Synthesis

Preparation and Properties

Carbodiphosphorane **259** was isolated initially in 1961 by Ramirez after deprotonation of methylene bis(triphenylphosphonium)dibromide salt **257**.[115] Initially, this deprotonation was achieved directly using two equivalents of potassium metal or sodium amide, but later it was discovered that it can also be performed stepwise using sodium carbonate and sodium hydride (Scheme 108).[116]

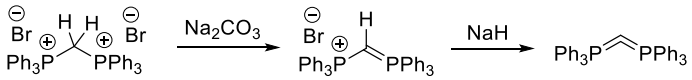

257 258 259

Scheme 108: Stepwise Formation of hexaphenylcarbodiphosphorane

Resulting compound **259** was described to have different resonance forms, which can be represented either in the neutral linear structure or as the ylidic or double-ylidic structures with a central sp^2- or sp^3-type hybridised carbon centre (Figure 13).

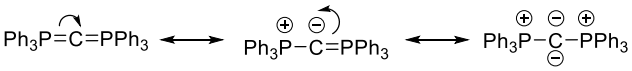

259

Figure 13: Resonance forms of CDP

Due to the double negative charge on the carbon, carbodiphosphoranes are dibasic and react rapidly with water (Scheme 109). The strong Brønsted basicity and the P=O stability provide a large driving force for the fast reaction with water so that hydrolysis occurs with atmospheric water as soon as the carbodiphosphorane is in solution.[117] Apart from their high reactivity with acidic substrates, carbodiphosphoranes are remarkably stable as they can be easily isolated as a bright-yellow powder with a high melting point of 210 °C.[115]

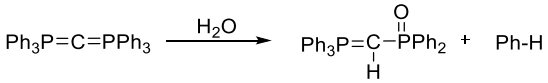

259 260

Scheme 109: CDP Reaction with water

After their initial discovery, carbodiphosphoranes and their protonated derivatives have been extensively studied in metal coordination (*vide infra*). More recent computational studies showed their potential as bases in catalysis and organic synthesis. The P–C–P bond angle of

135° and the P–C bond length of 166 pm show that they are best described as sp^2 hybridised at the carbon centre (Figure 14).[118]

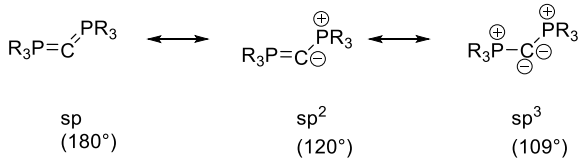

Figure 14: Hybridisation of CDP

DFT calculations showed that the central carbon atom has two orthogonal occupied orbitals, one with σ and one with π geometry.[119] Therefore, this class of compounds can be regarded as a divalent C(0) compound with two lone pairs on the central carbon atom that can be used as a four electron donor (Figure 15). In order to quantify the basicity of the compounds, their proton affinities (PAs) were calculated. Compared to the PA of *N*-heterocyclic carbenes (NHCs; 250 $kJmol^{-1}$), which are very strong bases, the first PA of carbodiphosphorane was found to exceed the NHC PA by about 30 $kJmol^{-1}$.[120] In addition, a second PA of the carbodiphosphoranes was found to be significant, with a value of 186 $kJmol^{-1}$. This double basicity is why both of its lone pairs may potentially be used in organocatalysis, metal or dual catalysis.

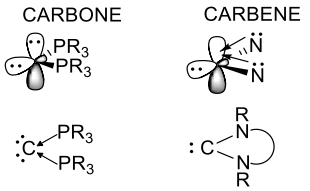

Figure 15: Orbitals of CDP vs. NHC

Synthetic Route

As described earlier, carbodiphosphoranes were traditionally prepared by deprotonation from their corresponding bromide salts. The required methylene bis(triphenylphosphonium) dibromide salt **257** was prepared from dibromomethane (**261**) and triphenylphosphine (Scheme 110, 1). Higher overall yields for the dibromide salt were obtained in the literature when performing the synthesis in two steps, where intermediate **262** was isolated after bromide substitution by one triphenylphosphine unit.[121] **262** was then subjected to the second substitution reaction at higher temperatures.[122] The dibromide salt has been deprotonated in one step using K^0 metal or $NaNH_2$ in liquid ammonia. Alternatively, the formation of the dibasic carbodiphosphorane was achieved in two steps, where initially only

one proton was abstracted by a carbonate base forming a stable monobasic carbodiphosphorane precursor salt (Scheme 110, 2).[121] This method resembled the synthesis of NHC where the protonated carbene salts are usually employed for an *in situ* preparation of the carbene using a base. The second CDP proton was subsequently removed using a stronger base, such as sodium hydride, to form **259** with two lone pairs at the central carbon atom.

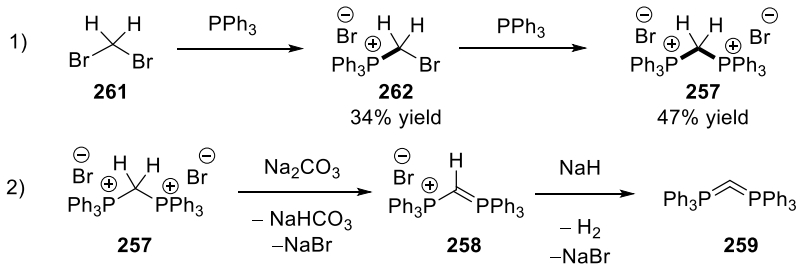

Scheme 110: Traditional method for CDP synthesis

A different approach was developed by Appel where triphenylphosphine (**263**) was directly reacted with tetrachloromethane (**264**) to give intermediate chloride salt **265** (Scheme 111).[123] This method did not display the common carbene precursor analogue, which required deprotonation, but contained a chlorine atom that was removed using an aminophosphine. Resulting carbodiphosphorane **259** could be successfully prepared using cheap and commercially available starting materials in two steps with good yields.

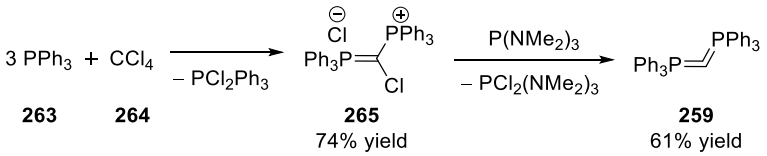

Scheme 111: Improved method for CDP synthesis

Literature-Known CDPs

Different derivatives of the carbodiphosphoranes have been prepared in the past 50 years, where the substituents on the phosphine unit were exchanged (Figure 16). Initial studies included the use of symmetrical and unsymmetrical substituents such as R,R' = Me (**266**)[124] or R,R' = Me/ Ph (**267** and **268**).[125] However, methyl-substitution allowed access for decomposition pathways through acidified C–H bonds that could be easily deprotonated by the central carbon atom. Other analogues included trialkylaminophosphine derivative **269**.[126] These carbones showed a higher stability than the trimethylphosphine analogues, but have been characterised by X-ray crystallography to have a linear P–C–P bond arrangement

and were therefore possibly not as basic as their aryl- and alkyl-homologues. However, the reason for this structural feature is yet to be elucidated. In 2013, Alcarazo described the preparation of pyridyl-substituted carbodiphosphorane **270**, where a pyridine ring aided the coordination to potential metal centres.[127] Other advances in the preparation of different carbodiphosphoranes include *P*-heterocyclic carbones (PHCs, **271**).[128] These compounds, in contrast to earlier cyclic versions of CDP,[129] showed a relatively high stability and have been used in metal coordination.[130]

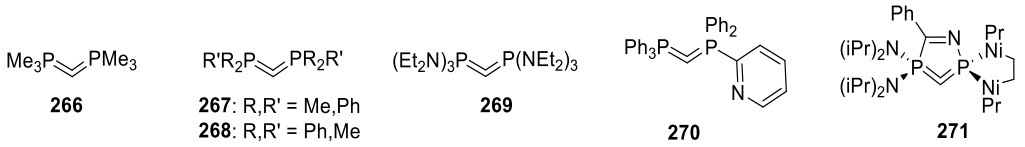

266 **267**: R,R' = Me,Ph **268**: R,R' = Ph,Me **269** **270** **271**

Figure 16: Different literature-known CDPs

Heteroatom-substituted phosphines such as $–PR_2=NR$ or $–PR_2=S$ (**273**) motifs form a different class of compounds, which can also be regarded as C(0) compounds (Scheme 112).[131] These compounds have an additional binding mode to metal centres through the heteroatoms (Scheme 112). Depending on the substituents, they showed donation of four electrons to a metal.[132] However, these bases can also be treated as pure carbene bases rather than true four electrons donors because a high charge density is located on the heteroatom.

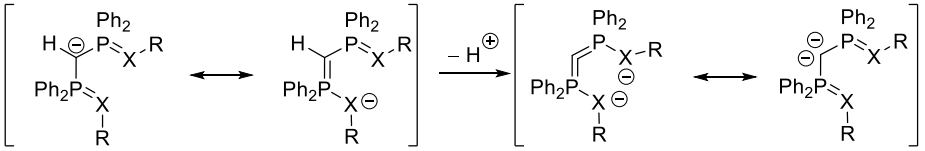

272 **273**

Scheme 112: Heteroatom-substituted CDPs with C(0) character

3.1.2 Stoichiometric Applications

Side Reactions: Ylide Chemistry

Due to their ylidic nature, carbodiphosphoranes have been used in reactions with reactive ketones, where the P–C–P motif is used in Wittig-type chemistry (Scheme 113). In principle, carbodiphosphoranes can be considered as extended Wittig reagents with a negative charge on the carbon centre and one single and one double bond to phosphorus.

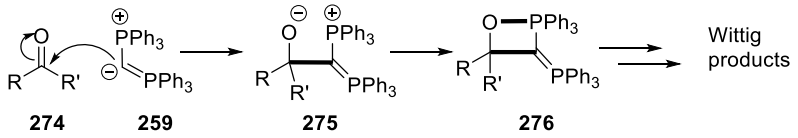

Scheme 113: CDP reaction with carbonyls

When CDP **259** attacked activated α-keto lactone **277**, the generated oxygen anion cyclised to form betaine **278**, which then led to the formation of triphenylphosphine oxide (**280**) and the replacement of the carbonyl group with a C=C bond giving heterocumulene **279** (Scheme 114).[133]

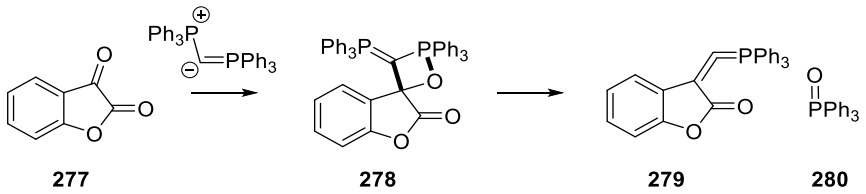

Scheme 114: Example of Wittig reaction

Furthermore, CDPs are not compatible with Brønsted acidic substrates like alcohols[134] or hydroxylamines[135] because the abstraction of a proton, like in the reaction with water, is thermodynamically favoured (Scheme 115). After protonation by phenol **281**, the CDP was attacked by the generated phenolate to form **282**. Further reactions using the second lone pair of electrons were still possible, but resulted in the integration of the carbodiphosphorane motif into complex structures like **283**.[136]

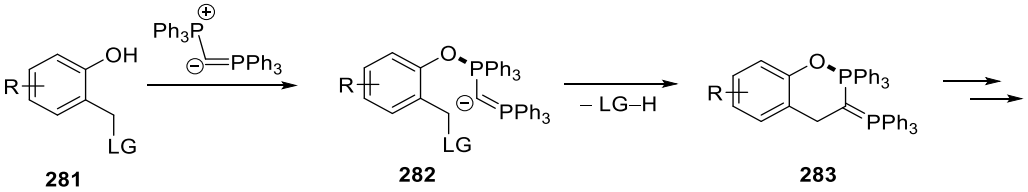

Scheme 115: CDP Reaction with alcohols

Mono- and Dimetallated Complexes

Metal complexes with CDP are numerous and can display different properties depending on the carbodiphosphorane and the nature of the metal. The first class of complexes are the monometallated species of type **284**, where the basic carbon atom on the carbodiphosphoranes coordinates to one metal centre bound to a ligand L (Figure 17, left). Late transition metals, predominantly in group XI (Cu, Ag, Au), have been studied.[137] To form these complexes, the carbodiphosphoranes were reacted with the corresponding metal salts or organometallic reagents to form a bond between the CDP and the metal, which was still bound to its ligand. Apart from the metals in group XI, other metals have been shown to display a similar reactivity, such as Zn(II) or Cd(II)[138]. A slight modification of the bonding situation was achieved when reacting two equivalents of CDP with one equivalent of the metal to form a linear complex where two CDPs coordinate to one metal (**285**; Figure 17, right).[139] Complexes including Ag, Hg and Cu(I) have been isolated with an overall cationic or neutral charge.

284

M = Cu, Ag, Au, Zn, Cd
L = Cl, Br, I, Cp, acetylene, acac

285

M = Ag, Hg, Cu

Figure 17: Literature-known mono and dimetallated complexes

Carbodiphosphoranes also reacted with transition metal carbonyl compounds upon loss of one CO ligand to give complexes of type **286** (Figure 18). W, Ni and Re have been observed to undergo this process.[140] In these complexes, it is possible to represent the carbon–metal bond in a carbene-type fashion where the carbodiphosphorane donates its second electron pair into the C–M bond. Also the reaction with $BeCl_2$ shows some proof for a double basic character on the carbodiphosphorane, as beryllium can be seen as a double Lewis acid and the coordination from the CDP would involve the donation of four electrons to the Be^{2+} centre.[141]

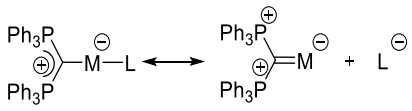

286

$W(CO)_5$, $Ni(CO)_2$, $Re(O_3)$, $BeCl_2$

Figure 18: Potential 4 electron donor complexes

Further evidence for the accessibility of two lone pairs for coordination was provided by the dimetallated CDP complex formed when two equivalents of methylgold (I) or gold (I) chloride were reacted with one equivalent of CDP **259** (Scheme 116).[142] Complex **287** displayed binding between both lone pairs on the central carbon atom of the CDP and showed that CDPs are not only more nucleophilic than commonly known Lewis bases, but also display sufficient reactivity to be bis-metallated. This double metallation meant that carbodiphosphoranes are not only double Brønsted bases as described in the original paper, but also double Lewis bases.

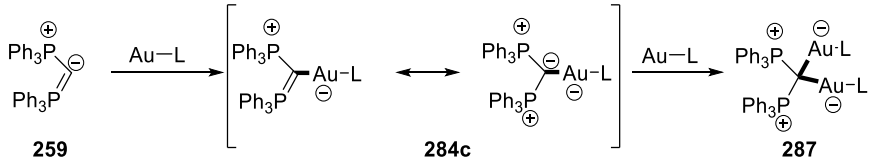

259 **284c** **287**

Scheme 116: Diauration of CDP

A more recent example of bis-metallation is the preparation of heterobimetallic CDP complex **289** (Scheme 117).[143] Here, pentaphenyl pyridyl carbodiphosphorane **270** was first reacted with a gold (I) complex to give **288**. Subsequently, a copper ion was coordinated by the second lone pair, where the pyridyl ligand formed a chelating complex to Cu(I) (**289**; Scheme 117). In addition to the demonstration of the double Lewis basic character of the central C atom, the heterobis-metallation also shows that the complexes can possibly be used as dual catalysts when two different metals are coordinated by one CDP.

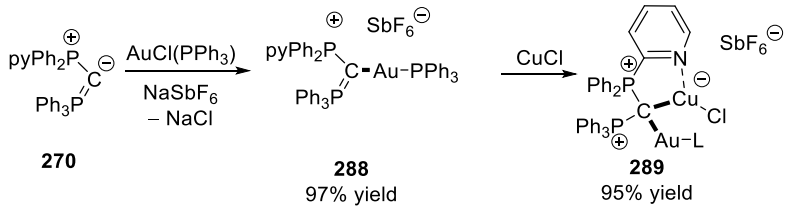

270

288
97% yield

289
95% yield

Scheme 117: Heterobimetallic complex formation

Further proof for the ability to act as a 4 electron donor was provided in the reaction of CDP with the dimeric borane B_2H_6 (Scheme 118).[144] The isolated complex **291** did not display

the coordination of each lone pair to one BH_3 as expected. Instead, it formed a tetravalent carbon intermediate with coordination to two boron atoms, bridged by one hydrogen atom, which is assumed to have rearranged from the initial double boration product (**291**).

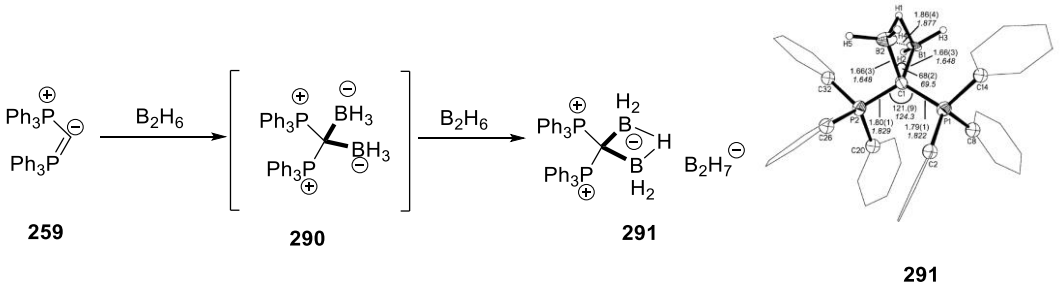

Scheme 118: Diboration of CDP

Complexes with other main group elements have also been published. In 2013, Alcarazo published the addition of CDP **259** to $GeCl_2$ and $SnCl_2$ (Scheme 119).[145] These adducts showed a high Lewis basicity and reactions with further metal resulted in the formation of a Ge–Ge bond.

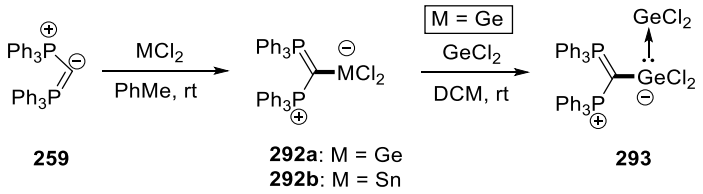

Scheme 119: CDP–Ge and CDP–Sn adducts

Further main group adducts with main group metals were synthesised using Al(III) or In(III) salts (Figure 19).[146] The reaction of CDP **259** with TMS–OTf was reported in 2014, where CDP–$SiMe_3$ adduct **292e** formed with a triflate counterion.[147]

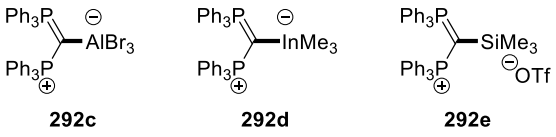

Figure 19: Main group CDP-adducts

Moreover, Vidovic reported a CDP–phosphorus complex **295** (Scheme 120).[148] Here, **259** reacted with an aminodichloro phosphine to form adduct **294**, which was dechlorinated using $AlCl_3$ to give dication **295**. Further studies demonstrated the application of this method to other carbodiphosphoranes, including crystal structures and bonding analyses.[149]

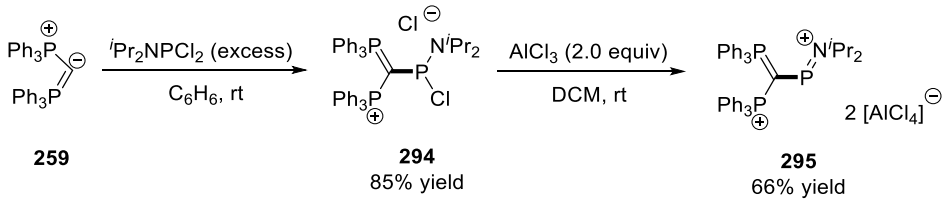

259 **294** 85% yield **295** 66% yield

Scheme 120: CDP–P adduct

CX_2 Adduct Formation (X = O, S, NR)

Carbodiphosphoranes have been known not only to coordinate to metals, but also to other molecules such as carbon dioxide.[150] Here, the *C*-centered nucleophile attacked a C=O bond of **296** and formed stable zwitterionic adduct **297** (Scheme 121). This inner salt was found to be reactive towards electrophiles such as methyl iodide, where the oxygen anion was methylated to form ester adduct **298**.

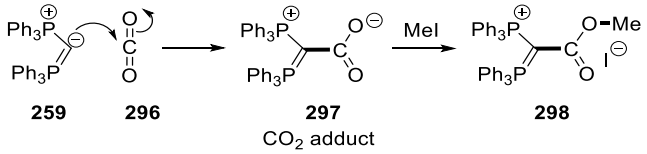

259 **296** **297** CO_2 adduct **298**

Scheme 121: Carbon dioxide adduct formation and E^+ trapping

Similar to the reaction with carbon dioxide, CDP adducts have been reported for CS_2, SCO and even carbodiimides **299** or isocyanates (Scheme 122).[151] However, adducts of type **300** have not been used further in synthesis or catalysis.

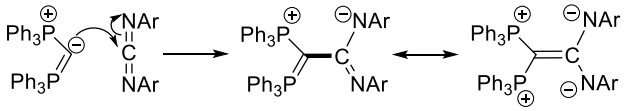

259 **299** **300**

Scheme 122: CDP adducts with carbodiimides

Stoichiometric Applications

As mentioned before, carbodiphosphoranes have been extensively studied in terms of their ability to form complexes with metals. Their use as catalysts has not been reported and only few examples of its use in organic synthesis were reported from the same group.

The first example was the reaction of the CDP with the Lewis acidic tris(perfluorophenyl) borane, $B(C_6F_5)$ (**301)**, where the CDP was initially thought to act as a potential Lewis base

for coordination to the boron centre (Scheme 123).[152] The reaction, which was carried out in toluene at –78 °C, showed that the CDP did not coordinate to the boron centre, but instead acted as a frustrated Lewis pair with the boron centre. Reaction product **302** resulted from the attack of the carbodiphosphorane at the *para*-position of one of the aryl substituents to displace a fluoride anion, which was then transferred to the boron Lewis acid. This example represents the first stoichiometric use of a CDP in organic synthesis (C–F bond activation).

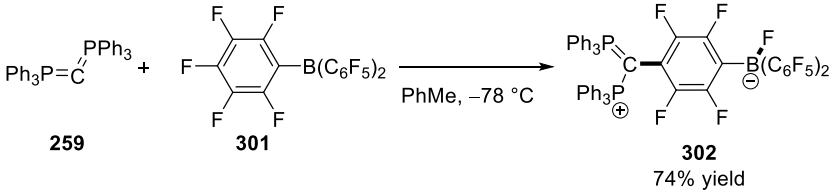

Scheme 123: C–F bond activation

Subsequent reactions were carried out to show the potential of CDPs to activate bonds while acting as Lewis or Brønsted bases. When reacted with terminal alkynes, CDP displayed Brønsted basic properties; alkyne **303** was deprotonated to form an acetylene anion and protonated CDP (**304)** (Scheme 124). The acetylene anion was then transferred, like the fluoride in the previous case, to the Lewis acidic boron centre. Thus, CDPs were also used for the activation of C(sp)–H bonds.

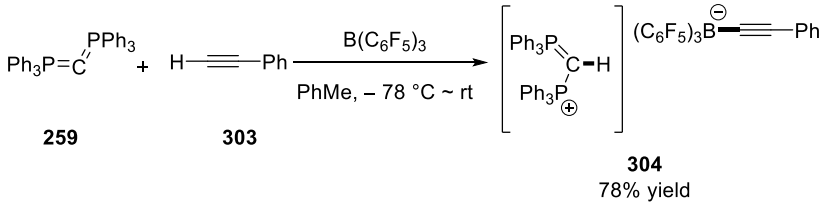

Scheme 124: C–H bond activation

In addition, CDPs have also been used as a Lewis base to activate B–H and Si–H bonds (Scheme 125). Here, the hydride donors, BH_3 and silane **307,** were attacked by *C*-centred Lewis base **259** to deliver a hydride to **301**. CDP–B or CDP–Si bonds were generated and boron-ate complexes **306** and **308** with high hydride donation ability were formed.[152-153]

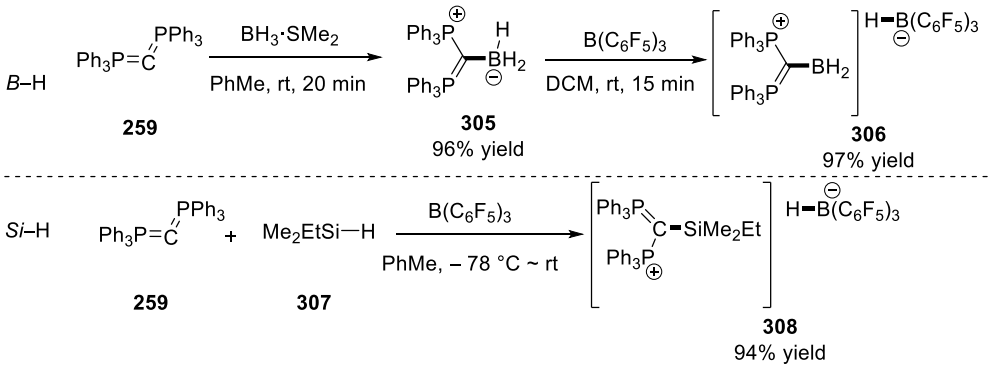

Scheme 125: B–H and Si–H bond activation

Finally, small molecule activation has also been achieved using the described frustrated Lewis pair.[152] When hydrogen gas was added to a cooled mixture of CDP **259** and borane **301**, a heterolytic cleavage of dihydrogen was observed, where the CDP abstracted a proton from molecular hydrogen, leaving a formal hydride that was transferred to the borane (Scheme 126). This sort of reactivity is usually expected from frustrated Lewis pairs and showed a great potential for catalysis.

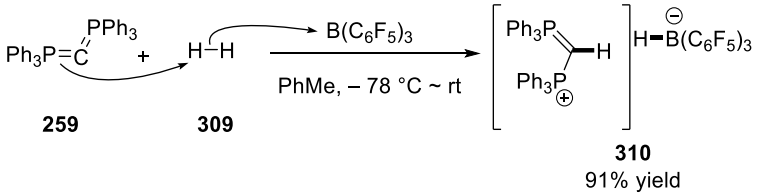

Scheme 126: Metal-free heterolytic dihydrogen activation

3.1.3 Applications of Carbones in Catalysis

At the outset of this project, the use of carbones in organocatalysis has not been reported. During the course of our study, Stephan postulated in a generic catalytic cycle the *in situ* generation of a CDP as a catalytically active species (Scheme 127).[154] The reduction of carbon dioxide (**296**) using phosphine **311** was achieved by forming CDP **314** *in situ*. The reaction of **314** with carbon dioxide led to expected adduct **315**, which, in the presence of a zinc Lewis acid catalyst, decomposed to phosphine oxide **312** and ketene **316**. In the reaction with further phosphine, **316** regenerated CDP **314** and gave carbon monoxide (**313**) as the final product.

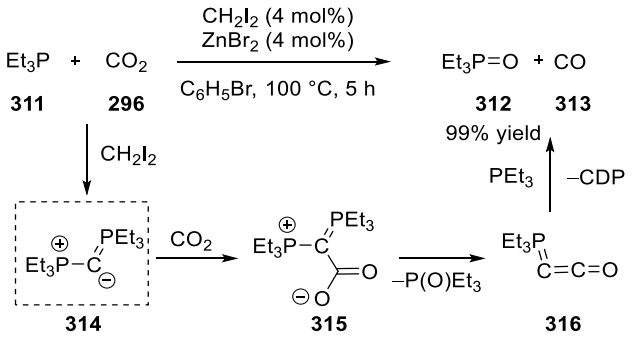

Scheme 127: *In situ* generation of a CDP catalyst

Despite being able to characterise several reaction intermediates, the reaction was not performed using CDP **314** directly, as its isolation proved challenging. Furthermore, a ^{31}P NMR chemical shift of +28 ppm was recorded for **314**, which markedly contrasted previously described data for CDPs (–29.6 ppm).[155]

The first direct use of a carbone in organocatalysis was reported by Ong in 2015.[156] The used carbone was not a carbodiphosphorane, but a related carbodicarbene (CDC). This class of compounds has originally been proposed by Frenking,[157] and analogues were subsequently prepared by the group of Bertrand and Fürstner.[158] Here, CDC **320** was prepared by deprotonation of **319**, which was synthesised from **317** and **318** (Scheme 128). CDCs like **320** have been calculated to display a high electron density at the central carbon atom, as they can be treated as a C(0) centre stabilised by two carbene donors, analogously to the CDP bonding situation.[157]

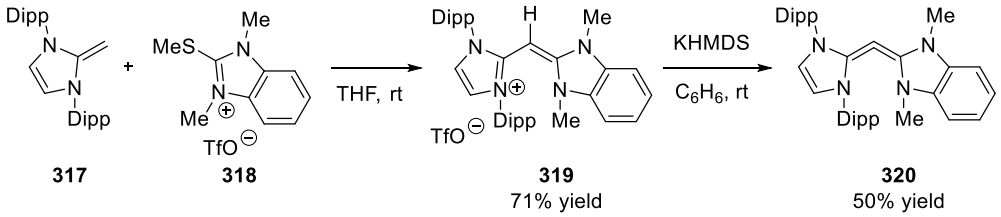

Scheme 128: Preparation of a CDC

This carbone was then used in the methylation reaction of primary and secondary amines using CO_2 as a carbon source (Scheme 129). The mechanism for this activation was shown to proceed through the addition of CDC **320** into the B–H bond of the reducing borane. This intermediate reacted with CO_2 to give a carboxylate, which subsequently reacted with borylated amine **323** to give formamide **324**. Finally, the CDC was assumed to also catalyse the reduction of **324** to give methylated amine **322**.

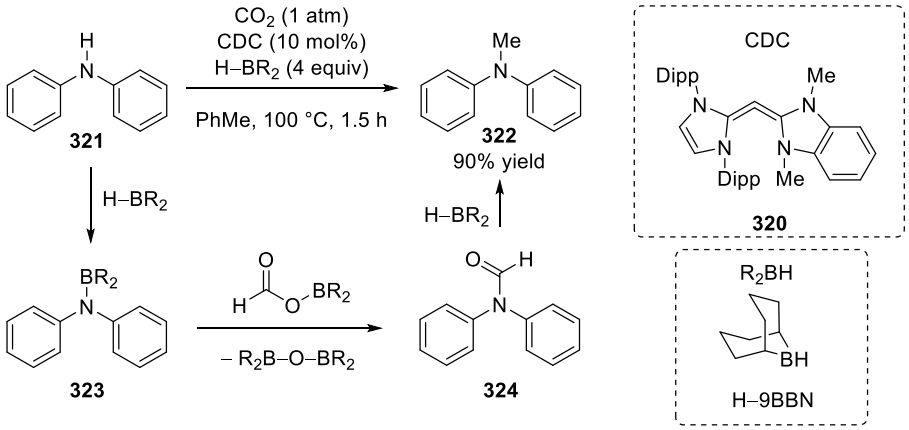

Scheme 129: CDC catalysis

3.2 Aims

The CDP's high basicity was thought to be applicable to organocatalysis, while its steric bulk suggested applications in frustrated Lewis pair (FLP) catalysis. In addition, the high electron-donating properties of the CDP showed a potential in metal catalysis where the CDP may act as a ligand. As two lone pairs were potentially available on the central carbon atom, these two areas were aimed to be combined for a potential dual activity of the catalyst.

One potential application for CDPs was their use in Brønsted or Lewis base catalysis (Scheme 130). As a Brønsted base (BB), the CDP could activate C–H bonds and subsequent reactions with electrophiles were assumed to lead to unprecedented C–C bond formations. As a Lewis base (LB), the CDP may activate boron-based pro-nucleophiles with a transferable R group that could react with electrophile *E*.

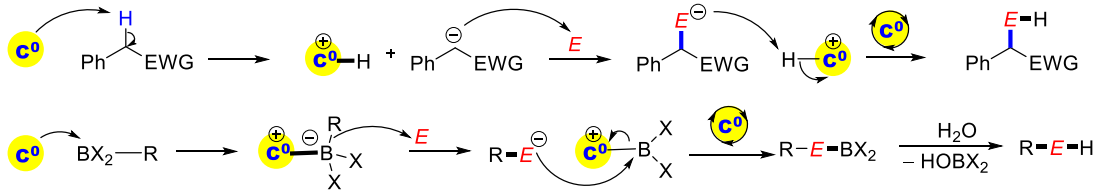

Scheme 130: CDP-catalysed C–H and B–R bond activations

Frustrated Lewis pair catalysis could also be developed, where the carbone and Lewis acids would not show direct reactivity. This type of reactivity could lead to the activation of small molecules such as CO_2 or H_2 .

Metal catalysis was another promising area for applications, where the CDP may act as a ligand to metal centres (Scheme 131). Due to the CDP's high basicity, the metal may be turned into a catalytically active intermediate that may then act as a novel catalyst.

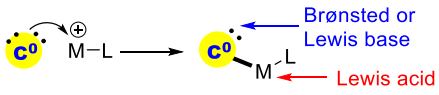

Scheme 131: CDP metal complexes

Furthermore, the potential for the two lone pairs at the carbon centre was to be used separately in dual catalysis. One lone pair may be used for coordination to a metal, which acted as a Lewis acid in a reaction to activate an electrophile. The second lone pair at the carbon may act as a Lewis or Brønsted base, which may catalytically activate an acidic pro-nucleophile. A different method to achieve dual catalysis could be the use of two metals that are ligated by one CDP. These metals would ideally be different and could act as sequential Lewis acid catalysts.

3.3 Results and Discussion

3.3.1 Preparation of CDPs

In order to prepare the hexaphenylcarbodiphosphorane, the modified synthetic route developed by Appel was chosen due to simplicity and higher reported yields (Scheme 132).[159]

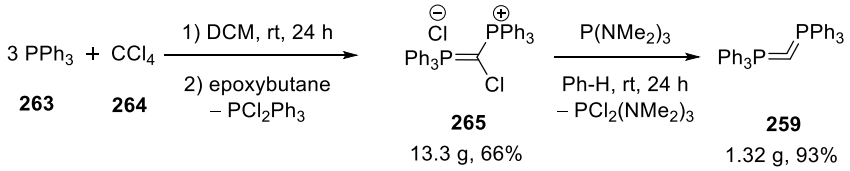

Scheme 132: Overall synthetic route

The first step in the synthesis involved the reaction of triphenylphosphine with tetrachloromethane. This step was carried out in DCM at room temperature for 24 h. In this reaction, two products were formed: The first equivalent of phosphine **263** abstracted a chlorine cation from tetrachloromethane (**264**) and the loss of a chloride anion formed **325**, which was insoluble in DCM and precipitated after several hours of stirring (Scheme 133). The resulting electrophilic carbene **326** was then attacked by a second molecule of **263** to form intermediate **327** that was attacked by a third equivalent of **263**, which displaced a chloride ion. Overall, the expected salt **265**, which was soluble in DCM, was formed.

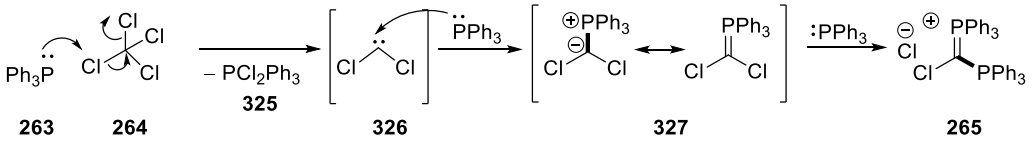

Scheme 133: Proposed mechanism for the formation of 265

Next, epoxide **328** was added once the reaction had come to completion in order to remove the insoluble by-product. The epoxide reacted with by-product **325** to the form triphenylphosphine oxide (**280**) and chlorinated hydrocarbon **329** that were both soluble in DCM (Scheme 134).

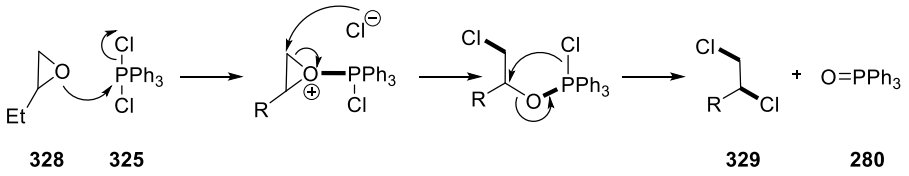

Scheme 134: Proposed mechanism for the removal of by-product

Once the by- products were removed, diethyl ether was added for the crystallisation of **265**, which was obtained in high yield and purity.

The second step of the CDP synthesis involved the dechlorination of intermediate **265** using aminophosphine **330** (Scheme 135). In this reaction, the Lewis basic phosphine abstracted a Cl^+ ion from the central carbon atom of **265** and formed a stable salt (**331**) that was insoluble in benzene.

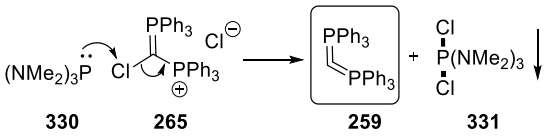

Scheme 135: Proposed mechanism for the dechlorination

Product **259** was purified and isolated using a hot benzene filtration to remove by-product **331**. The CDP in the filtrate crystallised immediately and was filtered off as a bright-yellow solid in high yields. ^{31}P NMR spectroscopic analysis showed a single signal at –4.8 ppm and two multiplets for the aromatic hydrogens were observed in ^{1}H NMR spectroscopy (C_6D_6; Chart 3).

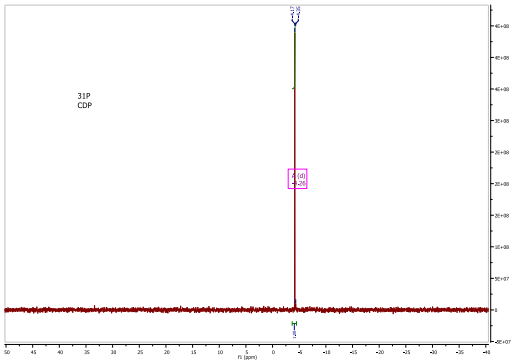

Chart 3: ^{31}P NMR spectrum for CDP

Residual water in the solvent caused severe contamination by the hydrolysed CDP (up to 15%; Scheme 136). ^{31}P NMR spectroscopic analysis of **260** showed two doublets at 23 ppm arising for the two phosphorus environments of this impurity. Therefore, it was important to use distilled and dried solvents in the purification process.

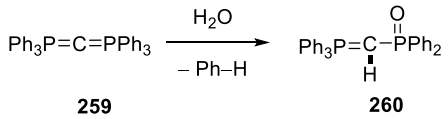

Scheme 136: Hydrolysis of CDP

A different C(0) complex was prepared according to the preparation of a pyridine-containing carbodiphosphorane reported by Alcarazo (Scheme 137).[143] As the literature reported synthesis did not offer a simplified preparation method like in the previous case, the original synthesis of CDPs was carried out.

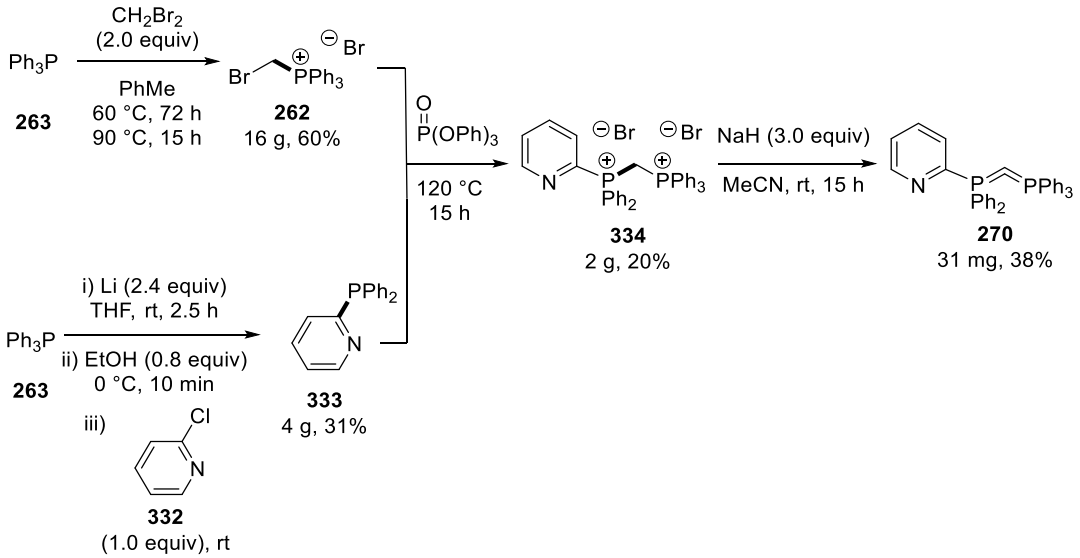

Scheme 137: Synthetic route to a heteroaromatic-substituted CDP

Similar to the original method of preparing hexaphenylcarbodiphosphorane, the route for making pyridyl-substituted carbone **270** started by condensing triphenylphosphine **263** and dibromomethane (Scheme 137). Product **262** was obtained and purified by recrystallization in a moderate yield. Pyridine-substituted phosphine **333** was then synthesised in a low yield from 2-chloropyridine (**332**) and triphenylphosphine (**263**) using Li metal. Despite the low yield, the reaction gave ca. 4 g of **333** from cheap starting material. Phosphine **333** and phosphonium salt **262** were then reacted in liquid triphenylphosphate at 120 ºC and dibromide salt **334** was extracted with toluene and recrystallised from methanol. The deprotonation of this carbone precursor was described in the literature by using $NaNH_2$ in liquid ammonia. This method was presumably chosen because the precursor salt is insoluble in most common solvents. It was found, however, that it dissolved at least partially in acetonitrile. Therefore, the deprotonation of **334** was attempted using KH in acetonitrile, which gave a yellow suspension after 15 h. Product **270** was then filtered off and the ^{31}P

NMR was recorded (Chart 4). A subsequent reaction was carried out using NaH, which gave a cleaner reaction and a yield of 38% starting from 105 mg of precursor **334**.

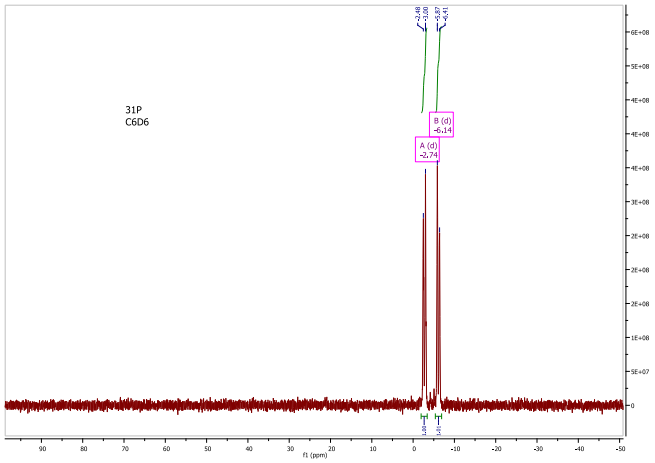

Chart 4: ^{31}P NMR spectrum of a pyridyl substituted CDP

Carbone **270** was particularly interesting in the context of metal complexes because of the additional binding interaction of the pyridyl nitrogen to a coordinated metal, forming a five membered chelate. As demonstrated by Alcarazo it did, however, not always participate in binding, which was the case for the diaurated complex where the crystal structure showed that the pyridine substituent pointed away from the gold centre.[160]

3.3.2 Reactions with Boron Lewis Acids

In order to determine the Lewis basicity of the synthesised CDP, it was reacted with different boron-containing compounds to form boron-ate complexes (Scheme 138). The chemical shift of the corresponding boron atom of the boron compounds in ^{11}B NMR spectroscopy was used as an indication for its Lewis acidity, where a more positive value represented a high electrophilicity at the boron atom. Once a Lewis base attacked the boron centre, a boron-ate complex formed. These tetravalent species display a low chemical shift between +5 and –40 ppm in ^{11}B NMR spectroscopy.

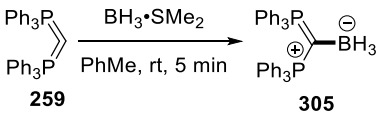

259 **305**

Scheme 138: CDP reaction with a borane

According to the literature preparation of CDP–BH_3 **(305)**, the borane–dimethylsulfide complex was reacted with CDP **259**.[144] The ^{11}B NMR spectrum of the generated complex

showed a signal at –22 ppm, which was in agreement with the literature data (Chart 5). Also the ^{1}H and ^{31}P NMR spectroscopic data corresponded to the previously described results, where the ^{31}P NMR shift appeared at +20 ppm. As the CDP was not entirely soluble in toluene, the reaction mixture needed to be stirred (5 min) upon which the CDP in solution reacted slowly with the borane and precipitated. Removal of the solvent *in vacuo* and dissolving the residue in $CDCl_3$ showed the formation of the *C–B* donor-acceptor complex.

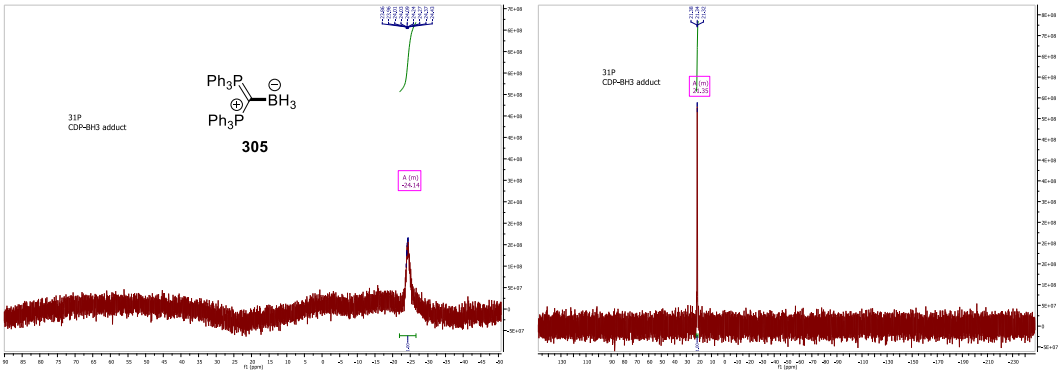

Chart 5: ^{11}B and ^{31}P NMR spectra of the CDP–BH_3 adduct

Other boranes were used in the binding study with CDP (Table 61). ^{31}P and ^{11}B NMR spectroscopy were used to analyse the formation of new adducts. ^{11}B NMR spectra were collected for all substrates. Reactions between CDP **259** and boron Lewis acids **335** (1.2 equiv) were carried out at room temperature in toluene; a slight excess of BR_3 was used in order to maintain an internal standard for the ^{11}B NMR chemical shift.

Table 61: Boron Binding Study

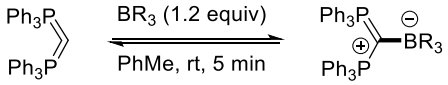

259
^{31}P = – 4.1 ppm

305, 336
^{11}B = –30 ~ +5 ppm

Entry	BR_3	BR_3 ^{11}B NMR shift (ppm)	Conv. (%)[a]	New ^{11}B NMR shift (ppm)	New ^{31}P NMR shift (ppm)
1	BH_3-SMe_2	–19	100%	–24	+22
2	BEt_3	+87	*NR*[b]	-	-
3	Bn–9BBN	+80	*NR*[b]	-	-
4	BPh_3	+60	*NR*[b]	-	-
5	MeO–9BBN	+57	*NR*[b]	-	-
6	Allyl–Bpin	+33	*NR*[b]	-	-
7	B_2pin_2	+32	*NR*[b]	-	-
8	H–Bpin	+28 (d)	10%[c]	-	+23 (d), –18 (d)
9	H–9BBN	+27 (d)	<10%[c]	-	+20, +30

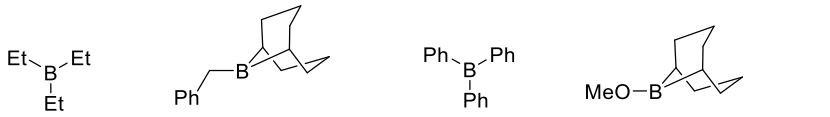

^{11}B NMR: δ =

335b
BEt_3
+87 ppm

335c
Bn-9BBN
+80 ppm

335d
BPh_3
+60 ppm

335e
MeO-9BBN
+57 ppm

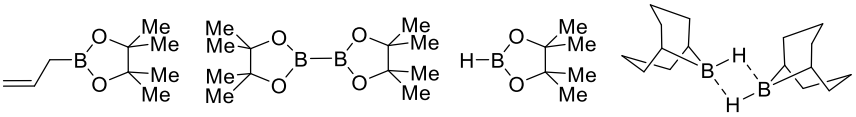

^{11}B NMR: δ =

15a
allyl-Bpin
+33 ppm

335g
B_2pin_2
+32 ppm

335h
H-Bpin
+28 ppm (d)

335i
$[H\text{-}9BBN]_2$
+27 ppm (d)

[a] The conversion was determined by ^{1}H NMR spectroscopy of with the entire reaction. [b] NR = no reaction; the desired product was not detectable, only starting materials were detected (^{1}H NMR analysis of a reaction aliquot). [c] The boron-ate complex could not be detected by ^{11}B NMR spectroscopy.

Other boranes did not display the same kind of reactivity as BH_3 (entry 1): The reaction of CDP with triethylborane (**335b**) did not proceed even at high temperature (80 °C, entry 2). The same results were observed for benzyl borabicyclo[3.3.1]nonane (**335c**, Bn–9BBN), triphenylborane (**335d**), methoxy borabicyclo[3.3.1]nonane (**335e**, MeO–9BBN), allyl boronic ester (**15a**, allyl–Bpin) and B_2pin_2 (**335g**; entries 3-7). H-substituted boron Lewis acids, such as pinacolatoborane (**335h**, H–Bpin) and H–9BBN (**335i**) showed around 10% of a new signal in ^{31}P NMR spectroscopy (entries 8 and 9). However, a boron-ate complex could not be confirmed by ^{11}B NMR spectroscopy, where only starting material was visible. The lack of binding showed how the binding equilibrium may be largely affected by steric effects and only less sterically demanding Lewis acids were attacked by the bulky C(0) centre.

The CDP only showed full binding to the least sterically hindered boron Lewis acid, BH_3. This observation suggested that the carbone was not a very good nucleophile. It was assumed, however, that the steric demand of the CDP prevented the Lewis base to bind to the boron centre in most cases. Other carbones have been studied in the group and were also found to react with BH_3. A carbodicarbene formed reactive boron-ate complex **337**, which underwent hydride transfer to the carbon centre, resulting in a chemical shift of 25 ppm in ^{11}B NMR spectroscopy (**338**; Scheme 139).[1] *C*,*P*-substituted carbone adduct **339** displayed a very low signal of –37 ppm in ^{11}B NMR spectroscopy, which was comparable to the carbene–BH_3 complexes formed using NHC Lewis bases.[2]

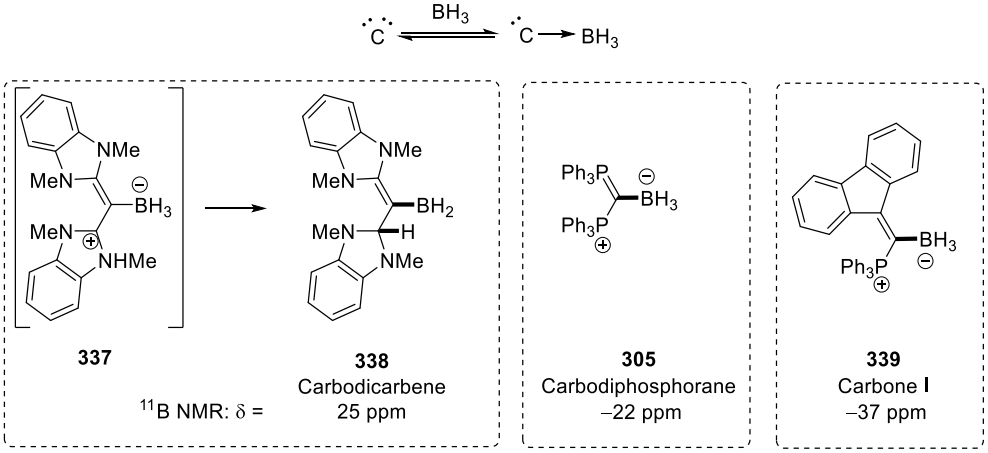

Scheme 139: Different C^0–BH_3 Complexes

In contrast to the other boron Lewis acids, tris(perfluorophenyl)borane (**301**) was described to form a different boron-ate complex in the literature (Scheme 140).[152] This complex underwent C–F bond activation, where the CDP attacked the aromatic *para*-position and the displaced fluoride was transferred to the boron.

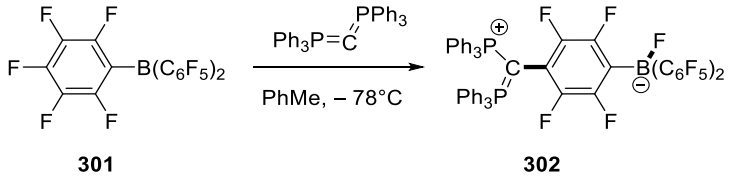

Scheme 140: C-F activation

This behaviour showed the 'frustration' between the carbon nucleophile and the boron electrophile. The steric bulk between the Lewis pair prevented direct attack of **259** at the highly Lewis acidic centre. Although only few boron-ate complexes were observed, the

[1] Reactions were carried out by Xun Lu.

[2] Reactions were carried out by Alexandros Papafilippou.

strong basic character of the carbone was demonstrated and its steric bulk offered a promising selectivity.

3.3.3 Stoichiometric Reactions

Reactions with Aldehydes and Imines

Studies of the reactivity of the carbodiphosphorane **259** with aldehydes and imines showed no reactivity. When the CDP and benzaldehyde were mixed and reacted overnight, a reaction did not occur even at elevated temperatures (Scheme 141). However, heating in the absence of molecular sieves (4Å, powder) lead to decomposition products being formed, as suggested by ^{31}P NMR spectroscopy.

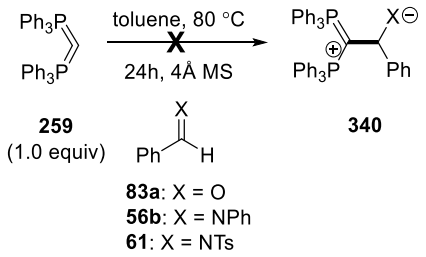

Scheme 141: CDP reactivity towards benzaldehyde

The same lack of reactivity was observed in the reactions of carbodiphosphorane **259** with benzaldimines. When a mixture of **259** and *N*-phenyl or *N*-Ts-benzaldimine in toluene was heated in the presence of molecular sieves, no change in the corresponding ^{31}P or ^{1}H NMR spectra was observed. More reactive electrophiles such as 1,2 dicarbonyls had been shown to react with CDPs in the literature.[133] Therefore, both electronic and steric factors also had to be considered when rationalising this lack of reactivity. However, it was shown that no Wittig or aza-Wittig products were formed. Furthermore, the lack of reactivity with aldehydes and imines allowed for the use of these substrates as electrophiles in CDP-catalysed activations of pro-nucleophiles.

Reactions with CO_2

Carbodiphosphoranes are known to react with carbon dioxide at ambient temperature and pressure.[150, 161] The attack of CDP **259** to the electrophilic carbon atom resulted in the formation of a carboxylate adduct **297** with a formal zwitterionic structure (Scheme 142).

This structure was potentially stabilised by an interaction of the oxygen anion with the phosphonium ion of the bound carbodiphosphorane.

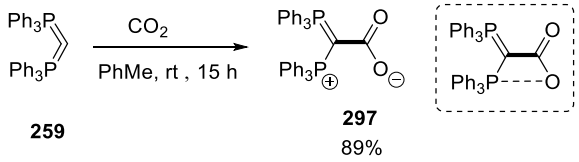

Scheme 142: Formation of the CO_2 adduct

As the product of this reaction was insoluble in toluene, product **297** could be easily purified by washing the colourless precipitate with toluene. However, the ^{31}P and ^{13}C NMR spectra had to be recorded in $CDCl_3$, which was acidic enough for the second lone pair to get protonated and displace the carboxylate group to give **258** (Scheme 143).

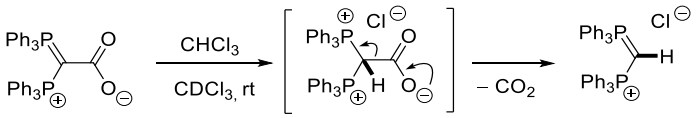

Scheme 143: Proposed decomposition pathway for the CDP–CO_2 adduct

This proposed decomposition was not very fast at room temperature so the corresponding signals of the adduct could be detected using NMR spectroscopy. Distinct signals in the ^{31}P NMR spectrum at 15.0 ppm and in the ^{13}C NMR spectrum 172.2 ppm confirmed the formation of the CDP–CO_2 adduct (Chart 6).

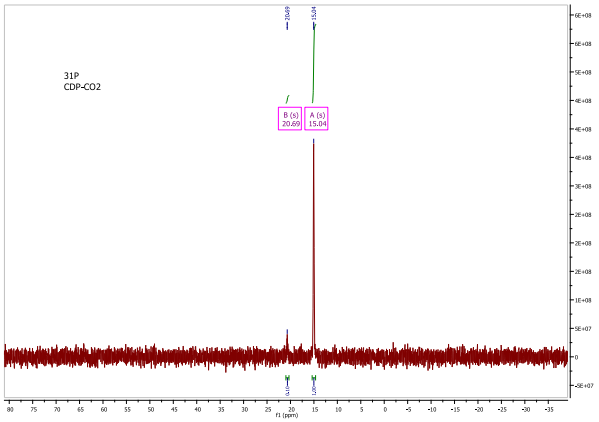

Chart 6: ^{31}P NMR spectrum of the CDP–CO_2 adduct

Metal Complexes

As many metal complexes with CDPs are literature-known, it was of interest to investigate the properties of CDPs as ligands to metal centres and the applications of these complexes in metal-catalysed reactions. As group XI metal complexes (Cu,[137a, 162] Ag, [162a, 163] Au[137c]) dominated the literature, representative gold-catalysed reactions were chosen as a model system, where Au acted as a π-acid. Literature precedence was also provided by the Gandon group, where π-acid catalysis had been achieved using NHC–Ga complexes (**343**; Scheme 144).[164]

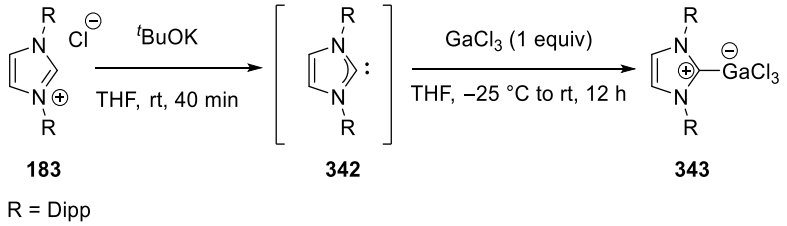

183 **342** **343**

R = Dipp

Scheme 144: NHC–$GaCl_3$ formation

This background inspired us to prepare novel metal complexes that could be potentially used in metal Lewis acid catalysis. The gallium complex **344** was synthesised using $GaCl_3$ and CDP in toluene (Scheme 145). The reaction was observed to be very fast, forming a colourless precipitate immediately upon addition of the Ga source to the suspension of CDP in toluene.

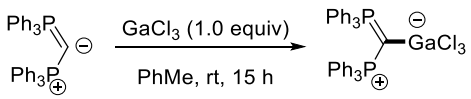

259 **344**

Scheme 145: CDP–Ga complex formation

As the complex was insoluble in toluene, isolation and purification with toluene was straightforward. Again, analysis was performed using ^{31}P NMR spectroscopy in $CDCl_3$, which showed a shift at 23.4 ppm (Chart 7). A small amount of impurity was observed in the ^{31}P NMR spectrum at 20.6 ppm, which was assigned to a small contamination by the CDP–H^+ chloride salt that could have potentially formed during the reaction. It is, however, also possible that this signal arose from the reaction with residual chloroform in the NMR solvent.

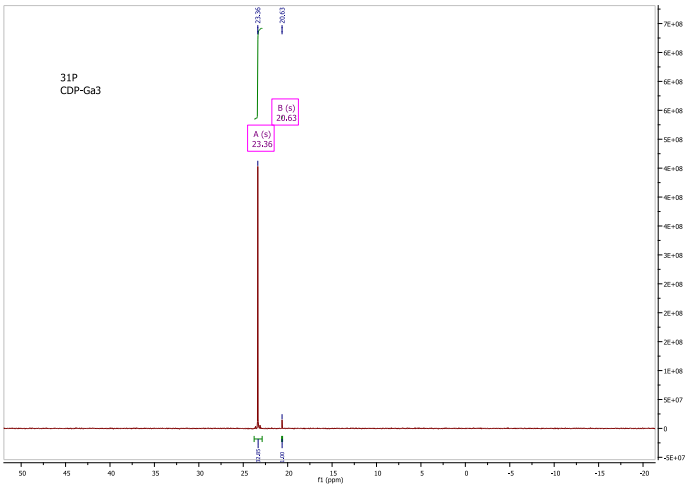

Chart 7: ^{31}P NMR spectrum of CDP–$GaCl_3$

Unfortunately, a crystal structure analysis could not be obtained; crystallisation of the compound from chlorinated solvents and toluene lead to the formation of the protonated CDP with a tetrachlorogallate counteranion **345** (Figure 20).

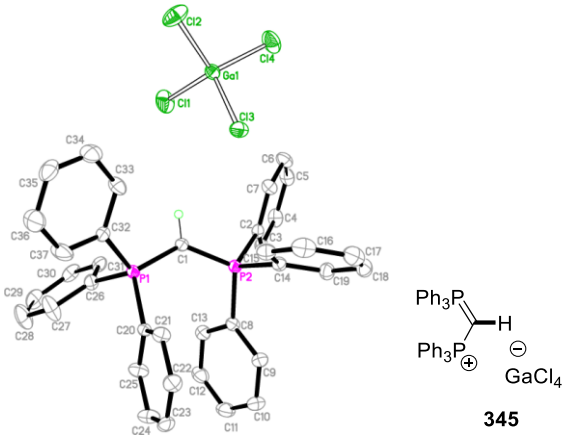

345

Figure 20: Crystal structure of $[CDP–H]^+[GaCl_4]^-$

^{71}Ga NMR spectroscopy of this complex did not show any signal, due to the low solubility of the complex even in chlorinated solvents. The absence of a hydrolysed product or starting material signal in ^{31}P NMR suggested the formation of the desired product.

During the course of this study, Gandon reported the synthesis of CDP–$GaCl_3$ adduct **344**. Spectral information were identical to the collected data.[165] Reaction conditions were similar, but the reaction was carried out in THF instead of toluene. Diffusion of Et_2O into a DCM-solution of **344** allowed for the formation of crystals, which were used for X-ray analysis, confirming the structure of **344** (Figure 21).

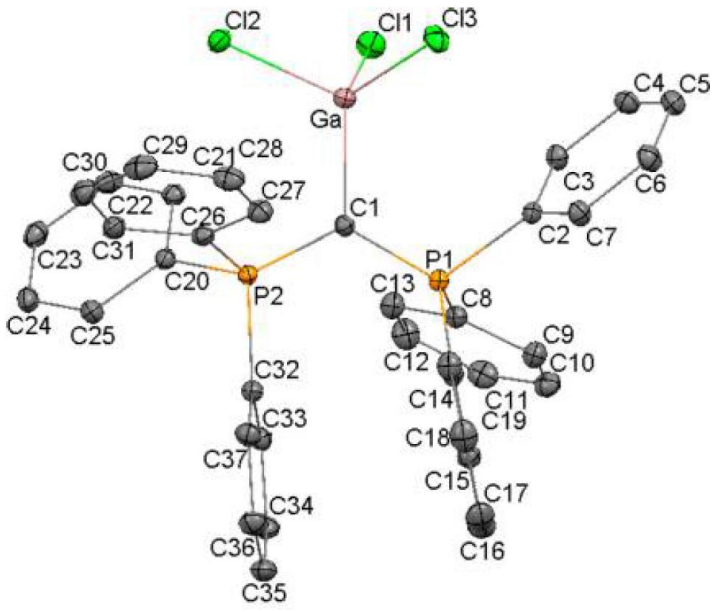

Figure 21: Reported crystal structure of CDP-$GaCl_3$

The CDP–Fe(II) and CDP–Fe(III) complexes were prepared using a similar method. The iron chloride salts were added to a suspension of CDP in toluene and reacted at room temperature overnight (Scheme 146). Monitoring the formation of these complexes was achieved using ^{31}P NMR spectroscopy in either C_6D_6 (consumption of starting material) or in $CDCl_3$ (product formation). As the solubility of these complexes even in chlorinated solvents was low, these complexes were reacted for prolonged periods of time and at higher temperatures until no starting material was visible in ^{31}P NMR spectroscopy.

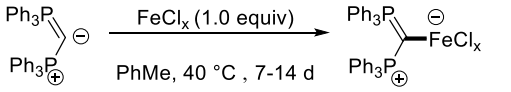

259

346: x = 2, 64%
347: x = 3, 73%

Scheme 146: Formation of CDP–Fe complexes

Isolation by filtration and washing with toluene gave both complexes in moderate yields [Fe(III): **346**, dark-purple solid, 64%; Fe(II): **347**, pale-brown solid, 73%]. ^{31}P NMR analysis of these complexes was attempted using chlorinated solvents, but proved to be challenging. The Fe(III) complex showed a weak ^{31}P NMR signal at 22.2 ppm, while the Fe(II) signal could not be recorded after isolation due to the lack of solubility in any common solvent. The aliquot ^{31}P NMR spectrum, however did show a signal at 22.3 ppm, which corresponded well to the expected shift. However, precise analysis of the metal coordination number could not be achieved using ^{31}P NMR spectroscopy. The ligands attached to the metal centre have

little influence on the ^{31}P NMR shift and therefore other forms of the complex could not be excluded from the predicted structure.

Further studies in the field of CDP–metal complexes were made while attempting to form digallated CDP complex **348** (Scheme 147). Neither the addition of $GaCl_3$ to the gallated CDP complex **344**, nor the reaction of CDP **259** with two equivalents of $GaCl_3$ resulted in the formation of any dimetallated species **348** to be observed, even at elevated temperatures. Next to the absence of electron density on the central C-atom, the low solubility of the CDP–$GaCl_3$ complex could also account for this lack or reactivity. Furthermore, CDP complex **344** did not react with the unhindered borane BH_3•SMe_2, which had shown coordination with the uncomplexed CDP. These results suggested that the coordinated $GaCl_3$ shielded the carbon centre from further reactions.

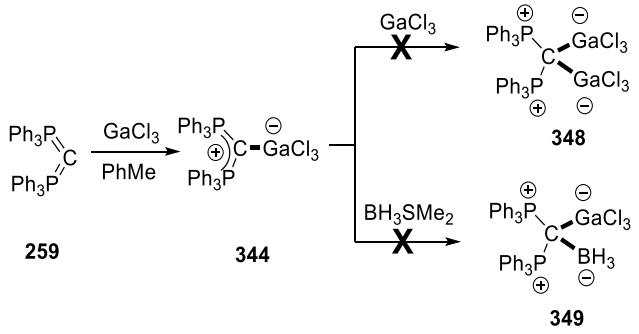

Scheme 147: Attempted double Lewis base reactions

3.3.4 Attempted Metal Catalysis

Gandon used the NHC–Ga complex **343** in π-acid catalysis by adding a catalytic amount of silver hexafluoroantimonate (Scheme 148).[164] The addition of a non-coordinating anion to the $GaCl_3$ complex was assumed to result in the abstraction of a chloride ligand and the formation of a cationic gallium catalyst. Complex **350** was assumed to be more π-acidic than precursor **343** and was therefore generated *in situ* in the reaction between alkyne **351** and **352**. This reaction included an intramolecular cycloisomerisation, followed by a Friedel-Crafts-type substitution, both of which were catalysed by a Lewis acidic metal.[166]

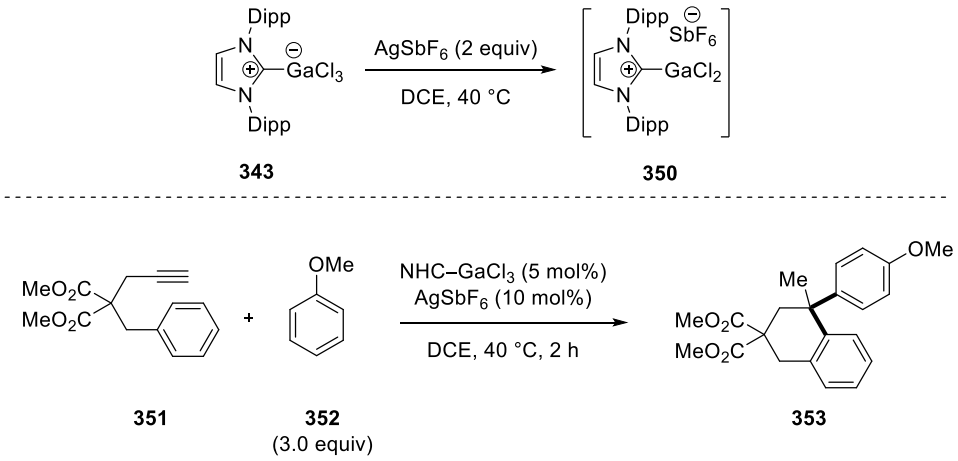

Scheme 148: π-acid catalysis

Inspired by this work, we aimed to apply this chemistry to the development of CDP–$GaCl_3$ catalysis (Scheme 149). As $AgSbF_6$ is an expensive reagent, Ga-complex **344** was thought to be activated by the use of $NaSbF_6$ or AgOTf. Reactions were carried out in *o*-C_6H_4BrF, a non-reactive polar solvent that has been used previously to crystallise CDP–metal complexes.[138] The formation of NaCl or AgCl was assumed to result in a counterion exchange to form complex **354**.

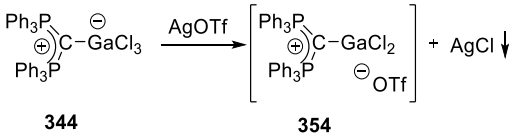

Scheme 149: Catalyst generation by anion exchange

Reactive gallium complex **354** may then act as a stronger π-acid, activating a π-base towards the attack of an external nucleophile. Phenyl acetylene (**303**), phenyl propyne (**355**) and diphenylacetylene (**356**) were chosen as π-bases, where the triple bond was assumed to be easily activated (Scheme 150). The nucleophile of choice was allyl trimethylsilane (**136a**), a reactive and commercially available compound. A similar reaction has been reported in the literature using catalytic amounts of $AlCl_3$, $InBr_3$ or stoichiometric $GaCl_3$.[167] In these reactions, the stable gallium catalyst would activate the alkyne for the attack of allylsilane **136a**, which would lead to silylated product **357**. Proto-desylilation would then give rise to 1,4-diene product **358**.

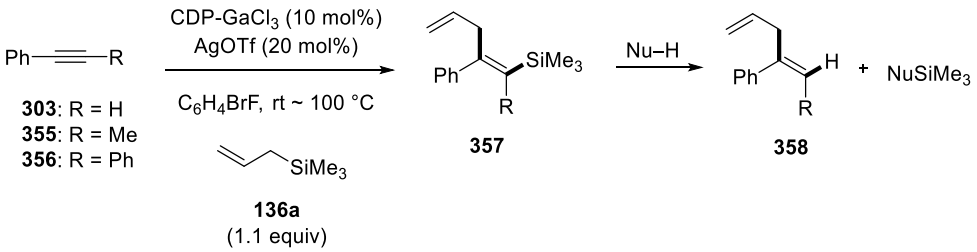

Scheme 150: CDP–Ga-catalysed allylation of alkynes

Different conditions were tested in this reaction. For each substrate, $GaCl_3$ was used for comparison and showed no reaction and complete recovery of starting materials in ^1H NMR spectroscopic analysis of reaction aliquots. ^1H NMR spectroscopy shifts in the allylic position of the silane **136a** (4.8 ppm) and the formation of allylic signals at 3.4-3.3 ppm for product **358** were monitored in this reaction (Table 62).

Table 62: π-Acid-catalysed allylation of alkynes

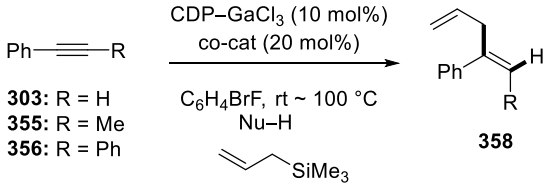

136a
(1.1 equiv)

Entry	R	Co-Catalyst	Conv (%)[a]
1	H	AgOTf	30
2	H	$NaSbF_6$	*NR*[b]
3	Me	AgOTf	5
4	Me	$NaSbF_6$	*NR*[b]
5	Ph	AgOTf	*NR*[b]
6	Ph	$NaSbF_6$	*NR*[b]

[a] The conversion was determined by ^{1}H NMR spectroscopy of a reaction aliquot without internal standard. [b] NR = no reaction; the desired product was not detectable, only starting materials were detected (^{1}H NMR analysis of a reaction aliquot).

No product was formed in the reactions below 80 °C. Prolonged heating at 100 °C lead to the formation of the desired product, where the silane was hydrolysed when using terminal alkyne **303** and a silver co-catalyst (entry 1). Using a sodium co-catalyst did not result in any product formation (entry 2). When methyl-substituted alkyne **355** was used, a similar pattern was observed, where the use of AgOTf resulted in 5% conversion to allylated product **358**, but no reaction was observed when the sodium salt was used (entries 3 and 4). Symmetrical alkyne **356** showed no reaction regardless of co-catalyst (entries 5 and 6).

Due to time contraints, reactions with **136a** were not investigated further at this point as the development of a catalytic method using both lone pairs on the carbone were of interest. However, some reactivity of the CDP–$GaCl_3$ in the field of π-acid catalysis has been observed.

3.3.5 Attempted Dual and FLP Catalysis

With the CDP–$GaCl_3$ complex in hand, dual catalysis was attempted by exploiting the potential for both CO_2 activation as well as metal coordination (Scheme 151). As both the reaction with carbon dioxide and gallium trichloride were fast, it was assumed that carboxylated CDP–$GaCl_3$ complex **359** could be formed *in situ*.

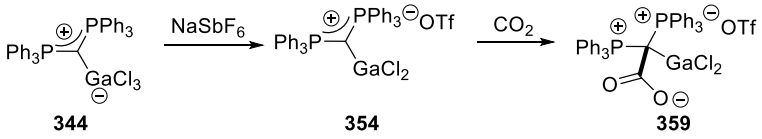

Scheme 151: Formation of carboxylated CDP–Ga

Complex **359** may then be used as a catalyst for the activation of a basic electrophile through coordination to the Lewis acidic metal (Scheme 152). The reaction of NHC–carboxylates with an epoxide is known to form the corresponding organic carbonate.[168] Therefore, gallium complex **344** was thought to activate epoxide **360** towards attack of the proposed *in situ* generated CDP–carboxylate **359** to generate carbonate **362**.

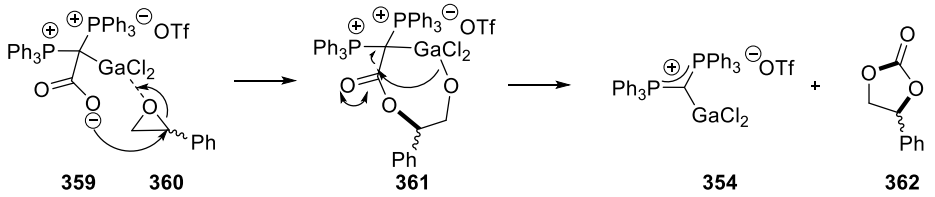

Scheme 152: Proposed mechanism for dual catalysis

$CDP–GaCl_3$ **344** (10 mol%) and $NaSbF_6$ (20 mol%) were used for the activation of epoxide **360** using atmospheric pressure of CO_2 in 1,2-bromofluorobenzene. Alternatively, **344** was replaced by a mixture of carbodiphosphorane **259** (20 mol%) and $GaCl_3$ (20 mol%) to generate **344** *in situ* (Scheme 153).

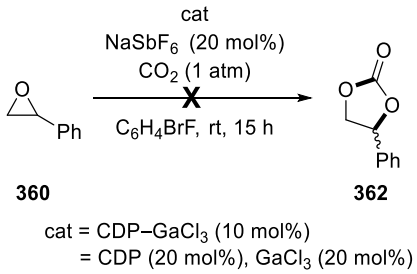

Scheme 153: CDP and CDP–$GaCl_3$-catalysed reactions

Unfortunately, neither of these reactions showed any product formation after 15 h at room temperature. Further heating of this mixture led to the loss of the styrene oxide without the formation of any product. Instead, polymerisation of the epoxide was indicated by broad signals in ^1H NMR spectroscopy.

The steric bulk that was assumed to prevent binding of CDP **259** to boron Lewis acids was assumed to be applicable to frustrated Lewis pair (FLP) catalysis.[169] Triethylborane (**335b**)

had been shown to be unreactive in the addition of CDP **259**. This FLP may be used in the activation of CO_2 by increasing the epoxide's electrophilicity by coordination to BEt_3 (Scheme 154). Simultaneously, the CO_2 could be turned into a nucleophile by the attack of CDP **259**. Both activated species could then react to form a carbonate, while regenerating the FLP catalysts after cyclisation.

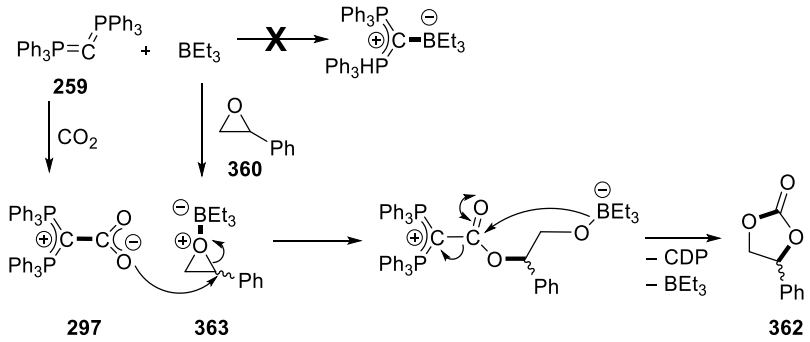

Scheme 154: Proposed mechanism for the carboxylation of epoxides

Initially, a stoichiometric version of this reaction was attempted, where the carboxylate adduct was reacted with the epoxide in the presence of the Lewis acid. No reaction was observed in $CDCl_3$, which could be due to the slow decomposition of the CO_2 adduct.

The *in situ* formation of adduct **297** was then attempted in toluene (Scheme 155). As the carboxylate was observed to precipitate, acetonitrile was added to increase solubility. However, no product was observed in this reaction. Further studies of this reaction showed that in the presence of CDP, styrene oxide (**360**) did not form a boron-ate complex with BEt_3, which was required in this reaction.

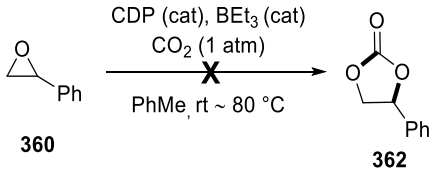

Scheme 155: Attempted catalytic cabonate formation

In summary, the activation of carbon dioxide was not achieved using CDP **259** as a catalyst. Despite the fast formation of adduct **297**, this compound did not show any reactivity towards (activated) electrophiles. The use of alternative electrophiles or other activators may be more successful in this field.

3.3.6 Brønsted Base Catalysis

As described previously, the Lewis basicity of the CDP was found to be low even in reactions with highly electrophilic aldehydes. No reaction was observed with benzaldehyde even at elevated temperatures suggesting that the attack of the CDP is slow or reversible (Scheme 156, right, cf. Scheme 141, p 162). This poor nucleophilicity may be related to the CDP's steric bulk, which may disfavour the attack of an electrophile. On the other hand, CDPs have been reported to yield Wittig-type products in the reaction with activated ketones (Scheme 156, left). This transformation liberates one equivalent of triphenylphosphine oxide, which is a good driving force for the reaction.

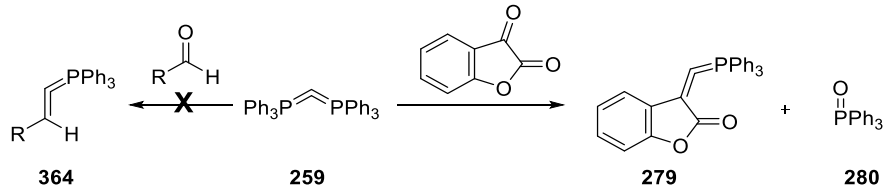

Scheme 156: Reaction of CDPs with carbonyls

The steric bulk of the CDP was assumed to be less pronounced when it acted as a Brønsted base catalyst. Here, the catalyst would deprotonate an acidic C–H bond to generate the protonated CDP cation and an alkyl anion (Scheme 157). This nucleophile may subsequently be used in the reaction with a suitable electrophile to generate a C–C bond.

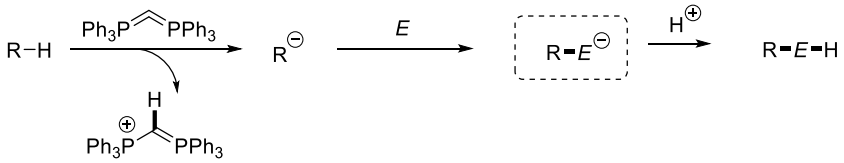

Scheme 157: BB activation using a CDP catalyst

Different acidic substrates may be used as pro-nucleophiles in this reaction. Depending on their pK_a values, these can be more or less difficult to be activated. Possible examples include nitroalkanes, ketones and alkyl nitriles (Figure 22).

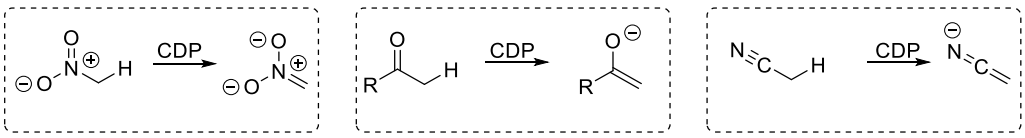

Figure 22: Potential pro-nucleophiles

Once deprotonated by the CDP catalyst, the corresponding nucleophilic carbanions generated may be used in C–C bond-forming reactions with neutral electrophiles. These

transformations would generate a negative charge on a heteroatom that can be protonated by either the substrate or the protonated catalyst to close the catalytic cycle. Carbonyls, imines, epoxides, aziridines and Michael acceptors are all potential electrophiles that would give rise to different kinds of products (Figure 23).

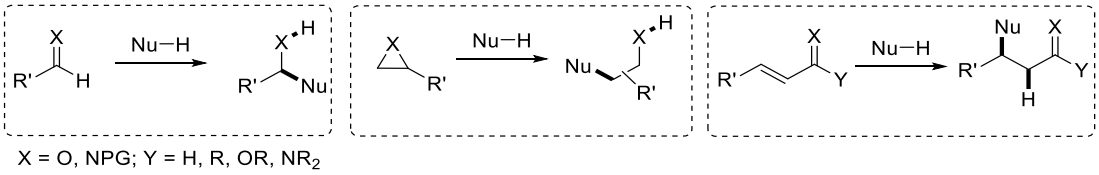

Figure 23: Potential electrophiles

Overall, the choice of pro-nucleophiles and electrophiles was limited by their reactivity with the catalyst. For acetophenone for example, both the nucleophilic attack and the deprotonation are competing reactions, where either the Wittig product or the enolate is produced (Scheme 158). If the reaction with the electrophile is fast, the equilibrium may be shifted towards the deprotonation. At the same time, the catalyst may also be deactivated by the reaction with the electrophile, if this is too electrophilic.

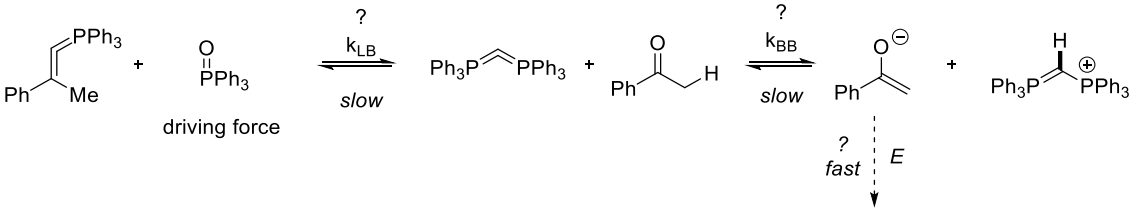

Scheme 158: LB and BB activation of a CDP with Acetophenone

Aldol and Mannich reactions

The aldol and the Mannich reaction are common C–C bond forming reactions, where an enolate nucleophile is added to aldehydes and imines.[3] As a variety of carbonyl-containing pro-nucleophiles were available for activation, this reaction depends largely on the pro-nucleophile's pK_a value (Figure 24).

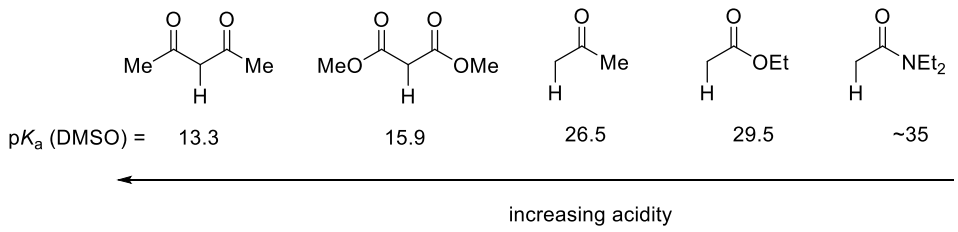

Figure 24: Acidity of α-carbonyl C–H bonds

While many bases are known for the activation of malonates, deprotonation of esters and amides are less explored. Drawing from the success of enamine catalysis in the aldol reaction,[170] a similar pathway was rationalised for the reactions with imines.[171] The use of a proline catalyst has been reported for the activation of ketones.[172] Both malonates as well as β-ketoesters were activated using chiral cinchona alkaloid catalysts[173] or a lithium binaphtholate catalyst[174] in the enantioselective catalytic Mannich reaction.

3.3.6.1 Carbonyl Compounds

1,2-additions

Acetophenone was chosen as an initial model substrate with a comparably low pK_a value of ca. 25 (DMSO).[37] First, the reaction between acetophenone and CDP was examined, showing no Wittig products being formed even when heating up to 60 °C (Scheme 159).

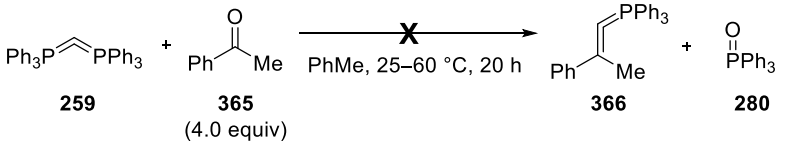

Scheme 159: Reaction of CDP with acetophenone

Catalytic reactions with benzaldehyde and imines were then carried out using 5–20 mol% CDP in toluene at 25 °C for 20 h (Table 63). In all cases a product mixture was obtained, which can be assigned to structures **367**-**369** based on comparison with literature ^{1}H NMR data.[175] Conversions were based on the relative integration of the product signals with respect to the acetophenone signals in ^{1}H NMR spectroscopy. For this analysis, C–H signals in the benzylic position [δ = 5.4 (X = O), δ = 4.9 (X = NPG) for **367** and δ = 4.1 ppm for **369**] or in the alkenyl region (δ = 7.8 ppm for **368**) were integrated.

Table 63: Aldol and Mannich reactions of acetophenone

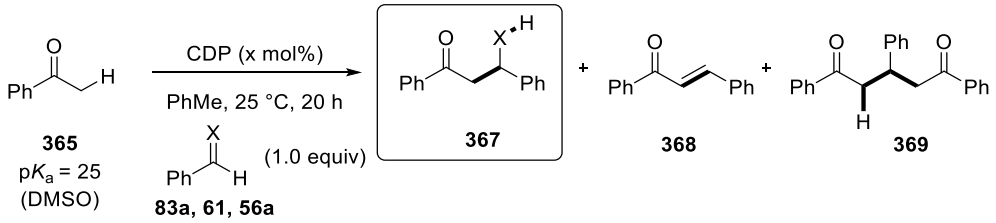

Entry	X	x (mol%)	Overall Conv (%)[a]	367:368:369 Conv (%)[a]
1	O	20	47	10:26:11
2	O	10	73	31:42:0
3	O	5	30	2:24:4
4[b]	O	5	35	18:15:2
5	NTs	10	15	15:0:0
6	NPh	10	5	5:0:0

[a] The conversion was determined by ^{1}H NMR spectroscopy of a reaction aliquot without internal standard. [b] Reaction carried out at 0 °C.

Although the expected aldol adducts **367** were detected (entries 1-4), these products underwent further transformations. Due to the acidic nature of the C_α–H bond in the aldol adduct, a dehydration reaction was observed, leading to the formation of chalcone (**368**; Scheme 160). One reason for this side-reaction could be the coordination of the OH in **367a** to the catalyst. Chalcone was then shown to act as an electrophile in a Michael addition with the *in situ* generated enolate of acetophenone.

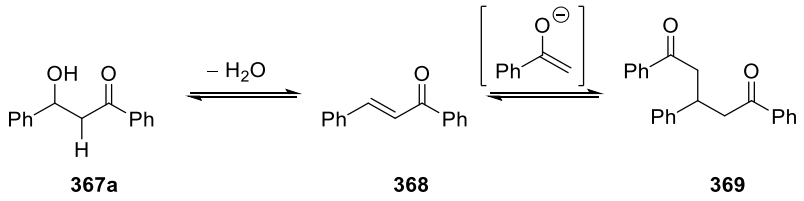

Scheme 160: Dehydration and further reaction of aldol adduct

Reactions with benzaldehyde as the electrophile achieved good conversions and catalyst turnover was achieved (TON up to 7, entries 1-4). However, low degrees of selectivity were obtained and a mixture of all three products was observed under almost all employed conditions, regardless of catalyst loading or temperature. By changing the nature of the electrophile, an improvement of selectivity was expected to be observed. The Mannich adducts **367b-c,** generated from imines, were assumed to be less likely to undergo a dehydroamination. By changing the *N*-protecting group, the imine can be either more (PG = Ts) or less (PG = Ph) reactive than benzaldehyde.[176]

In the reactions with imines, a higher degree of selectivity was indeed observed, where **367** (X = NTs or NPh) was the only observed product and no dehydroamination occurred (Table 63, entries 5 and 6). However, conversions were generally poor with levels of only up to 15% showing a limited turnover capacity, if any.

In order to suppress the undesired side-reactions, a solvent screening was performed under otherwise identical conditions and compared to the result in toluene (Table 64).

Table 64: Solvent screening for aldol reaction of acetophenone with benzaldehyde

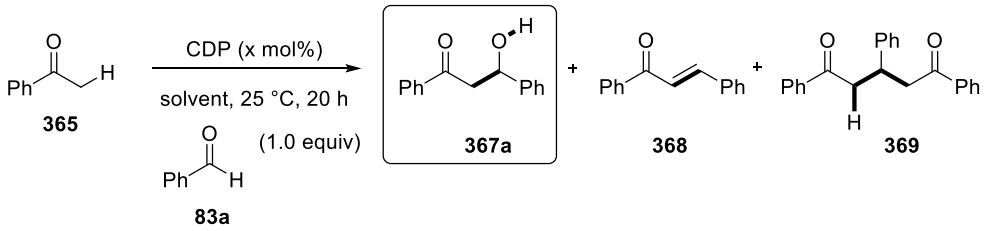

Entry	Solvent (Ɛ)	x (mol%)	Overall Conv (%)[a]	367a:368:369 Conv (%)[a]
1	PhMe (2.4)	5	30	2:24:4
2	Dioxane (2.3)	5	34	8:14:12
3	Et_2O (4.3)	5	40	3:29:8
4	2-Me-THF (7.0)	5	18	4:0:14
5	THF (7.5)	5	20	3:10:7
6	BTF (9.2)	5	13	3:7:3
7	THF (7.5)	10	42	30:12:0
8[b]	THF (7.5)	5	57	13:21:23

[a] The conversion was determined by ^{1}H NMR spectroscopy of a reaction aliquot without internal standard. [b] Reaction carried out at 0 °C.

Compared to the initial result in toluene (30%, mixture of **367a**, **368** and **369**; entry 1), none of the other aprotic solvents with different polarities (Ɛ = 2.3–9.2) showed a significant improvement in selectivity, and a general decrease in reactivity was observed (entries 2-6). This could be ascribed to a lower solubility of the catalyst in the chosen solvents. Due to the established solubility of CDPs in THF, reactions at a higher catalyst loading and at 0 °C were performed in this solvent (entries 7 and 8). Both the conversion and the selectivity for product **367a** increased when using 10 mol% catalyst loading, but products **367a** and **368** were obtained in a 3:1 ratio only (entry 7). Despite a good yield being obtained at 0 °C, unfortunately the product selectivity was poor (entry 8). Overall, best conversions were obtained in toluene and diethyl ether, but no satisfactory method for the selective preparation of aldol or Mannich adducts could be developed. However, it was noted that the nucleophilic addition of acetophenone to Michael acceptors was indeed observed, suggesting that direct selective Michael reactions may be more successful.

1,4-additions

As the Michael addition of acetophenone enolates to chalcone was observed as a side-reaction in previous experiments, this reaction was further investigated and extended to the use of α,β-unsaturated aldehydes and amides (Table 65). Previous reaction conditions (toluene, 25 °C, 20 h) were applied. The conversion was determined by quantification of the product signals in ^{1}H NMR spectra relative to the consumption of acetophenone.

Table 65: 1,4-addition of acetophenone to different Michael acceptors

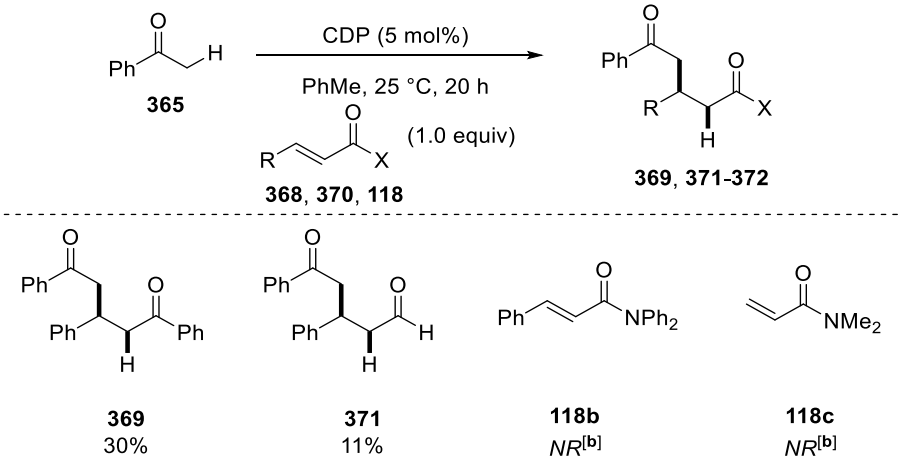

The conversion was determined by ^{1}H NMR spectroscopy of a reaction aliquot without internal standard. [b] NR = no reaction; the desired product was not detectable, only starting materials were detected (^{1}H NMR analysis of a reaction aliquot).

Reacting acetophenone (**365**) with chalcone (**368**) yielded the 1,5-dione product **369**, albeit in only 30% yield. Compound **369** had previously been identified as a side-product in the 1,2-addition experiments. The incomplete transformation shows that this side-reaction is slow, which may explain why chalcone was often the major side-product in the previous aldol reactions. The use of a more reactive Michael acceptor, cinnamaldehyde (**370**), gave only 11% conversion to dione product **371**. Here again, no side-products such as the 1,2-adduct were observed in ^{1}H NMR spectroscopy. The less reactive Michael amides (**118**) did not show any reactivity under the employed conditions, both for the β-substituted and unsubstituted substrates. In both cases, only the corresponding starting materials were recovered.

The choice of electrophile was somewhat limited in this type of reaction because the catalyst showed reactivity with many other Michael acceptors. These substrates were often decomposed or polymerised in the presence of catalytic amounts of CDP and were therefore considered less suitable in Michael additions. In turn, a different pro-nucleophile was considered for these Brønsted base-catalysed reactions.

3.3.6.2 Alkylnitriles - 1,2-Additions

Acetonitrile is a much more challenging substrate to activate than acetophenone. With a pK_a value of 31 (DMSO),[37] acetonitrile requires a much stronger base to get deprotonated than acetophenone (pK_a ~ 25, DMSO).[37] In 2008, Levacher reported the activation of acetonitrile using a Brønsted base catalyst in a Mannich reaction with imine **56a** (Scheme 161). The catalyst consisted of a combination of sodium phenoxide with an α-silyl ester, which was thought to be basic enough to generate the acetonitrile anion.

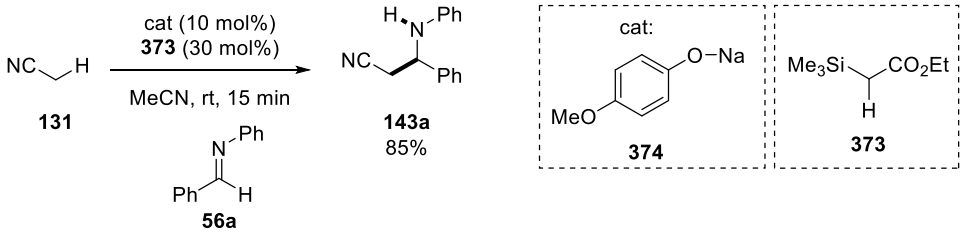

Scheme 161: Phenoxide-mediated C–H bond activation of acetonitrile

Therefore, reactions with acetonitrile were attempted in a similar manner to the experiments using acetophenone as a pro-nucleophile (Table 66). Imines and aldehydes were used initially as electrophiles in the 1,2-addition reaction. A similar reactivity pattern to the aldol reactions was observed in these experiments. The 1,2-adducts **143** were the desired products. However, these could undergo a dehydration or dehydroamination reaction to yield substituted acrylonitrile **375**, which could subsequently be attacked by another equivalent of the acetonitrile anion to give 1,3-dicyanoakane **376**. By using different electrophiles and solvents, the ratio of these products was attempted to be optimised.

Table 66: 1,2-additions of acetonitrile to aldehydes and imines

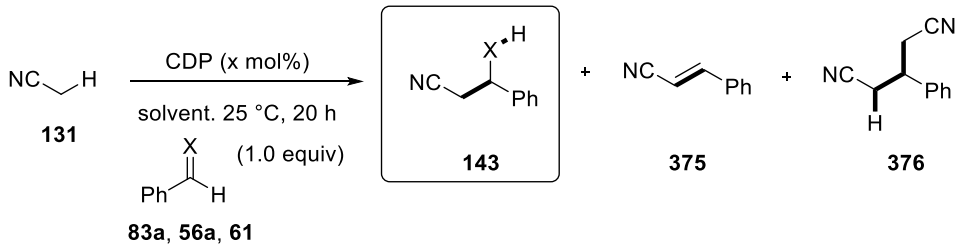

Entry	X	Solvent	x (mol%)	Overall Conv (%)[a]	143:375:376 Conv (%)[a]
1	O	PhMe	5	7	0:5:2
2	NPh	PhMe	5	*NR*[b]	-
3	O	MeCN (>50 equiv)	10	35	26:5:4
4	NPh	MeCN (>50 equiv)	10	62	52:0:10
5	NTs	MeCN (>50 equiv)	10	9	9:0:0

[a] The conversion was determined by ^{1}H NMR spectroscopy of a reaction aliquot without internal standard. [b] NR = no reaction; the desired product was not detectable, only starting materials were detected (^{1}H NMR analysis of a reaction aliquot).

First, the reactions using benzaldehyde or the *N*-Ph-protected benzaldimine as electrophiles were carried out in toluene (entries 1 and 2). In the case of benzaldehyde, a low conversion was observed with a slight preference for the formation of the dehydration side-product **375**. The reaction with the imine did not proceed at all; only starting materials were recovered. Acetonitrile is a popular organic solvent as it is more volatile than most other polar aprotic solvents. Thus, reactions were attempted using acetonitrile as both the solvent and pro-nucleophile (>50 equiv relative to the electrophile; entries 3-5). Furthermore, the catalyst loading was increased to 10 mol%. The reaction with benzaldehyde gave a much higher conversion and turnover of the catalyst was achieved (TON > 3, entry 3). However, further reactions of product **143** could not be suppressed entirely, and substantial amounts of both side-products were observed. As imines had previously shown an improvement in the selectivity in the reactions with acetophenone, these were used as alternative electrophiles (entries 4 and 5). Surprisingly, the reaction with *N*-Ph-benzaldimine gave a substantially higher conversion and a higher selectivity for product **143**. The reaction with *N*-Ts-protected benzaldimine gave exclusive formation of product **143**, although the conversion was only 9%.

The reaction with the *N*-Ph-protected imine showed that the 1,2-adduct could be formed selectively by using CDP as the catalyst. Further reactions of the product could not be suppressed entirely, but **376** appeared to be the only side-product in this reaction. This means

that the elimination product **375** also reacted quickly with the *in situ* generated acetonitrile anion.

Before investigating the Michael addition of acetonitrile, other alkylnitriles were examined in the 1,2-addition. Propionitrile has a higher pK_a value (32.5, DMSO)[37] than acetonitrile, due to the methyl group in α-position. By replacing the methyl with a phenyl group instead, the pK_a value is lowered to 22 (DMSO).[37] Both pro-nucleophiles were tested for their ability to react with aldehydes and imines (Table 67). Toluene was used as the solvent because these pro-nucleophiles are less commonly used as organic solvents.

Table 67: 1,2-addition of substituted acetonitrile with electrophiles

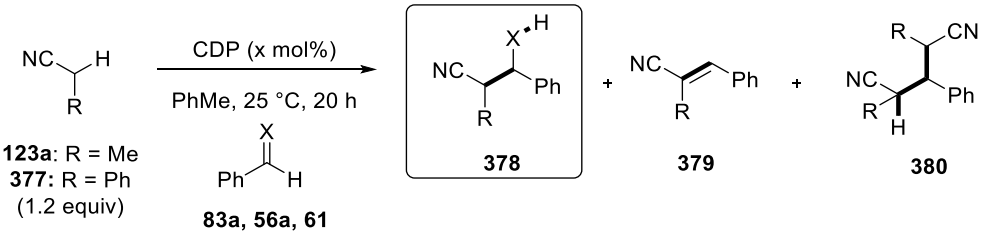

Entry	R	X	x (mol%)	Overall Conv (%)[a]	378:379:380 Conv (%)[a]
1	Me	O	5	*NR*[b]	-
2	Me	NPh	5	*NR*[b]	-
3	Ph	O	10	95	0:95:0
4	Ph	NPh	10	64	17:40:7
5	Ph	NTs	10	96	0:96:0

[a] The conversion was determined by ^{1}H NMR spectroscopy of a reaction aliquot without internal standard. [b] NR = no reaction; the desired product was not detectable, only starting materials were detected (^{1}H NMR analysis of a reaction aliquot).

No reactivity was observed when using propionitrile in the reaction with benzaldehyde or *N*-Ph-benzaldimine (entries 1 and 2). As this pro-nucleophile is more difficult to activate, lower conversions were expected. Benzylnitrile, in turn, was easier to activate due to the significantly increased acidity of the α-hydrogen. In the reaction with all three electrophiles, high conversions but very low selectivities for the desired product **378** were observed (entries 3-5). This may arise from the highly acidic proton in product **378**, leading to a facile elimination reaction producing **379** in high yields. In the absence of further pro-nucleophile, the reaction essentially stopped after the elimination. When the reaction had not gone to completion and pro-nucleophile was present when the alkene formed, this was also a suitable electrophile for the Michael addition and product **380** formed as well.

Overall, the activation of alkylnitriles provided promising results, but the selectivity in reactions with aldehydes and aldimines remained a challenge.

3.3.6.3 MeCN - 1,4-Additions

The addition of alkylnitriles to Michael acceptors is much less investigated and only one example is known in the literature. The Kobayashi group developed a Brønsted base-catalysed process, in which propionitrile was added to α,β-unsaturated amides in a diastereoselective fashion (Scheme 45, p 42).[61] Furthermore, the use of a chiral ligand for the employed potassium amide catalyst resulted in the enantioselective 1,4-addition with an optical purity of up to 65% (Scheme 162). *It is worth noting that the reaction using acetonitrile resulted in a 'messy' reaction mixture, and did not yield the desired 1,4 adduct.*

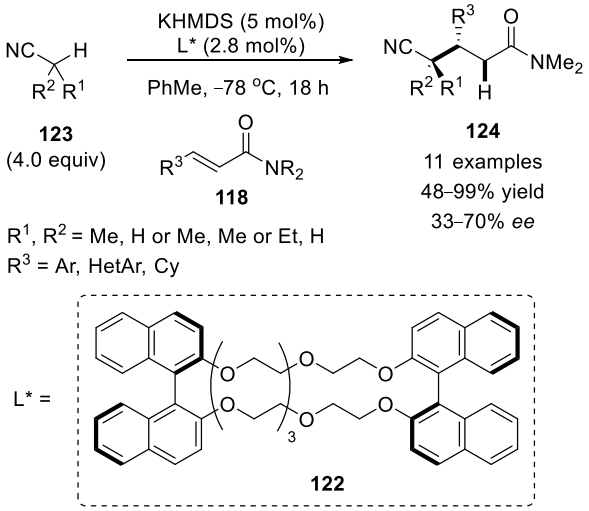

Scheme 162: BB-catalysed activation of alylnitriles in Michael additions

We decided to examine the CDP as a metal-free catalyst, which may address this gap in synthetic methodology. Different Michael acceptors, such as α,β-unsaturated aldehydes, ketones and amides, were selected for the reaction with acetonitrile (Table 68). In line with the previous results suggesting a higher reactivity using a large excess of the pro-nucleophile, reactions were carried out in acetonitrile as the solvent. This choice also simplified the ^{1}H NMR spectroscopic analysis as only one solvent signal was present. In order to quantify the results reliably, dibenzyl ether (DBE) was added as an internal standard after the specified reaction time. For ^{1}H NMR spectroscopic interpretation, the overlapping C–H signals of the α- and γ-positions of the 1,4 adduct were integrated (δ = 2.9 ppm, 4H).

Table 68: Michael additions of acetonitrile

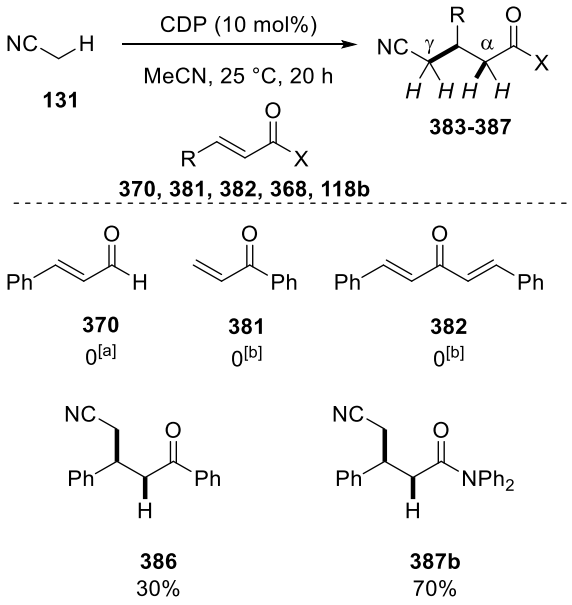

The yield was determined by ^{1}H NMR spectroscopy of a reaction aliquot; internal standard: dibenzyl ether (25 mol%). [a] 1,2-addition product observed (^{1}H NMR analysis of a reaction aliquot). [b] polymerisation observed (^{1}H NMR analysis of a reaction aliquot).

The reaction with cinnamaldehyde (**370**) showed no formation of the expected product, but instead gave rise to a different compound that was assumed to be the 1,2-adduct. Different ketones were then tested in this reaction. Both vinyl phenyl ketone (**381**) and dibenzylidene acetone (**382**) gave rise to broad signals in ^{1}H NMR spectroscopy, suggesting polymerisation, and no formation of the product. In contrast, the reaction with chalcone (**368**) proceeded, but the yield was only 30% after 20 h. Finally, the *N*,*N*-diphenyl-3-phenylacrylamide (**118b**) gave a promising yield of 70% for product **387b**. Interestingly, this substrate is very similar to the substrate used by the Kobayashi group.

Since less reactive Michael acceptors proved to be most suitable in the 1,4-addition of acetonitrile, similar electrophiles were screened next under otherwise unchanged conditions (Table 69).

Table 69: Electrophile screening for the Michael addition of acetonitrile

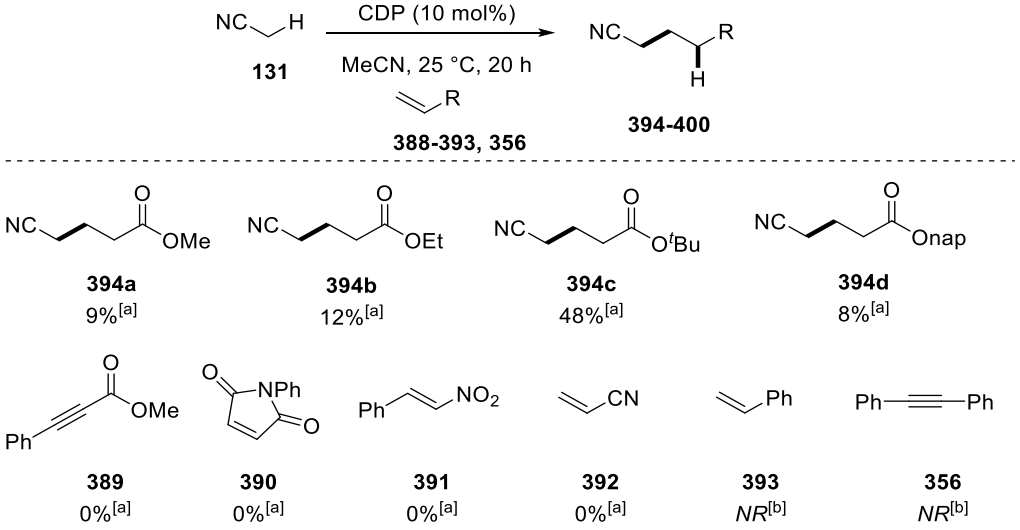

The yield was determined by ^{1}H NMR spectroscopy of a reaction aliquot; internal standard: dibenzyl ether (25 mol%). [a] Broad ^{1}H NMR signals were observed due to polymerisation of the starting material. [b] NR = no reaction; the desired product was not detectable, only starting materials were detected (^{1}H NMR analysis of a reaction aliquot). nap = 2-naphthyl.

Michael esters were expected to be slightly more reactive than amides, but are not known to undergo side-reactions such as the 1,2-addition, as seen with cinnamaldehyde. Unfortunately, none of the employed esters, including the alkynyl substrate, gave yields that were comparable with those obtained in the reaction with the Michael amide. In all cases, broad ^{1}H NMR signals were observed, suggesting polymerisation of the α,β-unsaturated esters. Similar results were obtained when using *N*-protected maleimide **390**, nitrostyrene **391** or acrylonitrile **392**. Indeed, when reacting these Michael acceptors with 10 mol% of CDP, decomposition of the starting material was observed by ^{1}H NMR analysis even in the absence of the pro-nucleophile. This background reaction suggested an attack of the CDP to the Michael acceptors leading to subsequent reactions with further equivalents of the Michael acceptor resulting in oligomeric or polymeric structures. On the other end of the spectrum, unactivated multiple bonds were also tested under these conditions. Both styrene **393** and diphenyl acetylene **356** showed no reactivity even when heating the reaction mixtures to 80 °C.

As α,β-unsaturated amides have been shown to be the most suitable electrophiles under mild reaction conditions, solvent screenings were performed for this class of substrates to decrease the equivalents of pro-nucleophile used. Despite the reaction resulting in a high yield when conducted in acetonitrile, its application may be limited when the pro-nucleophile is the limiting reagent. Reactions between acetonitrile (2.0 equiv) and the previously used Michael amide **118b** were carried out in THF, toluene, and dioxane (Table 70).

Table 70: Solvent screening for the Michael addition of acetonitrile I

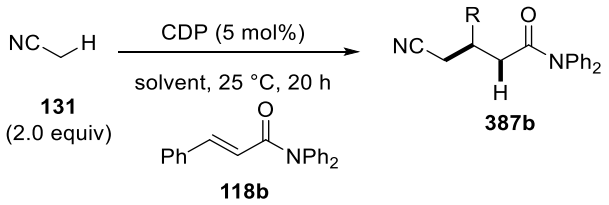

Entry	Solvent (Ɛ)	Yield (%)[a]
1	MeCN (37.5)	70
2	THF (7.5)	*NR*[b]
3	PhMe (2.4)	*NR*[b]
4	dioxane (2.3)	*NR*[b]

[a] The yield was determined by ^{1}H NMR spectroscopy of a reaction aliquot; internal standard: dibenzyl ether (25 mol%). [b] NR = no reaction; the desired product was not detectable, only starting materials were detected (^{1}H NMR analysis of a reaction aliquot).

No reactivity was observed under these conditions (entries 2-4). One reason for this lack of reactivity could be the decreased substrate concentration that led to a slow equilibration when forming the acetonitrile anion. Alternatively, the low polarity of the employed solvents compared with acetonitrile could destabilise the charged intermediates. Another reason could be the low reactivity of the chosen substrate, as the β-substitution may substantially increase the steric hindrance. Therefore, unsubstituted acrylamide **118d** was chosen as the electrophile and reactions were carried out in a range of more polar solvents (Table 71).

Table 71: Solvent screening for the Michael addition of acetonitrile II

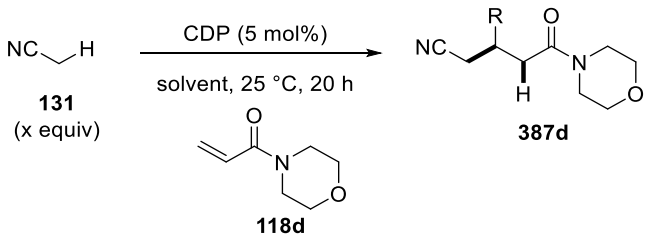

Entry	Solvent (Ɛ)	x (equiv)	Yield (%)[a]
1	MeCN (37.5)	40	86
2	PC (65.5)	2	8
3	DMF (36.7)	2	39
4	NMP (32.2)	2	23
5	PhCN (26.0)	2	*NR*[b]
6	THF / MeCN[c]	20	70
7	DMF / MeCN[c]	20	77

[a] The yield was determined by ^{1}H NMR analysis of a reaction aliquot; internal standard: dibenzyl ether (25 mol%). [b] NR = no reaction; the desired product was not detectable, only starting materials were detected (^{1}H NMR analysis of a reaction aliquot). [c] Solvent:MeCN = 1:1.

First, the reaction with this Michael acceptor was performed in acetonitrile to provide a benchmark yield for the solvent screening (86%, entry 1). Propylene carbonate (PC) was chosen as a solvent with a higher polarity than acetonitrile, but the observed yield was low (8%, entry 2). Both DMF and *N*-methyl-pyrrolidone (NMP) have a similar polarity to acetonitrile and contain an amide functional group that may be able to stabilise highly polar reaction intermediates. The use of these solvents resulted in higher yields for product **387d** than in the case of propylene carbonate, but could not compete with the result in acetonitrile alone (entries 3 and 4). Like acetonitrile, benzonitrile (PhCN) contains a nitrile functional group, but due to the lack of α-hydrogens, it cannot be activated itself. However, its polarity is rather low and no reaction was observed (entry 5). As some of these solvents were at least tolerated in this reaction, it was anticipated that a solvent mixture may be used in order to decrease the equivalents of pro-nucleophile. When using a 1:1 mixture of acetonitrile with THF or DMF, similar yields were observed to the reaction in pure acetonitrile (entries 6 and 7). This method allowed to decrease the amount of pro-nucleophile used by 50%, while maintaining a comparable yield.

As both pure acetonitrile and the binary solvent system with DMF were suitable conditions for this reaction, temperature screens were performed both solvent systems using Michael acceptor **118b** (Table 72).

Table 72: Temperature screening for the Michael addition of acetonitrile I

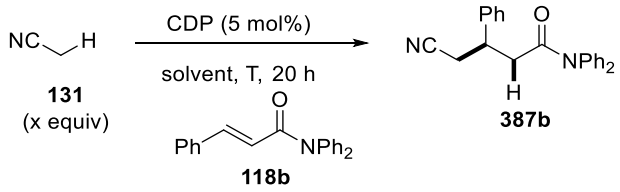

Entry	Solvent	x (equiv)	T (°C)	Yield (%)[a]
1[b]	MeCN	40	25	70
2	MeCN	40	40	60
3	MeCN	40	60	52
4	MeCN	40	80	78
5	DMF / MeCN[c]	20	25	39
6	DMF / MeCN[c]	20	40	50
7	DMF / MeCN[c]	20	60	42
8	DMF / MeCN[c]	20	80	52

[a] The yield was determined by ^{1}H NMR analysis of a reaction aliquot; internal standard: dibenzyl ether (25 mol%). [b] Reaction carried out using 10 mol% catalyst loading. [c] DMF:MeCN = 1:1.

It was found that increasing the temperature to 40–80 °C did not significantly increase the reactivity in pure acetonitrile. The use of the solvent mixture showed a substantially lower reactivity of this electrophile compared to the unsubstituted Michael acceptor **118d** (entry 5). Increasing the temperature in this case did generally increase the reactivity but only yields of up to 52% were observed (entry 8).

In order to verify these results, another temperature screening was carried out with the more reactive Michael acceptor **118d** in DMF or THF using only 2.0 equiv acetonitrile (Table 73).

Table 73: Temperature screening in DMF and THF

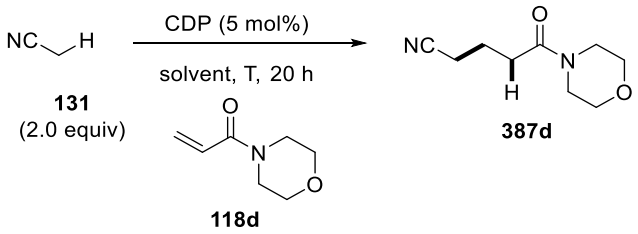

Entry	Solvent	T (°C)	Yield (%)[a]
1	DMF	25	39
2	DMF	60	47
3	DMF	80	44
4	THF	60	4
5	THF	80	25

[a] The yield was determined by ^{1}H NMR analysis of a reaction aliquot; internal standard: dibenzyl ether (25 mol%).

This screening showed a moderate improvement of reactivity in DMF when performing the reaction at 60–80 °C (entries 2 and 3) compared to the reaction at room temperature (entry 1). Interestingly, reactivity was also observed at elevated temperatures in THF, which had previously been proven to be an unsuitable solvent at room temperature (entries 4 and 5). Overall, changing the temperature does not have a substantial effect on the reactivity and as the reaction proceeded at room temperature when conducted in acetonitrile, the use of the pro-nucleophile as the solvent was considered the most convenient.

Other organobases were also tested as catalysts in the reaction between acetonitrile and Michael amides. Verkade and Schwesinger organosuperbases were screened under identical conditions to the CDP-catalysed reactions (Table 74).

Table 74: Catalyst screening for the 1,4-addition of acetonitrile to Michael amides

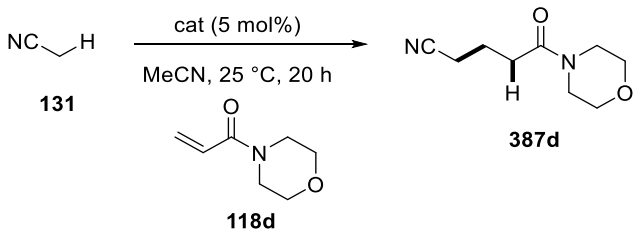

Entry	Cat	Yield (%)[a]
1	CDP	86
2	**102a** (Me)	*NR*[b]
3	**102a** (pyrr)	*NR*[b]
4	**103b**	62
5	**103a**	68
6	**104**	22
7	**105a** (Me)	66
8	**105b** (^{i}Pr)	86
9	**105c** (^{i}Bu)	46
10	NaHMDS	13[c]

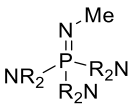

102
Me-P_1 (R^1)
Schwesinger

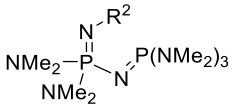

103
R^2-P_2
Schwesinger

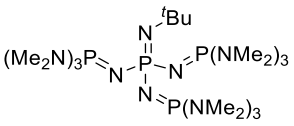

104
^{t}Bu-P_4
Schwesinger

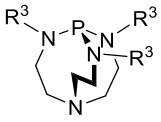

105
^{R3}Verkade

[a] The yield was determined by ^{1}H NMR analysis of a reaction aliquot; internal standard: dibenzyl ether (25 mol%). [b] NR = no reaction; the desired product was not detectable, only starting materials were detected (^{1}H NMR analysis of a reaction aliquot). [c] Mass balance = 13%.

Neither of the P_1 Schwesinger bases **102** was able to catalyse the reaction between **131** and **118d** (entries 2 and 3). However, P_2 Schwesinger bases **103** gave product **387d** in 62–68% yield (entries 4 and 5). The strongest Schwesinger P_4 base did not show a comparable reactivity and gave product **387d** in only 22% yield (entry 6). Also the Verkade bases **105** were able to catalyse the conjugate addition giving **387d** in 46–86% yield (entries 7-9). Although some of these catalysts were highly active in the Michael addition, their general potential in catalysis has already been demonstrated, so the CDP-catalysed reactions were investigated further. When NaHMDS was used for comparison, a low yield and a low mass balance was observed (entry 10). This observation confirmed the results obtained by Kobayashi, where a 'messy' reaction mixture was described in the Michael addition of acetonitrile (Scheme 162, p 182).

Finally, the electrophile scope of this reaction was investigated using the optimised conditions (Table 75).

Table 75: Electrophile scope for the addition of acetonitrile to acrylamides

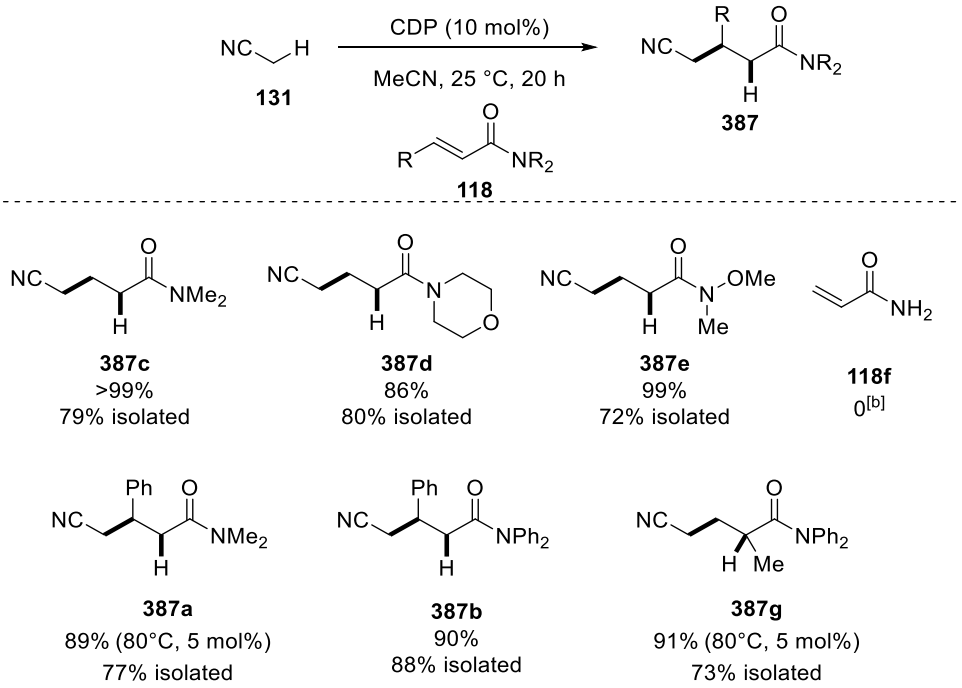

The yields were determined by ^{1}H NMR analysis of a reaction aliquot; internal standard: dibenzyl ether (25 mol%). [b] Broad ^{1}H NMR signals are observed due to polymerisation of the starting material (^{1}H NMR analysis of a reaction aliquot).

The unsubstituted acrylamides, as well as the Weinreb amide showed good reactivities towards the addition of acetonitrile and products **387c-e** were formed in good yields. The unprotected acrylamide **118f** did not give any product due to the polymerisation of the

starting material as suggested by ^{1}H NMR spectroscopy. The β-substituted amide products **387a** and **387b** could be obtained in high yields but more forcing conditions had to be used in the case of *N*,*N*-dimethyl acrylamide (**118a**), which did not show any reactivity under mild reaction conditions. Indeed, prolonged reaction times or heating (96 h at 40 °C or 20 h at 80 °C) were required to obtain the desired reactivity of this compound. For the α-methyl substituted *N*,*N*-diphenyl substrate, similar forcing conditions were required as its reactivity at room temperature was very low. After 20 h at 80 °C, excellent yields for product **387g** were obtained. Interestingly, no side-reactions or decomposition were observed when heating these substrates.

In order to investigate the catalytic cycle for this reaction, ^{31}P NMR spectroscopy was used as a simple tool to identify the nature of the catalyst before and after the reaction. To this end, CDP and acetonitrile were reacted neat in a 1:1 molar ratio at different temperatures and the ^{31}P NMR spectrum was recorded after 20 h (Scheme 163).

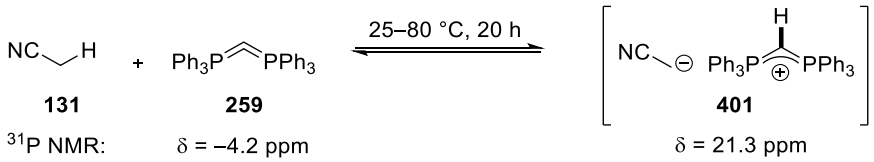

Scheme 163: Stoichiometric reaction of acetonitrile with CDP

The catalyst's ^{31}P NMR signal at δ = –4.2 ppm remained the major signal in this reaction even at elevated temperatures. However, a second signal at δ = 21.3 ppm was observed, which increased with increasing temperature, suggesting the formation of an ion pair between the acetonitrile anion and the protonated CDP, a delocalised phosphonium species (**401**). These results were confirmed by analysing the ^{31}P NMR spectra of reaction aliquots, where the only observed signals were either the unchanged CDP or its protonated form at δ = 21.3 ppm. The coexistence of the protonated and the original form of the catalyst suggested a slow deprotonation or a fast equilibrium between the two species. The *in situ* generated acetonitrile anion was then assumed to undergo a conjugate addition to the Michael acceptor leading to a basic enolate intermediate, the so-called product base (Scheme 164). This species had the choice to deprotonate either the catalyst's conjugate acid or the pro-nucleophile directly in order to close the catalytic cycle and form the observed product.

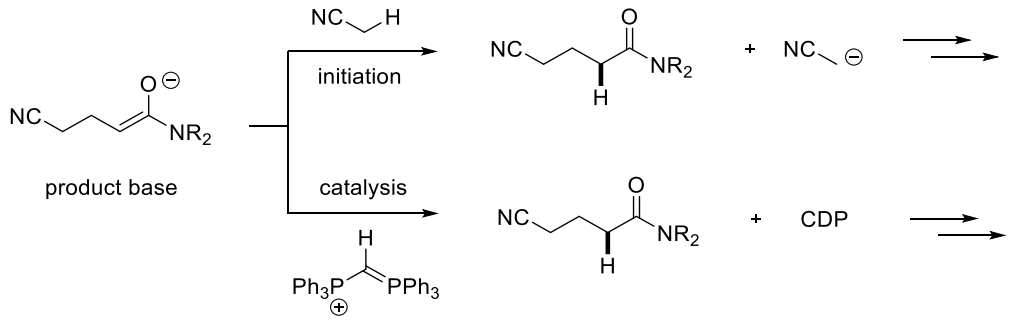

Scheme 164: Product base mechanisms

In summary, the first example of a 1,4-addition of acetonitrile to a variety of Michael acceptors has been developed. Furthermore, to the best of our knowledge the first catalytic use of a carbodiphosphorane has been demonstrated in this reaction, exploiting the catalyst's high Brønsted basicity together with its steric hindrance that prevents side-reactions in a very efficient manner.

3.3.6.4 EtCN - 1,4-Additions

To explore the scope of the CDP-catalysed 1,4-addition of alkylnitriles to acrylamides, substituted alkylnitriles were examined in this reaction with different electrophiles. As not all pro-nucleophiles are as readily available as acetonitrile, reactions were carried out in other solvents first. The CDP-triggered reaction of propionitrile in toluene or THF showed no activity for Michael aldehydes, ketones or amides.

In order to improve the reactivity of propionitrile, the reaction with unsubstituted acrylamide **118d** was performed in different solvents at various temperatures (Table 76).

Table 76: Solvent screening for the Michael addition of propionitrile

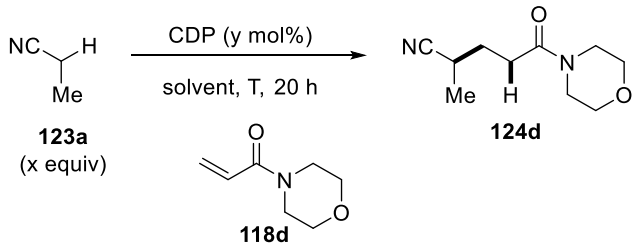

Entry	Solvent (Ɛ)	x (equiv)	y mol%	T (°C)	Yield (%)[a]
1	DMF (36.7)	2.0	5	25	13
2	PhCN (26.0)	2.0	5	25-80	*NR*[b]
3	THF (7.5)	2.0	10	25-40	*NR*[b]
4	Et_2O (4.3)	2.0	10	25-40	*NR*[b]
5	PhMe (2.4)	2.0	10	25-40	*NR*[b]
6	EtCN (27.7)	30	5	25	82
7	DMF / EtCN[c]	15	5	25	52

[a] The yield was determined by ^{1}H NMR analysis of a reaction aliquot; internal standard: dibenzyl ether (25 mol%). [b] NR = no reaction; the desired product was not detectable, only starting materials were detected (^{1}H NMR analysis of a reaction aliquot). [c] DMF:EtCN = 1:1.

The reaction of propionitrile (**123a**, 2.0 equiv) with electrophile **118d** did proceed in 13% yield when performed in a highly polar aprotic solvent such as DMF (entry 1). Solvents with a lower polarity did not prove to be suitable for this reaction and the product was not obtained in benzonitrile, THF, diethyl ether, or toluene (entries 2-5). To mimic the reaction conditions of acetonitrile, the reaction was performed in propionitrile as the solvent (ca. 30 equiv) and the product yield increased to 82% (entry 6). As both DMF and EtCN proved to be suitable solvents in this reaction, a 1:1 solvent mixture was also used, giving a yield of 52% (entry 7).

Under otherwise identical conditions, both solvent systems were then subjected to a temperature screening under otherwise identical conditions between 25 and 80 °C (Table 77).

Table 77: Temperature screening for the Michael addition of propionitrile

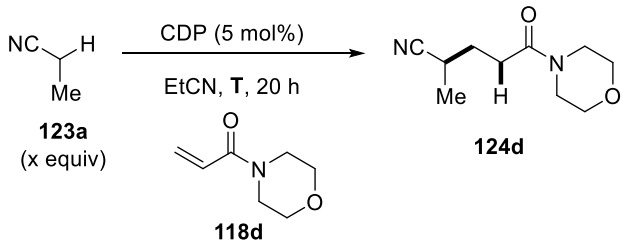

Entry	Solvent	x (equiv)	T (°C)	Yield (%)[a]
1	EtCN	30	25	82
2	EtCN	30	40	79
3	EtCN	30	60	60
4	EtCN	30	80	17
5	DMF / EtCN[b]	15	25	52
6	DMF / EtCN[b]	15	40	68
7	DMF / EtCN[b]	15	60	44
8	DMF / EtCN[b]	15	80	83

[a] The yield was determined by ^{1}H NMR analysis of a reaction aliquot; internal standard: dibenzyl ether (25 mol%). [b] DMF:EtCN = 1:1.

Like in the case of acetonitrile, the increase of temperature did not result in a significant improvement of the yield when using the pro-nucleophile as the solvent (entries 1-4). Indeed, the best result was obtained for the mildest conditions (entry 1). For the solvent mixture containing DMF, the increase of the reaction temperature did not give conclusive results (entries 5-8). Here, the best result was obtained at 80 °C (83%, entry 8), but a general correlation between temperature and yield could not be observed. Therefore, reaction conditions at 25 °C using 30 equivalents of the pro-nucleophile as the solvent were chosen as optimised reaction conditions for the electrophile scope (Table 78). For all three unsubstituted acrylamides, the reaction proceeded to give good to excellent yields for the corresponding Michael adducts. Due to the α-substitution of the pro-nucleophile, these reactions formed chiral products with one stereogenic centre in α-position to the cyano group.

Table 78: Electrophile scope for the reaction with propionitrile

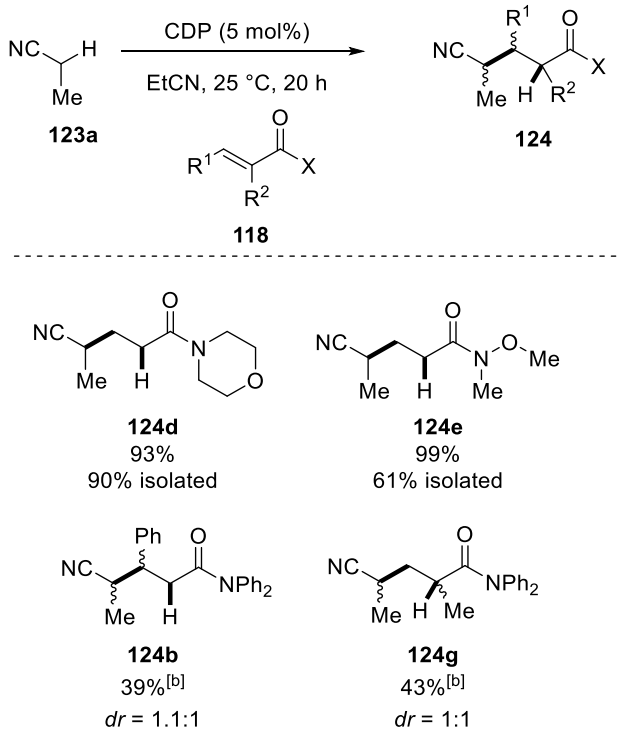

The yield was determined by ^{1}H NMR analysis of a reaction aliquot; internal standard: dibenzyl ether (25 mol%). [b] Reaction performed at 60–80 °C.

When substituted acrylamides were used in this reaction, the products contained two stereogenic centres, leading to diastereoisomers. These centres were vicinal in product **124b** and in a 1,3-relationship in product **124g**. Like in the case of acetonitrile, these products could not be obtained in high yields using the developed mild conditions, but heating to 60–80 °C resulted in acceptable yields for these substrates. However, the diastereoselectivity for both products **124b** and **124g** was poor and 1:1 mixtures of products were formed. A change of solvent was considered the most effective way to improve the selectivity of the reaction. However, the solvent screening had shown a low tolerance of solvents other than the pro-nucleophile for this reaction. Therefore, no alternative method could be developed at this stage.

Overall, the activation of propionitrile was achieved using a CDP catalyst. In contrast to the literature, this transformation constitutes the first organocatalytic 1,4-addition of propionitrile to Michael acceptors. However, both reactivity and diastereoselectivity present limitations for this new catalytic activity.

3.3.6.5 BnCN - 1,4-Additons

As previously discussed, phenyl acetonitrile is up to 10 orders of magnitude more acidic than the alkylnitriles, as suggested by its pK_a value of 22 (DMSO).[37] It is therefore not surprising that reactions with Michael acceptors were catalysed by CDP under mild reaction conditions in toluene (Table 79).

Table 79: Michael addition of benzylnitrile to Michael acceptors

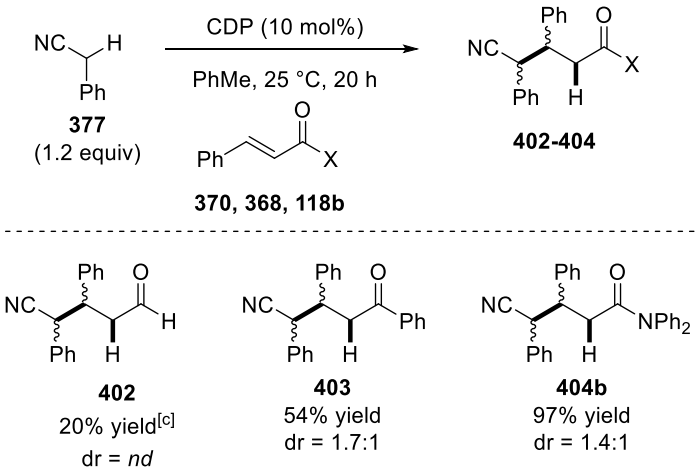

[a] The yield was determined by ^{1}H NMR spectroscopy of a reaction aliquot; internal standard: dibenzyl ether (25 mol%). [b] NR = no reaction; the desired product was not detectable, only starting materials were detected (^{1}H NMR analysis of a reaction aliquot). [c] 1,2-addition product also observed.

Both the Michael aldehyde and ketone gave poor to modest yields and resulted in a mixture of diastereoisomers with poor selectivity (entries 1 and 2). In the case of cinnamaldehyde, the 1,2-addition product was also observed in the reaction aliquot. The reaction with the Michael amide resulted in complete conversion to the desired product albeit with a low diastereoselectivity (1.4, entry 3). In order to improve this selectivity, a solvent screening was performed (Table 80).

Table 80: Solvent screening for the Michael addition of benzylnitrile I

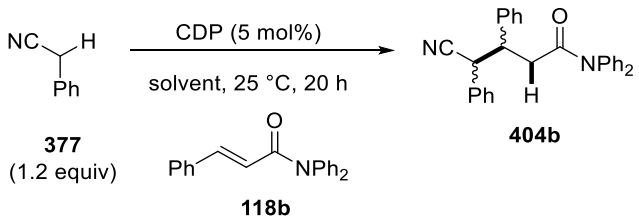

Entry	Solvent (Ɛ)	Yield (%)[a]	*syn:anti*
1	PhMe (2.4)	97	1:1.4
2	dioxane (2.3)	99	1:1.3
3	THF (7.5)	53	1:1.2
4	DMF (36.7)	99	1:1.4

[a] The yield was determined by ^{1}H NMR analysis of a reaction aliquot; internal standard: dibenzyl ether (25 mol%).

The reactions proceeded in toluene, dioxane and DMF in excellent yields (entries 1, 2 and 4). In THF, only a moderate yield was observed (entry 3). However, none of the more coordinating solvents was able to improve the diastereoselectivity of this reaction where the two stereogenic centres are in vicinal positions.

When an α-substituted acrylamide was used, the diastereoselectivity occurred in different positions. Again, a solvent screening was conducted to monitor the selectivities in different solvents (Table 81).

Table 81: Solvent screening for the Michael addition of benzylnitrile II

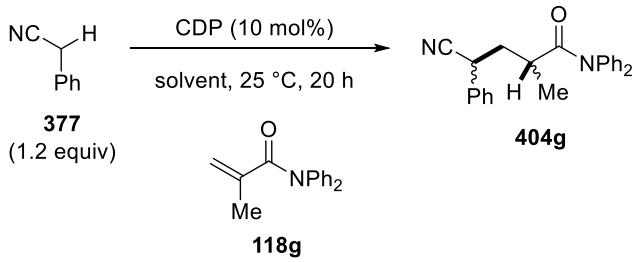

Entry	Solvent (Ɛ)	Yield (%)[a]	*syn:anti*
1	PhMe (2.4)	95	1:1.4
2	dioxane (2.3)	81	1:2.3
3	DMF (36.7)	62	1:1.4

[a] The yield was determined by ^{1}H NMR analysis of a reaction aliquot; internal standard: dibenzyl ether (25 mol%).

While the reaction yields were again moderate to excellent, the diastereoselectivities did not give satisfactory results. Despite a slightly improved selectivity for the reaction in dioxane

(entry 2), neither toluene nor DMF showed a significant diastereodifferentiation (entries 1 and 3).

The methyl-substituted analogue of benzyl nitrile, α-methyl benzylnitrile, was used as another synthetically interesting pro-nucleophile in this reaction. This substrate was particularly interesting because of its single acidic proton that, upon C–H activation and subsequent C–C bond formation, would give rise to a all-carbon quaternary stereogenic centre. The scope of benzylnitrile (**377**) and α-methyl benzylnitrile (**405**) was investigated in the same manner as before in toluene with different acrylamides (Table 82).

Table 82: Scope for the Michael addition of benzylnitriles

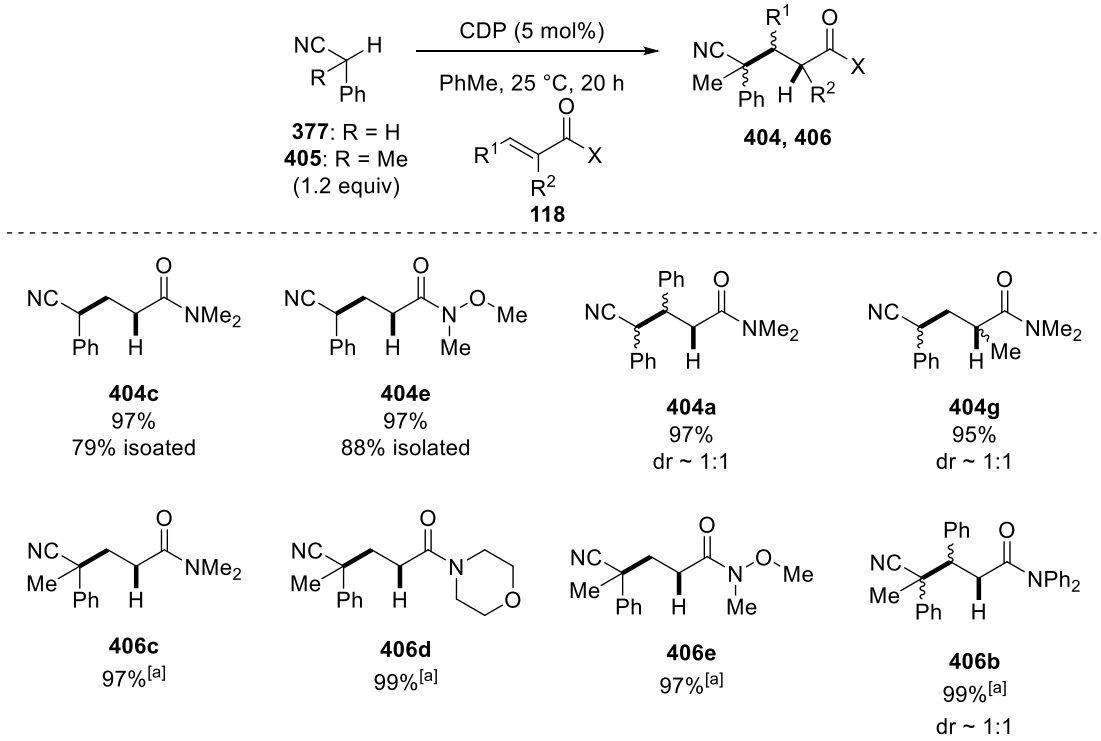

[a] The yield was determined by ^{1}H NMR analysis of a reaction aliquot; internal standard: dibenzyl ether (25 mol%).

The scope showed the facile formation of highly substituted products **404**. Products **404c** and **404e** were chosen to be isolated for proof of principle. Due to the poor diastereoselectivity when using substituted acrylamides, this process proved to be limited to unsubstituted acrylamides. Substituted benzylnitrile **405** showed similar reactivity and products **406** were obtained in excellent yields. However, as shown for substrate **377**, a 1:1 mixture of diastereoisomers was obtained for substituted acrylamides.

To expand the scope of this newly developed C–C bond-forming methodology, different substitution patterns at the α-carbon centre of acetonitrile were of interest. Initial results

using halogenated acetonitriles (X = Cl, Br) showed no reactivity, but due to time constraints this class of compounds was not investigated in depth. Among these compounds, fluoroacetonitrile is of particular interest, which has not been used in preliminary studies yet. Here, the formation of a fluorinated amide product **408** may be interesting in the area of pharmaceutically active compounds, while the method avoids the use of expensive electrophilic fluorine ('F^+') sources (Scheme 165).

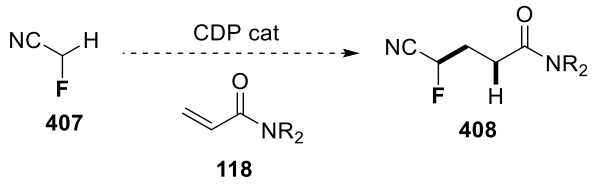

Scheme 165: Fluorinated alkylnitriles in Michael additions

Due to the highly diverse nature of the nitrile functional group, further modifications may open pathways for the selective formation of fluorinated compounds ranging from carboxylic acid derivatives (hydrolysis) to aldehydes or amines (reduction), as well as cyclisation products.

Further commercially pro-nucleophiles that have not been studied in this project include allyl cyanide **410** and adiponitrile **409** (Figure 25).

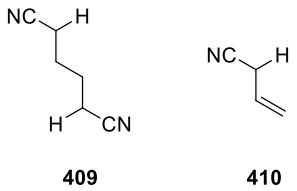

Figure 25: Alternative pronucleophiles

The dinitrile substrate may potentially show interesting reactivity, because the double addition to two equivalents of acrylamides would be possible. In the case of the allylic substrate, both α- and γ-additions are possible and a selective process would lead to highly functionalised products.

3.4 Conclusions and Future Work

Carbodiphosphoranes are a promising class of reagents for organic synthesis and catalysis. Their ease of preparation and good stability to anhydrous conditions offered a variety of applications in catalysis. The synthesised carbodiphosphorane has been shown to coordinate to BH_3 showing chemical shift of –22 ppm in ^{11}B NMR spectroscopy, thereby proving its Lewis basicity. More sterically demanding boron Lewis acids showed little or no reactivity with the C(0), which suggests a frustrated Lewis pair character. Further work regarding the deprotonation of the pyridyl-substituted carbodiphosphorane is required prior to its use in metal complexation and binding studies (Scheme 166). Cyclic carbones could also be prepared and used for the formation of metal complexes, as CDPs are calculated to be the most basic class of carbodiphosphoranes.

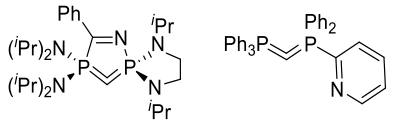

Scheme 166: Different CDPs

Protonated CDP–H^+ with only one lone pair of electrons could also be studied with respect to metal complex formation and boron binding. Indeed, the CDP–H^+ has been successfully used as a ligand for a variety of transition metals [Au(I),[137c] Ag(I),[162a] Fe(III),[177]; Scheme 167].

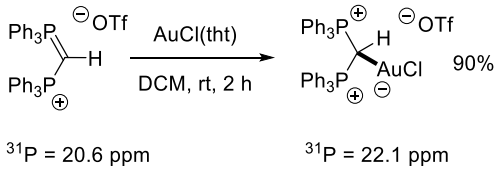

Scheme 167: Auration of CDP–H^+ Ligand

The metal complexes of this compound could then be deprotonated *in situ* in order to achieve dual catalysis, which was not achieved directly, yet. Therefore, such complexes can be regarded as 'protected' metallated CDPs, where the second lone pair on the carbon centre can be activated when required.

Initial experiments in the field of FLP catalysis showed that the activation of CO_2 is facile, while further reactions with electrophiles did not show the desired reactivity. A variety of metal complexes have also been prepared using the CDP as a ligand to the metal centre. These complexes have been shown to be unstable in protic solvents and display a low solubility in apolar solvents.

In the field of FLP catalysis, different boron Lewis acids can be used to activate carbon dioxide. The used electrophiles can also be varied, giving rise to a wider substrate scope. One example of using FLP catalysis would be the use of the CDP–BH_3 complex as a reducing agent. NHC–BH_3 complexes are known to reduce aldehydes, aldimines and ketones in the presence of Lewis acids.[178] The reduction of CO_2 to MeOH using a CDP–BH_3 complex would be of interest in the field of 'carbon capturing' (Scheme 168). Here, the CDP acts as a nucleophile to form an intermediary reactive ate complex with the borane, which could then reduce the LA-activated CO_2 in order to form methanol and water as the final products.

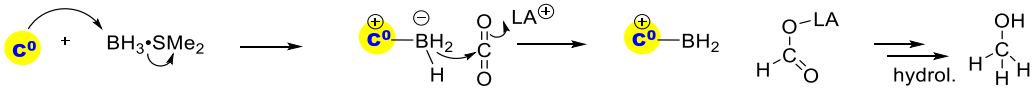

Scheme 168: FLP catalytic Reduction of CO_2

When reacted with different electrophiles, the CDP did not show any nucleophilic attack towards aldehydes or imines, even at elevated temperatures. This lack of reactivity demonstrated that reactivity may be limited to certain electrophiles, but at the same time side-reactions may be avoided and high substrate selectivity may be achieved.

The use of CDP as a Brønsted base, however, was more successful. CDPs have been shown to deprotonate α-carbonyl C–H bonds, which was used in the catalytic aldol, Mannich or Michael addition, albeit with low selectivities. The catalytic activation of acetonitrile was then demonstrated in the reaction with aldehydes and imines and was finally optimised for Michael amides (Scheme 169). The scope for other alkylnitriles showed applicability to alkyl and phenyl-substituted alkylnitriles.

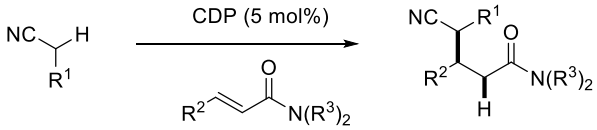

Scheme 169: 1,4-addition of alkylnitriles to Michael amides

A diastereoselective variation of this reaction was not developed yet, but modification on the catalyst, the use of a co-catalyst, or a different solvent could allow for a more selective 1,4-addition. One field of applications include the use of halogenated alkylnitriles, which would provide a useful alternative for the preparation of fluorinated amide products using BB catalysis.

Other pro-nucleophiles can also be screened in the catalytic BB activation using CDPs. Examples for this include indene or indole substrates with a pK_a ~ 20 (DMSO)[37] as well as more challenging substrates such as diphenylmethane, which could not be activated in the first chapter using a metal–base approach (Figure 26).

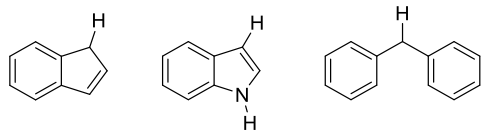

Figure 26: Different Acidic Substrates for BB Catalysis

In order to stabilise the intermediates formed in this reaction, it might be necessary to use the CDP as a ligand to a metal centre that can then be used to form a complex with the generated anion. This combination would lead to new developments in the field of metal catalysis using Brønsted basic complexes, which would combine both strands of research.

4 Experimental

4.1 General Experimental

^{1}H NMR spectra were recorded on Bruker AVA400 (400 MHz), Bruker AVA500 (500 MHz), Bruker PRO500 (500 MHz), or Bruker AVA600 (600 MHz) spectrometers. Chemical shifts (δ) are quoted in parts per million (ppm) downfield of tetramethylsilane, using TMS as an internal standard ($Si(CH_3)_4$, δ = 0.00 ppm). In the absence of TMS, deuterated solvents were used as an internal standard ($CDCl_3$, δ = 7.26 ppm or C_6D_6, δ = 7.16 ppm). Abbreviations used in the description of resonances are: s (singlet), d (doublet), t (triplet), q (quartet), m (multiplet) and br (broad). Coupling constants (*J*) are quoted to the nearest 0.1 Hz. ^{13}C NMR spectra were recorded on Bruker AVA500 (125 MHz), or Bruker AVA600 (150 MHz) spectrometers. Chemical shifts (δ) are quoted in parts per million (ppm) downfield of tetramethylsilane, using TMS as an internal standard ($Si(CH_3)_4$, δ = 0.00 ppm). In the absence of TMS, deuterated solvent was used as an internal standard ($CDCl_3$, δ = 77.0 ppm or C_6D_6, δ = 128.4 ppm). ^{7}Li NMR spectra were recorded on Bruker AVA400 (155 MHz) or Bruker PRO500 (194 MHz) spectrometers. Chemical shifts (δ) are quoted in parts per million (ppm) downfield of lithium chloride without internal standard. ^{11}B NMR spectra were recorded on Bruker AVA400 (128 MHz) or Bruker PRO500 (160 MHz) spectrometers. Chemical shifts (δ) are quoted in parts per million (ppm) downfield of trifluoroborate diethyletherate without internal standard. ^{19}F NMR spectra were recorded on Bruker AVA400 (376 MHz) or Bruker PRO500 (470 MHz) spectrometers. Chemical shifts (δ) are quoted in parts per million (ppm) downfield of trichlorofluoromethane without internal standard. ^{23}Na NMR spectra were recorded on Bruker AVA400 (106 MHz) or Bruker PRO500 (132 MHz) spectrometers. Chemical shifts (δ) are quoted in parts per million (ppm) downfield of sodium chloride without internal standard. ^{31}P NMR spectra were recorded on Bruker AVA400 (162 MHz) or Bruker PRO500 (202 MHz) spectrometers. Chemical shifts (δ) are quoted in parts per million (ppm) downfield of phosphoric acid without internal standard. Infra-red spectra were recorded on a Shimadzu IRAffinity-1 instrument on isolated samples using the attenuated total reflectance sampling technique provided in the School of Chemistry, The Univeristy of Edinburgh. High resolution mass spectra were recorded using electrospray ionisation (ESI) or electron ionisation (EI) techniques on a Finnigan MAT 900 XLT spectrometer in School of Chemistry, University of Edinburgh. Thin layer chromatography (TLC) was performed on Merck DFAlufoilien 60F254 0.2 mm pre-coated plates. Product spots were visualised by UV light at 254 nm. Preparative thin-layer Chromatography (PTLC) was carried out on self-prepared plates prepared from Wakogel B-

5F (particle size 45 μm) from WAKO. Flash column chromatography was performed using silica gel (Fisher Scientific 60 Å particle size 40-63 μm).

Unless otherwise stated, all reagents purchased from commercial suppliers were used directly and all catalytic reactions were carried out in a nitrogen glovebox with oven–dried glassware. All the solvents were stored in a nitrogen glove box over 4 Å molecular sieves. THF, toluene and diethyl ether were distilled over Na^0 with a benzophenone indicator and stored over 4 Å molecular sieves. Solvent dryness was analysed using a Carl-Fischer apparatus. Allylbenzene **36** was commercially available (98%; Acros) and distilled prior to use over CaH_2. Substituted allyltoluene **147** (97%; Aldrich) and **148** (97%; Aldrich), as well as allylanisole **149** (98%; Acros), trifluoromethyl allylbenzene **151** (95%; Aldrich) and fluoro allylbenzene **146** (97%; Aldrich) were stored over 4 Å molecular sieves. Perfluoro allylbenzene **150** (97%; Alfa) was purchased from VWR and stored in a nitrogen glove box over 4 Å molecular sieves. Allyl trimethylsilane (**136a**; Sigma-Aldrich) and benzaldehyde (**83a**; Sigma-Aldrich), were commercially available and stored in a nitrogen glove box over 4 Å molecular sieves. Allyl boronic ester **15a** was prepared and and purified by distillation by another member of the group. Dry acetonitrile was obtained from the departmental solvent supply and was stored without further purification in a nitrogen glove box over 4 Å molecular sieves. Propionitrile **123a** (99%; Acros), phenylacetonitrile **377** (>98%; Alfa), methyl-phenyl acetophenone **405** (96%; Sigma-Aldrich), as well as *N*,*N*-dimethyl acrylamide **118c** (99%; Sigma-Aldrich) and 4-acrylo morpholine **118d** (97%; Sigma-Aldrich) were stored in a nitrogen glove box over 4 Å molecular sieves.

The following catalysts were stored nitrogen glove box: potassium bis(trimethylsilyl)amide (Aldrich, 95%), Sodium bis(trimethylsilyl)amide (Acros, 95%), lithium bis(trimethylsilyl)amide (Aldrich, 97%), lithium 2,2,6,6-tetramethylpiperidide (Aldrich, 97%), lithium diisopropylamide (Aldrich, 97%) , sodium hydride (Aldrich, 95%), magnesium bis(hexamethyldisilazide) (Aldrich, 97%), tris[*N*,*N*-bis(trimethylsilyl)amide] gadolinium(III) (Alfa, 98%), tris[*N*,*N*-bis(trimethylsilyl)amide] europium(III) (Alfa, 98%), tris[*N*,*N*-bis(trimethylsilyl)amide] cerium(III) (Alfa, 96%), 2,8,9-triisobutyl-2,5,8,9-tetraaza-1-phosphabicyclo[3.3.3]undecane (**105c**; Aldrich, 97%), 2,8,9-triisopropyl-2,5,8,9-tetraaza-1-phosphabicyclo[3,3,3]undecane (**105b**; Aldrich), 2,8,9-trimethyl-2,5,8,9-tetraaza-1-phosphabicyclo[3.3.3]undecane (**105a**; Aldrich) and 1,8-diazabicyclo[5.4.0]undec-7-ene (**178**; Alfa, 99%). Potassium hydride (Aldrich, 30 wt% dispersion in mineral oil) was washed with PE and pulverised to powder then dried and stored in a nitrogen glove box. Phosphazene base P_1-^{t}Bu (**102a**; Aldrich, 97%), phosphazene base P_1-^{t}Bu-

tris(tetramethylene) (**102b**; Aldrich, 97%), phosphazene base P_2-^{t}Bu (**103b**; Aldrich, 2.0 M solution in THF), phosphazene base P_2-Et (**103a**; Aldrich, 98%) and Phosphazene base P_4-^{t}Bu solution (**104**; Aldrich, 0.8M solution in hexane) were stored in a freezer. Methyllithium (Acros, 1.6M solution in diethyl ether) and *n*-butyllithium (Acros, 1.6M solution in hexane) were stored in a fridge.

The following ligand were stored in a nitrogen glove box: [18]crown-6 (**188**; >99%, Alfa), [DB18]crown-6 (**189**; >98%, Alfa), [15]crown-5 (**187**; 98%; Alfa), as well as chiral ^{t}Bu-BOX ligand **176** (99%; Sigma-Aldrich) and carbene precursors IPr-HCl (**183**; 97%; Sigma-Aldrich) and IMes-HCl (**182**; 97%; Sigma-Aldrich). Carbene ligands SIPr (**231**; 97%; Sigma-Aldrich) and SIMes (**241**; 97%; Sigma-Aldrich) were stored in a freezer under nitrogen atmosphere at –20 °C.

4.2 Metal-Base Catalysis

4.2.1 General Methods

Preparation of Imines from Aldehydes and Anilines (GP–I)

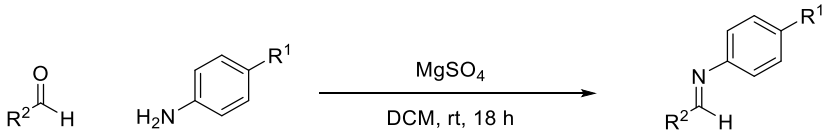

N-Ar-protected aldimines were prepared using a literature reported method.[179] In a dried flask under an Ar atmosphere, aniline (55.0 mmol) and benzaldehyde (60.0 mmol, 1.1 equiv) were stirred for 1 h at rt (in the absence of a solvent for the liquid amines). After 1 h, DCM (75 mL) and magnesium sulfate (10 g) were added and this mixture was stirred at rt for 15 h. The mixture was then filtered and the solvent removed *in vacuo* to give the crude imine, which was recrystallised from warm ethanol to yield the pure imines, which were ground and dried in THF over molecular sieves (4Å) before use.

Preparation of Imines from Ketones and Anilines (GP–II)

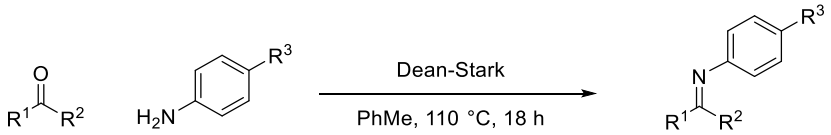

N-Ar-protected ketimines were prepared using a literature reported method.[180] In a dried flask under an Ar atmosphere, aniline (40 mmol) and ketone (40 mmol, 1.0 equiv) were stirred for 18 h under reflux in toluene (100 mL) using a Dean-Stark apparatus. The mixture was then cooled and the solvent was removed *in vacuo* to give the crude imine, which was recrystallized from warm ethanol to yield the pure imines, which were ground and dried in THF over molecular sieves (4Å) before use.

Preparation of Hexamethyldisilazide Salts (GP–III)

The alkaline earth metal hexamethyldisilazides were prepared according to a literature known procedure developed by Westerhausen.[53] In a glove box, the alkaline earth metal (10 mmol, 2.0 equiv) and tin bis(hexamethyldisilazide) (5 mmol) were reacted in toluene (10 mL) and stirred at room temperature for 48-96 h. The resulting suspension was filtered over a size 4 frit in the glove box and the solvent was removed *in vacuo*. The resulting solid was redissolved in toluene and crystallised at –20 °C overnight. The alkaline earth metal bis(hexamethyldisilazides) were then filtered and washed with petrol ether. ^{1}H and ^{13}C NMR analysis was in agreement with the literature data.

Catalytic Allylation of Imines (GP–IV)

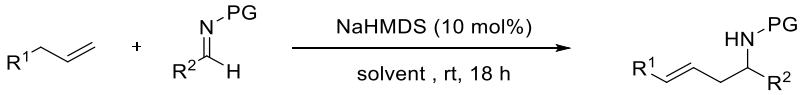

In a nitrogen glove box, a dry screw-capped vial with a magnetic stirring bar was charged with sodium hexamethyldisilazide (3.7 mg, 0.02 mmol, 10 mol%), the corresponding imine **56** (0.20 mmol), and dioxane (100 µL). To this mixture were added the corresponding alkene **36** or **146-151** (0.20–0.60 mmol, 1.00–3.00 equiv) and dioxane (200 µL). The reaction mixture was sealed and stirred at 25–60 °C for 18–72 h (*as indicated for the individual product*). The internal standard, dibenzyl ether, was added prior to ^{1}H NMR spectroscopic analysis using an aliquot of the reaction mixture. The solvent was removed *in vacuo*, and the residue was purified by PTLC on silica gel to give the corresponding product **57** or **152-157** (*as indicated for the individual product*).

Successive Addition of Pro-nucleophile in the Catalytic Allylation of Imines GP–V

In a nitrogen glove box, a dry screw-capped vial with a magnetic stirring bar was charged with sodium hexamethyldisilazide (3.7 mg, 0.02 mmol, 10 mol%), the corresponding imine **56** (0.20 mmol), and dioxane (100 µL). To this mixture were added the corresponding alkene **36** (0.20 mmol, 1.00 equiv) and dioxane (200 µL). The reaction mixture was sealed and stirred at 25 °C for 6 h. To this mixture under an inert atmosphere was re-added the corresponding alkene **36** (0.16–0.20 mmol, 0.80–1.00 equiv), and stirred at 25 °C for 6–12 h. If necessary, to this mixture under an inert atmosphere was re-added the corresponding alkene **36** (0.10 mmol, 0.50 equiv), and stirred at 25 °C for 6 h (*as indicated for the individual product*). The internal standard, dibenzyl ether, was added prior to ^{1}H NMR

spectroscopic analysis using an aliquot of the reaction mixture. The solvent was removed *in vacuo*, and the residue was purified by PTLC on silica gel to give the corresponding product **57** (*as indicated for the individual product*).

Catalytic Allylation of Imines in the Robustness Screening (GP–VI)

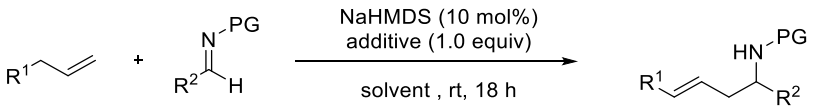

In a nitrogen glove box, a dry 10 mL screw cap vial with a magnetic stirring bar was charged with sodium hexamethyldisilazide (3.7 mg, 0.02 mmol, 10 mol%), benzaldimine (0.20 mmol), and dioxane (100 µL). To this mixture, the additive (0.20 mmol, 1.00 equiv) and allylbenzene (0.21 mmol, 1.05 equiv) were added and rinsed with dioxane (200 µL). This solution was sealed and stirred in a 25 °C sand bath for 18–24 h. The internal standard DBE (0.25 M, 0.20 mL) was added prior to ^{1}H NMR analysis using aliquot NMR. The mixtures were purified by PTLC on silica gel (Wako, Et_2O:PE = 1:9) to isolate the pure homoallylic amine (R_f ~ 0.3) as a yellow liquid.

Preparation of Substituted Allylic Substrates (GP–VII)

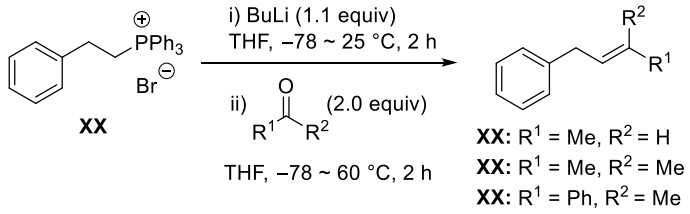

Substituted allylbenzenes were prepared using a literature reported method.[181] In a dried flask under Ar atmosphere, phosphonium salt **199** (7.5 mmol) and *n*-butyllithium (8.25 mmol, 1.1 equiv) were stirred for 1 h at -78 °C in THF (25 mL). After 1 h, the reaction was warmed to room temperature for 1 h. The mixture was then cooled again to -78 °C followed by the addition of the aldehyde or ketone (15 mmol, 2.0 equiv), which was stirred for 1 h at this temperature. The mixture was then warmed to room temperature and heated to 60 °C for 1 h. After having cooled to room temperature, the mixture was extracted into cyclohexane (20 mL) and washed with water (2 x 20 mL). The organic phase was dried ($MgSO_4$), filtered and the solvent was removed *in vacuo* to give the crude allylbenzenes, which were purified by silica gel chromatography (petrol ether) to give the substituted allylbenzenes.

Isomerisation of Allylbenzene (GP-VIII)

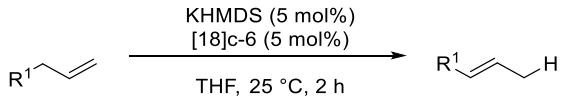

In a nitrogen glove box, a dry 10 mL screw cap vial with a magnetic stirring bar was charged with potassium hexamethyldisilazide (2.0 mg, 0.01 mmol, 5 mol%), the crown ether (2.6 mg, 0.01 mmol, 5 mol%) and THF (100 µL). To this mixture the allylbenzene (0.20 mmol, 1.00 equiv) was added and rinsed with THF (100 µL). This solution was sealed and stirred at 25 °C for 2 h. The internal standard DBE (0.25 M, 0.20 mL) was added prior to ^{1}H NMR analysis using a reaction aliquot. The mixtures were purified by PTLC on silica gel (Wako silica gel, PE) to isolate the allylbenzene (R_f ~ 0.3) as a colourless liquid. The solvent was removed on a rotary evaporator (>150 mbar) prior to NMR analysis.

Isomerisation of Functionalised Allylic Compounds (GP–IX)

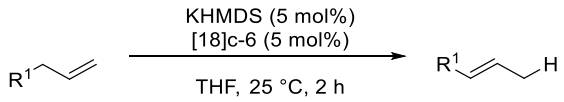

In a nitrogen glove box, a dry 10 mL screw cap vial with a magnetic stirring bar was charged with potassium hexamethyldisilazide (2.0 mg, 0.01 mmol, 5 mol%), the crown ether (2.6 mg, 0.01 mmol, 5 mol%) and THF (100 µL). To this mixture the allyl–M or allyl–FG (0.20 mmol, 1.00 equiv) was added and rinsed with THF (100 µL). This solution was sealed and stirred at 25 °C for 2 h. The internal standard DBE (0.25 M, 0.20 mL) was added prior to ^{1}H NMR analysis using a reaction aliquot.

Catalytic Allylation of Imines with Functionalised Allylic Substrates (GP–X)

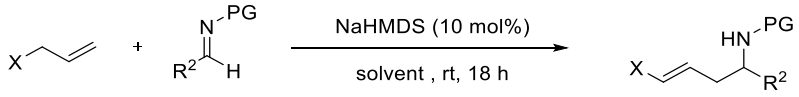

In a nitrogen glove box, a dry 10 mL screw cap vial with a magnetic stirring bar was charged with sodium hexamethyldisilazide (3.7 mg, 0.02 mmol, 10 mol%), benzaldimine (0.20 mmol), and dioxane (100 µL). To this mixture allylic substrate (0.21-0.30 mmol, 1.05-1.50 equiv) was added and rinsed with dioxane (200 µL). This solution was sealed and stirred at 25 °C for 18–24 h. The internal standard DBE (0.25 M, 0.20 mL) was added prior to ^{1}H NMR analysis of a reaction aliquot.

4.2.2 Aldimines

All Imines were prepared according to known literature procedures and spectral information is in agreement with the reported literature.

[(phenylimino)methyl]-benzenamine (56a)[179]

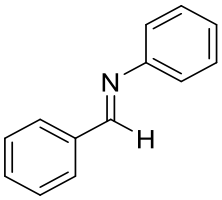

Compound **56a** was prepared according to *GP–I* and the obtained analytical data fitted accurately the literature reported data.

^{1}H NMR (500 MHz, $CDCl_3$): δ = 8.47 (s, 1H), 7.94–7.91 (m, 2H), 7.50–7.41 (m, 3H), 7.43–7.39 (m, 2H), 7.27–7.22 (m, 3H) ppm.

^{13}C NMR (125 MHz, $CDCl_3$): δ = 160.4, 152.0, 136.2, 131.4, 129.1 (2C), 128.82 (2C), 128.75 (2C), 125.9, 120.8 (2C) ppm.

[[(4-methoxyphenyl)imino]methyl]-benzenamine (56b)[182]

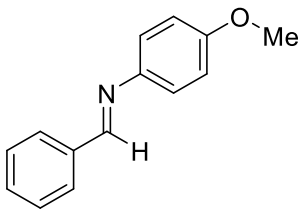

Compound **56b** was prepared according to *GP–I* and the obtained analytical data fitted accurately the literature reported data.

^{1}H NMR (500 MHz, $CDCl_3$): δ = 8.47 (s, 1H), 7.92–7.84 (m, 2H), 7.47–7.45 (m, 3H), 7.24 (d, *J* = 8.9 Hz, 2H), 6.94 (d, *J* = 8.9 Hz, 2H), 3.84 (s, 3H) ppm.

^{13}C NMR (125 MHz, $CDCl_3$): δ = 158.7, 158.4, 144.9, 136.5, 131.0, 128.7 (2C), 128.6 (2C), 122.2 (2C), 114.4 (2C), 55.5 ppm.

4-[[(4-methoxyphenyl)imino]methyl]-methyl-benzenamine (56c)[179]

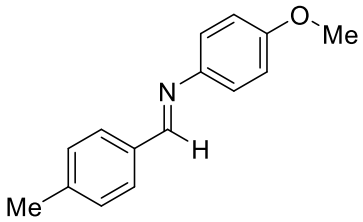

Compound **56c** was prepared according to *GP–I* and the obtained analytical data fitted accurately the literature reported data.

^{1}H NMR (500 MHz, $CDCl_3$): δ = 8.44 (s, 1H), 7.78 (d, *J* = 8.1 Hz, 2H), 7.28 (d, *J* = 8.1 Hz, 2H), 7.24 (d, *J* = 8.9 Hz, 2H), 6.93 (d, *J* = 8.9 Hz, 2H), 3.83 (s, 3H), 2.41 (s, 3H) ppm.

^{13}C NMR (125 MHz, $CDCl_3$): δ = 158.5, 158.2, 145.0, 141.6, 133.8, 129.5 (2C), 128.7 (2C), 122.2 (2C), 114.4 (2C), 55.5, 21.6 ppm.

2-[[(4-methoxyphenyl)imino]methyl]-methyl-benzenamine (56d)[183]

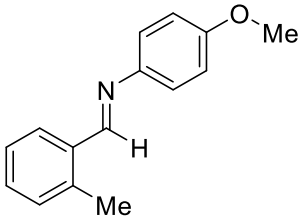

Compound **56d** was prepared according to *GP–I* and the obtained analytical data fitted accurately the literature reported data.

^{1}H NMR (500 MHz, $CDCl_3$): δ = 8.77 (s, 1H), 8.06 (dd, *J* = 8.0, 1.5 Hz, 1H), 7.37−7.27 (m, 2H), 7.25−7.19 (m, 3H), 6.94 (d, *J* = 9.0 Hz, 2H), 3.84 (s, 3H), 2.58 (s, 3H) ppm.

^{13}C NMR (125 MHz, $CDCl_3$): δ = 158.2, 157.1, 145.5, 138.3, 134.4, 130.9, 130.7, 127.5, 126.3, 122.1 (2C), 114.3 (2C), 55.5, 19.4 ppm.

4-[[(4-methoxyphenyl)imino]methyl]-trifluoromethyl-benzenamine (56e)[184]

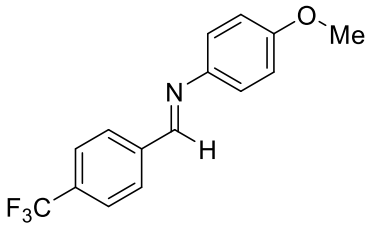

Compound **56e** was prepared according to *GP–I* and the obtained analytical data fitted accurately the literature reported data.

^{1}H NMR (500 MHz, $CDCl_3$): δ = 8.53 (s, 1H), 8.00 (d, *J* = 8.2 Hz, 2H), 7.71 (d, *J* = 8.2 Hz, 2H) 7.27 (d, *J* = 8.9 Hz, 2H), 6.97 (d, *J* = 8.9 Hz, 2H), 3.84 (s, 3H) ppm.

^{13}C NMR (125 MHz, $CDCl_3$): δ = 158.8, 156.2, 144.1, 139.6, 132.5 (q, *J* = 32.5 Hz), 128.7 (2C), 125.6 (q, *J* = 3.2 Hz, 2C), 123.9 (q, *J* = 127.2 Hz), 122.38 (2C), 114.5 (2C), 55.5 ppm.

^{19}F NMR (471 MHz, $CDCl_3$): δ = -62.9 (s) ppm.

4-[[(4-methoxyphenyl)imino]methyl]-fluoro-benzenamine (56f)[179]

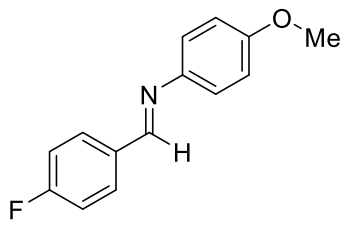

Compound **56f** was prepared according to *GP–I* and the obtained analytical data fitted accurately the literature reported data.

^{1}H NMR (500 MHz, $CDCl_3$): δ = 8.45 (s, 1H), 7.89 (t, *J* = 8.7, 5.5 Hz, 2H), 7.24 (t, *J* = 8.9 Hz, 2H), 7.15 (dd, *J* = 8.7, 8.7 Hz, 2H), 6.94 (d, *J* = 8.9 Hz, 2H), 3.84 (s, 3 H) ppm.

^{13}C NMR (125 MHz, $CDCl_3$): δ = 164.5 (d, *J* = 250.0 Hz), 158.3, 156.9, 144.7, 132.8, 130.5 (d, *J* = 8.0 Hz, 2C), 122.2 (2C), 115.9 (d, *J* = 22.0 Hz, 2C), 114.4 (2C), 55.5 ppm.

^{19}F NMR (471 MHz, $CDCl_3$): δ = -(108.7–108.8) ppm.

4-[[(4-methoxyphenyl)imino]methyl]-chloro-benzenamine (56g)[179]

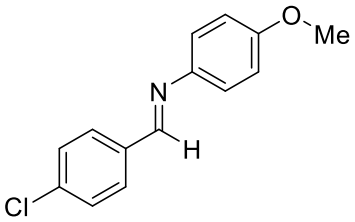

Compound **56g** was prepared according to *GP–I* and the obtained analytical data fitted accurately the literature reported data.

^{1}H NMR (500 MHz, $CDCl_3$): δ = 8.44 (s, 1H), 7.83 (d, *J* = 8.4 Hz, 2H), 7.44 (d, *J* = 8.4 Hz, 2H), 7.26 (d, *J* = 9.0 Hz, 2H), 6.94 (d, *J* = 9.0 Hz, 2H), 3.83 (s, 3H) ppm.

^{13}C NMR (125 MHz, $CDCl_3$): δ = 158.5, 156.7, 144.4, 137.0, 134.9, 129.8 (2C), 129.0 (2C), 122.3 (2C), 114.4 (2C), 55.5 ppm.

4-[[(4-methoxyphenyl)imino]methyl]-bromo-benzenamine (56h)[185]

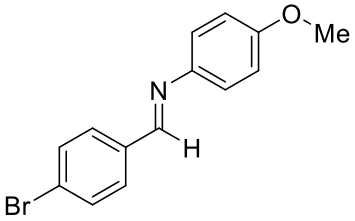

Compound **56h** was prepared according to *GP–I* and the obtained analytical data fitted accurately the literature reported data.

^{1}H NMR (500 MHz, $CDCl_3$): δ = 8.42 (s, 1H), 7.75 (d, *J* = 8.4 Hz, 2H), 7.58 (d, *J* = 8.4 Hz, 2H), 7.23 (*J* = 8.9 Hz, 2H), 6.93 (d, *J* = 8.9 Hz, 2H), 3.83 (s, 3H) ppm.

^{13}C NMR (125 MHz, $CDCl_3$): δ = 159.3, 154.8, 149.0, 143.5, 142.0, 129.1 (2C), 124.0 (2C), 122.7 (2C), 114.6 (2C), 55.5 ppm.

3-[[(4-methoxyphenyl)imino]methyl]-bromo-benzenamine (56i)[186]

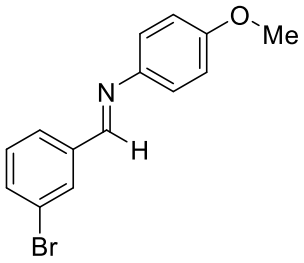

Compound **56i** was prepared according to *GP–I* and the obtained analytical data fitted accurately the literature reported data.

^{1}H NMR (500 MHz, $CDCl_3$): δ = 8.42 (s, 1H), 8.08 (dd , *J* = 1.8, 1.0 Hz, 1H), 7.77 (ddd, *J* = 7.6, 1.8, 1.8 Hz, 1H), 7.58 (ddd, *J* = 7.8, 1.8, 1.0 Hz, 1H), 7.33 (dd, *J* = 7.8, 7.6 Hz, 1H), 7.27 (d, *J* = 8.9 Hz, 2H), 6.94 (d, *J* = 8.9 Hz, 2H), 3.84 (s, 3H) ppm.

^{13}C NMR (125 MHz, $CDCl_3$): δ = 158.6, 156.3, 144.2, 138.5, 133.8, 131.1, 130.2, 127.3, 123.0, 122.3 (2C), 114.4 (2C), 55.5 ppm.

2-[[(4-methoxyphenyl)imino]methyl]-bromo-benzenamine (56j)[187]

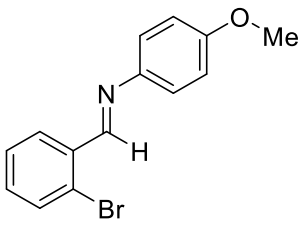

Compound **56j** was prepared according to *GP–I* and the obtained analytical data fitted accurately the literature reported data.

^{1}H NMR (500 MHz, $CDCl_3$): δ = 8.87 (s, 1H), 8.22 (dd, *J* = 7.8, 1.8 Hz, 1H), 7.61 (dd, *J* = 7.8, 0.9 Hz, 1H), 7.41–7.37 (m, 1H), 7.31–7.27 (m, 3H), 6.98–6.91 (d, *J* = 9.0 Hz, 2H), 3.84 (s, 3H) ppm.

^{13}C NMR (125 MHz, $CDCl_3$): δ = 158.6, 157.1, 144.6, 134.9, 133.2, 132.0, 128.8, 127.7, 125.8, 122.5 (2C), 114.5 (2C), 55.5 ppm.

1-[[(4-methoxyphenyl)imino]methyl]-naphthylamine (56k)[188]

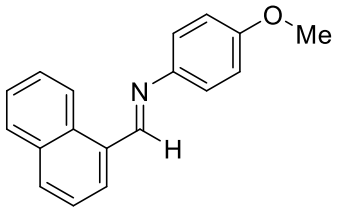

Compound **56k** was prepared according to *GP–I* and the obtained analytical data fitted accurately the literature reported data.

^{1}H NMR (500 MHz, $CDCl_3$): δ = 9.14 (s, 1H), 9.03 (d, *J* = 9.2 Hz, 1H), 8.10 (dd, *J* = 7.2, 1.3 Hz, 1H), 7.96 (d, *J* = 8.2 Hz, 1H), 7.92 (dd, *J* = 8.2, 1.3 Hz, 1H), 7.62 (ddd, *J* = 8.5, 6.8, 1.3 Hz, 1H), 7.59 – 7.53 (m, 2H), 7.32 (d, *J* = 8.9 Hz, 2H), 6.98 (d, *J* = 8.9 Hz, 2H), 3.86 (s, 3H) ppm.

^{13}C NMR (125 MHz, $CDCl_3$): δ = 158.4, 158.0, 145.7, 134.0, 131.8, 131.6, 131.5, 129.3, 128.8, 127.3, 126.2, 125.3, 124.2, 122.2 (2C), 114.5 (2C), 55.6 ppm.

2-[[(4-methoxyphenyl)imino]methyl]-naphthylamine (56l)[189]

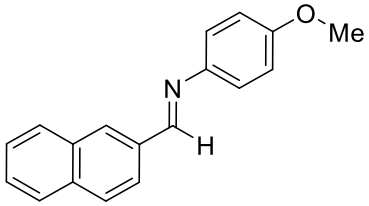

Compound **56l** was prepared according to *GP–I* and the obtained analytical data fitted accurately the literature reported data.

^{1}H NMR (500 MHz, $CDCl_3$): δ = 8.64 (s, 1H), 8.18 (s, 1H), 8.16 (dd, *J* = 8.5, 1.7 Hz, 1H), 7.95 – 7.85 (m, 3H), 7.56 – 7.50 (m, 2H), 7.29 (d, *J* = 8.9 Hz, 2H), 6.96 (d, *J* = 8.9 Hz, 2H), 3.85 (s, 3H) ppm.

^{13}C NMR (125 MHz, $CDCl_3$): δ = 158.37, 158.30, 144.98, 134.91, 134.24, 133.19, 130.75, 128.71, 128.60, 127.93, 127.34, 126.55, 123.95, 122.26 (2C), 114.45 (2C), 55.52 ppm.

4-[[(4-methoxyphenyl)imino]methyl]-methoxy-benzenamine (56m)[179]

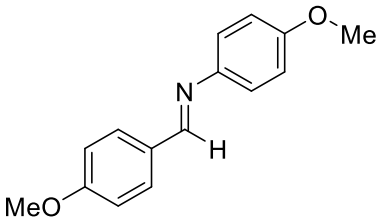

Compound **56m** was prepared according to *GP–I* and the obtained analytical data fitted accurately the literature reported data.

^{1}H NMR (500 MHz, $CDCl_3$): δ = 8.41 (s, 1H), 7.86 (d, *J* = 8.0 Hz, 2H), 7.25−7.22 (m, 2H), 6.98 (d, *J* = 8.9 Hz, 2H), 6.93 (d, *J* = 8.9 Hz, 2H), 3.87 (s, 3H), 3.83(s, 3H) ppm.

^{13}C NMR (125 MHz, $CDCl_3$): δ = 162.0, 158.0, 157.9, 145.3, 130.4 (2C), 129.6, 122.1 (2C), 114.4 (2C), 114.1 (2C), 55.5, 55.4 ppm.

4-[[(4-methoxyphenyl)imino]methyl]-*N*,*N*-dimethyl-benzenamine (56n)[190]

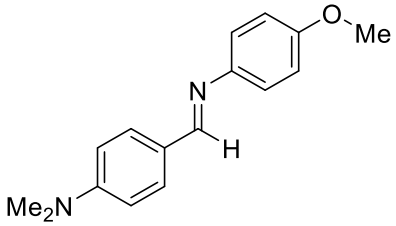

Compound **56n** was prepared according to *GP–I* and the obtained analytical data fitted accurately the literature reported data.

^{1}H NMR (500 MHz, $CDCl_3$): δ = 8.34 (s, 1H), 7.75 (d, *J* = 8.9 Hz, 2H), 7.18 (d, *J* = 8.9 Hz, 2H), 6.91 (d, *J* = 8.9 Hz, 2H), 6.73 (d, *J* = 8.9 Hz, 2H), 3.82 (s, 3H), 3.05 (s, 6H) ppm.

^{13}C NMR (125 MHz, $CDCl_3$): δ = 158.6, 157.5, 152.3, 146.0, 130.2 (2C), 124.8, 122.0 (2C), 114.3 (2C), 111.6 (2C), 55.5, 40.2 (2C) ppm.

4-[[(4-methoxyphenyl)imino]methyl]-cyano-benzenamine (56o)[191]

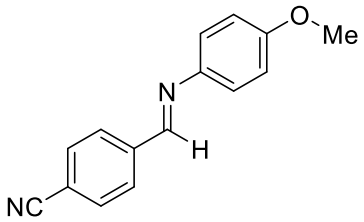

Compound **56o** was prepared according to *GP–I* and the obtained analytical data fitted accurately the literature reported data.

^{1}H NMR (500 MHz, $CDCl_3$): δ = 8.52 (s, 1H), 7.99 (d, *J* = 8.2 Hz, 1H), 7.74 (d, *J* = 8.2 Hz, 1H), 7.28 (d, *J* = 9.0 Hz, 2H), 6.95 (d, *J* = 9.0 Hz, 2H), 3.84 (s, 3H) ppm.

^{13}C NMR (125 MHz, $CDCl_3$): δ = 159.1, 155.4, 143.7, 140.3, 132.5 (2C), 128.9(2C), 122.6 (2C), 118.6, 114.5 (2C), 113.9, 55.5 ppm.

[[(4-methoxyphenyl)imino]methyl]-nitro-benzenamine (56p)[185]

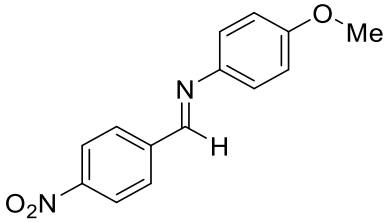

Compound **56p** was prepared according to *GP–I* and the obtained analytical data fitted accurately the literature reported data.

^{1}H NMR (500 MHz, $CDCl_3$): δ = 8.57 (s, 1H), 8.30 (d, *J* = 8.8 Hz, 2H), 8.05 (d, *J* = 8.8 Hz, 2H), 7.31 (d, *J* = 9.0 Hz, 2H), 6.96 (d, *J* = 9.0 Hz, 2H), 3.85 (s, 3H) ppm.

^{13}C NMR (125 MHz, $CDCl_3$): δ = 159.3, 154.8, 149.0, 143.6, 142.0, 129.1 (2C), 124.0 (2C), 122.6 (2C), 114.6 (2C), 55.5 ppm.

4-[[(4-methoxyphenyl)imino]methyl]-benzoic acid methyl ester (56q)[185]

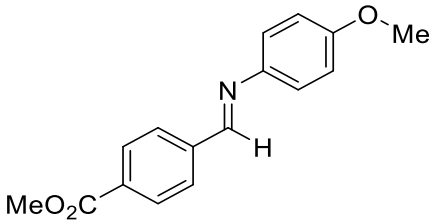

Compound **56q** was prepared according to *GP–I* and the obtained analytical data fitted accurately the literature reported data.

^{1}H NMR (500 MHz, $CDCl_3$): δ = 8.53 (s, 1H), 8.12 (d, *J* = 8.2 Hz, 2H), 7.95 (d, *J* = 8.2 Hz, 2H), 7.27 (d, *J* = 8.9 Hz, 2H), 6.95 (d, *J* = 8.9 Hz, 2H), 3.95 (s, 3H), 3.84 (s, 3H) ppm.

^{13}C NMR (125 MHz, $CDCl_3$): δ = 166.7, 158.8, 156.8, 144.3, 140.4, 132.0, 130.0 (2C), 128.4 (2C), 122.4 (2C), 114.5 (2C), 55.5, 52.3 ppm.

4-methoxy-*N*-(3-phenyl-2-propen-1-ylidene)-benzenamine (56r)[192]

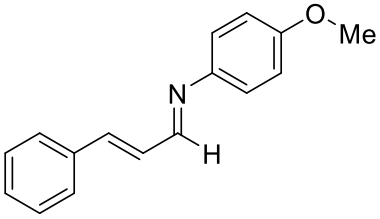

Compound **56r** was prepared according to *GP–I* and the obtained analytical data fitted accurately the literature reported data.

^{1}H NMR (500 MHz, $CDCl_3$): δ = 8.28 (dd, *J* = 4.7, 3.6 Hz, 1H), 7.55–7.49 (m, 2H), 7.40–7.35 (m, 2H), 7.35–7.30 (m, 1H), 7.20 (d, *J* = 9.0 Hz, 2H), 7.12–7.08 (m, 2H), 6.91 (d, *J* =9.0 Hz, 2H), 3.81 (s, 3H) ppm.

^{13}C NMR (125 MHz, $CDCl_3$): δ = 159.5, 158.4, 144.6, 143.0, 135.8, 129.4, 128.9 (2C), 128.8, 127.4 (2C), 122.2 (2C), 114.4 (2C), 55.5 ppm.

2-[(4-methoxyphenyl)imino]-acetic acid ethyl ester (56s)[193]

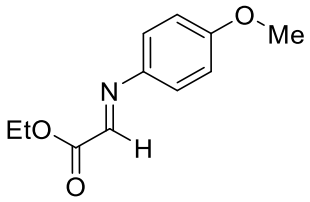

Compound **56s** was prepared according to *GP–I* and the obtained analytical data fitted accurately the literature reported data.

^{1}H NMR (500 MHz, $CDCl_3$): δ = 7.93 (s, 1H), 7.38 (d, *J* = 8.9 Hz, 2H), 6.90 (d, *J* = 8.9 Hz, 2H), 4.41 (q, *J* = 7.1 Hz, 2H), 3.84 (s, 1H), 1.41 (t, *J* = 7.1 Hz, 3H) ppm.

^{13}C NMR (125 MHz, $CDCl_3$): δ = 163.6, 160.5, 148.0, 141.4, 123.6, 114.5, 61.9, 55.5, 14.2 ppm.

2,6-bis(1-methylethyl)-*N*-(phenylmethylene)-benzenamine (56t)[194]

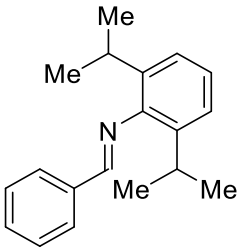

Compound **56t** was prepared according to *GP–I* and the obtained analytical data fitted accurately the literature reported data.

^{1}H NMR (500 MHz, $CDCl_3$): δ = 8.20 (s, 1H), 7.91 (d, *J* = 7.4 Hz, 2H), 7.52–7.47 (m, 3H), 7.15 (d, *J* = 7.4 Hz, 2H), 7.12–7.07 (m, 1H), 2.98 (hept, *J* = 6.9 Hz, 2H), 1.17 (d, *J* = 6.9 Hz, 12H) ppm.

^{13}C NMR (125 MHz, $CDCl_3$): δ = 162.0, 149.3, 137.6 (2C), 136.1, 131.4, 128.8 (2C), 128.6 (2C), 124.1, 123.0 (2C), 27.9, 23.5 ppm.

1,3,5-trimethyl-*N*-(phenylmethylene)-benzenamine (56u)[195]

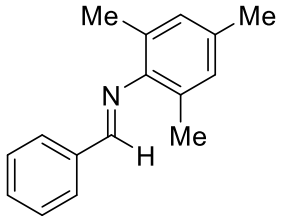

Compound **56u** was prepared according to *GP–I* and the obtained analytical data fitted accurately the literature reported data.

^{1}H NMR (500 MHz, $CDCl_3$): δ = 8.25 (s, 1H), 7.97–7.93 (m, 2H), 7.57–7.50 (m, 3H), 6.93 (s, 2H), 2.33 (s, 3H), 2.16 (s, 6H) ppm.

^{13}C NMR (125 MHz, $CDCl_3$): δ = 162.7, 148.7, 136.2, 133.0, 131.3, 128.7 (2C), 128.7 (2C), 128.4 (2C), 127.0 (2C), 20.7, 18.2 (2C) ppm.

4-methoxy-*N*-(2-thienylmethylene)-benzenamine (56v)[196]

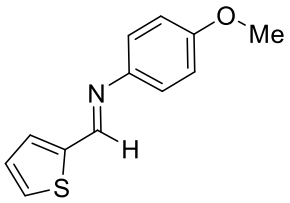

Compound **56v** was prepared according to *GP–I* and the obtained analytical data fitted accurately the literature reported data.

^{1}H NMR (500 MHz, $CDCl_3$): δ = 8.58 (s, 1H), 7.50 (d, *J* = 5.0 Hz, 1H), 7.47 (d, *J* = 3.6 Hz, 1H), 7.25 (d, *J* = 8.8 Hz, 2H), 7.15 (dd, *J* = 5.0, 3.6 Hz, 1H), 6.94 (d, *J* = 8.8 Hz, 2H), 3.78 (s, 3H) ppm.

^{13}C NMR (125 MHz, $CDCl_3$): δ = 158.3, 151.1, 144.4, 143.2, 132.0, 130.1, 127.8, 122.5 (2C), 114.2 (2C), 55.5 ppm.

4-methoxy-*N*-(2-furylmethylene)-benzenamine (56ø)[197]

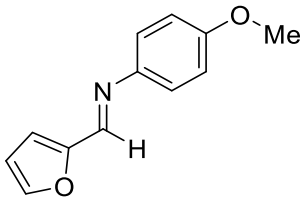

Compound **56ø** was prepared according to *GP–I* and the obtained analytical data fitted accurately the literature reported data.

^{1}H NMR (500 MHz, $CDCl_3$): δ = 8.30 (s, 1H), 7.59 (d, *J* = 1.7 Hz, 1H), 7.26 (d, *J* = 9.0 Hz, 2H), 6.92 (d, *J* = 9.0 Hz, 2H), 6.91 (d, *J* = 3.3 Hz, 1H), 6.54 (dd, *J* = 3.3, 1.7, 1H), 3.82 (s, 3H) ppm.

^{13}C NMR (125 MHz, $CDCl_3$): δ = 158.5, 152.3, 145.7, 145.3, 144.3, 122.3 (2C), 115.5, 114.4 (2C), 112.1, 55.5 ppm.

4-methoxy-*N*-[(1-methyl-1H-pyrrol-2-yl)methylene]-benzenamine (56x)[198]

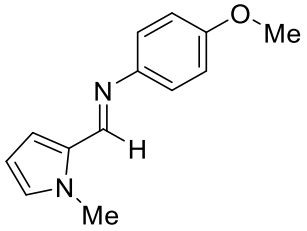

Compound **56x** was prepared according to *GP–I* and the obtained analytical data fitted accurately the literature reported data.

^{1}H NMR (500 MHz, $CDCl_3$): δ = 8.30 (s, 1H), 7.13 (d, *J* = 8.8 Hz, 2H), 6.90 (d, *J* = 8.8 Hz, 2H), 6.77 (d, *J* = 2.0 Hz, 1H), 6.64 (dd, *J* = 3.8, 2.0 Hz, 1H), 6.19 (dd, *J* = 3.8, 2.6 Hz, 1H), 4.05 (s, 3H), 3.82 (s, 3H) ppm.

^{13}C NMR (125 MHz, $CDCl_3$): δ = 157.6, 151.3, 146.5, 130.2, 128.7, 121.7 (2C), 118.7, 114.4 (2C), 108.7, 55.6, 36.7 ppm.

4-methoxy-*N*-(2-quinolinylmethylene)-benzenamine (56y)[197]

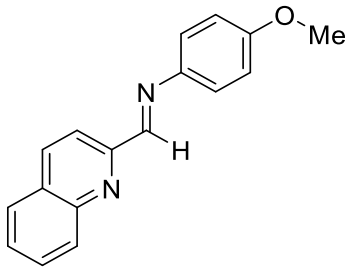

Compound **56y** was prepared according to *GP–I* and the obtained analytical data fitted accurately the literature reported data.

^{1}H NMR (500 MHz, $CDCl_3$): δ = 8.81 (s, 1H), 8.34 (d, *J* = 8.5 Hz, 1H), 8.21 (t, *J* = 7.4 Hz, 1H), 8.15 (d, *J* = 8.5 Hz, 1H), 7.83 (t, *J* = 5.9 Hz, 1H), 7.74 (t, *J* = 7.4 Hz, 1H), 7.60–7.53 (m, 1H), 7.40 (d, *J* = 8.2 Hz, 2H), 6.96 (d, *J* = 8.2 Hz, 2H), 3.83 (s, 3H) ppm.

^{13}C NMR (125 MHz, $CDCl_3$): δ = 159.2, 158.4, 155.2, 148.0, 143.5, 136.5, 129.8, 129.6, 128.8, 127.7, 127.5, 122.9 (2C), 118.6, 114.5 (2C), 55.5 ppm.

4-methoxy-*N*-(2-pyridinylmethylene)-benzenamine (56ö)[199]

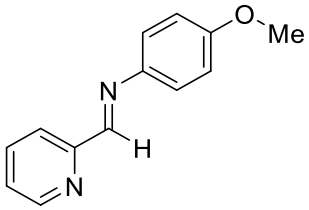

Compound **56ö** was prepared according to *GP–I* and the obtained analytical data fitted accurately the literature reported data.

^{1}H NMR (500 MHz, $CDCl_3$): δ = 8.71 (d, *J* = 4.8 Hz, 1H), 8.66 (s, 1H), 8.21 (d, *J* = 7.9 Hz, 1H), 7.83 (dd, *J* = 7.9, 6.7 Hz, 1H), 7.37 (dd, *J* = 6.7, 4.8 Hz, 2H), 7.35 (d, *J* = 8.9 Hz, 2H), 6.97 (d, *J* = 8.9 Hz, 2H), 3.85 (s, 3H) ppm.

^{13}C NMR (125 MHz, $CDCl_3$): δ = 158.9, 158.2, 154.8, 149.5, 143.6, 136.6, 124.8, 122.6 (2C), 121.6, 114.4 (2C), 55.7 ppm.

4-methoxy-*N*-(3-pyridinylmethylene)-benzenamine (56ä)[200]

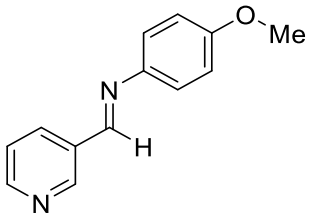

Compound **56ä** was prepared according to *GP–I* and the obtained analytical data fitted accurately the literature reported data.

^{1}H NMR (500 MHz, $CDCl_3$): δ = 9.00 (d, *J* = 1.8 Hz, 1H), 8.68 (dd, *J* = 4.8, 1.8 Hz, 1H), 8.52 (s, 1H), 8.27 (app dt, *J* = 7.9, 1.8 Hz, 1H), 7.39 (dd, *J* = 7.9, 4.8 Hz, 1H), 7.27 (d, *J* = 8.9 Hz, 2H), 6.95 (d, *J* = 8.9 Hz, 2H), 3.84 (s, 3H) ppm.

^{13}C NMR (125 MHz, $CDCl_3$): δ = 158.8, 154.9, 151.7, 150.8, 144.2, 134.6, 132.1, 123.8, 122.3 (2C), 114.5 (2C), 55.5 ppm.

4-methoxy-*N*-(4-pyridinylmethylene)-benzenamine (56z)[201]

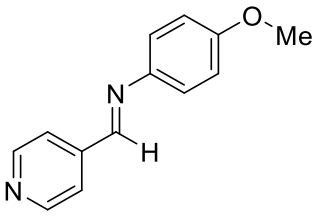

Compound **56z** was prepared according to *GP–I* and the obtained analytical data fitted accurately the literature reported data.

^{1}H NMR (500 MHz, $CDCl_3$): δ = 8.73 (d, *J* = 4.2 Hz, 2H), 8.45 (s, 1H), 7.72 (d, *J* = 4.2 Hz, 2H), 7.28 (d, *J* = 6.8 Hz, 2H), 6.94 (d, *J* = 6.8 Hz, 2H), 3.83 (s, 3H) ppm.

^{13}C NMR (125 MHz, $CDCl_3$): δ = 159.2, 155.3, 150.5 (2C), 143.6, 143.1, 122.6 (2C), 122.1 (2C), 114.5 (2C), 55.5 ppm.

***N*-(2,2-dimethylpropylidene)-4-methoxy-benzenamine (56ü)**[202]

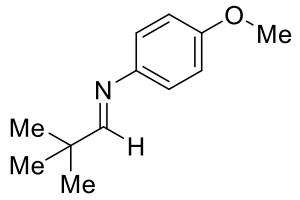

Compound **56ü** was prepared according to *GP–I* and the obtained analytical data fitted accurately the literature reported data.

^{1}H NMR (500 MHz, $CDCl_3$): δ = 7.70 (s, 1H), 7.30 (d, *J* = 8.8 Hz, 2H), 6.86 (d, *J* = 8.8 Hz, 2H), 3.80 (s, 3H). 1.17 (s, 9H) ppm.

^{13}C NMR (125 MHz, $CDCl_3$): δ = 171.6, 157.6, 145.6, 121.6 (2C), 114.1 (2C), 55.4, 36.6, 26.8 (3C) ppm.

2-formyl-1*H*-Pyrrole-1-carboxylic acid 1,1-dimethylethyl ester (411)[203]

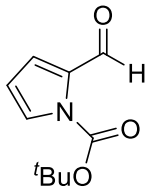

411 was prepared from pyrrole-2-carboxaldehyde (11 mmol), di(*tert*-butyl) dicarbonate (12.1 mmol, 1.1 equiv) and sodium hydride (13.2 mmol, 1.2 equiv) in THF (70 mL). After stirring this mixture for 20 h at room temperature, saturated ammonium chloride solution (30 mL) was added. The mixture was extracted into diethyl ether (20 mL) and washed with water (20 mL) and brine (20 mL). The organic solvents were dried over $MgSO_4$, filtered and the solvents were removed *in vacuo*. The pale yellow solid was used without further purification and the obtained spectral data fitted accurately with literature reported data.

^{1}H NMR (500 MHz, $CDCl_3$): δ = 10.32 (s, 1H), 7.44 (dd, *J* = 3.1, 1.7 Hz, 1H), 7.19 (dd, *J* = 3.7, 1.7 Hz, 1H), 6.28 (dd, *J* = 3.7, 3.1 Hz, 1H), 1.65 (s, 9H) ppm.

4-methoxy-*N*-[(1-Boc-1H-pyrrol-2-yl)methylene]-benzenamine (56æ)

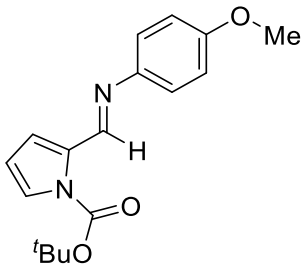

Compound **56æ** was prepared according to *GP–I*.

^{1}H NMR (500 MHz, $CDCl_3$): δ = 9.07 (s, 1H), 7.37 (dd, *J* = 3.2, 1.7 Hz, 1H), 7.22 (d, *J* = 9.0, 2H), 7.13 (dd, *J* = 3.6, 1.7 Hz, 1H), 6.90 (d, *J* = 9.0, 2H), 6.27 (dd, *J* = 3.6, 3.2 Hz, 1H), 3.82 (s, 3H), 1.62 (s, 9H) ppm.

3-formyl-1*H*-Indole-1-carboxylic acid 1,1-dimethylethyl ester (412)[204]

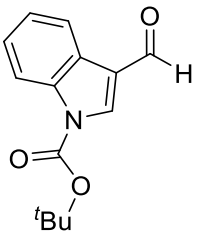

412was prepared from indole-3carboxaldehyde (7 mmol), di(*tert*-butyl) dicarbonate (7.7 mmol, 1.1 equiv) and potassium hydroxide (> 20 mmol) in toluene (10 mL) in the presence of TBAB (0.7 mmol, 10 mol%). After stirring this mixture for 1 h at room temperature, the crude yellow liquid was recrystallised from diethyl ether at -20 °C to give a colourless solid. The obtained spectral data fitted accurately with literature reported data.

^{1}H NMR (500 MHz, $CDCl_3$): δ = 10.09 (s, 1H), 8.28 (d, *J* = 7.7 Hz, 1H), 8.22 (s, 1H), 8.15 (d, *J* = 8.2 Hz, 1H), 7.41 (dd, *J* = 8.2, 7.5 Hz, 1H), 7.37 (dd, *J* = 7.5, 7.7 Hz, 1H), 1.71 (s, 9H) ppm.

^{13}C NMR (125 MHz, $CDCl_3$): δ = 185.8, 148.8, 136.5, 136.0, 126.1, 126.1, 124.6, 122.1, 121.6, 115.2, 85.7, 28.1 (3C) ppm.

3-[(*E*)-[(4-methoxyphenyl)imino]methyl]-1*H*-Indole-1-carboxylic acid 1,1-dimethylethyl ester (56å)[205]

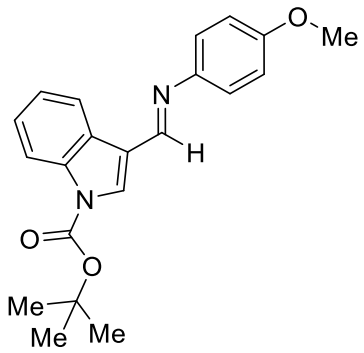

Compound **56å** was prepared according to *GP–I* and the obtained analytical data fitted accurately the literature reported data.

^{1}H NMR (500 MHz, $CDCl_3$): δ = 8.65 (s, 1H), 8.55 (d, *J* = 7.8 Hz, 1H), 8.17 (d, *J* = 8.2 Hz, 1H), 7.99 (s, 1H), 7.40 (ddd, *J* = 8.2, 7.8, 1.3 Hz, 1H), 7.36 (ddd, *J* = 7.5, 7.3, 1.3 Hz, 1H) 7.25 (d, *J* = 8.9 Hz, 2H), 6.94 (d, *J* = 8.9 Hz, 2H), 3.83 (s, 3H), 1.70 (s, 9H) ppm.

^{13}C NMR (125 MHz, $CDCl_3$): δ = 158.0, 152.0, 145.7, 130.6, 127.6, 125.5, 123.8, 122.7, 122.0 (2C), 119.7, 115.0, 114.4 (2C), 84.6, 55.5, 28.2 (3C) ppm.

1-methyl-1*H*-Indole-3-carboxaldehyde (413)[206]

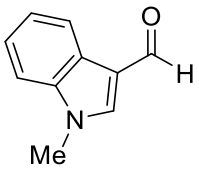

413 was prepared from indole-3carboxaldehyde (13.8 mmol), methyl iodide (16.5 mmol, 1.2 equiv) and sodium hydride (16.5 mmol, 1.2 equiv) in DMF (30 mL). After stirring this mixture for 1 h at room temperature, the mixture was extracted into ethyl acetate (50 mL) and washed with water (5 x 50 mL). The organic layer was dried ($MgSO_4$), filtered and the solvent was removed *in vacuo*. The crude product was recrystallised from diethyl ether and light petroleum ether at 0 °C to give a colourless solid. The obtained spectral data fitted accurately with literature reported data.

^{1}H NMR (500 MHz, $CDCl_3$): δ = 9.89 (s, 1H), 8.29 (d, *J* = 6.8 Hz, 1H), 7.52 (s, 1H), 7.36–7.17 (m, 3H), 3.72 (s, 3H) ppm.

4-methoxy-*N*-[(1-methyl-1*H*-indol-3-yl)methylene]-benzenamine (56w)[207]

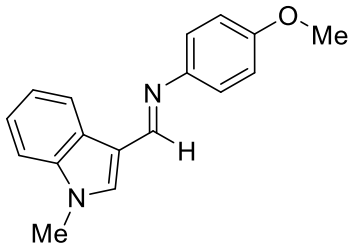

Compound **56w** was prepared according to *GP–I* and the obtained analytical data fitted accurately the literature reported data.

^{1}H NMR (500 MHz, $CDCl_3$): δ = 8.64 (s, 1H), 8.46 (d, *J* = 7.8 Hz, 1H), 7.51 (s, 1H), 7.37 – 7.32 (m, 2H), 7.32–7.26 (m, 1H), 7.22 (d, *J* = 8.9 Hz, 2H), 6.93 (d, *J* = 8.9 Hz, 2H), 3.85 (s, 3H), 3.83 (s, 3H) ppm.

^{13}C NMR (125 MHz, $CDCl_3$): δ = 157.2, 152.5, 146.5, 137.7, 133.5, 125.9, 123.1, 122.0, 121.7 (2C), 121.3, 115.0, 114.2 (2C), 109.3, 55.4, 33.1 ppm.

***N*-phenyl-2-furyl aldimine (56ð)**[208]

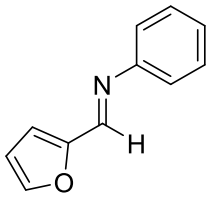

Compound **56ð** was prepared according to *GP–I* and the obtained analytical data fitted accurately the literature reported data.

^{1}H NMR (500 MHz, $CDCl_3$): δ = 8.28 (s, 1H), 7.60 (s, 1H), 7.38 (ddd, *J* = 7.4, 7.3, 1.7 Hz, 2H), 7.25–7.20 (m, 3H), 6.94 (d, *J* = 3.5 Hz, 1H), 6.54 (dd, *J* = 3.4, 1.7 Hz, 1H) ppm.

^{13}C NMR (125 MHz, $CDCl_3$): δ = 152.1, 151.4, 147.7, 145.6, 129.2 (2C), 126.2, 121.0 (2C), 116.2, 112.2 ppm.

***N*-phenyl-2-thienyl aldimine (56þ)**[208]

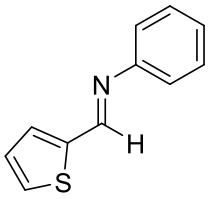

Compound **56þ** was prepared according to *GP–I* and the obtained analytical data fitted accurately the literature reported data.

^{1}H NMR (500 MHz, $CDCl_3$): δ = 8.54 (s, 1H), 7.48 (d, *J* = 5.0 Hz, 1H), 7.45 (d, *J* = 3.7 Hz, 1H), 7.39–7.34 (m, 2H), 7.23–7.18 (m, 3H), 7.10 (dd, *J* = 5.0, 3.7 Hz, 1H) ppm.

^{13}C NMR (125 MHz, $CDCl_3$): δ = 153.0, 151.4, 142.9, 132.2, 130.3, 129.1 (2C), 127.7, 126.0, 121.0 (2C) ppm.

***N*-phenyl-4-pyridyl aldimine (56ë)**[209]

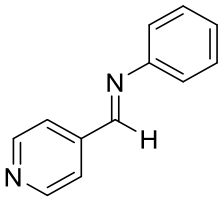

Compound **56ë** was prepared according to *GP–I* and the obtained analytical data fitted accurately the literature reported data.

^{1}H NMR (500 MHz, $CDCl_3$): δ = 8.78–8.73 (m, 2H), 8.45 (s, 1H), 7.80–7.72 (m, 2H), 7.42 (ddd, *J* = 7.7, 6.7, 1.7 Hz, 2H), 7.31–7.26 (m, 1H), 7.26–7.23 (m, 1H) ppm.

^{13}C NMR (125 MHz, $CDCl_3$): δ = 157.9, 151.0, 150.6 (2C), 142.8, 129.3 (2C), 127.0, 122.3 (2C), 120.9 (2C) ppm.

4-Methyl-*N*-(phenylmethylene)-benzenesulfonamide (61)[210]

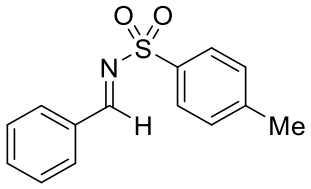

Compound **61** had been previously prepared in the group and the obtained analytical data fitted accurately the literature reported data.

^{1}H NMR ($CDCl_3$, 500 MHz): δ = 9.06 (s, 1H), 7.96-7.91 (m, 4H), 7.62-7.53 (m, 1H), 7.51-7.46 (m, 2H), 7.37 (d, *J* = 8.1 Hz, 2H), 2.46 (s, 3H) ppm.

^{13}C NMR ($CDCl_3$, 125.8 MHz): δ = 170.1, 144.6, 135.2, 134.9, 132.1, 131.3 (2C), 129.8 (2C), 129.2 (2C), 128.1 (2C), 21.7 ppm.

Benzaldehyde-*O*-methyloxime (60)[211]

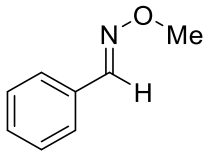

Compound **60** had been previously prepared in the group and the obtained analytical data fitted accurately the literature reported data.

^{1}H NMR (500 MHz, $CDCl_3$): δ = 8.05 (s, 1H), 7.59–7.55 (m, 2H), 7.37–7.32 (m, 3H), 3.96 (s, 3H) ppm.

^{13}C NMR (125 MHz, $CDCl_3$): δ = 148.5, 132.2, 129.8, 128.7 (2C), 127.0 (2C), 62.0 ppm.

2-Methyl-*N*-(phenylmethylene)-2-propanamine (59)[212]

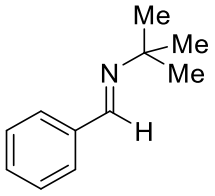

Compound **59** had been previously prepared in the group and the obtained analytical data fitted accurately the literature reported data.

^{1}H NMR (500 MHz, $CDCl_3$): δ = 8.27 (s, 1H), 7.76–7.73 (m, 2H), 7.41–7.36 (m, 3H), 1.29 (s, 9H) ppm.

^{13}C NMR (125 MHz, $CDCl_3$): δ = 155.1, 137.2, 130.1, 128.5 (2C), 127.9 (2C), 57.2, 29.7 (3C) ppm.

4.2.3 Ketimines

***N*-(1-phenylethylidene)- 4-methoxy-benzenamine (144a)**[213]

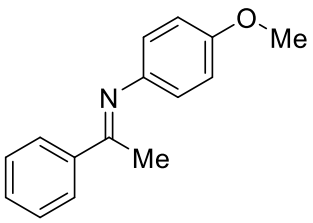

Compound **144a** was prepared according to *GP–II* and the obtained analytical data fitted accurately the literature reported data.

^{1}H NMR (500 MHz, $CDCl_3$): δ = 7.98–7.94 (m, 2H), 7.47–7.40 (m, 3H), 6.91 (d, *J* = 8.8 Hz, 2H), 6.75 (d, *J* = 8.8 Hz, 2H), 3.81 (s, 3H), 2.25 (s, 3H) ppm.

^{13}C NMR (125 MHz, $CDCl_3$): δ = 165.7, 156.0, 144.8, 139.8, 130.3, 128.3 (2C), 127.1 (2C), 120.7 (2C), 114.3 (2C), 55.5, 17.3 ppm.

***N*-(2,2,2-trifluoro-1-phenylethylidene)-4-methoxy-benzenamine (144b)**[214]

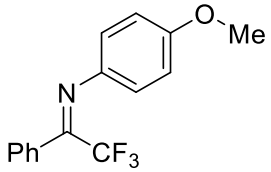

Compound **144b** was prepared according to *GP–II* and the obtained analytical data fitted accurately the literature reported data.

^{1}H NMR (500 MHz, $CDCl_3$): δ = 7.42–7.31 (m, 3H), 7.28–7.21 (m, 2H), 6.79–6.68 (m, 4H), 3.70 (s, 3H) ppm.

^{13}C NMR (125 MHz, $CDCl_3$): δ = 157.8, 155.3 (q, *J* = 33.5 Hz), 139.6, 130.5, 130.2 (2C), 128.7 (2C), 128.4, 123.2 (2C), 120.1 (q, *J* = 278.7 Hz), 114.1 (2C), 55.2 ppm.

^{19}F NMR (376 MHz, $CDCl_3$): δ = 92.1 ppm.

***N*-(diphenylmethylene)-4-methoxy-benzenamine (144c)**[215]

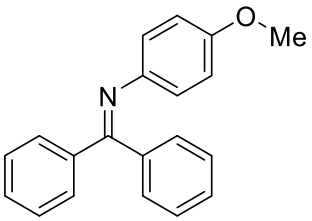

Compound **144c** was prepared according to *GP–II* and the obtained analytical data fitted accurately the literature reported data.

^{1}H NMR (500 MHz, $CDCl_3$): δ = 7.74–7.71 (m, 2H), 7.44 (tt, *J* = 7.2, 2.3 Hz, 1H), 7.40–7.36 (m, 2H), 7.29–7.24 (m, 3H), 7.14–7.10 (m, 2H), 6.7–6.65 (m, 4H), 3.71 (s, 3H) ppm.

^{13}C NMR (125 MHz, $CDCl_3$): δ = 167.7, 155.9, 144.4, 140.1, 136.6, 130.5, 129.6 (2C), 129.2 (2C), 128.5, 128.1 (2C), 128.0 (2C), 122.6 (2C), 113.8 (2C), 55.3 ppm.

***N*-cyclohexylidene-4-methoxy-benzenamine (144d)**[216]

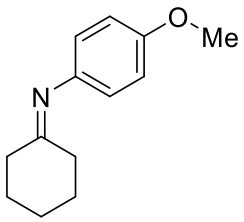

Compound **144d** was prepared according to *GP–II* and the obtained analytical data fitted accurately the literature reported data.

^{1}H NMR (500 MHz, $CDCl_3$): δ = 6.84 (d, *J* = 8.9 Hz, 2H), 6.63 (d, *J* = 8.9 Hz m, 2H), 3.74 (s, 3H), 2.40 (t, *J* = 6.0 Hz, 2H), 2.22 (t, *J* = 6.0 Hz, 2H), 1.91–1.83 (m, 2H), 1.67–1.61 (m, 4H) ppm.

^{13}C NMR (125 MHz, $CDCl_3$): δ = 175.3, 155.6, 144.0, 120.9 (2C), 114.0 (2C), 55.4, 39.5, 31.1, 27.8, 27.6, 25.8 ppm.

α-[(4-Methoxyphenyl)imino]-benzeneacetic acid ethyl ester (144e)[217]

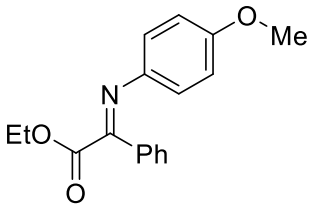

Compound **144e** was prepared according to *GP–II* and the obtained analytical data fitted accurately the literature reported data.

Mostly *E*-isomer, residual signals from *Z*-isomer.

^{1}H NMR (500 MHz, $CDCl_3$): δ = 7.87–7.83 (m, 2H), 7.47–7.42 (m, 3H), 6.94 (d, *J* = 9.0 Hz, 2H), 6.84 (d, *J* = 9.0 Hz, 2H), 4.15 (q, *J* = 7.1 Hz, 2H), 3.76 (s, 3H), 1.06 (t, *J* = 7.1 Hz, 3H) ppm.

1,3-Dihydro-3-[(4-methoxyphenyl)imino]-1-methyl-2*H*-Indol-2-one (144f)[218]

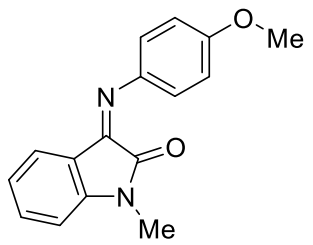

Compound **144f** was prepared according to *GP–II* and the obtained analytical data fitted accurately the literature reported data.

Ratio *E:Z* isomers = 6:1.

***E*-isomer**: **^{1}H NMR** (500 MHz, $CDCl_3$): δ = 7.39 (dd, *J* = 7.9, 7.6 Hz, 1.2, 0H), 7.05 (d, *J* = 9.0 Hz, 2H), 6.99 (d, *J* = 9.0 Hz, 2H), 6.98–6.92 (m, 1H), 6.88 (d, *J* = 7.9 Hz, 0H), 6.82 (d, *J* = 7.6 Hz, 1H), 3.87 (s, 3H), 3.33 (s, 3H) ppm.

***E*-isomer**: **^{13}C NMR** (125 MHz, $CDCl_3$): δ = 162.4, 157.3, 153.5, 147.5, 143.0, 134.1, 125.1, 122.5, 119.8 (2C), 115.4, 114.8 (2C), 110.2, 55.6, 26.0 ppm.

***Z*-isomer**: **^{1}H NMR** (500 MHz, $CDCl_3$): δ = 7.46 (d, *J* = 7.7 Hz, 1H), 7.26 (d, *J* = 8.9 Hz, 2H), 7.14 (d, *J* = 7.7, 7.2 Hz, 1H), 7.09–7.01 (m, 2H), 6.96–6.92 (m, 1H), 6.87–6.80 (m, 1H), 3.86 (s, 3H), 3.21 (s, 3H) ppm.

***Z*-isomer**: **^{13}C NMR** (125 MHz, $CDCl_3$): δ = 165.5, 159.5, 157.2, 143.2, 134.0, 131.4, 128.6 (2C), 127.7 (2C), 121.1 (2C), 114.0 (2C), 61.7, 55.4, 13.8 ppm.

4.2.4 Pronucleophiles

Allylbenzene (36)[219]

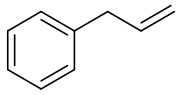

Compound **36** is commercially available and the obtained analytical data fitted accurately the literature reported data.

^{1}H NMR (500 MHz, $CDCl_3$): δ = 7.52–7.38 (m, 2H), 7.42–7.38 (m, 3H), 5.97 (ddt, *J* = 16.9, 10.1, 6.7 Hz, 1H), 5.10–5.05 (m, 1H), 3.59 (d, *J* = 6.7 Hz, 2H) ppm.

^{13}C NMR (125 MHz, $CDCl_3$): δ = 140.0, 137.4, 128.6 (2C), 128.4 (2C), 126.0, 115.8, 40.2 ppm.

4-Fluoro-allylbenzene (146)[219]

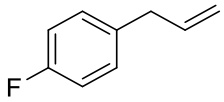

Compound **146** is commercially available and the obtained analytical data fitted accurately the literature reported data.

^{1}H NMR (500 MHz, $CDCl_3$): δ = 7.15 (dd, *J* = 8.7, 5.5 Hz, 2H), 6.97 (dd, *J* = 8.7, 8.7 Hz, 2H), 6.03–5.89 (m, 1H), 5.10–5.05 (m, 1H), 3.37 (d, *J* = 6.6 Hz, 2H) ppm.

^{13}C NMR (125 MHz, $CDCl_3$): δ = 161.4 (d, *J* = 243.0 Hz), 137.3, 135.6 (d, *J* = 2.9 Hz), 129.9 (d, *J* = 7.8 Hz, 2C), 115.9, 115.1 (d, *J* = 21.1 Hz, 2C), 39.4 ppm.

^{19}F NMR (376 MHz, $CDCl_3$): δ = –(117.5–117.6) (m) ppm.

4-Methyl-allylbenzene (147)[220]

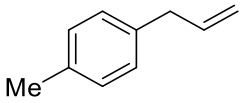

Compound **147** is commercially available and the obtained analytical data fitted accurately the literature reported data.

^{1}H NMR (500 MHz, $CDCl_3$): δ = 7.10 (d, *J* = 8.2 Hz, 2H), 7.07 (d, *J* = 8.2 Hz, 2H), 6.03–5.91 (m, 1H), 5.11–5.04 (m, 2H), 3.36 (d, *J* = 6.7 Hz, 2H), 2.33 (s, 3H) ppm.

^{13}C NMR (125 MHz, $CDCl_3$): δ = 140.0, 137.4, 128.6 (2C), 128.4 (2C), 126.0, 115.8, 40.2, 21.1 ppm.

2-Methyl-allylbenzene (148)[221]

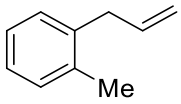

Compound **148** is commercially available and the obtained analytical data fitted accurately the literature reported data.

^{1}H NMR (500 MHz, $CDCl_3$): δ = 7.16–7.10 (m, 4H), 6.02–5.89 (m, 1H), 5.08–4.96 (m, 2H) 3.36 (d, *J* = 6.6 Hz, 2H), 2.28 (s, 3H) ppm.

^{13}C NMR (125 MHz, $CDCl_3$): δ = 138.1, 136.6, 136.3, 130.1, 129.1, 126.2, 126.0, 115.6, 37.7, 19.3 ppm.

4-Methoxy-allylbenzene (149)[219]

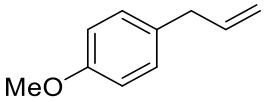

Compound **149** is commercially available and the obtained analytical data fitted accurately the literature reported data.

^{1}H NMR (500 MHz, $CDCl_3$): δ = 7.16 (d, *J* = 8.6 Hz, 2H), 6.90 (d, *J* = 8.6 Hz, 2H), 6.06–5.97 (m, 1H), 5.15–5.09 (m, 2H), 3.85 (s, 3H), 3.39 (d, *J* = 6.6 Hz, 2H) ppm.

^{13}C NMR (125 MHz, $CDCl_3$): δ = 158.0, 137.9, 132.1, 129.5 (2C), 115.4, 113.8 (2C), 55.2, 39.3 ppm.

4-Trifluoromethyl-allylbenzene (151)[221]

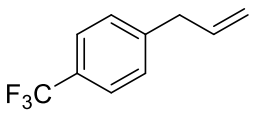

Compound **151** is commercially available and the obtained analytical data fitted accurately the literature reported data.

^{1}H NMR (500 MHz, $CDCl_3$): δ = 7.55 (d, *J* = 7.9 Hz, 2H), 7.30 (d, *J* = 7.9 Hz, 2H), 5.95 (ddt, *J* = 16.9, 10.2, 6.6 Hz, 1H), 5.14–5.07 (m, 2H), 3.44 (d, *J* = 6.6 Hz, 2H) ppm.

^{13}C NMR (125 MHz, $CDCl_3$): δ = 144.1, 136.3, 128.9 (2C), 128.5 (q, *J* = 32.2 Hz), 125.3 (q, *J* = 3.8 Hz, 2C), 124.3 (q, *J* = 272.1 Hz), 116.7, 39.9 ppm.

^{19}F NMR (376 MHz, $CDCl_3$): δ = –62.4 ppm.

3-Allylpyridine (158)[221]

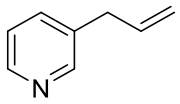

Compound **158** had been previously prepared in the group and the obtained analytical data fitted accurately the literature reported data.

^{1}H NMR (500 MHz, $CDCl_3$): δ = 8.47 (app s, 2H), 7.50 (d, *J* = 7.8 Hz, 1H), 7.22 (dd, *J* = 7.8, 4.8 Hz, 1H), 5.95 (ddt, *J* = 16.8, 10.1, 6.6 Hz, 1H), 5.14–5.07 (m, 2H), 3.39 (d, *J* = 6.6 Hz, 2H) ppm.

^{13}C NMR (125 MHz, $CDCl_3$): δ = 150.1, 147.7, 136.2, 136.0, 135.3, 123.4, 116.8, 37.2 ppm.

3-Phenylpropane-1-triphenylphosphonium bromide (199)[222]

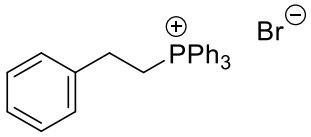

199 was prepared from 2-bromo ethylbenzene (75 mmol) and triphenylphosphine (75 mmol, 1.0 equiv) in the absence of solvent. After stirring this mixture at 130 °C for 24 h, the mixture was cooled to room temperature, whereupon it solidified to a colourless solid, which was used without further purification. The obtained spectral data fitted accurately with literature reported data.

^{1}H NMR (500 MHz, $CDCl_3$): δ = 7.91–7.84 (m, 6H), 7.84–7.77 (m, 3H), 7.74–7.68 (m, 6H), 7.66 (td, *J* = 7.9, 3.5 Hz, 1H), 7.31 (d, *J* = 7.3 Hz, 2H), 7.25–7.22 (m, 2H), 7.19–7.15 (m, 1H), 4.21 (dd, *J* = 20.4, 7.8 Hz, 2H), 3.09 (dd, *J* = 20.7, 7.8 Hz, 2H), 1.84 (dd, *J* = 19.1, 7.2 Hz, 1H) ppm.

^{31}P NMR (202 MHz, $CDCl_3$): δ = 24.6–24.3 ppm.

1,1-Dimethylallylbenzene (201)[223]

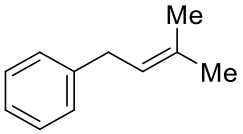

201 was prepared according to *GP-VII* and spectral data fitted the literature reported data accurately.

^{1}H NMR (500 MHz, $CDCl_3$): δ = 7.38–7.33 (m, 2H), 7.28–7.23 (m, 3H), 5.45–5.39 (m, 1H), 3.42 (d, *J* = 5.3 Hz, 2H), 1.83 (s, 3H), 1.80 (s, 3H) ppm.

^{13}C NMR (125 MHz, $CDCl_3$): δ = 141.9, 132.5, 128.4 (2C), 128.4 (2C), 125.7, 123.3, 34.4, 25.8, 17.9 ppm.

(*E*/*Z*)-1-methylallylbenzene (200)[224]

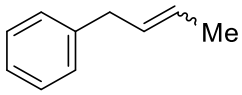

200 was prepared according to *GP–VII* and spectral data fitted the literature reported data accurately. E:Z = 1:3.

***Z*-isomer**:

^{1}H NMR (500 MHz, $CDCl_3$): δ = 7.27 (t, *J* = 7.3 Hz, 2H), 7.19–7.16 (m, 3H), 5.61 – 5.58 (m, 2H), 3.40 (d, *J* = 4.9 Hz, 2H), 1.72 (d, *J* = 4.8 Hz, 3H) ppm.

^{13}C NMR (125 MHz, $CDCl_3$): δ = 141.2, 129.0, 128.4 (2C), 128.4 (2C), 125.8, 124.8, 33.2, 12.8 ppm.

***E*-isomer**:

^{1}H NMR (500 MHz, $CDCl_3$): δ = 7.27 (t, *J* = 7.3 Hz, 2H), 7.19–7.16 (m, 3H), 5.88–5.83 (m, 1H), 5.54–5.47 (m, 1H), 3.31 (d, *J* = 6.5 Hz, 2H), 1.68 (d, *J* = 6.2 Hz, 3H) ppm.

***(E*/*Z*)-1-methyl-1-phenyl allylbenzene (202)**[225]

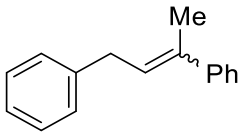

202 was prepared according to *GP–VII* and spectral data fitted the literature reported data accurately. *E:Z* = 2:5.

***E*-isomer**: **^{1}H NMR** (500 MHz, $CDCl_3$): δ = 7.36–7.32 (m, 2H), 7.32–7.28 (m, 2H), 7.27–7.22 (m, 4H), 7.18–7.11 (m, 2H), 5.66 (tq, *J* = 7.5, 1.3 Hz, 1H), 3.32 (d, *J* = 7.5 Hz, 2H), 2.08 (q, *J* = 1.3 Hz, 3H) ppm.

^{13}C NMR (125 MHz, $CDCl_3$): δ = 141.8, 141.5, 137.4, 128.4 (2C), 128.3 (2C), 128.2 (2C), 127.9 (2C), 126.7, 125.8, 125.7, 35.3, 25.7 ppm.

***Z*-isomer**: **^{1}H NMR** (500 MHz, $CDCl_3$): δ = 7.42–7.38 (m, 2H), 7.32–7.28 (m, 2H), 7.27–7.22 (m, 4H), 7.19–7.16 (m, 2H), 5.97 (tq, *J* = 7.4, 1.4 Hz, 1H), 3.57 (d, *J* = 7.4 Hz, 2H), 2.14 (q, *J* = 1.4 Hz, 3H) ppm.

^{13}C NMR (125 MHz, $CDCl_3$): δ = 143.7, 141.0, 135.7, 128.5 (2C), 128.4 (2C), 128.2 (2C), 127.9 (2C), 126.7, 126.0, 125.7, 35.0, 16.0 ppm.

4.2.5 Functionalised Allylic Starting Materials

***N*,*N*-diphenylallylamine (222b)**[226]

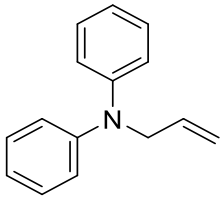

222b was prepared from allyl bromide (**132**, 50 mmol, 2.0 equiv), diphenylamine (**133**, 25 mmol) and K_2CO_3 (50 mmol, 2.0 equiv) in acetonitrile (40 mL) and water (0.5 mL) in the presence of TBAI (0.75 mmol, 3 mol%). After stirring this mixture for 48 h under reflux, the mixture cooled to room temperature. The solvent was removed *in vacuo* and the crude product was extracted into ethyl acetate (20 mL) and washed with water (2 x 20 mL). The organic phase was dried ($MgSO_4$), filtered and the solvent removed *in vacuo*. The crude product was then purified by silica gel flash chromatography (Petrol ether) to give the title compound as a colourless liquid. The obtained spectral data fitted accurately with literature reported data.

^{1}H NMR (500 MHz, $CDCl_3$): δ = 7.25–7.20 (m, 4H), 7.04–6.99 (m, 4H), 6.93–6.88 (m, 2H), 5.95–5.87 (m, 1H), 5.25 (d, *J* = 17.2 Hz, 1H), 5.14 (d, *J* = 10.4 Hz, 1H), 4.33 (d, *J* = 5.9 Hz, 2H) ppm.

^{13}C NMR (125 MHz, $CDCl_3$): δ = 147.8 (2C), 134.3, 129.2 (4C), 121.2 (2C), 120.7 (4C), 116.3, 54.7 ppm.

3-(2-propen-1-yl)-2,4,5-imidazolidinetrione (254)

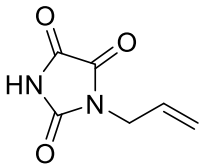

254 was prepared from allyl urea **253** (10 mmol) and oxalyl chloride (12 mmol, 1.2 equiv) in dioxane (30 mL). After stirring this mixture for 72 h at room temperature, the solvent and excess reagent were removed *in vacuo* and the crude product was used directly as a pale yellow solid.

^{1}H NMR (500 MHz, $CDCl_3$): δ = 7.86 (br s, 1H), 5.87 (ddt, *J* = 16.6, 10.1, 6.1 Hz, 1H), 5.36 (d, *J* = 16.6 Hz, 1H), 5.33 (d, *J* = 10.1 Hz, 1H), 4.29 (d, *J* = 6.1 Hz, 2H) ppm.

1-methyl-3-(2-propen-1-yl)-2,4,5-imidazolidinetrione (222c)

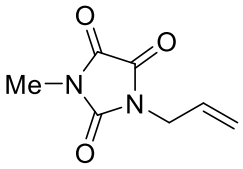

222c was prepared from trione **254** (7.5 mmol), methyl iodide (11.2 mmol, 1.5 equiv) and KOH (8.95 mmol, 1.2 equiv) in ethanol (20 mL). After stirring this mixture for 24 h under reflux, the mixture cooled to room temperature. The solvent was removed *in vacuo* and the crude product was recrystallised from diethyl ether at -20 °C.

^{1}H NMR (500 MHz, $CDCl_3$): δ = 5.84 (ddt, *J* = 17.1, 10.2, 6.1 Hz, 1H), 5.32 (dtd, *J* = 17.1, 1.3, 0.9, 1H), 5.28 (app dq, *J* = 10.2, 1.1 Hz, 1H), 4.25 (dt, *J* = 6.1, 1.3 Hz, 2H), 3.19 (s, 3H) ppm.

^{13}C NMR (125 MHz, $CDCl_3$): δ = 156.7, 156.4, 153.6, 129.8, 119.8, 41.3, 25.0 ppm.

IR (neat): ν = 2947.2, 1728.2, 1699.3, 1647.2, 1448.5, 1431.2, 1388.8, 1136.1, 935.5, 758.0, 732.9 cm^{-1}.

HRMS (EI): calculated for $C_7H_9N_2O_3^+$ = [MH^+]: *m*/*z* = 169.0608, found: *m*/*z* = 169.0599; calculated for $C_7H_8NaN_2O_3^+$ = [MNa^+]: *m*/*z* = 191.0427, found: *m*/*z* = 191.0418.

4.2.6 Anilines

***N*-(*N*-4-methoxyphenyl)benzylamine (171b)**[227]

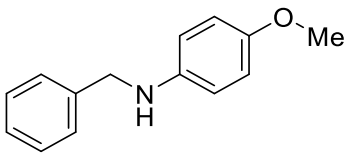

According to a literature procedure[228], in a mortar, benzaldehyde (11 mmol, 1.1 equiv), and *p*-anisidine (10 mmol) were ground in the presence of boric acid (10 mmol, 1.0 equiv) with a pestle until the mixture was ground to a uniform powder. Next, sodium borohydride (10 mmol, 1 equiv) was added in three portions and ground for 30 min. The resulting liquid was dissolved in ethanol and product **171b** crystallised as a colourless solid at -20 °C. The collected spectral information fitted the literature reported data accurately.

^{1}H NMR (500 MHz, $CDCl_3$): δ = 7.38–7.31 (m, 4H), 7.28–7.23 (m, 1H), 6.77 (d, *J* = 8.8 Hz, 1H), 6.59 (d, *J* = 8.8 Hz, 2H), 4.27 (s, 2H), 3.76 (br s, 1H), 3.73 (s, 3H) ppm.

^{13}C NMR (125 MHz, $CDCl_3$): δ = 152.2, 142.5, 139.7, 128.6 (2C), 127.5 (2C), 127.2, 114.9 (2C), 114.1 (2C), 55.8, 49.3 ppm.

***N*-phenyl-*N*-benzylamine (171a)**[227]

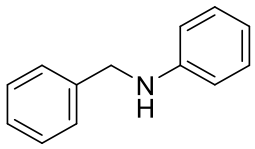

According to a literature procedure[228], in a mortar, benzaldehyde (11 mmol, 1.1 equiv), and aniline (10 mmol) were ground in the presence of boric acid (10 mmol, 1.0 equiv) with a pestle until the mixture was ground to a uniform powder. Next, sodium borohydride (10 mmol, 1 equiv) was added in three portions and ground for 30 min. The resulting liquid was dissolved in ethanol and product **171a** crystallised as a colourless solid at -20 °C. The collected spectral information fitted the literature reported data accurately.

^{1}H NMR (500 MHz, $CDCl_3$): δ = 7.40–7.31 (m, 4H), 7.27 (t, *J* = 7.1 Hz, 1H), 7.21–7.13 (m, 2H), 6.71 (t, *J* = 6.8 Hz, 1H), 6.64 (d, *J* = 7.7 Hz, 2H), 4.33 (s, 2H), 4.01 (s, 1H) ppm.

^{13}C NMR (125 MHz, $CDCl_3$): δ = 148.2, 139.4, 129.3 (2C), 128.6 (2C), 127.5 (2C), 127.2, 117.6, 112.8 (2C), 48.3 ppm.

4.2.7 Homoallylic Amines: Imine-Scope

(*E*)-*N*-(1,4-Diphenylbut-3-enyl)-4-methoxyaniline (57b)

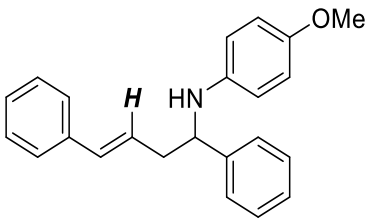

Compound **57b** was prepared according to *GP–IV* from allylbenzene (**36**; 26.5 µL, 0.20 mmol, 1.00 equiv) and imine **56b** (42.2 mg, 0.20 mmol), using NaHMDS (3.7 mg, 0.02 mmol, 10 mol%) as the catalyst, in dioxane (300 µL) at 25 °C for 18 h. **57b** was purified by PTLC on silica gel (Et_2O/PE = 1:9; *eluted once*).

Yellow liquid.

Yield: 60.0 mg (91%; *E*:*Z* = 99:1).

^{1}H NMR (600 MHz, $CDCl_3$): δ = 7.38–7.37 (m, 2H), 7.33–7.27 (m, 6H), 7.24–7.19 (m, 2H), 6.67–6.65 (m, 2H), 6.49 (d, *J* = 15.8 Hz, 1H), 6.46–6.43 (m, 2H), 6.16–6.11 (m, 1H, *E*-CH=C<u>H</u>), 5.69 (ddd, *J* = 10.8, 7.1, 7.1 Hz, 1H, *Z*-CH=C<u>H</u>), 4.42–4.36 (m, 1H), 3.95 (br s, 1H), 3.65 (s, 3H), 2.74–2.70 (m, 1H), 2.65–2.60 (m, 1H) ppm.

^{13}C NMR (150 MHz, $CDCl_3$): δ = 152.1, 143.8, 141.5, 137.1, 133.2, 128.6 (2C), 128.6 (2C), 127.4, 127.0, 126.4 (2C), 126.2 (2C), 114.8 (3C), 114.8 (2C), 58.4, 55.7, 42.5 ppm.

IR (neat): ν = 3389, 3024, 2930, 2830, 1508, 1234, 818, 741, 692 cm^{-1}.

HRMS (EI): calculated for $C_{23}H_{23}NO^+ = [M^+]$: *m*/*z* = 329.1774, found: *m*/*z* = 329.1772.

(*E*)-*N*-(1,4-Diphenylbut-3-enyl)aniline (57a)[229]

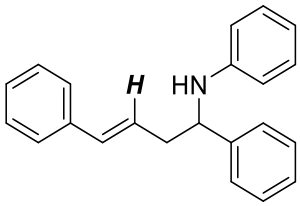

Compound **57a** was prepared according to *GP–IV* from allylbenzene (**36**; 29.2 µL, 0.22 mmol, 1.10 equiv) and imine **56a** (36.2 mg, 0.20 mmol), using NaHMDS (3.7 mg, 0.02 mmol, 10 mol%) as the catalyst, in dioxane (300 µL) at 25 °C for 18 h. **57a** was purified by PTLC on silica gel (Et_2O/PE = 1:9; *eluted once*).

Yellow liquid.

Yield: 57.5 mg (96%; *E*:*Z* = 49:1).

^{1}H NMR (500 MHz, $CDCl_3$): δ = 7.49–7.48 (m, 2H), 7.44–7.38 (m, 6H), 7.35–7.29 (m, 2H), 7.28–7.15 (m, 2H), 6.74 (dd, *J* = 7.3, 7.3 Hz, 1H), 6.63–6.59 (m, 3H), 6.24 (ddd, *J* = 15.9, 7.4, 7.0 Hz, 1H, *E*-CH=C<u>H</u>), 5.79 (ddd, *J* = 11.9, 7.0, 6.1 Hz, 1H, *Z*-CH=C<u>H</u>), 4.57 (dd, *J* = 6.3, 6.3 Hz, 1H), 4.30 (br s, 1H), 2.93–2.83 (m, 1H), 2.78–2.72 (m, 1H) ppm.

^{13}C NMR (125 MHz, $CDCl_3$): δ = 147.2, 143.5, 137.0, 133.3 (2C), 129.1 (2C), 128.6 (2C), 128.6 (2C), 127.4, 127.0, 126.3 (2C), 126.2 (2C), 126.0, 117.4, 113.5, 57.4, 42.4 ppm.

IR (neat): ν = 3412, 3024, 2922, 1601, 1503, 1265, 734, 691 cm^{-1}.

HRMS (EI): calculated for $C_{22}H_{21}N^+ = [M^+]$: *m*/*z* = 299.1669, found: *m*/*z* = 299.1668.

(*E*)-*N*-[1-(4-Methylphenyl)-4-phenylbut-3-enyl]-4-methoxyaniline (57c)

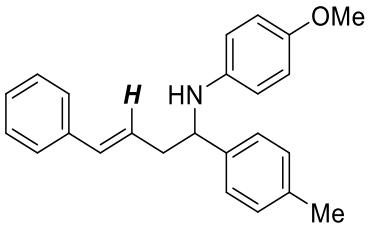

Compound **57c** was prepared according to *GP–IV* from allylbenzene (**36**; 29.2 µL, 0.22 mmol, 1.10 equiv) and imine **56c** (45.1 mg, 0.20 mmol), using NaHMDS (3.7 mg, 0.02 mmol, 10 mol%) as the catalyst, in dioxane (300 µL) at 25 °C for 18 h. **57c** was purified by PTLC on silica gel (Et_2O/PE = 1:9; *eluted once*).

Yellow liquid.

Yield: 63.2 mg (92%; *E*:*Z* = 32:1).

^{1}H NMR (500 MHz, $CDCl_3$): δ = 7.37 (d, *J* = 7.4 Hz, 2H), 7.35–7.29 (m, 2H), 7.28–7.18 (m, 3H), 7.10 (d, *J* = 7.7 Hz, 2H), 6.65 (dd, *J* = 8.9, 1.5 Hz, 2H), 6.48–6.39 (m, 3H), 6.08 (ddd, *J* = 14.5, 7.2, 7.2 Hz, 1H, *E*-CH=C<u>H</u>), 5.64 (ddd, *J* = 12.1, 7.1, 7.1 Hz, 1H, *Z*-CH=C<u>H</u>), 4.42–4.31 (m, 1H), 3.96 (br s, 1H), 3.66 (s, 3H), 2.77–2.67 (m, 1H), 2.67–2.54 (m, 1H), 2.32 (s, 3H) ppm.

^{13}C NMR (125 MHz, $CDCl_3$): δ = 152.0, 143.8, 141.6, 137.2, 134.3, 133.1, 129.2 (2C), 128.6 (2C), 127.0, 126.4 (2C), 126.1 (2C), 125.1, 114.7 (2C), 114.7 (2C), 58.4, 55.7, 42.6, 21.2 ppm.

IR (neat): ν = 3401, 3024, 2920, 2832, 1508, 1236, 816, 735, 692 cm^{-1}.

HRMS (EI): calculated for $C_{24}H_{25}NO^+ = [M^+]$: *m*/*z* = 343.1931, found: *m*/*z* = 343.1938.

(*E*)-*N*-[1-(2-Methylphenyl)-4-phenylbut-3-enyl]-4-methoxyaniline (57d)

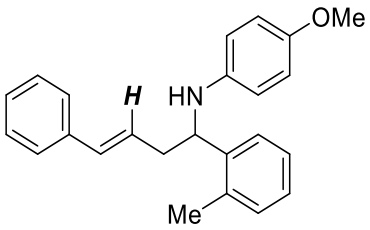

Compound **57d** was prepared according to *GP–IV* from allylbenzene (**36**; 29.2 µL, 0.22 mmol, 1.10 equiv) and imine **56d** (45.1 mg, 0.20 mmol), using NaHMDS (3.7 mg, 0.02 mmol, 10 mol%) as the catalyst, in dioxane (300 µL) at 25 °C for 18 h. **57d** was purified by PTLC on silica gel (Et_2O/PE = 1:9; *eluted once*).

Yellow liquid.

Yield: 55.0 mg (80%; *E*:*Z* = 99:1).

^{1}H NMR (500 MHz, $CDCl_3$): δ = 7.42–7.37 (m, 1H), 7.32–7.22 (m, 4H), 7.21–7.08 (m, 4H), 6.62 (d, *J* = 8.9 Hz, 2H), 6.49 (d, *J* = 15.8 Hz, 1H), 6.34 (d, *J* = 8.9 Hz, 2H), 6.14 (ddd, *J* = 15.8, 7.2, 7.2 Hz, 1H, *E*-CH=C<u>H</u>), 5.68 (ddd, *J* = 11.9, 7.0, 7.0 Hz, 1H, *Z*-CH=C<u>H</u>), 4.57 (dd, *J* = 8.1, 4.8 Hz, 1H), 3.91 (br s, 1H), 3.63 (s, 3H), 2.71–2.63 (m, 1H), 2.58–2.47 (m, 1H), 2.43 (s, 3H) ppm.

^{13}C NMR (125 MHz, $CDCl_3$): δ = 152.0, 141.6, 141.4, 137.1, 134.6, 133.2, 130.7, 128.6 (2C), 127.4, 126.8, 126.5, 126.4, 126.2 (2C), 125.5, 114.8 (2C), 114.5 (2C), 55.8, 54.6, 40.7, 19.2 ppm.

IR (neat): ν = 3395, 3025, 2928, 2832, 1508, 1234, 818, 735, 692 cm^{-1}.

HRMS (EI): calculated for $C_{24}H_{25}NO^+ = [M^+]$: *m*/*z* = 343.1931, found: *m*/*z* = 343.1930.

(*E*)-*N*-[1-(4-Trifluoromethylphenyl)-4-phenylbut-3-enyl]-4-methoxyaniline (57e)

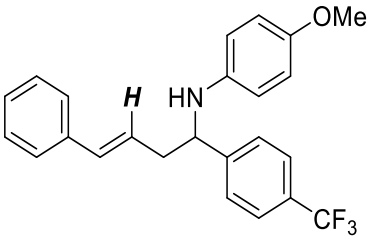

Compound **57e** was prepared according to *GP–IV* from allylbenzene (**36**; 29.2 µL, 0.22 mmol, 1.10 equiv) and imine **56e** (55.9 mg, 0.20 mmol), using NaHMDS (3.7 mg, 0.02 mmol, 10 mol%) as the catalyst, in dioxane (300 µL) at 25 °C for 18 h. **57e** was purified by PTLC on silica gel (Et_2O/PE = 1:9; *eluted twice*).

Yellow liquid.

Yield: 64.4 mg (81%; *E*:*Z* = 99:1).

^{1}H NMR (500 MHz, $CDCl_3$): δ = 7.65 (d, *J* = 7.9 Hz, 2H), 7.57 (d, *J* = 7.9 Hz, 2H), 7.40–7.35 (m, 4H), 7.31–7.28 (m, 1H), 6.74 (d, *J* = 8.8 Hz, 2H), 6.58 (d, *J* = 15.8 Hz, 1H), 6.48 (d, *J* = 8.8 Hz, 2H), 6.18 (ddd, *J* = 15.8, 6.8, 5.9 Hz, 1H, *E*-CH=C<u>H</u>), 5.73 (ddd, *J* = 12.3, 7.1, 7.1 Hz, 1H, *Z*-CH=C<u>H</u>), 4.51 (dd, *J* = 7.1, 6.1 Hz, 1H), 4.09 (br s, 1H), 3.74 (s, 3H), 2.83–2.78 (m, 1H), 2.71–2.65 (m, 1H) ppm.

^{13}C NMR (125 MHz, $CDCl_3$): δ = 152.3, 148.0, 141.0, 136.8, 133.8, 129.3 (q, *J* = 32.3 Hz), 128.6 (2C), 127.6, 126.7 (2C), 126.2 (2C), 125.6 (q, *J* = 3.7 Hz, 2C), 125.3, 123.9 (q, *J* = 272.6 Hz), 114.8 (4C), 58.1, 55.7, 42.4 ppm.

^{19}F NMR (470 MHz, $CDCl_3$): δ = –62.3 (s, 3F) ppm.

IR (neat): ν = 3391, 3026, 2932, 2833, 1510, 1323, 1236, 1109, 1065, 818, 737, 692 cm^{-1}.

HRMS (EI): calculated for $C_{24}H_{22}F_3NO^+ = [M^+]$: *m*/*z* = 397.1648, found: *m*/*z* = 397.1646.

(*E*)-*N*-[1-(4-Fluorophenyl)-4-phenylbut-3-enyl]-4-methoxyaniline (57f)

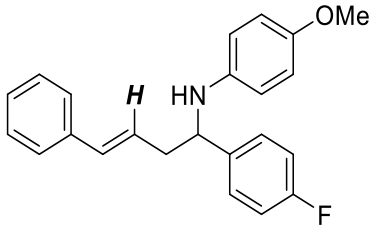

Compound **57f** was prepared according to *GP–IV* from allylbenzene (**36**; 29.2 µL, 0.22 mmol, 1.10 equiv) and imine **56f** (45.9 mg, 0.20 mmol), using NaHMDS (3.7 mg, 0.02 mmol, 10 mol%) as the catalyst, in dioxane (300 µL) at 40 °C for 18 h. **57f** was purified by PTLC on silica gel (Et_2O/PE = 1:9; *eluted once*).

Yellow liquid.

Yield: 68.8 mg (99%; *E*:*Z* = 49:1).

^{1}H NMR (400 MHz, $CDCl_3$): δ = 7.41–7.24 (m, 6H), 7.24–7.16 (m, 1H), 7.00 (dd, *J* = 8.7, 8.7 Hz, 2H), 6.67 (d, *J* = 8.9 Hz, 2H), 6.49 (d, *J* = 15.8 Hz, 1H), 6.43 (d, *J* = 8.9 Hz, 2H), 6.11 (ddd, *J* = 15.8, 7.2, 7.2 Hz, 1H, *E*-CH=C<u>H</u>), 5.66 (ddd, *J* = 11.7, 7.0, 7.0 Hz, 1H, *Z*-CH=C<u>H</u>), 4.37 (dd, *J* = 7.6, 5.3 Hz, 1H), 3.94 (br s, 1H), 3.67 (s, 3H), 2.75–2.65 (m, 1H), 2.65–2.54 (m, 1H) ppm.

^{13}C NMR (125 MHz, $CDCl_3$): δ = 161.8 (d, *J* = 244.7 Hz), 152.1, 141.3, 139.4 (d, *J* = 2.9 Hz), 137.0, 133.5, 128.6 (2C), 127.8 (d, *J* = 7.9 Hz, 2C), 127.5, 126.2 (2C), 125.8, 115.4 (d, *J* = 21.3 Hz, 2C), 114.8 (2C), 114.7 (2C), 57.8, 55.7, 42.6 ppm.

^{19}F NMR (376 MHz, $CDCl_3$): δ = –115.9 (s) ppm.

IR (neat): ν = 3385, 3026, 2930, 2832, 1506, 1234, 1219, 818, 735, 692 cm^{-1}.

HRMS (EI): calculated for $C_{23}H_{22}FNO^+ = [M^+]$: *m*/*z* = 347.1680, found: *m*/*z* = 347.1683.

(*E*)-*N*-[1-(4-Chlorophenyl)-4-phenylbut-3-enyl]-4-methoxyaniline (57g)

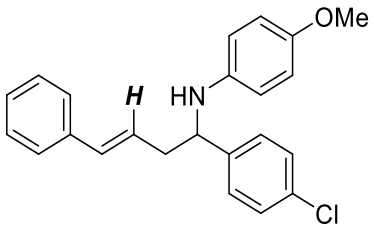

Compound **57g** was prepared according to *GP–IV* from allylbenzene (**36**; 29.2 µL, 0.22 mmol, 1.10 equiv) and imine **56g** (49.1 mg, 0.20 mmol), using NaHMDS (3.7 mg, 0.02 mmol, 10 mol%) as the catalyst, in dioxane (300 µL) at 25 °C for 18 h. **57g** was purified by PTLC on silica gel (Et_2O/PE = 1:9, *eluted once*).

Yellow liquid.

Yield: 58.2 mg (80%; *E*:*Z* = 49:1).

^{1}H NMR (500 MHz, $CDCl_3$): δ = 7.38–7.26 (m, 8H), 7.25–7.15 (m, 1H), 6.67 (d, *J* = 8.9 Hz, 2H), 6.50 (d, *J* = 15.8 Hz, 1H), 6.41 (d, *J* = 8.9 Hz, 2H), 6.10 (ddd, 15.8, 7.8, 7.3 Hz, 1H, *E*-CH=C<u>H</u>), 5.65 (ddd, *J* = 11.8, 7.0, 7.0 Hz, 1H, *Z*-CH=C<u>H</u>), 4.36 (dd, *J* = 5.7, 5.7 Hz, 1H), 3.93 (br s, 1H), 3.67 (s, 3H), 2.76–2.65 (m, 1H), 2.65–2.52 (m, 1H).

^{13}C NMR (125 MHz, $CDCl_3$): δ = 152.2, 142.4, 141.2, 137.0, 133.6, 132.6, 128.8 (2C), 128.7 (2C), 127.8 (2C), 127.6, 126.3 (2C), 125.7, 114.8 (2C), 114.8 (2C), 57.9, 55.8, 42.5 ppm.

IR (neat): ν = 3402, 3024, 2930, 2832, 1510, 1238, 818, 744, 694 cm^{-1}.

HRMS (EI): calculated for $C_{23}H_{22}{}^{35}ClNO^+$ = [M^+]: *m*/*z* = 363.1384, found: *m*/*z* = 363.1391.

(*E*)-*N*-[1-(4-Bromophenyl)-4-phenylbut-3-enyl]-4-methoxyaniline (57h)

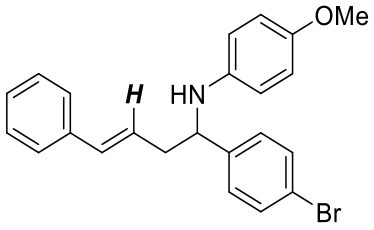

Compound **57h** was prepared according to *GP–IV* from allylbenzene (**36**; 29.2 µL, 0.22 mmol, 1.10 equiv) and imine **56h** (58.0 mg, 0.20 mmol), using NaHMDS (3.7 mg, 0.02 mmol, 10 mol%) as the catalyst, in dioxane (300 µL) at 25 °C for 18 h. **57h** was purified by PTLC on silica gel (Et_2O/PE = 1:9; *eluted once*).

Yellow liquid.

Yield: 69.4 mg (85%; *E*:*Z* = 99:1).

^{1}H NMR (500 MHz, $CDCl_3$): δ = 7.44 (d, *J* = 8.4 Hz, 2H), 7.34–7.18 (m, 7H), 6.66 (d, *J* = 8.9 Hz, 2H), 6.49 (d, *J* = 15.8 Hz, 1H), 6.41 (d, *J* = 8.9 Hz, 2H), 6.09 (ddd, *J* = 15.8, 7.2, 7.2 Hz, 1H, *E*-CH=C<u>H</u>), 5.64 (ddd, *J* = 11.8, 7.1, 7.1 Hz, 1H, *Z*-CH=C<u>H</u>), 4.34 (ddd, *J* = 8.7, 4.8, 4.1 Hz 1H), 3.93 (d, *J* = 4.1 Hz, 1H), 3.66 (s, 3H), 2.75–2.64 (m, 1H), 2.63–2.51 (m, 1H) ppm.

^{13}C NMR (125 MHz, $CDCl_3$): δ = 152.2, 142.9, 141.1, 136.9, 133.6, 131.7 (2C), 128.6 (2C), 128.2 (2C), 127.5, 126.2 (2C), 125.6, 120.7, 114.8 (2C), 114.7 (2C), 57.8, 55.7, 42.4 ppm.

IR (neat): ν = 3401, 3026, 2926, 2832, 1510, 1236, 818, 741, 694 cm^{-1}.

HRMS (EI): calculated for $C_{23}H_{22}{}^{79}BrNO^+$ = [M^+]: *m*/*z* = 407.0879, found: *m*/*z* = 407.0884.

(*E*)-*N*-[1-(3-Bromophenyl)-4-phenylbut-3-enyl]-4-methoxyaniline (57i)

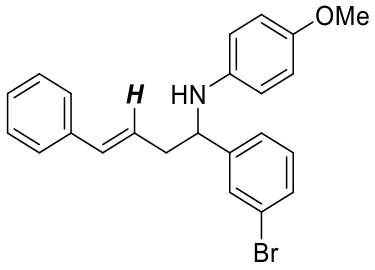

Compound **57i** was prepared according to *GP–IV* from allylbenzene (**36**; 30.5 µL, 0.23 mmol, 1.15 equiv) and imine **56i** (58.0 mg, 0.20 mmol), using NaHMDS (3.7 mg, 0.02 mmol, 10 mol%) as the catalyst, in dioxane (300 µL) at 25 °C for 18 h. **57i** was purified by PTLC on silica gel (EtOAc/PE = 1:9; *eluted twice*).

Yellow liquid.

Yield: 78.4 mg (96%; *E*:*Z* = 49:1).

^{1}H NMR (400 MHz, $CDCl_3$): δ = 7.55 (dd, *J* = 1.8, 1.8 Hz, 1H), 7.39–7.26 (m, 6H), 7.24–7.13 (m, 2H), 6.69 (d, *J* = 9.0 Hz, 2H), 6.50 (d, *J* = 15.8 Hz, 1H), 6.43 (d, *J* = 9.0 Hz, 2H), 6.10 (ddd, *J* = 15.8, 7.8, 6.6 Hz, 1H, *E*-CH=C<u>H</u>), 5.65 (ddd, *J* = 11.7, 7.1, 7.1 Hz, 1H, *Z*-CH=C<u>H</u>), 4.34 (dd, *J* = 8.0, 5.0, 1H), 4.00 (br s, 1H), 3.67 (s, 3H), 2.76–2.66 (m, 1H), 2.65–2.53 (m, 1H) ppm.

^{13}C NMR (125 MHz, $CDCl_3$): δ = 152.3, 146.4, 141.1, 136.9, 133.7, 130.2, 130.2, 129.5, 128.6 (2C), 127.5, 126.2 (2C), 125.6, 125.1, 122.9, 114.8 (2C), 114.8 (2C), 58.1, 55.7, 42.5 ppm.

IR (neat): *ν* = 3395, 3024, 2930, 2830, 1508, 1234, 818, 739, 692 cm^{-1}.

HRMS (EI): calculated for $C_{23}H_{22}{}^{79}BrNO^+$ = [M^+]: *m*/*z* = 407.0879, found: *m*/*z* = 407.0879.

(*E*)-*N*-[1-(2-Bromophenyl)-4-phenylbut-3-enyl]-4-methoxyaniline (57j)

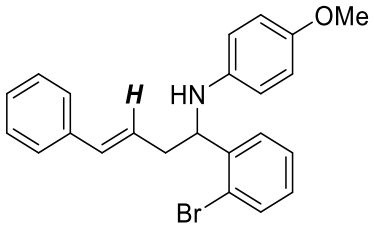

Compound **57j** was prepared according to *GP–IV* from allylbenzene (**36**; 29.2 µL, 0.22 mmol, 1.10 equiv) and imine **56j** (58.0 mg, 0.20 mmol), using NaHMDS (3.7 mg, 0.02 mmol, 10 mol%) as the catalyst, in dioxane (300 µL) at 25 °C for 18 h. **57j** was purified by PTLC on silica gel (EtOAc/PE = 1:9; *eluted once*).

Yellow liquid.

Yield: 73.5 mg (90%; *E*:*Z* = 49:1).

^{1}H NMR (500 MHz, $CDCl_3$): δ = 7.58 (dd, *J* = 7.8, 1.1 Hz, 1H), 7.45 (dd, *J* = 7.8, 1.7 Hz, 1H), 7.35 (dd, *J* = 7.8, 1.1 Hz, 2H), 7.30 (dd, *J* = 7.6, 7.6 Hz, 2H), 7.24 (dd, *J* = 7.6, 7.6 Hz 2H), 7.10 (ddd, *J* = 7.6, 7.6, 1.7 Hz, 1H), 6.67 (d, *J* = 9.0 Hz, 2H), 6.54 (d, *J* = 15.8 Hz, 1H), 6.38 (d, *J* = 9.0 Hz, 2H), 6.19 (ddd, *J* = 15.7, 7.8, 6.7 Hz, 1H, *E*-CH=C<u>H</u>), 5.74 (ddd, *J* = 11.8, 8.1, 5.9 Hz, 1H, *Z*-CH=C<u>H</u>), 4.81 (dd, *J* = 8.3, 4.2 Hz, 1H), 4.05 (br s, 1H), 3.67 (s, 3H), 2.85–2.80 (m, 1H), 2.57–2.50 (m, 1H) ppm.

^{13}C NMR (125 MHz, $CDCl_3$): δ = 152.1, 141.9, 141.0, 137.0, 133.5, 133.1, 128.6 (2C), 128.6, 127.9, 127.9, 127.5, 126.3 (2C), 125.9, 123.0, 114.8 (2C), 114.6 (2C), 57.0, 55.7, 40.2 ppm.

IR (neat): ν = 3402, 3024, 2930, 2830, 1508, 1236, 1020, 818, 743, 692 cm^{-1}.

HRMS (EI): calculated for $C_{23}H_{22}{}^{79}BrNO^+$ = [M^+]: *m*/*z* = 407.0879, found: *m*/*z* = 407.0880.

(*E*)-*N*-[1-(1-Naphthyl)-4-phenylbut-3-enyl]-4-methoxyaniline (57k)

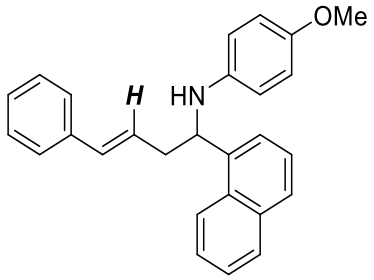

Compound **57k** was prepared according to *GP–IV* from allylbenzene (**36**; 29.2 µL, 0.22 mmol, 1.10 equiv) and imine **56k** (52.3 mg, 0.20 mmol), using NaHMDS (3.7 mg, 0.02 mmol, 10 mol%) as the catalyst, in dioxane (300 µL) at 25 °C for 20 h. **57k** was purified by PTLC on silica gel (Et_2O/PE = 1:9; *eluted once*).

Yellow liquid.

Yield: 74.4 mg (98%; *E*:*Z* = 24:1).

^{1}H NMR (500 MHz, $CDCl_3$): δ = 8.21 (d, *J* = 8.5 Hz, 1H), 7.91 (d, *J* = 8.2 Hz, 1H), 7.75 (d, *J* = 8.2 Hz, 1H), 7.66 (d, *J* = 7.2, 1H), 7.56 (dd, *J* = 7.6, 7.4 Hz, 1H), 7.51 (dd, *J* = 7.6, 7.4 Hz, 1H), 7.41 (dd, *J* = 7.7, 7.7 Hz, 1H), 7.33–7.26 (m, 4H), 7.22–7.19 (m, 1H), 6.61 (d, *J* = 8.9 Hz, 2H), 6.55 (d, *J* = 15.8 Hz, 1H), 6.40 (d, *J* = 8.9 Hz, 2H), 6.22 (ddd, *J* = 15.4, 7.1, 7.1 Hz, 1H, *E*-CH=C<u>H</u>), 5.80 (ddd, *J* = 11.7, 7.2, 7.2 Hz, 1H, *Z*-CH=C<u>H</u>), 5.23 (dd, *J* = 7.7, 3.9 Hz, 1H), 4.17 (br s, 1H), 3.62 (s, 3H), 2.98–2.93 (m, 1H), 2.72–2.66 (m, 1H) ppm.

^{13}C NMR (125 MHz, $CDCl_3$): δ = 151.9, 141.4, 138.3, 137.0, 134.2, 133.2, 130.7, 129.2, 128.6 (2C), 127.5, 127.4, 126.4, 126.2 (2C), 126.1, 125.82, 125.4, 123.3, 122.4, 114.7 (2C), 114.5 (2C), 55.7, 54.0, 41.0 ppm.

IR (neat): ν = 3404, 3026, 2932, 2830, 1508, 1236, 1036, 818, 779, 734, 692 cm^{-1}.

HRMS (EI): calculated for $C_{27}H_{25}NO^+$ = [M^+]: *m*/*z* = 379.1931, found: *m*/*z* = 379.1922.

(*E*)-*N*-[1-(2-Naphthyl)-4-phenylbut-3-enyl]-4-methoxyaniline (57l)

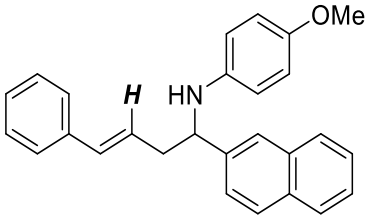

Compound **57l** was prepared according to *GP–IV* from allylbenzene (**36**; 29.2 µL, 0.22 mmol, 1.10 equiv) and imine **56l** (52.3 mg, 0.20 mmol), using NaHMDS (3.7 mg, 0.02 mmol, 10 mol%) as the catalyst, in dioxane (300 µL) at 25 °C for 20 h. **57l** was purified by PTLC on silica gel (Et_2O/PE = 1:9; *eluted once*).

Yellow liquid.

Yield: 66.0 mg (87%; *E*:*Z* = 24:1).

^{1}H NMR (500 MHz, $CDCl_3$): δ = 7.83–7.78 (m, 4H), 7.51 (d, *J* = 8.6 Hz, 1H), 7.46–4.40 (m, 2H), 7.32–7.25 (m, 4H), 7.22–7.18 (m, 1H), 6.64 (d, *J* = 7.9 Hz, 2H), 6.52 (d, *J* = 15.9 Hz, 1H, *E*-CH=C<u>H</u>), 6.48 (d, *J* = 7.9 Hz, 2H), 6.15 (ddd, *J* = 15.9, 8.1, 6.7 Hz, 1H), 5.71 (ddd, *J* = 12.7, 7.2, 7.2 Hz, 1H, *Z*-CH=C<u>H</u>), 4.54 (dd, *J* = 7.9, 5.1 Hz, 1H), 4.04 (br s, 1H), 3.63 (s, 3H), 2.83–2.78 (m, 1H), 2.72–2.66 (m, 1H) ppm.

^{13}C NMR (125 MHz, $CDCl_3$): δ = 152.1, 141.5, 141.3, 137.0, 133.6, 133.3, 132.8, 128.6 (2C), 128.4, 127.9, 127.7, 127.4, 126.2 (2C), 126.1, 126.0, 125.5, 125.0, 124.7, 114.8 (2C), 114.7 (2C), 58.6, 55.7, 42.5 ppm.

IR (neat): ν = 3402, 3024, 2930, 2830, 1508, 1236, 1036, 818, 746, 692 cm^{-1}.

HRMS (EI): calculated for $C_{27}H_{25}NO^+$ = [M^+]: *m*/*z* = 379.1931, found: *m*/*z* = 379.1929.

(*E*)-*N*-[1-(4-Methoxyphenyl)-4-phenylbut-3-enyl]-4-methoxyaniline (57m)

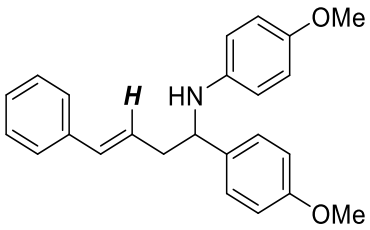

Compound **57m** was prepared according to *GP–V* from allylbenzene (**36**; 47.7 µL, 0.36 mmol, 1.80 equiv) and imine **56m** (48.3 mg, 0.20 mmol), using NaHMDS (3.7 mg, 0.02 mmol, 10 mol%) as the catalyst, in dioxane (300 µL) at 25 °C for 18 h. **57m** was purified by PTLC on silica gel (EtOAc/PE = 1:9; *eluted twice*).

Yellow liquid.

Yield: 52.5 mg (73%; *E*:*Z* = 99:1).

^{1}H NMR (600 MHz, $CDCl_3$): δ = 7.33–7.28 (m, 6H), 7.24–7.20 (m, 1H), 6.87 (d, *J* = 8.9 Hz, 2H), 6.67 (d, *J* = 8.9 Hz, 2H), 6.50 (d, *J* = 15.8 Hz, 1H), 6.46 (d, *J* = 8.9 Hz, 2H), 6.14 (ddd, *J* = 15.8, 7.6, 6.9 Hz, 1H, *E*-CH=C<u>H</u>), 5.68 (ddd, *J* = 11.8, 7.7, 6.3 Hz, 1H, *Z*-CH=C<u>H</u>), 4.35 (dd, *J* = 7.4, 5.6 Hz, 1H), 3.92 (br s, 1H), 3.79 (s, 3H), 3.68 (s, 3H), 2.74–2.69 (m, 1H), 2.66–2.61 (m, 1H) ppm.

^{13}C NMR (125 MHz, $CDCl_3$): δ = 158.6, 152.0, 141.6, 137.1, 135.7, 133.1, 128.6 (2C), 127.4 (2C), 127.4, 126.3, 126.2 (2C), 114.8 (2C), 114.7 (2C), 114.0 (2C), 57.8, 55.7, 55.3, 42.7 ppm.

IR (neat): ν = 3399, 3024, 2932, 2832, 1508, 1238, 1034, 820, 742, 694 cm^{-1}.

HRMS (EI): calculated for $C_{24}H_{25}NO_2^+ = [M^+]$: *m*/*z* = 359.1880, found: *m*/*z* = 359.1884.

(*E*)-*N*-[1-(4-*N*,*N*-Dimethylaminophenyl)-4-phenylbut-3-enyl]-4-methoxyaniline (57n)

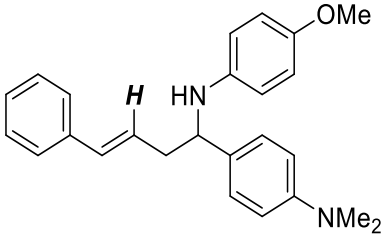

Compound **57n** was prepared according to *GP–V* from allylbenzene (**36**; 66.4 µL, 0.50 mmol, 2.50 equiv) and imine **56n** (50.9 mg, 0.20 mmol), using NaHMDS (3.7 mg, 0.02 mmol, 10 mol%) as the catalyst, in dioxane (300 µL) at 25 °C for 18 h. **57n** was purified by PTLC on silica gel (EtOAc/PE = 1:9; *eluted twice*).

Yellow liquid.

Yield: 67.1 mg (90%; *E*:*Z* = 49:1).

^{1}H NMR (601 MHz, $CDCl_3$): δ = 7.34–7.32 (m, 2H), 7.28 (dd, *J* = 7.7, 7.3 Hz, 2H), 7.24 (d, *J* = 8.7 Hz, 2H), 7.20 (dd, *J* = 7.3, 7.3 Hz, 1H), 6.72 (d, *J* = 8.7 Hz, 2H), 6.67 (d, *J* = 8.9 Hz, 2H), 6.50 (d, *J* = 15.5 Hz, 1H), 6.47 (d, *J* = 8.9 Hz, 2H), 6.16 (ddd, *J* = 15.5, 7.6, 6.8 Hz, 1H, *E*-CH=C<u>H</u>), 5.69 (ddd, *J* = 11.8, 7.7, 6.3 Hz, 1H, *Z*-CH=C<u>H</u>), 4.32 (dd, *J* = 7.5, 5.5 Hz, 1H), 4.02 (br s, 1H), 3.68 (s, 3H), 2.93 (s, 6H), 2.73–2.69 (m, 1H), 2.66–2.61 (m, 1H) ppm.

^{13}C NMR (125 MHz, $CDCl_3$): δ = 151.9, 149.7, 141.9, 137.3, 132.8, 131.5, 128.5 (2C), 127.3, 127.1 (2C), 126.8, 126.2 (2C), 114.8 (2C), 114.7 (2C), 112.8 (2C), 57.8, 55.8, 42.6, 40.7 (2C) ppm.

IR (neat): *ν* = 3395, 3024, 2916, 2830, 1508, 1234, 1036, 818, 733, 692 cm^{-1}.

HRMS (EI): calculated for $C_{25}H_{28}N_2O^+$ = [M^+]: *m*/*z* = 372.2196, found: *m*/*z* = 372.2188.

(*E*)-*N*-[1-(4-cyanophenyl)-4-phenylbut-3-enyl]-4-methoxyaniline (57o)

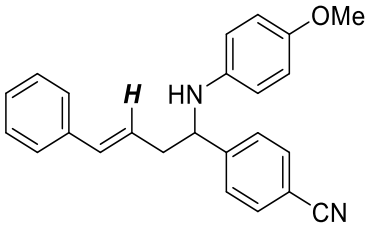

Compound **57o** was prepared according to *GP–IV* from allylbenzene (**36**; 79.5 µL, 0.60 mmol, 3.00 equiv) and imine **56o** (47.3 mg, 0.20 mmol), using NaHMDS (3.7 mg, 0.02 mmol, 10 mol%) as the catalyst, in dioxane (300 µL) at 25 °C for 20 h. **57o** was purified by PTLC on silica gel (EtOAc/PE = 1:9; *eluted twice*).

Yellow liquid.

Yield: 35.4 mg (50%; *E*:*Z* = >99:1).

^{1}H NMR (500 MHz, $CDCl_3$): δ = 7.66 (d, *J* = 8.3 Hz, 2H), 7.54 (d, *J* = 8.3 Hz, 2H), 7.37–7.31 (m, 4H), 7.28–7.25 (m, 1H), 6.70 (d, *J* = 9.0 Hz, 2H), 6.54 (d, *J* = 15.8 Hz, 1H), 6.41 (d, *J* = 9.0 Hz, 2H), 6.11 (ddd, *J* = 15.8, 7.8, 6.7 Hz, 1H), 4.47 (dd, *J* = 7.9, 5.1 Hz, 1H), 4.01 (br s, 1H), 3.71 (s, 3H), 2.80–2.73 (m, 1H), 2.68–2.61 (m, 1H) ppm.

The Z-isomer could not be detected.

^{13}C NMR (125 MHz, $CDCl_3$): δ = 152.5, 149.6, 140.7, 136.7, 134.1, 132.6 (2C), 128.7 (2C), 127.7, 127.2 (2C), 126.2 (2C), 124.9, 118.9, 114.8 (4C), 111.0, 58.2, 55.7, 42.2 ppm.

IR (neat): ν = 3390, 3026, 2926, 2225, 1510, 1238, 1035, 820, 748, 694 cm^{-1}.

HRMS (EI): calculated for $C_{24}H_{22}N_2O^+$ = [M^+]: *m*/*z* = 354.1727, found: *m*/*z* = 354.1716.

(*E*)-*N*-[1-(Thiophen-2-yl)-4-phenylbut-3-enyl]-4-methoxyaniline (57v)

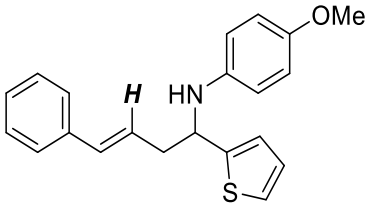

Compound **57v** was prepared according to *GP–IV* from allylbenzene (**36**; 39.8 µL, 0.30 mmol, 1.50 equiv) and imine **56v** (43.5 mg, 0.20 mmol), using NaHMDS (3.7 mg, 0.02 mmol, 10 mol%) as the catalyst, in dioxane (300 µL) at 60 °C for 72 h. **57v** was purified by PTLC on silica gel (Et_2O/PE = 1:9; *eluted once*).

Yellow liquid.

Yield: 60.4 mg (90%; *E*:*Z* = 99:1).

^{1}H NMR (500 MHz, $CDCl_3$): δ = 7.33–7.28 (m, 4H), 7.24–7.17 (m, 2H), 6.99 (d, *J* = 3.4 Hz, 1H), 6.95 (dd, *J* = 4.9, 3.4 Hz, 1H), 6.72 (d, *J* = 8.9 Hz, 2H), 6.57 (d, *J* = 8.9 Hz, 2H), 6.52 (d, *J* = 15.8 Hz, 1H), 6.19 (ddd, *J* = 15.8, 7.3, 7.3 Hz, 1H, *E*-CH=C<u>H</u>), 5.72 (ddd, *J* = 11.8, 6.9, 6.9 Hz, 1H, *Z*-CH=C<u>H</u>), 4.72 (dd, *J* = 6.3, 6.3 Hz, 1H), 3.94 (br s, 1H), 3.71 (s, 3H), 2.83–2.79 (m, 2H) ppm.

^{13}C NMR (125 MHz, $CDCl_3$): δ = 152.5, 149.0, 141.1, 137.1, 133.6, 128.6 (2C), 127.5, 126.8, 126.2 (2C), 125.6, 123.8, 123.5, 115.2 (2C), 114.8 (2C), 55.7, 54.8, 42.4 ppm.

IR (neat): ν = 3387, 3026, 2928, 2832, 1508, 1234, 818, 735, 692 cm^{-1}.

HRMS (EI): calculated for $C_{21}H_{21}NO^{32}S^+ = [M^+]$: *m*/*z* = 335.1338, found: *m*/*z* = 335.1342.

(*E*)-*N*-[1-(1-Methyl-1*H*-indol-3-yl)-4-phenylbut-3-enyl]-4-methoxyaniline (57w)

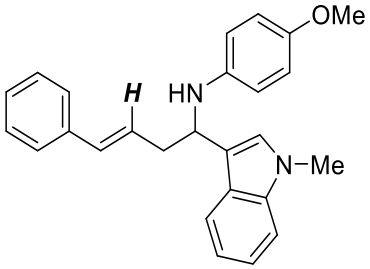

Compound **57w** was prepared according to *GP–V* from allylbenzene (**36**; 53.0 µL, 0.40 mmol, 2.00 equiv) and imine **56w** (52.9 mg, 0.20 mmol), using NaHMDS (3.7 mg, 0.02 mmol, 10 mol%) as the catalyst, in dioxane (300 µL) at 25 °C for 20 h. **57w** was purified by PTLC on silica gel (Et_2O/PE = 1:9; *eluted three times*).

Yellow liquid.

Yield: 61.2 mg (80%; *E*:*Z* = 99:1).

^{1}H NMR (500 MHz, $CDCl_3$): δ = 7.71 (d, *J* = 7.9 Hz, 1H), 7.33–7.26 (m, 5H), 7.25–7.22 (m, 1H), 7.22–7.18 (m, 1H), 7.13 (ddd, *J* = 7.9, 7.0, 1.0 Hz, 1H), 6.97 (s, 1H), 6.70 (d, *J* = 9.0 Hz, 2H), 6.57 (d, *J* = 9.0 Hz, 2H), 6.53 (d, *J* = 15.8 Hz, 1H), 6.24 (ddd, *J* = 15.8, 7.2, 7.2 Hz, 1H, *E*-CH=C<u>H</u>), 5.78 (ddd, *J* = 11.6, 7.1, 7.1 Hz, 1H, *Z*-CH=C<u>H</u>), 4.78 (dd, *J* = 6.2, 6.2 Hz, 1H), 3.91 (br s, 1H), 3.73 (s, 3H), 3.70 (s, 3H), 2.97–2.91 (m, 1H), 2.86–2.81 (m, 1H) ppm.

^{13}C NMR (125 MHz, $CDCl_3$): δ = 151.9, 142.0, 137.5, 137.3, 132.7, 128.5 (2C), 127.2, 127.0, 126.6, 126.3, 126.1 (2C), 121.6, 119.3, 118.9, 116.7, 114.8 (2C), 114.7 (2C), 109.4, 55.7, 51.7, 40.5, 32.7 ppm.

IR (neat): ν = 3435, 3358, 3022, 3022, 2831, 1510, 1238, 824, 738, 692 cm^{-1}.

HRMS (ESI): calculated for $C_{26}H_{27}N_2O^+ = [M+H]^+$: *m*/*z* = 383.2118, found: *m*/*z* = 383.2140.

(*E*)-*N*-[1-(1-Methyl-1*H*-pyrrol-2-yl)-4-phenylbut-3-enyl]-4-methoxyaniline (57x)

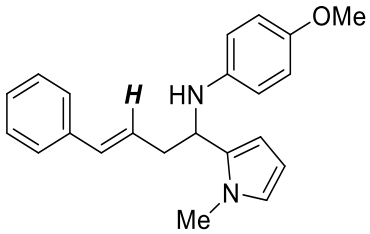

Compound **57x** was prepared according to *GP–IV* from allylbenzene (**36**; 29.2 µL, 0.22 mmol, 1.10 equiv) and imine **56x** (42.9 mg, 0.20 mmol), using NaHMDS (3.7 mg, 0.02 mmol, 10 mol%) as the catalyst, in dioxane (300 µL) at 25 °C for 18 h. **57x** was purified by PTLC on silica gel (EtOAc/PE = 1:9; *eluted twice*).

Yellow liquid.

Yield: 53.2 mg (80%; *E*:*Z* = >99:1).

^{1}H NMR (500 MHz, $CDCl_3$): δ = 7.31–7.24 (m, 4H), 7.21–7.18 (m, 1H), 6.76 (d, *J* = 8.9 Hz, 2H), 6.62–6.52 (m, 3H), 6.48 (d, *J* = 15.9 Hz, 1H), 6.22 (ddd, *J* = 15.9, 7.3, 7.3 Hz, 1H), 6.18 (dd, *J* = 3.4, 1.5 Hz, 1H), 6.08 (dd, *J* = 3.4, 2.8 Hz, 1H), 4.47 (dd, *J* = 7.3, 5.8 Hz, 1H), 3.73 (s, 3H), 3.57 (s, 3H), 3.56 (br s, 1H), 2.89–2.84 (m, 1H), 2.82–2.76 (m, 1H) ppm.

The Z-isomer could not be detected.

^{13}C NMR (125 MHz, $CDCl_3$): δ = 152.2, 141.3, 137.3, 133.4, 132.6, 128.5 (2C), 127.2, 126.8, 126.1 (2C), 122.5, 115.0 (2C), 114.8 (2C), 106.7, 106.5, 55.8, 51.5, 38.3, 34.0 ppm.

IR (neat): ν = 3379, 3024, 2916, 2832, 1508, 1236, 1034, 818, 735, 712, 692 cm^{-1}.

HRMS (EI): calculated for $C_{22}H_{24}N_2O^+ = [M^+]$: *m*/*z* = 332.1883, found: *m*/*z* = 332.1887.

(*E*)-*N*-(2,2-Dimethyl-6-phenylhex-5-en-3-yl)-4-methoxyaniline (57ü)

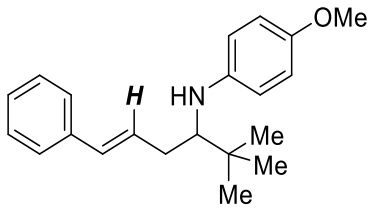

Compound **57ü** was prepared according to *GP–V* from allylbenzene (**36**; 53.0 µL, 0.40 mmol, 2.00 equiv) and imine **56ü** (38.3 mg, 0.20 mmol), using NaHMDS (3.7 mg, 0.02 mmol, 10 mol%) as the catalyst, in dioxane (300 µL) at 25 °C for 18 h. **57ü** was purified by PTLC on silica gel (Et_2O/PE = 1:9; *eluted once*).

Yellow liquid.

Yield: 53.8 mg (87%; *E*:*Z* = 49:1).

^{1}H NMR (600 MHz, $CDCl_3$): δ = 7.21–7.18 (m, 2H), 7.15–7.10 (m, 3H), 6.72 (d, *J* = 8.5 Hz, 2H), 6.55 (d, *J* = 8.5 Hz, 2H), 6.38 (d, *J* = 15.8 Hz, 1H), 6.16 (ddd, *J* = 15.8, 8.1, 8.1 Hz, 1H, *E*-CH=C<u>H</u>), 5.69 (ddd, *J* = 11.5, 6.9, 6.9 Hz, 1H, *Z*-CH=C<u>H</u>), 3.72 (s, 3H), 3.24 (br s, 1H), 3.12 (dd, *J* = 9.4, 3.5 Hz, 1H), 2.61–2.57 (m, 1H), 2.22–2.17 (m, 1H), 1.00 (s, 9H) ppm.

^{13}C NMR (150 MHz, $CDCl_3$): δ = 151.4, 143.9, 137.7, 131.2, 129.3, 128.4 (2C), 126.8, 126.0 (2C), 115.0 (2C), 114.4 (2C), 63.9, 55.9, 35.9, 35.9, 27.1 (3C) ppm.

IR (neat): ν = 3404, 3024, 2951, 2832, 1508, 1232, 816, 739, 692 cm^{-1}.

HRMS (EI): calculated for $C_{21}H_{27}NO^+ = [M^+]$: *m*/*z* = 309.2087, found: *m*/*z* = 309.2091.

4.2.8 Homoallylic Amines: Pro-nucleophile-Scope

(*E*)-*N*-[4-(4-Fluorophenyl)-1-phenylbut-3-enyl]-4-methoxyaniline (152b)

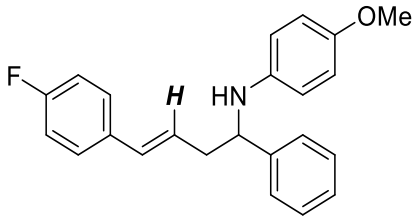

Compound **152b** was prepared according to *GP–IV* from the substituted allylbenzene **146** (29.7 µL, 0.22 mmol, 1.10 equiv) and imine **56b** (42.2 mg, 0.20 mmol), using NaHMDS (3.7 mg, 0.02 mmol, 10 mol%) as the catalyst, in dioxane (300 µL) at 25 °C for 20 h. **152b** was purified by PTLC on silica gel (EtOAc/PE = 1:9; *eluted once*).

Yellow liquid.

Yield: 68.8 mg (99%; *E*:*Z* = 49:1).

^{1}H NMR (500 MHz, $CDCl_3$): δ = 7.37 (d, *J* = 7.3 Hz, 2H), 7.32 (dd, *J* = 7.6, 7.6 Hz, 2H), 7.29–7.21 (m, 3H), 6.96 (dd, *J* = 8.7, 8.7 Hz, 2H), 6.66 (d, *J* = 9.0 Hz, 2H), 6.49–6.40 (m, 3H), 6.04 (ddd, *J* = 15.8, 7.2, 7.2 Hz, 1H, *E*-CH=C<u>H</u>), 5.67 (ddd, *J* = 11.7, 7.1, 7.1 Hz, 1H, *Z*-CH=C<u>H</u>), 4.38 (dd, *J* = 7.8, 5.3 Hz, 1H), 3.94 (br s, 1H), 3.65 (s, 3H), 2.74–2.66 (m, 1H), 2.65–2.56 (m, 1H) ppm.

^{13}C NMR (125 MHz, $CDCl_3$): δ = 162.2 (d, *J* = 246.6 Hz), 152.1, 143.7, 141.5, 133.2 (d, *J* = 3.3 Hz), 132.0, 128.6 (2C), 127.6 (d, *J* = 7.9, 2C), 127.0, 126.4, 126.0 (d, *J* = 2.1, 2C), 115.5, 115.3, 114.7 (2C), 114.6 (2C), 58.4, 55.7, 42.4 ppm.

^{19}F NMR (376 MHz, $CDCl_3$): δ = –114.6 (ddd, *J* = 13.2, 6.7, 3.9 Hz) ppm.

IR (neat): ν = 3402, 3026, 2931, 2832, 1506, 1229, 818, 737, 700 cm^{-1}.

HRMS (EI): calculated for $C_{23}H_{22}FNO^+ = [M^+]$: *m*/*z* = 347.1680, found: *m*/*z* = 347.1687.

(*E*)-*N*-[4-(4-Methylphenyl)-1-phenylbut-3-enyl]-4-methoxyaniline (153b)

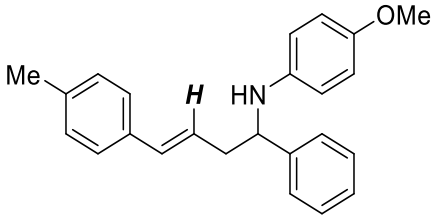

Compound **153b** was prepared according to *GP–IV* from the substituted allylbenzene **147** (33.7 µL, 0.22 mmol, 1.10 equiv) and imine **56b** (42.2 mg, 0.20 mmol), using NaHMDS (3.7 mg, 0.02 mmol, 10 mol%) as the catalyst, in dioxane (300 µL) at 25 °C for 20 h. **153b** was purified by PTLC on silica gel (EtOAc/PE = 1:9; *eluted once*).

Yellow liquid.

Yield: 68.0 mg (99%; *E*:*Z* = 99:1).

^{1}H NMR (500 MHz, $CDCl_3$): δ = 7.38 (d, *J* = 7.2 Hz, 2H), 7.36–7.30 (m, 3H), 7.26–7.21 (m, 1H), 7.13 (d, *J* = 3.1 Hz, 3H), 6.76–6.64 (m, 3H), 6.46 (d, *J* = 9.0 Hz, 2H), 6.01 (ddd, *J* = 15.6, 7.8, 6.7 Hz, 1H, *E*-CH=C<u>H</u>), 5.73 (ddd, *J* = 11.4, 7.3, 7.3 Hz, 1H, *Z*-CH=C<u>H</u>), 4.40 (ddd, *J* = 7.6, 5.0, 4.4 Hz, 1H), 3.98 (d, *J* = 4.4 Hz, 1H), 3.67 (s, 3H), 2.79–2.72 (m, 1H), 2.70–2.63 (m, 1H), 2.31 (s, 3H) ppm.

^{13}C NMR (125 MHz, $CDCl_3$): δ = 152.0, 143.8, 141.6, 137.2, 134.3, 133.1, 129.2 (2C), 128.6 (2C), 127.0, 126.4 (2C), 126.1 (2C), 125.1, 114.7 (2C), 114.7 (2C), 58.4, 55.7, 42.6, 21.2 ppm.

IR (neat): ν = 3397, 3024, 2930, 2830, 1510, 1236, 818, 746, 700 cm^{-1}.

HRMS (EI): calculated for $C_{24}H_{25}NO^+ = [M^+]$: *m*/*z* = 343.1931, found: *m*/*z* = 343.1945.

(*E*)-*N*-[4-(2-Methylphenyl)-1-phenylbut-3-enyl]-4-methoxyaniline (154b)

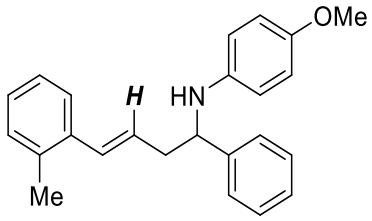

Compound **154b** was prepared according to *GP–IV* from the substituted allylbenzene **148** (33.7 µL, 0.22 mmol, 1.10 equiv) and imine **56b** (42.2 mg, 0.20 mmol), using NaHMDS (3.7 mg, 0.02 mmol, 10 mol%) as the catalyst, in dioxane (300 µL) at 25 °C for 20 h. **154b** was purified by PTLC on silica gel (EtOAc/PE = 1:9; *eluted once*).

Yellow liquid.

Yield: 58.4 mg (85%; *E*:*Z* = 49:1).

^{1}H NMR (500 MHz, $CDCl_3$): δ = 7.37 (d, *J* = 7.3 Hz, 2H), 7.31 (dd, *J* = 7.5, 7.3 Hz, 2H), 7.24–7.21 (m, 3H), 7.09 (d, *J* = 7.5 Hz, 2H), 6.65 (d, *J* = 8.9 Hz, 2H), 6.48–6.43 (m, 3H), 6.08 (ddd, *J* = 14.7, 7.2, 7.2 Hz, 1H, *E*-CH=C<u>H</u>), 5.64 (ddd, *J* = 11.5, 7.2, 6.4 Hz, 1H, *Z*-CH=C<u>H</u>) 4.37 (dd, *J* = 6.4, 6.4 Hz, 1H), 3.95 (br s, 1H), 3.65 (s, 3H), 2.73–2.69 (m, 1H), 2.63–6.57 (m, 1H), 2.31 (s, 3H) ppm.

^{13}C NMR (125 MHz, $CDCl_3$): δ = 152.1, 143.8, 141.6, 136.3, 135.1, 131.3, 130.3, 128.6 (2C), 127.6, 127.4, 127.0, 126.5 (2C), 126.1, 125.7, 114.8 (2C), 114.8 (2C), 58.4, 55.8, 42.8, 19.9 ppm.

IR (neat): ν = 3399, 3024, 2924, 2830, 1508, 1234, 816, 750, 700 cm^{-1}.

HRMS (EI): calculated for $C_{24}H_{25}NO^+ = [M^+]$: *m*/*z* = 343.1931, found: *m*/*z* = 343.1922.

(*E*)-*N*-[4-(4-Methoxyphenyl)-1-phenylbut-3-enyl]-4-methoxyaniline (155b)

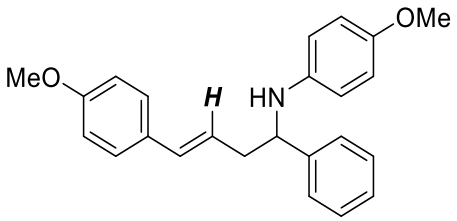

Compound **155b** was prepared according to *GP–IV* from the substituted allylbenzene **149** (33.8 µL, 0.22 mmol, 1.10 equiv) and imine **56b** (42.2 mg, 0.20 mmol), using NaHMDS (3.7 mg, 0.02 mmol, 10 mol%) as the catalyst, in dioxane (300 µL) at 40 °C for 20 h. **155b** was purified by PTLC on silica gel (EtOAc/PE = 1:9; *eluted twice*).

Yellow liquid.

Yield: 55.4 mg (77%; *E*:*Z* = 24:1).

^{1}H NMR (500 MHz, $CDCl_3$): δ = 7.38–7.37 (m, 2H), 7.32–7.30 (m, 2H), 7.26–7.21 (m, 3H), 6.83 (d, *J* = 8.7 Hz, 2H), 6.66 (d, *J* = 8.7 Hz, 2H), 6.46–6.43 (m, 3H), 5.99 (ddd, *J* = 15.6, 7.2, 7.2 Hz, 1H, *E*-CH=C<u>H</u>), 5.59 (ddd, *J* = 12.0, 7.0, 7.0 Hz, 1H, *Z*-CH=C<u>H</u>), 4.37 (dd, *J* = 5.7, 5.7 Hz, 1H), 3.97 (br s, 1H), 3.78 (s, 3H), 3.66 (s, 3H), 2.73–2.68 (m, 1H), 2.62–2.56 (m, 1H) ppm.

^{13}C NMR (125 MHz, $CDCl_3$): δ = 159.1, 152.0, 143.9, 141.6, 132.6, 129.0, 128.6 (2C), 127.3 (2C), 126.9, 126.4 (2C), 123.9, 114.7 (4C), 114.0 (2C), 58.4, 55.7, 55.3, 42.6 ppm

IR (neat): ν = 3397, 3026, 2932, 2832, 1508, 1236, 1032, 818, 752, 700 cm^{-1}.

HRMS (EI): calculated for $C_{24}H_{25}NO_2^+ = [M^+]$: *m*/*z* = 359.1880, found: *m*/*z* = 359.1878.

(*E*)-*N*-[4-(Pyridin-3-yl)-1-(pyridin-4-yl)but-3-enyl]-4-methoxyaniline (159z)

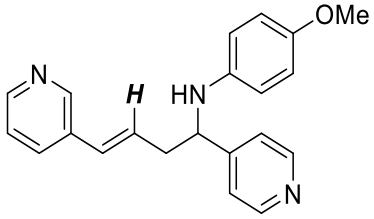

Compound **159z** was prepared according to *GP–IV* from 3-allyl pyridine (**158**; 35.8 mg, 0.30 mmol, 1.50 equiv) and imine **56z** (42.4 mg, 0.20 mmol), using NaHMDS (3.7 mg, 0.02 mmol, 10 mol%) as the catalyst, in dioxane (300 µL) at 25 °C for 20 h. **159z** was purified by PTLC on silica gel (NEt_3/Et_2O/PE = 1:2:17; *eluted twice*).

Yellow liquid.

Yield: 49.7 mg (75%; *E*:*Z* = 32:1).

^{1}H NMR (500 MHz, $CDCl_3$): δ = 8.57 (d, *J* = 6.0 Hz, 2H), 8.55 (d, *J* = 1.8 Hz, 1H), 8.47 (d, *J* = 4.7 Hz, 1H), 7.63 (dt, *J* = 7.9, 1.8 Hz, 1H), 7.32 (d, *J* = 6.0 Hz, 2H), 7.23 (dd, *J* = 7.9, 4.7 Hz, 1H), 6.69 (d, *J* = 8.9 Hz, 2H), 6.49 (d, *J* = 15.9 Hz, 1H), 6.42 (d, *J* = 8.9 Hz, 2H), 6.19 (ddd, *J* = 15.9, 7.5, 7.5 Hz, 1H, *E*-CH=C<u>H</u>), 5.81 (ddd, *J* = 11.7, 7.1, 7.1 Hz, 1H, *Z*-CH=C<u>H</u>), 4.42 (dd, *J* = 7.5, 5.2 Hz, 1H), 3.98 (br s, 1H), 3.69 (s, 3H), 2.80–2.75 (m, 1H), 2.70–2.64 (m, 1H) ppm.

^{13}C NMR (125 MHz, $CDCl_3$): δ = 152.7, 152.5, 150.2 (2C), 148.8, 148.2, 140.6, 132.6, 132.3, 130.4, 127.5, 123.5, 121.7 (2C), 114.9 (2C), 114.8 (2C), 57.5, 55.7, 41.8 ppm

IR (neat): ν = 3287, 3028, 2930, 2832, 1597, 1508, 1236, 1034, 818, 731, 706 cm^{-1}.

HRMS (EI): calculated for $C_{21}H_{21}N_3O^+ = [M^+]$: *m*/*z* = 331.1679, found: *m*/*z* = 331.1695.

(*E*)-*N*-[4-(pyridin-3-yl)-1-(thiophen-2-yl)phenylbut-3-enyl]-4-methoxyaniline (159v)

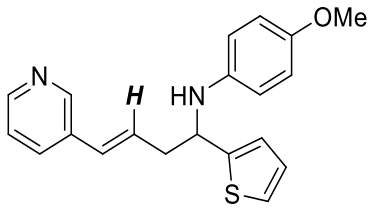

Compound **159v** was prepared according to *GP–IV* from allyl pyridine (**158**; 35.8 mg, 0.30 mmol, 1.50 equiv) and aldimine **56v** (43.5 mg, 0.20 mmol), using NaHMDS (3.7 mg, 0.02 mmol, 10 mol%) as the catalyst, in dioxane (300 µL) at 25 °C for 20 h. **159v** was purified by PTLC (NEt_3:Et_2O:PE = 1:2:17, *eluted twice*).

Yellow liquid.

Yield: 38.4 mg (57%, *E*:*Z* = 32:1).

^{1}H NMR (500 MHz, $CDCl_3$): δ = 8.55 (d, *J* = 1.7 Hz, 1H), 8.45 (dd, *J* = 4.6, 1.2 Hz, 1H), 7.63 (dt, *J* = 7.9, 1.7 Hz, 1H), 7.23–7.18 (m, 2H), 6.99–6.95 (m, 2H), 6.73 (d, *J* = 8.9 Hz, 2H), 6.58 (d, *J* = 8.9 Hz, 2H), 6.49 (d, *J* = 16.0 Hz, 1H), 6.27 (ddd, *J* = 16.0, 7.2, 7.2 Hz, 1H, *E*-CH=C<u>H</u>), 5.87 (ddd, *J* = 11.6, 7.2, 7.2 Hz, 1H, *Z*-CH=C<u>H</u>), 4.74 (dd, *J* = 6.4, 6.4 Hz, 1H), 3.90 (br s, 1H), 3.71 (s, 3H), 2.85–2.82 (m, 2H) ppm.

^{13}C NMR (125 MHz, $CDCl_3$): δ = 152.6, 148.6, 148.5, 148.2, 141.0, 132.6, 132.6, 129.9, 128.2, 126.9, 124.0, 123.6, 123.4, 115.2 (2C), 114.8 (2C), 55.7, 54.7, 42.3 ppm.

IR (neat): ν = 3379, 3287, 3028, 2926, 2832, 1508, 1234, 1036, 818, 702 cm^{-1}.

HRMS (EI): calculated for $C_{20}H_{20}N_2OS^+ = [M^+]$: *m*/*z* =336.1291, found: *m*/*z* = 336.1300.

(*E*)-*N*-[4-(pyridin-3-yl)-1-(furan-2-yl)phenylbut-3-enyl]-4-methoxyaniline (159ø)

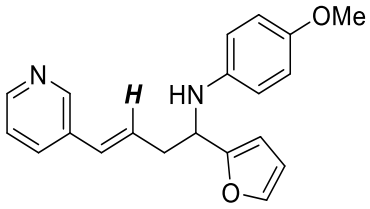

Compound **159ø** was prepared according to *GP–IV* from allyl pyridine (**158**; 35.8 mg, 0.30 mmol, 1.50 equiv) and aldimine **56ø** (40.2 mg, 0.20 mmol), using NaHMDS (3.7 mg, 0.02 mmol, 10 mol%) as the catalyst, in dioxane (300 µL) at 25 °C for 20 h. **159ø** was purified by PTLC (NEt_3:Et_2O:PE = 1:2:17, *eluted twice*).

Yellow liquid.

Yield: 26.3 mg (41%, *E*:*Z* = 32:1).

^{1}H NMR (500 MHz, $CDCl_3$): δ = 8.53 (d, *J* = 2.0 Hz, 1H), 8.44 (dd, *J* = 4.8, 1.6 Hz, 1H), 7.61 (dt, *J* = 8.0, 2.0 Hz, 1H), 7.36 (s, 1H), 7.20 (dd, *J* = 8.0, 4.8 Hz, 1H), 6.74 (d, *J* = 8.9 Hz, 2H), 6.59 (d, *J* = 8.9 Hz, 2H), 6.45 (d, *J* = 15.8 Hz, 1H), 6.29 (dd, *J* = 3.3, 1.9 Hz, 1H), 6.22 (ddd, *J* = 15.8, 7.2, 7.2 Hz, 1H, *E*-CH=C<u>H</u>), 6.17 (d, *J* = 7.2 Hz, 1H), 5.85 (ddd, *J* = 12.3, 7.4, 7.4 Hz, 1H, *Z*-CH=C<u>H</u>), 4.57 (t, *J* = 6.4 Hz, 1H), 3.78 (br s, 1H), 3.72 (s, 3H), 2.84–2.82 (m, 2H) ppm.

^{13}C NMR (125 MHz, $CDCl_3$): δ = 155.6, 152.6, 148.4, 148.2, 141.6, 140.9, 132.7, 132.6, 129.6, 128.3, 123.4, 115.3 (2C), 114.8 (2C), 110.2, 106.3, 55.7, 52.7, 38.6 ppm

IR (neat): ν = 3366, 3275, 3028, 2932, 2832, 1508, 1234, 1034, 818, 733, 706 cm^{-1}.

HRMS (EI): calculated for $C_{20}H_{20}N_2O_2^+$ = [M^+]: *m*/*z* = 320.1519, found: *m*/*z* = 320.1510.

(*E*)-*N*-[4-(Pyridin-3-yl)-1-phenylbut-3-enyl]-aniline (159a)

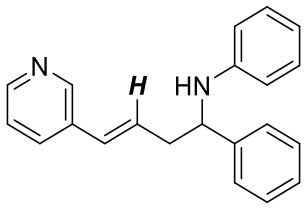

Compound **159a** was prepared according to *GP–IV* from 3-allyl pyridine (**158**; 35.8 mg, 0.30 mmol, 1.50 equiv) and imine **56a** (36.2 mg, 0.20 mmol), using NaHMDS (3.7 mg, 0.02 mmol, 10 mol%) as the catalyst, in dioxane (300 µL) at 25 °C for 20 h. **159a** was purified by PTLC on silica gel (NEt_3/Et_2O/PE = 1:2:17; *eluted twice*).

Yellow liquid.

Yield: 39.7 mg (66%; *E*:*Z* = 99:1).

^{1}H NMR (500 MHz, $CDCl_3$): δ = 8.54 (d, *J* = 1.8 Hz, 1H), 8.44 (dd, *J* = 4.7, 1.4 Hz, 1H), 7.61 (ddd, *J* = 7.9, 1.8, 1.8 Hz, 1H), 7.39–7.32 (m, 4H), 7.26–7.23 (m, 1H), 7.20 (dd, *J* = 7.9, 4.7 Hz, 1H), 7.09–7.06 (m, 2H), 6.64 (dd, *J* = 7.3, 7.3 Hz, 1H), 6.51 (d, *J* = 8.4 Hz, 2H), 6.47 (d, *J* = 15.9 Hz, 1H), 6.21 (ddd, *J* = 15.9, 7.2, 7.2 Hz, 1H, *E*-CH=C<u>H</u>), 5.84 (ddd, *J* = 11.7, 7.2, 7.2 Hz, 1H, *Z*-CH=C<u>H</u>), 4.51–4.49 (m, 1H), 4.19 (br s, 1H), 2.80–2.74 (m, 1H), 2.73–2.67 (m, 1H) ppm.

^{13}C NMR (125 MHz, $CDCl_3$): δ = 148.5, 148.2, 147.1, 143.2, 132.6, 132.6, 129.6, 129.1 (2C), 128.7 (2C), 128.7, 127.2, 126.3 (2C), 123.4, 117.6, 113.5 (2C), 57.5, 42.4 ppm

IR (neat): ν = 3406, 3287, 3026, 2922, 2851, 1601, 1501, 1317, 964, 748, 692 cm^{-1}.

HRMS (EI): calculated for $C_{21}H_{20}N_2^+$ = [M^+]: *m*/*z* = 300.1621, found: *m*/*z* = 300.1621.

(*E*)-*N*-[4-(Pyridin-3-yl)-1-(pyridin-4-yl)but-3-enyl]-aniline (159ë)

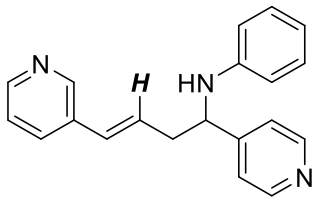

Compound **159ë** was prepared according to *GP–IV* from 3-allyl pyridine (**158**; 35.8 mg, 0.30 mmol, 1.50 equiv) and aldimine **56ë** (36.4 mg, 0.20 mmol), using NaHMDS (3.7 mg, 0.02 mmol, 10 mol%) as the catalyst, in dioxane (300 µL) at 25 °C for 20 h. **159ë** was purified by PTLC on silica gel (NEt_3:Et_2O:PE = 1:2:17; eluted twice).

Yellow liquid.

Yield: 49.4 mg (82%; *E*:*Z* = 99:1).

^{1}H NMR (500 MHz, $CDCl_3$): δ = 8.57 (d, *J* = 5.4 Hz, 2H), 8.55 (s, 1H), 8.47 (d, *J* = 4.8 Hz, 1H), 7.63 (d, *J* = 7.9 Hz, 1H), 7.32 (d, *J* = 5.4 Hz, 2H), 7.23 (dd, *J* = 7.9, 4.8 Hz, 1H), 7.13–7.06 (m, 3H), 6.69 (t, *J* = 7.4 Hz, 1H), 6.50 (d, *J* = 15.9, 1H), 6.46 (d, *J* = 7.8 Hz, 2H), 6.18 (ddd, *J* = 15.9, 7.4, 6.9 Hz, 1H, *E*-CH=C<u>H</u>), 5.81 (ddd, *J* = 11.6, 7.0, 4.8 1H, *Z*-CH=C<u>H</u>), 4.49 (d, *J* = 5.9, 5.0 Hz, 2H), 4.18 (br s, 1H), 2.84–2.75 (m, 1H), 2.74–2.64 (m, 1H) ppm.

^{13}C NMR (125 MHz, $CDCl_3$): δ = 152.4, 150.3 (2C), 148.8, 148.2, 146.5, 132.6, 132.2, 130.5, 129.3 (2C), 127.4, 123.5, 121.6 (2C), 118.2, 113.5 (2C), 56.7, 41.7 ppm

IR (neat): ν = 3285, 3026, 2931, 2852, 1599, 1507, 1238, 965, 731, 699 cm^{-1}.

HRMS (EI): calculated for $C_{20}H_{19}N_3^+$ = [M^+]: *m*/*z* = 301.1573, found: *m*/*z* = 301.1572.

(*E*)-*N*-[4-(Pyridin-3-yl)-1-(thiophen-2-yl)but-3-enyl]-aniline (159þ)

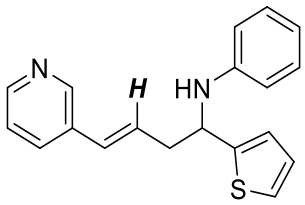

Compound **159þ** was prepared according to *GP–IV* from 3-allyl pyridine (**158**; 47.7 mg, 0.40 mmol, 2.00 equiv) and imine **56þ** (37.5 mg, 0.20 mmol), using NaHMDS (3.7 mg, 0.02 mmol, 10 mol%) as the catalyst, in dioxane (300 µL) at 25 °C for 20 h. **159þ** was purified by PTLC on silica gel (NEt_3/Et_2O/PE = 1:2:17; *eluted twice*).

Yellow liquid.

Yield: 44.7 mg (73%; *E*:*Z* = 32:1).

^{1}H NMR (500 MHz, $CDCl_3$): δ = 8.54 (d, *J* = 1.8 Hz, 1H), 8.45 (dd, *J* = 4.8, 1.8 Hz, 1H), 7.62 (d, *J* = 7.9 Hz, 1H), 7.23–7.17 (m, 2H), 7.13 (dd, *J* = 8.6, 7.4 Hz, 2H), 7.02–6.99 (m, 1H), 6.96 (dd, *J* = 5.0, 3.5 Hz, 1H), 6.71 (dd, *J* = 7.6, 7.1 Hz, 1H), 6.62 (d, *J* = 7.6 Hz, 2H), 6.49 (d, *J* = 15.9 Hz, 1H), 6.26 (ddd, *J* = 15.9, 7.2, 7.2 Hz, 1H, *E*-CH=C<u>H</u>), 5.87 (ddd, *J* = 11.7, 7.1, 7.1 Hz, 1H, *Z*-CH=C<u>H</u>), 4.87–4.79 (m, 1H), 4.13 (br s, 1H), 2.89–2.80 (m, 2H) ppm.

^{13}C NMR (125 MHz, $CDCl_3$): δ = 148.6, 148.2, 148.1, 146.8, 132.6, 132.6, 130.0, 129.2 (2C), 128.1, 126.9, 124.0, 123.7, 123.4, 118.2, 113.7 (2C), 53.7, 42.2 ppm.

IR (neat): ν = 3408, 3273, 3028, 2924, 1600, 1501, 1412, 1313, 1263, 966, 732, 692 cm^{-1}.

HRMS (EI): calculated for $C_{19}H_{18}N_2S^+$ = [M^+]: *m*/*z* = 306.1208, found: *m*/*z* = 306.1185.

(*E*)-*N*-[4-(Pyridin-3-yl)-1-(furan-2-yl)but-3-enyl]-aniline (159ð)

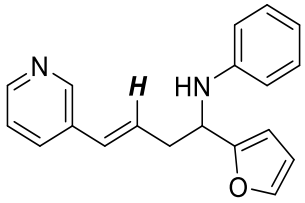

Compound **159ð** was prepared according to *GP–IV* from 3-allyl pyridine (**158**; 35.8 mg, 0.30 mmol, 1.50 equiv) and imine **56ð** (34.2 mg, 0.20 mmol), using NaHMDS (3.7 mg, 0.02 mmol, 10 mol%) as the catalyst, in dioxane (300 µL) at 25 °C for 20 h. **159ð** was purified by PTLC on Al_2O_3 (EtOAc/PE = 1:9; *eluted twice*).

Yellow liquid.

Yield: 46.6 mg (80%; *E*:*Z* = 19:1).

^{1}H NMR (500 MHz, $CDCl_3$): δ = 8.56 (d, *J* = 2.1 Hz, 1H), 8.47 (dd, *J* = 4.8, 1.8 Hz, 1H), 7.65 (ddd, *J* = 7.9, 2.1, 1.7 Hz, 1H), 7.40 (dd, *J* = 1.7, 0.8 Hz, 1H), 7.23 (dd, *J* = 7.9, 4.8 Hz, 1H), 7.16 (d, *J* = 8.6, 7.6 Hz, 2H), 6.74 (dd, *J* = 8.6, 0.8 Hz, 1H), 6.66 (d, *J* = 7.6 Hz, 2H), 6.49 (d, *J* = 15.9 Hz, 1H), 6.33 (dd, *J* = 3.2, 1.8 Hz, 1H), 6.26 (ddd, *J* = 15.9, 7.2, 7.2 Hz, 1H, *E*-CH=C<u>H</u>), 6.22 (d, *J* = 3.2 Hz, 1H), 5.85 (ddd, *J* = 11.7, 7.2, 7.2 Hz, 1H, *Z*-CH=C<u>H</u>), 4.69 (dd, *J* = 6.3, 6.3 Hz, 1H), 4.03 (br s, 1H), 2.89–2.84 (m, 2H) ppm.

^{13}C NMR (125 MHz, $CDCl_3$): δ = 155.3, 148.5, 148.2, 146.8, 141.7, 132.7, 132.6, 129.7, 129.2 (2C), 128.1, 123.4, 118.1, 113.6 (2C), 110.2, 106.4, 51.7, 38.5 ppm.

IR (neat): ν = 3410, 3288, 3028, 2926, 1597, 1498, 1413, 1313, 1265, 968, 732, 692 cm^{-1}.

HRMS (EI): calculated for $C_{19}H_{18}N_3O^+ = [M^+]$: *m*/*z* = 290.1474, found: *m*/*z* = 290.1473.

(*E*/*Z*)-*N*-(1-phenylhexa-3,5-dienyl)-4-methoxyaniline (163b)

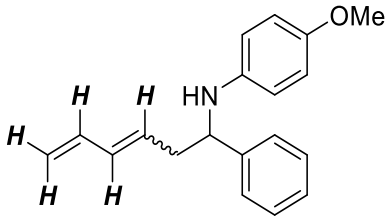

Compound **163b** was prepared according to *GP–IV* from 1,4-pentadiene (**160**; 15.0 mg, 0.22 mmol, 1.10 equiv) and imine **56b** (42.2 mg, 0.20 mmol), using NaHMDS (3.7 mg, 0.02 mmol, 10 mol%) as the catalyst, in dioxane (300 µL) at 25 °C for 20 h. **163b** was purified by PTLC on silica gel (Et_2O/PE = 1:9; *eluted once*).

Yellow liquid.

Yield: 53.1 mg (95%; *E*:*Z* = 3:1).

^{1}H NMR (500 MHz, $CDCl_3$): δ = 7.41–7.27 (m, 4H), 7.24–7.17 (m, 1H), 6.67 (d, *J* = 8.8 Hz, 2H), 6.64–6.55 (m, *Z*-C<u>H</u>=CH_2, 1H), 6.44 (d, *J* = 8.8 Hz, 2H), 6.29 (ddd, *J* = 17.0, 10.3, 10.1 Hz, *E*-C<u>H</u>=CH_2, 1H), 6.17 (dd, *J* = 15.0, 10.3 Hz, 1H), 5.62 (ddd, *J* = 15.0, 7.3, 7.3 Hz, *E*-CH=C<u>H</u>, 1H), 5.49–5.37 (m, *Z*-CH=C<u>H</u>, 1H), 5.25 (d, *J* = 16.9 Hz, *Z*-CH=C<u>H_2</u>, 1H), 5.16 (d, *J* = 9.4 Hz, *Z*-CH=C<u>H_2</u>, 1H), 5.15 (d, *J* = 17.0 Hz, *E*-CH=C<u>H_2</u>, 1H), 5.03 (d, *J* = 10.1 Hz, *E*-CH=C<u>H_2</u>, 1H), 4.31 (dd, *J* = 7.9, 5.2 Hz, 1H), 3.87 (br s, 1H), 3.67 (s, 3H), 2.72–2.56 (m, 1H), 2.55–2.44 (m, 1H) ppm.

^{13}C NMR (125 MHz, $CDCl_3$): δ = 152.0, 143.7 (*E*), 143.6 (*Z*), 141.6 (*Z*), 141.5 (*E*), 136.6 (*E*), 134.2 (*E*), 132.3 (*Z*), 131.7 (*Z*), 130.4 (*E*), 128.6 (2C), 127.8 (*Z*), 127.0, 126.3 (2C), 118.6 (*Z*), 116.3 (*E*), 114.7 (2C), 114.7 (2C), 58.6 (*Z*), 58.3 (*E*), 55.7, 42.1 (*E*), 37.0 (*Z*) ppm.

(*E*/*Z*)-*N*-(1-tienyl-3,5-dienyl)-4-methoxyaniline (163v)

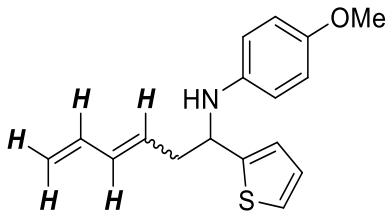

Compound **163v** was prepared according to *GP–IV* from 1,4-pentadiene (**160**; 20.5 mg, 0.30 mmol, 1.50 equiv) and imine **56v** (43.5 mg, 0.20 mmol), using NaHMDS (3.7 mg, 0.02 mmol, 10 mol%) as the catalyst, in dioxane (300 µL) at 25 °C for 20 h. **163v** was purified by PTLC on silica gel (Et_2O/PE = 1:9; *eluted once*).

Yellow liquid.

Yield: 51.4 mg (90%; *E*:*Z* = 4:1).

^{1}H NMR (500 MHz, $CDCl_3$): δ = 7.21 (dd, *J* = 4.8, 1.3 Hz, 1H), 7.05–6.93 (m, 2H), 6.77 (d, *J* = 8.8 Hz, 2H), 6.70–6.63 (m, *Z*-C<u>H</u>=CH_2, 1H), 6.61 (d, *J* = 8.8 Hz, 2H), 6.35 (ddd, *J* = 17.0, 10.4, 10.2 Hz, *E*-C<u>H</u>=CH_2, 1H), 6.23 (dd, *J* = 15.0, 10.4 Hz, 1H), 5.72 (ddd, *J* = 15.0, 7.3, 7.3 Hz, *E*-CH=C<u>H</u>, 1H), 5.58–5.46 (m, *Z*-CH=C<u>H</u> 1H), 5.31 (d, *J* = 16.5 Hz, *Z*-CH=C<u>H</u>$_2$, 1H), 5.22 (d, *J* = 10.9 Hz, *Z*-CH=C<u>H</u>$_2$, 1H), 5.21 (d, *J* = 17.0 Hz, *E*-CH=C<u>H</u>$_2$, 1H), 5.09 (d, *J* = 10.2 Hz, *E*-CH=C<u>H</u>$_2$, 1H), 4.68 (dd, *J* = 6.4, 6.4 Hz, 1H), 3.90 (br s, 1H), 3.76 (s, 3H), 2.88–2.79 (m, *Z*-CH-C<u>H</u>$_2$, 2H), 2.78–2.65 (m, *E*-CH-C<u>H</u>$_2$, 2H) ppm.

^{13}C NMR (125 MHz, $CDCl_3$): δ = 152.5, 148.9 (*E*), 148.8 (*Z*), 141.1, 136.7 (*E*), 134.6 (*E*), 132.5 (*Z*), 131.8 (*Z*), 129.7 (*E*), 127.2 (*Z*), 126.8, 123.9 (*Z*), 123.8 (*E*), 123.6 (*Z*), 123.5 (*E*), 118.7 (*Z*), 116.5 (*E*), 115.2 (2C), 114.8 (2C), 55.7, 55.0 (*Z*), 54.7 (*E*), 42.0 (*E*), 36.9 (*Z*) ppm.

4.2.9 Styrenes and 1,3-Dienes

(*E*)-1-phenyl-1-propene (58)[77a]

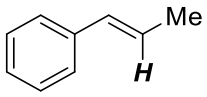

58 was prepared according to *GP–VIII* from allylbenzene (**36**; 26.5 µL, 0.20 mmol, 1.00 equiv) using KHMDS (2.0 mg, 0.01 mmol, 5 mol%) and [18]crown-6 (2.6 mg, 0.01 mmol, 5 mol%) as the catalyst, in THF (200 µL) at 25 °C for 2 h. **58** was purified by PTLC on silica gel (petrol ether) and spectral data fitted the literature reported data accurately.

Colourless liquid, 92% NMR yield, *E:Z* = >99:1.

^{1}H NMR (500 MHz, $CDCl_3$): δ = 7.41–7.29 (m, 4H), 7.22 (dd, *J* = 7.2, 7.2 Hz, 1H), 6.44 (dq, *J* = 15.7, 1.5 Hz, 1H), 6.28 (dq, *J* = 15.7, 6.6 Hz, 1H, *E*-CH=C<u>H</u>), 5.83 (dq, *J* = 11.7, 7.2 Hz, 1H, *Z*-CH=C<u>H</u>), 1.92 (dd, *J* = 6.6, 1.5 Hz, 3H) ppm.

^{13}C NMR (125 MHz, $CDCl_3$): δ = 138.0, 131.1, 128.5 (2C), 126.7, 125.8 (2C), 125.7, 18.5 ppm.

(*E/Z*)-1-(4-methylphenyl)-1-propene (191)[77a]

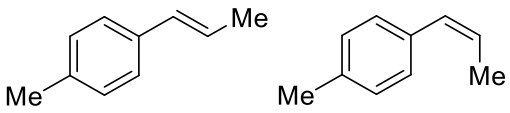

191 was prepared according to *GP–VIII* from 4-allyltoluene (**148**; 30.6 µL, 0.20 mmol, 1.00 equiv) using KHMDS (2.0 mg, 0.01 mmol, 5 mol%) and [18]crown-6 (2.6 mg, 0.01 mmol, 5 mol%) as the catalyst, in THF (200 µL) at 25 °C for 2 h. **191** was purified by PTLC on silica gel (petrol ether) and spectral data fitted the literature reported data accurately.

Colourless liquid, 87% NMR yield, *E:Z* = >49:1.

***E*-isomer**

^{1}H NMR (500 MHz, $CDCl_3$): δ = 7.22 (d, *J* = 7.9 Hz, 2H), 7.09 (d, *J* = 7.9 Hz, 2H), 6.36 (dq, *J* = 15.8, 1.4 Hz, 1H), 6.17 (dq, *J* = 15.5, 6.6 Hz, 1H), 2.32 (s, 3H), 1.86 (dd, *J* = 6.6, 1.4 Hz, 3H) ppm.

^{13}C NMR (125 MHz, $CDCl_3$): δ = 136.4, 135.2, 130.9, 129.2 (2C), 125.7 (2C), 124.6, 21.1, 18.4 ppm.

***Z*-isomer**

^{1}H NMR (500 MHz, $CDCl_3$): δ = 7.20 (d, *J* = 7.8 Hz, 2H), 7.14 (d, *J* = 7.8 Hz, 2H), 6.39 (dq, *J* = 12.1, 1.3 Hz, 1H), 5.74 (dq, *J* = 12.1, 7.2 Hz, 2H), 2.34 (s, 3H), 1.89 (dd, *J* = 7.2, 1.3 Hz, 3H) ppm.

(*E*/*Z*)-1-(2-methylphenyl)-1-propene (192)[77a]

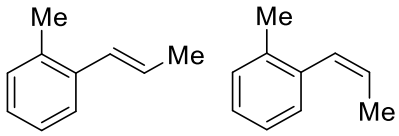

192 was prepared according to *GP–VIII* from 2-allyltoluene (**147**; 29.5 µL, 0.20 mmol, 1.00 equiv) using KHMDS (2.0 mg, 0.01 mmol, 5 mol%) and [18]crown-6 (2.6 mg, 0.01 mmol, 5 mol%) as the catalyst, in THF (200 µL) at 25 °C for 2 h. **192** was purified by PTLC on silica gel (petrol ether) and spectral data fitted the literature reported data accurately.

Colourless liquid, 91% NMR yield, *E:Z* = >19:1.

***E*-isomer**

^{1}H NMR (500 MHz, $CDCl_3$): δ = 7.38 (d, *J* = 7.4 Hz, 1H), 7.18–7.07 (m, 3H), 6.59 (dq, *J* = 15.6, 1.7 Hz, 1H), 6.10 (dq, *J* = 15.6, 6.6 Hz, 1H), 2.32 (s, 3H), 1.90 (dd, *J* = 6.6, 1.7 Hz, 3H) ppm.

^{13}C NMR (125 MHz, $CDCl_3$): δ = 137.1, 134.8, 130.1, 128.9, 127.0, 126.7, 126.0, 125.4, 19.8, 18.8 ppm.

***Z*-isomer**

^{1}H NMR (500 MHz, $CDCl_3$): δ = 7.18–7.07 (m, 4H), 6.45 (dq, *J* = 12.5, 1.8 Hz, 1H), 5.82 (dq, *J* = 12.5, 7.0 Hz, 1H), 2.25 (s, 3H), 1.73 (dd, *J* = 7.0, 1.8, 3H) ppm.

(*E*/*Z*)-1-(4-methoxyphenyl)-1-propene (193)[77a]

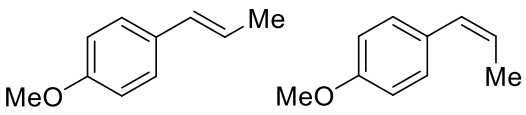

193 was prepared according to *GP–VIII* from 4-allylanisole (**149**; 30.7 µL, 0.20 mmol, 1.00 equiv) using KHMDS (2.0 mg, 0.01 mmol, 5 mol%) and [18]crown-6 (2.6 mg, 0.01 mmol, 5 mol%) as the catalyst, in THF (200 µL) at 25 °C for 2 h. **193** was purified by PTLC on silica gel (petrol ether) and spectral data fitted the literature reported data accurately.

Colourless liquid, 95% NMR yield, *E:Z* = >49:1.

***E*-isomer**

^{1}H NMR (500 MHz, $CDCl_3$): δ = 7.25 (d, *J* = 8.7 Hz, 2H), 6.82 (d, *J* = 8.7 Hz, 2H), 6.34 (dq, *J* = 15.7, 1.7 Hz, 1H), 6.08 (dq, *J* = 15.7, 6.6 Hz, 1H), 3.78 (s, 3H), 1.85 (dd, *J* = 6.6, 1.7 Hz, 3H) ppm.

^{13}C NMR (125 MHz, $CDCl_3$): δ = 158.6, 130.8, 130.4, 126.9 (2C), 123.5, 113.9 (2C), 55.3, 18.4 ppm.

***Z*-isomer**

^{1}H NMR (500 MHz, $CDCl_3$): δ = 7.26 (d, *J* = 8.6 Hz, 2H), 6.87 (d, *J* = 8.6 Hz, 2H), 6.38 (dq, *J* = 11.3, 1.9 Hz, 1H), 5.69 (dq, *J* = 11.3, 7.2 Hz, 1H), 3.80 (s, 3H), 1.88 (dd, *J* = 7.2, 1.9 Hz, 3H) ppm.

(*E*/*Z*)-1-(4-fluorophenyl)-1-propene (194)[77a]

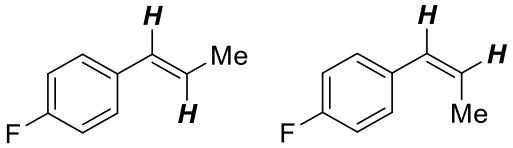

194 was prepared according to *GP–VIII* from 4-fluoro-allylbenzene (**146**; 27.0 µL, 0.20 mmol, 1.00 equiv) using KHMDS (2.0 mg, 0.01 mmol, 5 mol%) and [18]crown-6 (2.6 mg, 0.01 mmol, 5 mol%) as the catalyst, in THF (200 µL) at 25 °C for 2 h. *Due to polymerisation, the isolation of this compound was unsuccessful. Analysis of ^{1}H NMR spectroscopic data of a reaction aliquot using the listed signals allowed for identification and quantification of the title compound.* Spectral data fitted the literature reported data.

68% NMR yield, *E:Z* = >99:1.

***E*-isomer**

^{1}H NMR (500 MHz, $CDCl_3$): δ = 6.36 (dq, *J* = 15.7, 1.7 Hz, 1H), 6.14 (dq, *J* = 15.7, 6.6 Hz, 1H) ppm.

***Z*-isomer**

^{1}H NMR (500 MHz, $CDCl_3$): δ = 5.54 (qd, *J* = 6.7, 0.8 Hz, 1H) ppm.

(*E/Z*)-1-(4-trifluoromethylphenyl)-1-propene (195)[78a]

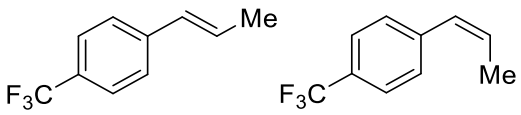

195 was prepared according to *GP–VIII* from 4-(trifluoromethyl)-allylbenzene (**151**; 33.5 µL, 0.20 mmol, 1.00 equiv) using KHMDS (2.0 mg, 0.01 mmol, 5 mol%) and [18]crown-6 (2.6 mg, 0.01 mmol, 5 mol%) as the catalyst, in THF (200 µL) at 25 °C for 24 h. **195** was purified by PTLC on silica gel (petrol ether) and spectral data fitted the literature reported data accurately.

Colourless liquid, 60% NMR yield, *E:Z* = >99:1.

***E*-isomer**

^{1}H NMR (500 MHz, $CDCl_3$): δ = 7.53 (d, *J* = 8.2 Hz, 2H), 7.40 (d, *J* = 8.2 Hz, 2H), 6.43 (d, *J* = 15.8 Hz, 1H), 6.34 (dq, *J* = 15.8 Hz, 6.3 Hz, 1H), 1.91 (d, *J* = 6.3 Hz, 3H) ppm.

^{13}C NMR (125 MHz, $CDCl_3$): δ = 141.4, 129.9, 128.7, 128.6 (q, *J* = 32.1 Hz), 125.9 (2C), 125.4 (q, *J* = 3.8 Hz, 2C), 124.3 (q, *J* = 271.7 Hz), 18.6 ppm.

^{19}F NMR (471 MHz, $CDCl_3$): **δ** = -62.4 (s) ppm.

***Z*-isomer**

^{1}H NMR (500 MHz, $CDCl_3$): δ = 7.58 (d, *J* = 8.1 Hz, 2H), 7.38 (d, *J* = 8.1 Hz, 2H), 6.45 (dq, *J* = 11.6, 1.7 Hz, 1H), 5.90 (dq, *J* = 11.6, 7.2 Hz, 1H), 1.90 (dd, *J* = 7.2, 1.7 Hz, 3H) ppm.

(*E/Z*)-1-(pentafluorophenyl)-1-propene (196)[73b]

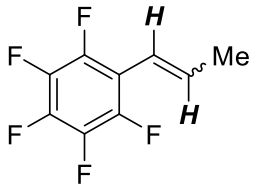

196 was prepared according to *GP–VIII* from pentafluoro-allylbenzene (**150**; 27.0 µL, 0.20 mmol, 1.00 equiv) using KHMDS (2.0 mg, 0.01 mmol, 5 mol%) and [18]crown-6 (2.6 mg, 0.01 mmol, 5 mol%) as the catalyst, in THF (200 µL) at 25 °C for 24 h. *Due to polymerisation, the isolation of this compound was unsuccessful. Analysis of ^{1}H NMR spectroscopic data of a reaction aliquot using the listed signals allowed for identification and quantification of the title compound.* Spectral data fitted the literature reported data.

6% NMR yield, *E:Z = nd*

^{1}H NMR (500 MHz, $CDCl_3$): δ = 6.57 (dq, *J* = 16.9, 6.8 Hz, 1H), 6.29 (dq, *J* = 16.1, 1.8 Hz, 1H) ppm.

(*E/Z*)-1-(3-pyridyl)-1-propene (197)[77a]

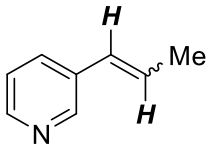

197 was prepared according to *GP–VIII* from 3-allylpyridine (**158**; 23.8 mg, 0.20 mmol, 1.00 equiv) using KHMDS (2.0 mg, 0.01 mmol, 5 mol%) and [18]crown-6 (2.6 mg, 0.01 mmol, 5 mol%) as the catalyst, in THF (200 µL) at 25 °C for 2 h. *Due to polymerisation, the isolation of this compound was unsuccessful. Analysis of ^{1}H NMR spectroscopic data of a reaction aliquot using the listed signals allowed for identification and quantification of the title compound.* Spectral data fitted the literature reported data.

50% NMR yield, *E:Z = nd*

^{1}H NMR (500 MHz, $CDCl_3$): δ = 6.38 (dq, *J* = 16.0, 1.2, 1H), 6.31 (dq, *J* = 16.0, 6.2, 1H) ppm.

(*E/Z*)-1-phenyl-1-butene (203)[78b]

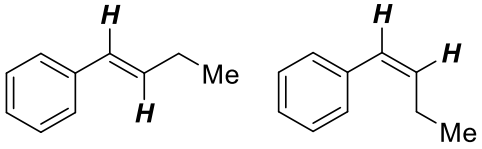

203 was prepared according to *GP–VIII* from alkene **200** (26.4 mg, 0.20 mmol, 1.00 equiv) using KHMDS (2.0 mg, 0.01 mmol, 5 mol%) and [18]crown-6 (2.6 mg, 0.01 mmol, 5 mol%) as the catalyst, in THF (200 µL) at 25 °C for 48 h. *Due to polymerisation, the isolation of this compound was unsuccessful. Analysis of ^{1}H NMR spectroscopic data of a reaction aliquot using the listed signals allowed for identification and quantification of the title compound.* Spectral data fitted the literature reported data.

87% NMR yield, *E:Z* = >12:1.

***E*-isomer: ^{1}H NMR** (500 MHz, $CDCl_3$): δ = 6.38 (dt, *J* = 15.9, 1.5 Hz, 1H), 6.27 (dt, *J* = 15.9, 6.4 Hz, 1H) ppm.

***Z*-isomer: ^{1}H NMR** (500 MHz, $CDCl_3$): δ = 5.86 (dt, *J* = 6.6, 1.3 Hz, 1H) ppm.

(*E*)-3-methyl-1-phenyl-1-butene (204)[78c]

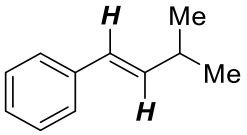

204 was prepared according to *GP–VIII* from alkene **201** (29.2 mg, 0.20 mmol, 1.00 equiv) using KHMDS (2.0 mg, 0.01 mmol, 5 mol%) and [18]crown-6 (2.6 mg, 0.01 mmol, 5 mol%) as the catalyst, in THF (200 µL) at 25 °C for 24 h. *Due to polymerisation, the isolation of this compound was unsuccessful. Analysis of ^{1}H NMR spectroscopic data of a reaction aliquot using the listed signals allowed for identification and quantification of the title compound.* Spectral data fitted the literature reported data.

67% NMR yield, *E:Z* = >99:1.

^{1}H NMR (500 MHz, $CDCl_3$): δ = 6.36 (d, *J* = 15.8 Hz, 1H), 6.22 (dd, *J* = 16.0, 6.9 Hz, 1H), 2.49 (dhept, *J* = 6.9, 6.7, 1H), 1.11 (d, *J* = 6.7 Hz, 6H) ppm.

(*E/Z*)-1,3-diphenyl-1-butene (205)[78d]

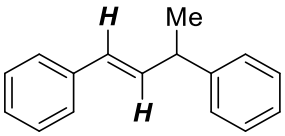

205 was prepared according to *GP–VIII* from alkene **202** (41.7 mg, 0.20 mmol, 1.00 equiv) using KHMDS (2.0 mg, 0.01 mmol, 5 mol%) and [18]crown-6 (2.6 mg, 0.01 mmol, 5 mol%) as the catalyst, in THF (200 µL) at 25 °C for 7 h. *Due to polymerisation, the isolation of this compound was unsuccessful. Analysis of ^{1}H NMR spectroscopic data of a reaction aliquot using the listed signals allowed for identification and quantification of the title compound.* Spectral data fitted the literature reported data.

33% NMR yield, *E:Z* = >99:1.

^{1}H NMR (500 MHz, $CDCl_3$): δ = 6.41–6.39 (m, 2H), 3.64 (dq, *J* = 7.0, 5.4 Hz, 1H), 1.47 (d, *J* = 7.0 Hz, 3H) ppm.

(*E*/*Z*)-1,3-pentadiene (207)[114]

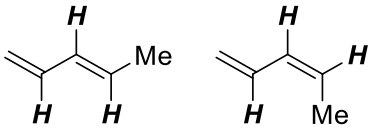

207 was prepared according to *GP–VIII* from 1,4-pentadiene **160** (13.6 mg, 0.20 mmol, 1.00 equiv) using KHMDS (2.0 mg, 0.01 mmol, 5 mol%) and [18]crown-6 (2.6 mg, 0.01 mmol, 5 mol%) as the catalyst, in THF (200 µL) at 25 °C for 2 h. Compound **207** is commercially available (CAS: 2004-70-8, 1574-41-0) and was not isolated due to volatility. *Analysis of ^{1}H NMR spectroscopic data of a reaction aliquot using the listed signals allowed for identification and quantification of the title compound.* Spectral data fitted the literature reported data.

99% NMR yield, *E:Z* = >2:1.

***E*-isomer**: **^{1}H NMR** (500 MHz, $CDCl_3$): δ = 6.33 (ddd, *J* = 17.0, 10.5, 10.1 Hz, 1H), 6.13–6.01 (m, 1H), 5.82–5.68 (m, 1H), 5.09 (d, *J* = 17.0 Hz, 1H), 4.96 (d, *J* = 10.1, 1H), 1.78 (d, *J* = 5.2, 3H) ppm.

***Z*-isomer**: **^{1}H NMR** (500 MHz, $CDCl_3$): δ = 6.69 (ddd, *J* = 16.9, 11.2, 10.1, 1H), 6.13–6.01 (m, 1H), 5.59–5.51 (m, 1H), 5.20 (d, *J* = 16.9 Hz, 1H), 5.11 (d, *J* = 10.1 Hz, 1H), 1.79 (d, *J* = 8.9 Hz, 3H) ppm.

(*E*/*Z*)-3-methyl-1,3-pentadiene (208)[114]

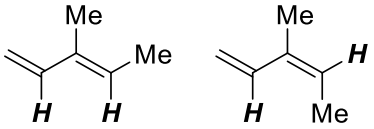

208 was prepared according to *GP–VIII* from 3-methyl-1,4-pentadiene **161** (16.4 mg, 0.20 mmol, 1.00 equiv) using KHMDS (2.0 mg, 0.01 mmol, 5 mol%) and [18]crown-6 (2.6 mg, 0.01 mmol, 5 mol%) as the catalyst, in THF (200 µL) at 25 °C for 1 h. Compound **208** is commercially available (CAS: 2787-43-1, 2787-45-3) and was not isolated due to volatility. *Analysis of ^{1}H NMR spectroscopic data of a reaction aliquot using the listed signals allowed for identification and quantification of the title compound.* Spectral data fitted the literature reported data.

99% NMR yield, *E:Z* = >8:1.

***E*-isomer**: **^{1}H NMR** (500 MHz, $CDCl_3$): δ = 6.39 (dd, *J* = 17.4, 10.6 Hz, 1H), 5.59 (q, *J* = 7.5 Hz, 1H), 5.09 (d, *J* = 17.4 Hz, 1H), 4.93 (d, *J* = 10.6 Hz, 1H), 1.76 (s, 3H) ppm.

***Z*-isomer**: **^{1}H NMR** (500 MHz, $CDCl_3$): δ = 5.89–5.79 (m, 1H), 5.52–5.45 (m, 1H), 5.12–5.10 (m, 1H), 5.06–4.97 (m, 1H), 1.75 (s, 3H) ppm.

1,3-Cyclohexadiene (209)[114]

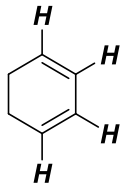

209 was prepared according to *GP–VIII* from 1,4-cyclohexadiene **206** (16.0 mg, 0.20 mmol, 1.00 equiv) using KHMDS (2.0 mg, 0.01 mmol, 5 mol%) and [18]crown-6 (2.6 mg, 0.01 mmol, 5 mol%) as the catalyst, in THF (200 µL) at 25 °C for 1 h. Compound **209** is commercially available (CAS: 592-57-4) and was not isolated due to volatility. *Analysis of ^{1}H NMR spectroscopic data of a reaction aliquot using the listed signals allowed for identification and quantification of the title compound.* Spectral data fitted the literature reported data.

55% NMR yield.

^{1}H NMR (500 MHz, $CDCl_3$): δ = 5.96–5.85 (m, 2H), 5.82–5.76 (m, 2H), 2.74–2.63 (m, 4H) ppm.

4.2.10 Functional Isomerisation

(*E*/*Z*)-1-trimethylsilyl-1-propene (216a)[84]

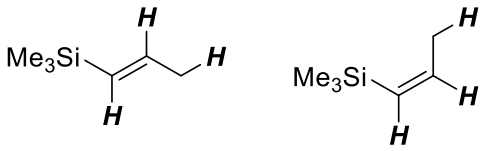

216a was prepared according to *GP–VIX* from trimethyl allylsilane **136a** (22.8 mg, 0.20 mmol, 1.00 equiv) using KHMDS (2.0 mg, 0.01 mmol, 5 mol%) as the catalyst, in THF (200 µL) at 30 °C for 20 h. **216a** *was not isolated*. *Analysis of ^{1}H NMR spectroscopic data of a reaction aliquot using the listed signals allowed for identification and quantification of the title compound.* Spectral data fitted the literature reported data.

66% NMR yield, *E:Z* = >24:1.

***E*-isomer**: **^{1}H NMR** (500 MHz, $CDCl_3$): δ = 6.05 (dq, *J* = 18.4, 6.2 Hz, 1H), 5.66 (dq, *J* = 18.4, 1.7 Hz, 1H) 1.81 (dd, *J* = 6.2, 1.7 Hz, 3H) ppm.

***Z*-isomer**: **^{1}H NMR** (500 MHz, $CDCl_3$): δ = 6.39 (dq, *J* = 14.0, 6.9 Hz, 1H), 5.50 (dq, *J* = 14.0, 1.5 Hz, 1H), 1.84 (d, *J* = 6.9, 1.5 Hz, 3H) ppm.

(*E*/*Z*)-1-trimethoxysilyl-1-propene (216b)[85]

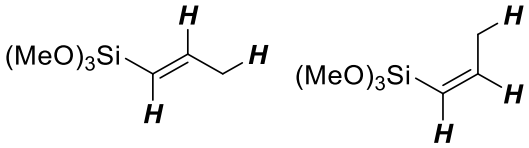

216b was prepared according to *GP–VIX* from trimethyl siloxane **136b** (32.4 mg, 0.20 mmol, 1.00 equiv) using KHMDS (2.0 mg, 0.01 mmol, 5 mol%) and [18]crown-6 (2.6 mg, 0.01 mmol, 5 mol%) as the catalyst, in THF (200 µL) at 25 °C for 2 h. **216b** *was not isolated*. *Analysis of ^{1}H NMR spectroscopic data of a reaction aliquot using the listed signals allowed for identification and quantification of the title compound.* Spectral data fitted the literature reported data.

64% NMR yield, *E:Z* = >9:1.

***E*-isomer: ^{1}H NMR** (500 MHz, $CDCl_3$): δ = 6.46 (dq, *J* = 18.8, 6.3 Hz, 1H), 5.42 (dq, *J* = 18.7, 1.7 Hz, 1H), 1.87 (dd, *J* = 6.3, 1.7, 3H) ppm.

***Z*-isomer: ^{1}H NMR** (500 MHz, $CDCl_3$): δ = 6.66 (dd, *J* = 14.2, 6.9 Hz, 1H), 5.31 (dd, *J* = 14.2, 1.5 Hz, 1H), 1.91 (dd, *J* = 6.9, 1.5 Hz, 3H) ppm.

(*E*/*Z*)-1-pinacolatoborane-1-propene (217)[82a, 230]

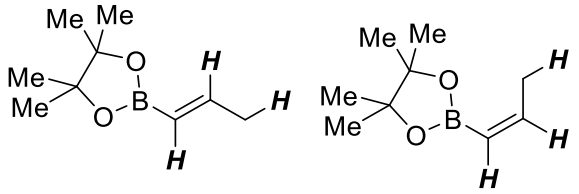

217 was prepared according to *GP–VIX* from allyl boronic acid pinacol ester **15a** (33.6 mg, 0.20 mmol, 1.00 equiv) using KHMDS (2.0 mg, 0.01 mmol, 5 mol%) as the catalyst in THF (200 µL) at 30 °C for 20 h. **217** *was not isolated*. *Analysis of ^{1}H NMR spectroscopic data of a reaction aliquot using the listed signals allowed for identification and quantification of the title compound.* Spectral data fitted the literature reported data.

75% NMR yield, *E:Z = nd.*

^{1}H NMR (500 MHz, $CDCl_3$): δ = 6.65 (dq, *J* = 17.8, 6.5 Hz, 1H), 5.46 (dq, *J* = 17.8, 1.7 Hz, 1H), 1.72 (dd, *J* = 6.5, 1.7 Hz, 3H) ppm.

(*E*/*Z*)-1-methylthio-1-propene (225a)[231]

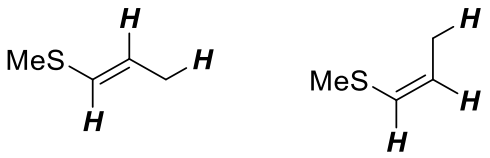

225a was prepared according to *GP–VIX* from allyl methyl thioether **219a** (17.6 mg, 0.20 mmol, 1.00 equiv) using KHMDS (2.0 mg, 0.01 mmol, 5 mol%) and [18]crown-6 (2.6 mg, 0.01 mmol, 5 mol%) as the catalyst, in THF (200 µL) at 25 °C for 2 h. ***225a** was not isolated. Analysis of ^{1}H NMR spectroscopic data of a reaction aliquot using the listed signals allowed for identification and quantification of the title compound.* Spectral data fitted the literature reported data.

99% NMR yield, *E:Z* = 1:1.

***E*-isomer: ^{1}H NMR** (500 MHz, $CDCl_3$): δ = 5.97 (dq, *J* = 14.9, 1.6 Hz, 1H), 5.48 (dq, *J* = 14.9, 6.6 Hz, 1H), 1.76 (dd, *J* = 6.6, 1.6 Hz, 3H) ppm.

***Z*-isomer: ^{1}H NMR** (500 MHz, $CDCl_3$): δ = 5.89 (dq, *J* = 9.3, 1.5 Hz, 1H), 5.59 (dq, *J* = 9.3, 6.8 Hz, 1H), 1.71 (dd, *J* = 6.8, 1.5 Hz, 3H) ppm.

(*E*/*Z*)-1-phenylthio-1-propene (225b)[54]

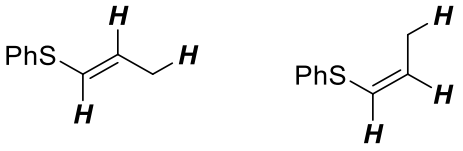

225b was prepared according to *GP–VIX* from allyl phenyl thioether **219b** (30.0 mg, 0.20 mmol, 1.00 equiv) using KHMDS (3.2 mg, 0.016 mmol, 8 mol%) and SIPr (7.8 mg, 0.02 mmol, 10 mol%) as the catalyst system in *m*-xylene (200 µL) at 25 °C for 1 h. **225b** *was not isolated*. *Analysis of ^{1}H NMR spectroscopic data of a reaction aliquot using the listed signals allowed for identification and quantification of the title compound.* Spectral data fitted the literature reported data.

99% NMR yield, *E:Z* = 1:6.

Minor *E*-isomer: ^{1}H NMR (500 MHz, $CDCl_3$): δ = 6.14 (dq, *J* = 14.8, 1.5 Hz, 1H) 5.99 (dq, *J* = 14.8, 6.7 Hz, 1H) , 1.84 (dd, *J* = 6.7, 1.5, 3H) ppm.

Major *Z*-isomer: ^{1}H NMR (500 MHz, $CDCl_3$): δ = 6.21 (dq, *J* = 9.2, 1.6 Hz, 1H) 5.88 (dq, *J* = 9.2, 6.8 Hz, 1H), 1.83 (dd, *J* = 6.8, 1.6 Hz, 3H) ppm.

(*E*/*Z*)-1-diphenylphosphino-1-propene (226a)[93b, 93c]

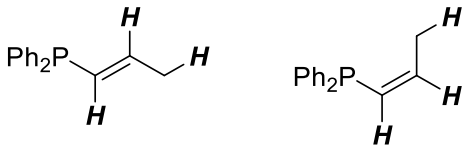

226a was prepared according to *GP–VIX* from diphenyl allylphosphine **220** (45.2 mg, 0.20 mmol, 1.00 equiv) using KHMDS (4.0 mg, 0.02 mmol, 10 mol%) as the catalyst in THF (200 µL) at 25 °C for 4 h. **226a** *was not isolated*. *Analysis of ^{1}H NMR spectroscopic data of a reaction aliquot using the listed signals allowed for identification and quantification of the title compound.* Spectral data fitted the literature reported data.

83% NMR yield, *E:Z* = >19:1.

***E*-isomer: ^{1}H NMR** (500 MHz, $CDCl_3$): δ = 6.34–6.18 (m, 2H), 1.91 (d, *J* = 5.3 Hz, 3H) ppm.

***Z*-isomer: ^{1}H NMR** (500 MHz, $CDCl_3$): δ = 6.57–6.46 (m, 2H), 1.98 (d, *J* = 6.9 Hz, 3H) ppm.

(*E*/*Z*)-1-dimethylamino-1-propene (228a)[94]

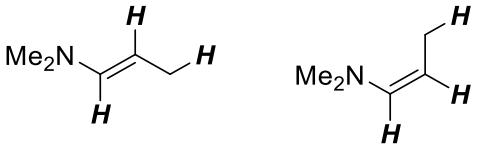

228a was prepared according to *GP–VIX* from dimethyl allylamine **222a** (17.0 mg, 0.20 mmol, 1.00 equiv) using LTMP (2.9 mg, 0.02 mmol, 10 mol%) as the catalyst in THF (200 µL) at 60 °C for 20 h. **228a** *was not isolated*. *Analysis of ^{1}H NMR spectroscopic data of a reaction aliquot using the listed signals allowed for identification and quantification of the title compound.* Spectral data fitted the literature reported data.

68% NMR yield, *E:Z* = 1:1.

Minor *E*-isomer: ^{1}H NMR (500 MHz, $CDCl_3$): δ = 5.89 (d, *J* = 13.7 Hz, 1H), 4.20 (dq, *J* = 13.7, 7.1 Hz, 1H), 1.70 (d, *J* = 7.1, 3H) ppm.

Major *Z*-isomer: ^{1}H NMR (500 MHz, $CDCl_3$): δ = 5.55 (d, *J* = 9.0 Hz, 1H), 4.32 (dq, *J* = 9.0, 6.4 Hz, 1H) 1.63 (d, *J* = 6.4 Hz, 3H) ppm.

(*E*/*Z*)-1-diphenylamino-1-propene (228b)[111]

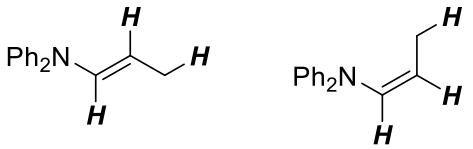

228b was prepared according to *GP–VIX* from diphenyl allylamine **222b** (41.8 mg, 0.20 mmol, 1.00 equiv) using KHMDS (2.9 mg, 0.02 mmol, 10 mol%) as the catalyst and [18]crown-6 (5.2 mg, 0.02 mmol, 10 mol%) as the ligand in THF (200 µL) at 25 °C for 2 h. **228b** *was not isolated. Analysis of ^{1}H NMR spectroscopic data of a reaction aliquot using the listed signals allowed for identification and quantification of the title compound.* Spectral data fitted the literature reported data.

99% NMR yield, *E:Z* = 1:>10.

Minor *E*-isomer: ^{1}H NMR (500 MHz, $CDCl_3$): δ = 6.58 (dq, *J* = 13.7, 1.4 Hz, 1H), 4.68 (dq, *J* = 13.5, 6.7 Hz, 1H), 1.69 (dd, *J* = 6.7, 1.4 Hz, 3H) ppm.

Major *Z*-isomer: ^{1}H NMR (500 MHz, $CDCl_3$): δ = 6.12 (dq, *J* = 8.2, 1.6 Hz, 1H), 5.00 (dq, *J* = 8.2, 7.1 Hz, 1H), 1.25 (dd, *J* = 7.1, 1.6 Hz, 3H) ppm.

(*Z*)-1-methoxy-1-propene (227a)[97]

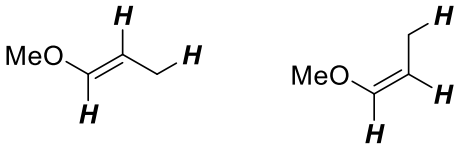

227a was prepared according to *GP–VIX* from allyl methyl ether **221a** (14.4 mg, 0.20 mmol, 1.00 equiv) using LTMP (2.9 mg, 0.02 mmol, 10 mol%) as the catalyst in THF (200 µL) at 25 °C for 2 h. **227a** *was not isolated*. *Analysis of ^{1}H NMR spectroscopic data of a reaction aliquot using the listed signals allowed for identification and quantification of the title compound.* Spectral data fitted the literature reported data.

99% NMR conversion, *E:Z* = 1:>99.

^{1}H NMR (500 MHz, $CDCl_3$): δ = 5.88 (dq, *J* = 6.2, 1.7 Hz, 1H), 4.38 (dq, *J* = 6.9, 6.2 Hz, 1H), 1.57 (dd, *J* = 6.9, 1.7 Hz, 3H) ppm.

(*E*/*Z*)-1-phenoxy-1-propene (227b)[96]

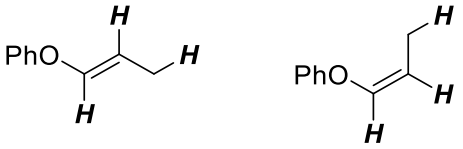

227b was prepared according to *GP–VIX* from allyl phenyl ether **221b** (26.8 mg, 0.20 mmol, 1.00 equiv) using KHMDS (2.0 mg, 0.01 mmol, 5 mol%) as the catalyst and [18]crown-6 (2.6 mg, 0.01 mmol, 5 mol%) as the ligand in THF (200 µL) at 25 °C for 4 h. **227b** *was not isolated*. *Analysis of ^{1}H NMR spectroscopic data of a reaction aliquot using the listed signals allowed for identification and quantification of the title compound.* Spectral data fitted the literature reported data.

99% NMR yield, *E:Z* = 1:>24.

Minor *E*-isomer: ^{1}H NMR (500 MHz, $CDCl_3$): δ = 6.42 (dq, *J* = 12.1, 1.7 Hz, 1H), 5.37 (dq, *J* = 12.1, 6.9 Hz, 1H), 1.67 (dd, *J* = 6.9, 1.7 Hz, 3H) ppm.

Major *Z*-isomer: ^{1}H NMR (500 MHz, $CDCl_3$): δ = 6.40 (dq, *J* = 6.1, 1.7 Hz, 1H), 4.90 (dq, *J* = 6.9, 6.1 Hz, 1H), 1.74 (dd, *J* = 6.9, 1.7 Hz, 3H) ppm.

4.2.11 Functionalised Allylation

(*E*)-*N*-(1-phenyl-4-trimethylsilyl-3-butenyl)-4-methoxyaniline (236a)

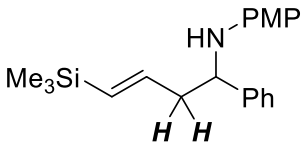

236a was prepared according to *GP–X* from trimethyl allylsilane **136a** (25.1 mg, 0.22 mmol, 1.10 equiv) and imine **56b** (42.2 mg, 0.20 mmol) using KHMDS (4.0 mg, 0.02 mmol, 10 mol%) as the catalyst in dioxane (300 µL) at 25 °C for 20 h. *Due to its instability to PTLC conditions,* **236a** *was not isolated. Analysis of ^{1}H NMR spectroscopic data of a reaction aliquot using the listed signals allowed for identification and quantification of the title compound.*

37% NMR yield.

^{1}H NMR (500 MHz, $CDCl_3$): δ = 2.6–2.5 (m, 2H) ppm.

(*E*)-*N*-(1-phenyl-4-trimethoxysilyl-3-butenyl)-4-methoxyaniline (236b)

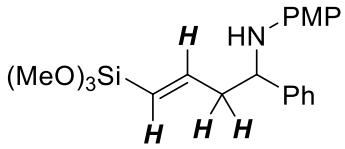

236b was prepared according to *GP–X* from trimethyl allylsilane **136b** (48.6 mg, 0.30 mmol, 1.50 equiv) and imine **56b** (42.2 mg, 0.20 mmol) using NaHMDS (3.7 mg, 0.02 mmol, 10 mol%) as the catalyst in dioxane (300 µL) at 25 °C for 20 h. *Due to its instability to PTLC conditions,* **236b** *was not isolated. Analysis of ^{1}H NMR spectroscopic data of a reaction aliquot using the listed signals allowed for identification and quantification of the title compound.*

96% NMR yield.

^{1}H NMR (500 MHz, $CDCl_3$): δ = 6.39 (ddd, *J* = 18.8, 7.2, 6.1 Hz, 1H), 5.55 (d, *J* = 18.9 Hz, 1H), 4.39 (ddd, *J* = 8.1, 5.1, 5.1 Hz, 1H), 2.77–2.68 (m, 1H), 2.67–2.59 (m, 1H) ppm.

(*E*)-*N*-(1-phenyl-4-pinacolatoborane-3-butenyl)-4-methoxyaniline (238a)

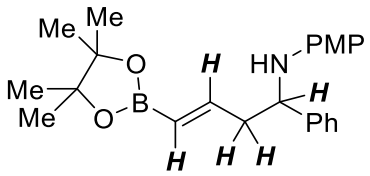

238a was prepared according to *GP–X* from allylboronic acid pinacol ester **15a** (37.0 mg, 0.22 mmol, 1.10 equiv) and imine **56b** (42.2 mg, 0.20 mmol) using NaHMDS (3.7 mg, 0.02 mmol, 10 mol%) as the catalyst in DMF (300 µL) at 25 °C for 20 h. *Due to its instability to PTLC conditions,* **238a** *was not isolated. Analysis of* ^{1}*H NMR spectroscopic data of a reaction aliquot using the listed signals allowed for identification and quantification of the title compound.*

72% NMR yield.

^{1}H NMR (500 MHz, $CDCl_3$): δ = 6.63 (d, *J* = 17.8 Hz, 1H), 5.62 (dd, *J* = 17.8, 1.4 Hz, 1H), 4.74 (dt, *J* = 7.9, 3.7 Hz, 1H), 2.80–2.74 (m, 2H) ppm.

(*E/Z*)-*N*-(1-phenyl-4-phenylthio-3-butenyl)-4-methoxyaniline (247b)

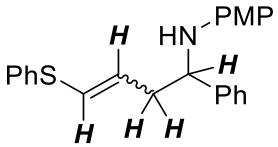

247b was prepared according to *GP–X* from allyl phenyl thioether **219b** (33.0 mg, 0.22 mmol, 1.10 equiv) and imine **56b** (42.2 mg, 0.20 mmol) using NaHMDS (3.7 mg, 0.02 mmol, 10 mol%) as the catalyst in dioxane (300 µL) at 25 °C for 20 h. *Due to its instability to PTLC conditions,* **247b** *was not isolated. Analysis of* ^{1}*H NMR spectroscopic data of a reaction aliquot using the listed signals allowed for identification and quantification of the title compound.*

91% NMR yield; *E:Z* = 2:1.

***E*-isomer**: **^{1}H NMR** (500 MHz, $CDCl_3$): δ = 6.25 (d, *J* = 14.9 Hz, 1H), 5.88 (dd, *J* = 14.9, 7.5 Hz, 1H), 4.40–4.35 (m, 1H), 2.72–2.60 (m, 2H) ppm.

***Z*-isomer**: **^{1}H NMR** (500 MHz, $CDCl_3$): δ = 6.37 (d, *J* = 9.3 Hz, 1H), 5.83 (d, *J* = 9.3 Hz, 1H), 4.47–4.40 (m, 1H), 2.85–2.72 (m, 2H) ppm.

(*Z*)-*N*-(1-phenyl-4-phenoxy-3-butenyl)-4-methoxyaniline (249b)

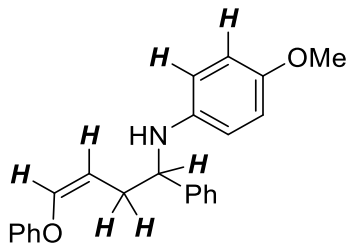

249b was prepared according to *GP–X* from allyl phenyl ether **221b** (53.6 mg, 0.40 mmol, 2.00 equiv) and imine **56b** (42.2 mg, 0.20 mmol) using NaHMDS (3.7 mg, 0.02 mmol, 10 mol%) as the catalyst and [18]crown-6 (5.6 mg, 0.02 mmol, 10 mol%) as the ligand in dioxane (300 µL) at 60 °C for 20 h. *Due to its instability to PTLC conditions,* **249b** *was not isolated. Analysis of* ^{1}*H NMR spectroscopic data of a reaction aliquot using the listed signals allowed for identification and quantification of the title compound.*

49% NMR yield.

^{1}H NMR (500 MHz, $CDCl_3$): δ = 6.69 (d, *J* = 9.0 Hz, 2H), 6.53 (d, *J* = 6.1 Hz, 1H), 6.46 (d, *J* = 9.0 Hz, 2H), 4.85 (dd, *J* = 8.0, 6.1 Hz, 1H), 4.35 (dd, *J* = 8.0, 5.2 Hz, 1H), 2.84–2.74 (m, 1H), 2.70–2.62 (m, 1H) ppm.

(*Z*)-*N*-[1-phenyl-4-(*N*,*N*-diphenlamino)-3-butenyl]-4-methoxyaniline (250b)

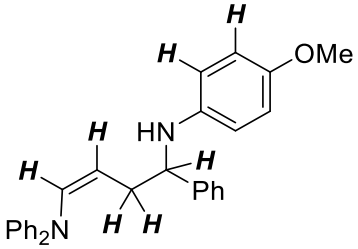

250b was prepared according to *GP–X* from allyl phenyl ether **221b** (83.6 mg, 0.40 mmol, 2.00 equiv) and imine **56b** (42.2 mg, 0.20 mmol) using NaHMDS (3.7 mg, 0.02 mmol, 10 mol%) as the catalyst and [18]crown-6 (5.6 mg, 0.02 mmol, 10 mol%) as the ligand in dioxane (300 µL) at 60 °C for 20 h. *Due to its instability to PTLC conditions,* **250b** *was not isolated. Analysis of* ^{1}*H NMR spectroscopic data of a reaction aliquot using the listed signals allowed for identification and quantification of the title compound.*

65% NMR yield.

^{1}H NMR (500 MHz, $CDCl_3$): δ = 6.67 (d, *J* = 8.9 Hz, 2H), 6.40 (d, *J* = 8.9 Hz, 2H), 6.25 (d, *J* = 8.3 Hz, 1H), 4.95 (ddd, *J* = 8.3, 7.6, 7.6 Hz, 1H), 4.17 (dd, *J* = 6.7, 7.2 Hz, 1H), 2.19–2.10 (m, 2H) ppm.

(*E*)-*N*-[1-phenyl-4-(*N*,*N*-diphenylphosphino)-3-butenyl]-4-methoxyaniline (255b)

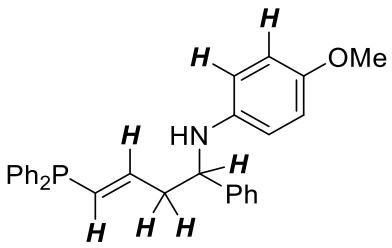

255b was prepared according to *GP–X* from diphenyl allylphosphine **220** (67.8 mg, 0.30 mmol, 1.50 equiv) and imine **56b** (42.2 mg, 0.20 mmol) using NaHMDS (3.7 mg, 0.02 mmol, 10 mol%) as the catalyst in dioxane (300 µL) at 25 °C for 20 h. *Due to its instability to PTLC conditions,* **255b** *was not isolated. Analysis of* ^{1}*H NMR spectroscopic data of a reaction aliquot using the listed signals allowed for identification and quantification of the title compound.*

82% NMR yield.

^{1}H NMR (500 MHz, $CDCl_3$): δ = 6.67 (d, *J* = 9.0 Hz, 2H), 6.40 (d, *J* = 9.0 Hz, 2H), 6.31 (d, *J* = 16.5 Hz, 1H), 6.13 (dd, *J* = 16.5, 7.0 Hz, 1H), 4.41–4.32 (m, 1H), 2.80–2.61 (m, 2H) ppm.

4.3 Carbodiphosphoranes

4.3.1 General Methods

General Procedure for the carbone boron binding study (GP–XI)

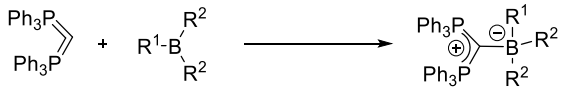

The carbone solution in toluene (0.02 mmol) was added to a vial containing the Lewis acid (0.022 mmol) and C_6D_6 (0.4 mL) was added. The solution was mixed and transferred into an NMR tube for direct ^{11}B and ^{31}P NMR spectroscopy.

General Procedure for the FLP catalysis (GP–XII)

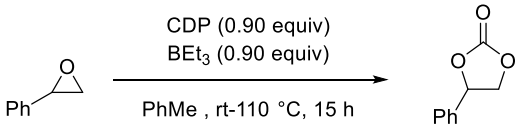

A Radleys vial was charged with hexaphenylcarbodiphosphorane **259** (96.6 mg, 0.18 mmol, 0.90 equiv), triethylborane (180 µL, 0.18 mmol, 0.90 equiv) and styrene oxide (23.2 µL, 0.20 mmol) and sealed under N_2 atmosphere. The vial was then evacuated and flushed with CO_2 gas on a Schlenk line. Toluene (4.0 mL) was added and the suspension stirred for 15 h. A colourless solid precipitated formed which indicated the presence of the CDP-CO_2 adduct. Acetonitrile (3.0 mL) was added, which instantaneously dissolved the solution. Aliquot ^{1}H NMR spectroscopy was used to monitor the reaction between 25–110 °C. No consumption of the epoxide was observed. ^{31}P NMR spectroscopy revealed the decomposition of the catalyst with new peaks at 25.9 and 25.3 ppm.

General procedure for the CDP–Ga^{III} catalysis (GP–XIII)

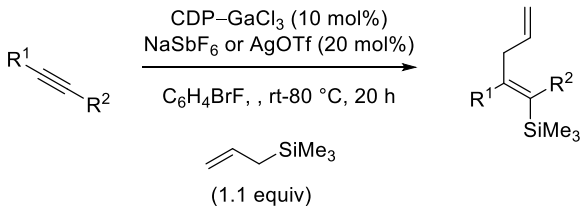

In a vial CDP-$GaCl_3$ complex **344** (14.3 mg, 0.02 mmol, 10 mol%) was mixed with silver triflate (10.3 mg, 0.04 mmol, 20 mol%) or sodium hexafluoroantimonate (10.3 mg, 0.04 mmol, 20 mol%) and 1,2-bromofluorobenzene (0.5 mL). After 5 min alkyne **303**, **355** or **356** (0.20 mmol) was added, followed by the allylsilane **136a** (35.1 µL, 0.22 mmol, 1.1 equiv). After 24 h the mixture was analysed using ^{1}H NMR in $CDCl_3$.

Catalytic Michael addition of alkylnitriles to Amides (GP–XIV)

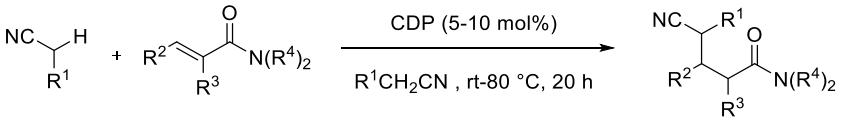

In a glove box, a dry 10 mL screw cap vial with a magnetic stirring bar was charged with CDP **259** (5.2 mg, 0.01 mmol, 10 mol%) and alkylnitrile (100 µL). To this mixture the acrylamide **118** (0.10 mmol) was added and rinsed with alkylnitrile (100 µL). This solution was sealed and stirred in a 25 °C sand bath for 20 h. The internal standard DBE (0.25 M, 0.10 mL) was added prior to ^{1}H NMR analysis using aliquot NMR. The mixtures were purified by PTLC on silica gel (Wako, Et_2O:PE = 1:1) to isolate the pure amides **387** (R_f ~ 0.15) as a colourless liquid.

Catalytic Michael addition of benzylnitrile to Amides (GP–XV)

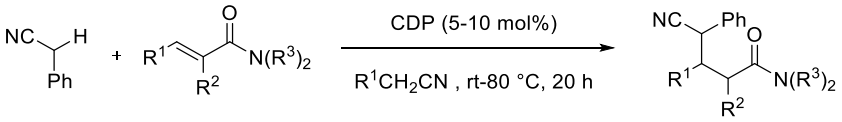

In a glove box, a dry 10 mL screw cap vial with a magnetic stirring bar was charged with CDP **259** (5.2 mg, 0.01 mmol, 10 mol%) and toluene (100 µL). To this mixture the acrylamide **118** (0.10 mmol) and benzylnitrile (14.0 µL, 0.12 mmol, 1.2 equiv) were added and rinsed with toluene (100 µL). This solution was sealed and stirred in a 25 °C sand bath for 20 h. The internal standard DBE (0.25 M, 0.10 mL) was added prior to ^{1}H NMR analysis using aliquot NMR. The mixtures were purified by PTLC (Wacko silica gel, Et_2O:PE = 1:1) to isolate the pure amides **404** or **406** (R_f ~ 0.15) as a colourless liquid.

4.3.2 Synthesis

1-Chloro-methylenebis(triphenylphosphonium) chloride (265)[159b]

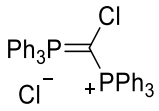

To a solution of triphenylphosphine (26.23 g, 100.0 mmol, 1.5 equiv) in DCM (50 mL) tetrachloromethane (6.43 mL, 66.7 mmol) was added dropwise at room temperature. The mixture was stirred for 26 h upon which the solution changed colour from yellow to brown and a colourless precipitate formed. To remove the precipitated by-product, 1,2-epoxybutane (5.80 mL, 66.7 mmol, 1.0 equiv) was added while ensuring that the temperature did not rise above 20 °C. The colourless precipitate dissolved and ether (50 mL) was added dropwise until turpidity occurred upon addition. The product crystallised at 0 °C and was then filtered, washed with DCM (2 x 2 mL) and Et_2O (2 x 2 mL) and recrystallised from DCM (30 mL) and Et_2O (10 mL) to form the light yellow crystals of **265** 13.3 g **(**66%).

^{1}H NMR (C_6D_6): δ = 7.89–7.81 (m, 12H), 7.03–6.95 (m, 18H) ppm.

^{31}P NMR (C_6D_6): δ = 25.7 (s) ppm.

Hexaphenylcarbodiphosphorane (259)[123a]

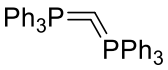

Benzene (6 mL) was added to a mixture of **265** (1.60 g, 2.64 mmol) and tris (dimethylamino)phosphine (0.43 g, 2.64 mmol, 1.0 equiv) and the mixture was stirred at room temperature. After 1 h a bright yellow solution had formed and after 3 h a colourless solid precipitated. After 24 h the solution was heated to 100 °C and the precipitate was separated from the hot solution which crystallised at room temperature and was filtered, washed with Et_2O (2 mL) to give the bright yellow powder of **259** (1.32g, 93%).

^{1}H NMR (C_6D_6): δ = 7.89–7.85 (m, 12H), 7.08–6.95 (m, 18H) ppm.

^{31}P NMR (C_6D_6): δ = -4.12 (s) ppm.

Diphenyl pyridyl phosphine (333)[232]

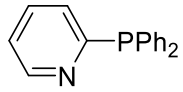

THF (150 mL) was added to a dry flask containing triphenylphosphine (**263**; 13.11 g, 50 mmol) and Li metal (6.94 g, 120 mmol, 2.4 equiv) was added. The brown solution was stirred at rt for 2.5 h and then cooled to 0 °C in an ice bath. Ethanol (2.33 mL, 40 mmol) was then added upon which the solution turned black. At the same temperature, chloropyridine **332** (4.73 mL, 50 mmol) was added and the reaction was warmed up to rt. The THF was then distilled off at atmospheric pressure until dryness. The mixture was then worked up by extracting with DCM (50 mL) and washing with ammonium chloride solution (3 M, 50 mL) and water (50 mL). The organic solution was then dried over $MgSO_4$, filtered and purified by flash column chromatography (silica, 20% EtOAc in hexane, R_f = 0.27) to yield product **333** (4.06 g, 31%). Spectral information fitted the reported literature data.

^{1}H NMR ($CDCl_3$): δ = 8.72 (ddd, *J* = 4.8, 1.7, 0.9 Hz, 1H), 7.56 (tt, *J* = 7.7, 1.9 Hz, 1H), 7.45–7.32 (m, 10H), 7.17 (ddt, 1H, *J* = 7.6, 4.8, 1.1 Hz, 1H), 7.08 (ddd, 1H, *J* = 7.8, 2.1, 1.0 Hz, 1H) ppm.

^{31}P NMR ($CDCl_3$): δ = -4.0 (s) ppm.

Methylene 1,1-bromo-briphenylphosphonium bromide (262)[233]

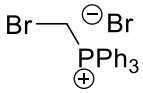

To a solution of triphenylphosphine (**263**; 15.74 g, 60.0 mmol) in toluene (25 mL) was added dibromomethane (5.61 mL, 80.0 mmol, 1.33 equiv) in one portion. The mixture was stirred at 60 °C for 72 h and the resulting crystals were filtered and washed with toluene. The remaining solution was stirred at 90 °C after the addition of an additional amount of dibromomethane (2.50 mL, 35.6 mmol). The combined filtered and washed solids were recrystallised from propan-2-ol to yield the bromide salt **262** (15.65 g, 60%). Spectral information fitted the reported literature data.

^{1}H NMR ($CDCl_3$): δ = 8.02–7.89 (m, 6H), 7.81 (t, *J* = 6.7 Hz, 3H), 7.74–7.66 (m, 6H), 5.90–5.77 (m, 2H) ppm.

^{31}P NMR (C_6D_6): δ = 23.6–23.1 (m) ppm.

Methylene 1,1-triphenylphosphonium-diphenylpyridylphosphonium dibromide (334)[127]

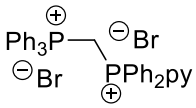

Triphenylphosphate (22.61 g) was melted in a flask under vacuum at 60 °C for 3 h. Bromide salt **262** (6.59 g, 15.1 mmol) and phosphine **333** (3.99 g, 15.2 mmol, 1.01 equiv) were then added to the phosphate and heated to 120 °C over night. The brown solution was then extracted by stirring vigorously in toluene (100 mL) for 3 h until a grey solid suspension formed. The solid was filtered off, dissolved directly in methanol (30 mL) and recrystallised using Et_2O (50 mL) to yield the pale brown crystals of **334** (2.02 g, 19%). Spectral information fitted the reported literature data.

^{1}H NMR ($CDCl_3$): δ = 8.22–8.08 (m, 12H), 8.04–7.94 (m, 1H), 7.78 (t, *J* = 16.4 Hz, 2H), 7.64–7.54 (m, 5H), 7.48–7.40 (m, 11H) ppm.

^{31}P NMR ($CDCl_3$): δ = 20.9–20.4 (m), 15.7–15.2 (m) ppm.

Pentaphenyl pyridyl carbodiphosphorane (270)[127]

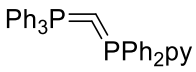

Powdered sodium hydride (12.0 mg, 0.50 mmol, 3.33 equiv) was added in one portion to the stirred solution of the precursor salt **334** (104.9 mg, 0.15 mmol) in acetonitrile (2 mL) After stirring for 15 h, the yellow suspension was filtered and washed with acetonitrile. The solid was then filtered and washed with toluene, which was removed *in vacuo* and dried to give the carbone **270** (31.0 mg, 38%).

^{31}P NMR (C_6D_6): δ = -2.7 (d, *J* = 83.8 Hz), -6.1 (d, *J* = 87.6 Hz) ppm.

4.3.3 Stoichiometric Reactions

Hexaphenylcarbodiphosphorane CO_2 adduct (297)[150]

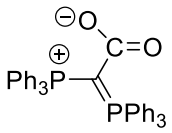

A Radley's vial was charged with hexaphenylcarbodiphosphorane **259** (268.3 mg, 0.50 mmol) and sealed under N_2 atmosphere. The vial was then flushed with CO_2 gas on a Schlenk line. Toluene (5 mL) was added and the suspension stirred for 15 h. A colourless solid precipitated, which was then filtered off, washed with toluene (2 mL) and dried to give the complex **297** (258.0 mg, 89%).

^{31}P NMR ($CDCl_3$): δ = 15.0 ppm.

Hexaphenylcarbodiphosphorane $GaCl_3$ complex (344)[165]

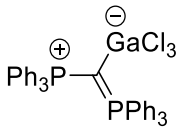

Hexaphenylcarbodiphosphorane **259** (268.3 mg, 0.50 mmol) was suspended in toluene (2.0 mL) and $GaCl_3$ (88.0 mg, 0.50 mmol) was added and rinsed with toluene (3.0 mL). The suspension was stirred over night at rt upon which a colourless precipitate formed. The solid was filtered off, washed with toluene (2.0 mL) and dried to give the complex **344** (346.0 mg, 97%).

^{31}P NMR ($CDCl_3$): δ = 23.4 ppm.

Hexaphenylcarbodiphosphorane Fe(III)Cl_3 complex (347)

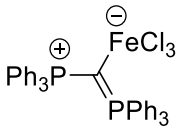

Hexaphenylcarbodiphosphorane **259** (134.2 mg, 0.25 mmol) was suspended in toluene (1.0 mL) and $FeCl_3$ (40.6 mg, 0.25 mmol) was added and rinsed with toluene (1.0 mL). The suspension was stirred for 7 d at rt and for 2 d at 40 °C until aliquot ^{31}P NMR in C_6D_6 showed the absence of starting material. The dark purple precipitate was filtered off, washed with toluene (2.0 mL) and dried to give the complex **347** (111.1 mg, 64%).

^{31}P NMR ($CDCl_3$): δ = 22.2 ppm.

Hexaphenylcarbodiphosphorane Fe(II)Cl_2 complex (346)

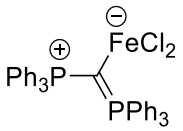

Hexaphenylcarbodiphosphorane **259** (134.2 mg, 0.25 mmol) was suspended in toluene (1.0 mL) and $FeCl_2$ (31.7 mg, 0.25 mmol) was added and rinsed with toluene (1.0 mL). The suspension was stirred for 7 d at rt and for 2 d at 40 °C until aliquot ^{31}P NMR in C_6D_6 showed the absence of starting material. The pale orange precipitate was filtered off, washed with toluene (2.0 mL) and dried to give the complex **346** (100.4 mg, 73%).

^{31}P NMR ($CDCl_3$): δ = 22.3 ppm.

4.3.4 Nitrile BB Starting Materials

Acetonitrile (131)[114]

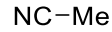

131 is commercially available. The obtained spectral data fitted accurately with literature reported data.

^{1}H NMR (500 MHz, $CDCl_3$): δ = 2.00 (s, 3H) ppm.

^{13}C NMR (125 MHz, $CDCl_3$): δ = 116.9, 1.8 ppm.

Propionitrile (123a)[114]

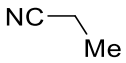

123a is commercially available. The obtained spectral data fitted accurately with literature reported data.

^{1}H NMR (500 MHz, $CDCl_3$): δ = 2.31 (q, *J* = 7.6 Hz, 2H), 1.29 (t, *J* = 7.6 Hz, 3H) ppm.

^{13}C NMR (125 MHz, $CDCl_3$): δ = 121.0, 10.9, 10.6 ppm.

1-phenyl acetonitrile (377)[234]

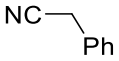

377 is commercially available. The obtained spectral data fitted accurately with literature reported data.

^{1}H NMR (500 MHz, $CDCl_3$): δ = 7.39–7.36 (m, 2H), 7.34–7.31 (m, 3H), 3.74 (s, 2H) ppm.

^{13}C NMR (125 MHz, $CDCl_3$): δ = 129.9, 129.1 (2C), 128.1, 127.9 (2C), 117.9, 23.6 ppm.

1-methyl-1-phenyl acetonitrile (405)[235]

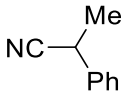

405 is commercially available. The obtained spectral data fitted accurately with literature reported data.

^{1}H NMR (500 MHz, $CDCl_3$): δ = 7.41–7.30 (m, 5H), 3.90 (q, *J* = 7.3 Hz, 1H), 1.64 (d, *J* = 7.3 Hz, 3H) ppm.

^{13}C NMR (125 MHz, $CDCl_3$): δ = 137.1, 129.2 (2C), 128.1, 126.7 (2C), 121.6, 31.3, 21.5 ppm.

***N*-dimethyl-2-propenamide (118c)**[114]

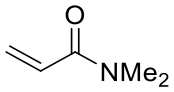

118c is commercially available. The obtained spectral data fitted accurately with literature reported data.

^{1}H NMR (500 MHz, $CDCl_3$): δ = 6.59 (dd, *J* = 16.8, 10.5 Hz, 1H), 6.30 (d, *J* = 16.8 Hz, 1H), 5.67 (d, *J* = 10.5 Hz, 1H), 3.09 (s, 3H), 3.02 (s, 3H) ppm.

^{13}C NMR (125 MHz, $CDCl_3$): δ = 166.6, 127.7, 127.5, 37.3, 35.6 ppm.

***N*-morpholino-2-propenamide (118d)**[236]

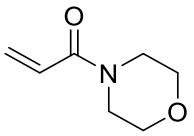

118d is commercially available. The obtained spectral data fitted accurately with literature reported data.

^{1}H NMR (500 MHz, $CDCl_3$): δ = 6.54 (dd, *J* = 16.8, 10.5 Hz, 1H), 6.32 (dd, *J* = 16.8, 1.9 Hz, 1H), 5.72 (dd, *J* = 10.5, 1.9 Hz, 1H), 3.72–3.64 (m, 6H), 3.61–3.50 (m, 2H) ppm.

^{13}C NMR (125 MHz, $CDCl_3$): δ = 165.5, 128.3, 127.1, 66.8 (2C), 46.2, 42.3 ppm.

***N*-methoxy-*N*-methyl-2-propenamide (118e)**[237]

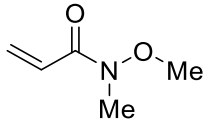

118e was prepared from acrolyl chloride (22 mmol, 1.1 equiv), *N,O*-dimethyl-hydroxylamine hydrochloride (20 mmol) and pyridine (44 mmol, 2.2 equiv) in chloroform (40 mL). After stirring this mixture for 20 h at room temperature, the reaction was worked by acidification with HCl (2 M, 50 mL), extraction of organic impurities followed by neutralisation with $NaHCO_3$ (sat. 100 mL) and extraction into chloroform (50 mL). The organic solution was dried ($MgSO_4$), filtered and the solvent removed *in vacuo*. The crude product was then subjected to silica gel flash chromatography (5% Et_2O in petrol ether) giving the title compound as a colourless liquid. The obtained spectral data fitted accurately with literature reported data.

^{1}H NMR (500 MHz, $CDCl_3$): δ = 6.73 (dd, *J* = 17.1, 10.4 Hz, 1H), 6.42 (dd, *J* = 17.1, 2.0 Hz, 1H), 5.75 (dd, *J* = 10.4, 2.0 Hz, 1H), 3.71 (s, 3H), 3.26 (s, 3H) ppm.

^{13}C NMR (125 MHz, $CDCl_3$): δ = 166.5, 128.9, 126.0, 61.8, 32.3 ppm.

***N,N*-diphenyl-2-methyl-2-propenamide (118g)**[238]

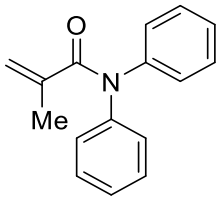

118g was prepared from methacrolyl chloride (15 mmol, 1.5 equiv), diphenylamine (10 mmol) and K_2CO_3 (15 mmol, 1.5 equiv) in toluene (15 mL). After stirring this mixture for 20 h under reflux, the reaction was worked up by washing with water (2 x 10 mL) and brine (10 mL). The organic solution was dried ($MgSO_4$), filtered and the solvent removed *in vacuo*. The crude solid was then recrystallised from diethyl ether at -20 °C giving the title compound as a light orange solid. The obtained spectral data fitted accurately with literature reported data.

^{1}H NMR (500 MHz, $CDCl_3$): δ = 7.35–7.30 (m, 4H), 7.24–7.19 (m, 2H), 7.19–7.14 (m, 4H), 5.23 (q, *J* = 1.0 Hz, 1H), 5.17 (q, *J* = 1.5 Hz, 1H), 1.84 (dd, *J* = 1.5, 1.0 Hz, 3H) ppm.

^{13}C NMR (125 MHz, $CDCl_3$): δ = 171.8, 143.5 (2C), 141.2, 129.1 (4C), 127.2 (4C), 126.5 (2C), 120.9, 19.9 ppm.

***N*,*N*-dimethyl-3-phenyl-2-propenamide (118a)**[239]

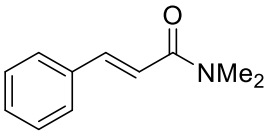

118a was prepared from dimethyl acetamide (100 mL, >50 equiv), benzaldehyde (20 mmol) and K_2CO_3 (10 mmol, 1.0 equiv) in dimethylacetamide and diethylcarbonate (1:1, 200 mL). After stirring this mixture for 100 h at 150 °C, the product was isolated by distillation of the solvents, leaving behind a solid residue. The crude product was recrystallised from diethyl ether at -20 °C giving the title compound as a light orange solid. The obtained spectral data fitted accurately with literature reported data.

^{1}H NMR (500 MHz, $CDCl_3$): δ = 7.67 (d, *J* = 15.5 Hz, 1H), 7.55–7.49 (m, 2H), 7.39–7.33 (m, 3H), 6.89 (d, *J* = 15.5 Hz, 1H), 3.16 (s, 3H), 3.06 (s, 3H) ppm.

^{13}C NMR (125 MHz, $CDCl_3$): δ = 166.7, 142.3, 135.4, 129.5, 128.8 (2C), 127.8 (2C), 117.5, 37.4, 35.9 ppm.

3-phenyl-2-propenyl acyl chloride (414)[238]

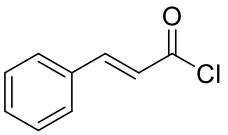

414 was prepared from cinnamic acid (20 mmol) and thionyl chloride (80 mmol, 4.0 equiv) in DCM (30 mL). After stirring this mixture for 20 h under reflux, the reaction was cooled to room temperature and the solvent was removed *in vacuo*. The crude liquid was used directly in the next step. The obtained spectral data fitted accurately with literature reported data.

^{1}H NMR (500 MHz, $CDCl_3$): δ = 7.87 (d, *J* = 15.6 Hz, 1H), 7.63–7.59 (m, 2H), 7.54–7.44 (m, 3H), 6.68 (d, *J* = 15.6 Hz, 1H) ppm.

***N,N*-diphenyl-3-phenyl-2-propenamide (118b)**[238]

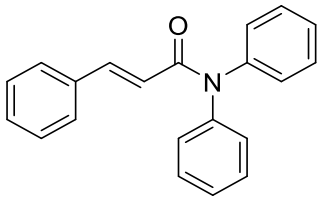

118b was prepared from cinnamyl chloride **414** (10 mmol) and diphenylamine (10 mmol, 1.0 equiv) in DCM (15 mL). After stirring this mixture for 20 h under reflux, the mixture was extracted in ethyl acetate (250 mL) and washed with aqueous $NaHCO_3$ (sat, 100 mL) and brine (100 mL). The organic phase was dried ($MgSO_4$), filtered and the solvent was removed *in vacuo*. The crude product was recrystallised from a mixture of isopropanol and DCM (19:1) at -20 °C giving the title compound as a colourless solid. The obtained spectral data fitted accurately with literature reported data.

^{1}H NMR (500 MHz, $CDCl_3$): δ = 7.77 (d, *J* = 15.5 Hz, 1H), 7.41–7.33 (m, 6H), 7.32–7.25 (m, 9H), 6.48 (d, *J* = 15.5 Hz, 1H) ppm.

^{13}C NMR (125 MHz, $CDCl_3$): δ = 166.2, 142.8 (2C), 142.6, 135.1, 129.7, 129.3 (4C), 128.7 (2C), 128.0 (2C), 126.9 (br, 6C), 119.8 ppm.

4.3.5 Alkylnitrile Michael Additions

***N,N*-dimethyl-4-cyano-butanamide (387c)**

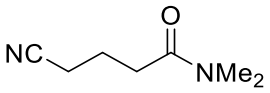

Compound **387c** was prepared according to *GP–XV* from acetonitrile (xs reagent as solvent) and acrylamide **118c** (9.9 mg, 0.10 mmol), using CDP (5.2 mg, 0.01 mmol, 10 mol%) as the catalyst, in acetonitrile (200 µL) at 25 °C for 20 h. **387c** was purified by PTLC on silica gel (EtOAc:PE = 1:1).

Colourless liquid.

Yield: 11.1 mg (79%).

^{1}H NMR (500 MHz, $CDCl_3$): δ = 3.02 (s, 3H), 2.96 (s, 3H), 2.52 (t, *J* = 7.0 Hz, 2H), 2.49 (t, *J* = 6.8 Hz, 2H), 2.00 (tt, *J* = 7.0, 6.8 Hz, 2H) ppm.

^{13}C NMR (125 MHz, $CDCl_3$): δ = 170.8, 119.6, 37.0, 35.4, 30.9, 20.8, 16.7 ppm.

IR (neat): ν = 2936, 2245, 1634, 1400, 1142 cm^{-1}.

HRMS (ESI): calculated for $C_7H_{13}N_2O^+$ = [MH^+]: *m*/*z* = 141.1022, found: *m*/*z* = 141.1040; calculated for $C_7H_{12}N_2NaO^+$ = [MNa^+]: *m*/*z* = 163.0842, found: *m*/*z* = 163.0847.

***N,N*-morpholino-4-cyano-butanamide (387d)**

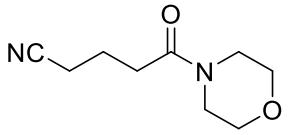

Compound **387d** was prepared according to *GP–XV* from acetonitrile (xs reagent as solvent) and acrylamide **118d** (14.1 mg, 0.10 mmol), using CDP (5.2 mg, 0.01 mmol, 10 mol%) as the catalyst, in acetonitrile (200 µL) at 25 °C for 20 h. **387d** was purified by PTLC on silica gel (EtOAc:PE = 1:1).

Colourless liquid.

Yield: 14.5 mg (80%).

^{1}H NMR (500 MHz, $CDCl_3$): δ = 3.71–3.66 (m, 4H), 3.64–3.60 (m, 2H), 3.49–3.46 (m, 2H), 2.52 (t, *J* = 6.7 Hz, 2H), 2.49 (t, *J* = 6.8 Hz, 2H), 2.02 (tt, *J* = 6.8, 6.7 Hz, 2H) ppm.

^{13}C NMR (125 MHz, $CDCl_3$): δ = 169.5, 119.5, 66.8, 66.5, 45.7, 42.0, 30.6, 20.7, 16.7 ppm.

IR (neat): ν = 2967, 2922, 2859, 2245, 1640, 1437, 1238, 1115 cm^{-1}.

HRMS (ESI): calculated for $C_7H_{13}N_2O^+$ = [MH^+]: *m*/*z* = 183.1128, found: *m*/*z* = 183.1138; calculated for $C_7H_{12}N_2NaO^+$ = [MNa^+]: *m*/*z* = 205.0948, found: *m*/*z* = 205.0959.

***N*-methoxy-*N*-methyl-4-cyano-butanamide (387e)**

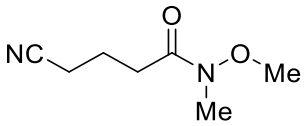

Compound **387e** was prepared according to *GP–XV* from acetonitrile (xs reagent as solvent) and acrylamide **118e** (11.5 mg, 0.10 mmol), using CDP (5.2 mg, 0.01 mmol, 10 mol%) as the catalyst, in MeCN (200 µL) at 25 °C for 20 h. **387e** was purified by PTLC on silica gel (EtOAc:PE = 1:1).

Colourless liquid.

Yield: 11.3 mg (72%).

^{1}H NMR (500 MHz, $CDCl_3$): δ = 3.73 (s, 3H), 3.21 (s, 3H), 2.64 (t, *J* = 6.8 Hz, 2H), 2.51 (t, *J* = 7.0 Hz, 2H), 2.01 (tt, *J* = 7.0, 6.8 Hz, 2H) ppm.

^{13}C NMR (125 MHz, $CDCl_3$): δ = 172.5, 119.4, 61.3, 32.2, 29.9, 20.2, 16.7 ppm.

IR (neat): ν = 2941, 2247, 1653, 1420, 1389, 991, 731 cm^{-1}.

HRMS (ESI): calculated for $C_7H_{13}N_2O_2^+$ = [MH^+]: *m*/*z* = 157.0971, found: *m*/*z* = 157.0968; calculated for $C_8H_{14}N_2NaO_2^+$ = [MNa^+]: *m*/*z* = 179.0791, found: *m*/*z* = 179.0777.

***N*,*N*-dimethyl-4-cyano-3-phenyl-butanamide (387a)**

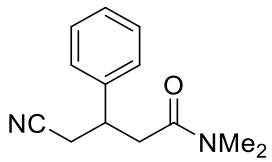

Compound **387a** was prepared according to *GP–XV* from acetonitrile (xs reagent as solvent) and acrylamide **118a** (17.5 mg, 0.10 mmol), using CDP (2.6 mg, 0.005 mmol, 5 mol%) as the catalyst, in acetonitrile (200 µL) at 80 °C for 20 h. **387a** was purified by PTLC on silica gel (EtOAc:PE = 1:1).

Colourless liquid.

Yield: 16.7 mg (77%).

^{1}H NMR (500 MHz, $CDCl_3$): δ: = 7.42–7.21 (m, 5H), 3.61 (dddd, *J* = 9.5, 7.0, 4.9, 4.9 Hz, 1H), 2.97 (s, 3H), 2.94 (s, 3H), 2.92–2.76 (m, 3H), 2.71 (dd, *J* = 16.3, 4.9 Hz, 1H) ppm.

^{13}C NMR (125 MHz, $CDCl_3$): δ: = 170.0, 141.7, 129.0 (2C), 127.6, 127.2 (2C), 118.5, 37.7, 37.5, 37.1, 35.5, 24.1 ppm.

IR (neat): ν = 2930, 2243, 1636, 1495, 1398, 1144, 764, 700 cm^{-1}.

HRMS (ESI): calculated for $C_{13}H_{17}N_2O^+$ = [MH^+]: *m*/*z* = 217.1335, found: *m*/*z* = 217.1343; calculated for $C_{13}H_{16}N_2NaO^+$ = [MNa^+]: *m*/*z* = 239.1155, found: *m*/*z* = 239.1162.

***N*,*N*-diphenyl-4-cyano-3-phenyl-butanamide (387b)**

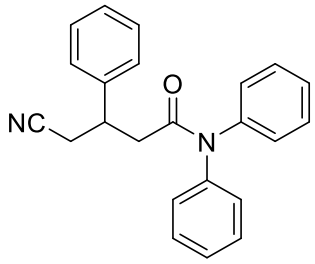

Compound **387b** was prepared according to *GP–XV* from acetonitrile (xs reagent as solvent) and acrylamide **118b** (29.9 mg, 0.10 mmol), using CDP (5.2 mg, 0.01 mmol, 10 mol%) as the catalyst, in acetonitrile (200 µL) at 25 °C for 20 h. **387b** was purified by PTLC on silica gel (EtOAc:PE = 1:1).

Colourless liquid.

Yield: 30.0 mg (88%).

^{1}H NMR (500 MHz, $CDCl_3$): δ: = 7.42–7.22 (m, 8H), 7.22–7.12 (m, 3H), 7.10 (d, *J* = 7.2 Hz, 4H) 3.65 (dddd, *J* = 7.6, 7.0, 6.8, 6.1 Hz, 1H), 2.83 (dd, *J* = 16.7, 7.0 Hz, 1H), 2.77 (dd, *J* = 15.7, 7.6 Hz, 1H), 2.73 (dd, *J* = 16.7, 6.1 Hz, 1H), 2.68 (dd, *J* = 15.7, 6.8 Hz, 1H) ppm.

^{13}C NMR (125 MHz, $CDCl_3$): δ: = 170.2, 142.3 (2C), 141.0, 130.0 (2C), 128.9 (2C), 128.6 (4C), 127.7, 127.3 (2C), 126.4 (4C), 118.3, 39.7, 38.6, 23.9 ppm.

IR (neat): ν = 3061, 3030, 2245, 1663, 1593, 1489, 1379, 1289, 698 cm^{-1}.

HRMS (ESI): calculated for $C_{23}H_{21}N_2O^+$ = [MH^+]: *m*/*z* = 341.1648, found: *m*/*z* = 341.1652; calculated for $C_{23}H_{20}N_2NaO^+$ = [MNa^+]: *m*/*z* = 363.1468, found: *m*/*z* = 363.1461.

***N,N*-diphenyl-4-cyano-2-methyl-butanamide (387g)**

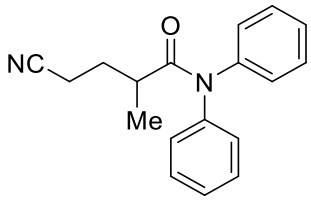

Compound **387g** was prepared according to *GP–XV* from acetonitrile (xs reagent as solvent) and acrylamide **118g** (23.7 mg, 0.10 mmol), using CDP (2.6 mg, 0.005 mmol, 5 mol%) as the catalyst, in acetonitrile (200 µL) at 80 °C for 20 h. **387g** was purified by PTLC on silica gel (EtOAc:PE = 1:1).

Colourless liquid.

Yield: 20.2 mg (73%).

^{1}H NMR (500 MHz, $CDCl_3$): δ = 7.54–7.12 (m, 10H), 2.83 (dqd, *J* = 9.4, 6.8, 4.9 Hz, 1H), 2.50–2.35 (m, 2H), 2.14 (ddt, *J* = 13.5, 9.4, 6.3 Hz, 1H), 1.67 (dddd, *J* = 13.5, 8.4, 7.0, 4.9 Hz, 1H), 1.16 (d, *J* = 6.8 Hz, 3H) ppm.

^{13}C NMR (125 MHz, $CDCl_3$): δ = 175.0, 142.4 (2C), 130.1 (2C), 129.0 (2C), 128.8 (2C), 128.3, 126.4 (3C), 119.5, 36.3, 29.4, 18.1, 15.2 ppm.

IR (neat): ν = 2972, 2934, 2243, 1665, 1591, 1491, 1387, 1267, 702 cm^{-1}.

HRMS (ESI): calculated for $C_{18}H_{19}N_2O^+$ = [MH^+]: *m*/*z* = 279.1492, found: *m*/*z* = 279.1500; calculated for $C_{18}H_{18}N_2NaO^+$ = [MNa^+]: *m*/*z* = 301.1311, found: *m*/*z* = 301.1310.

***N,N*-morpholino-4-cyano-pentanamide (124d)**

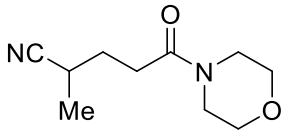

Compound **124d** was prepared according to *GP–XV* from propionitrile (xs reagent as solvent) and acrylamide **118d** (14.1 mg, 0.10 mmol), using CDP (5.2 mg, 0.01 mmol, 10 mol%) as the catalyst, in propionitrile (200 µL) at 25 °C for 20 h. **124d** was purified by PTLC on silica gel (EtOAc:PE = 1:1).

Colourless liquid.

Yield: 17.6 mg (90%).

^{1}H NMR (500 MHz, $CDCl_3$): δ = 3.71–3.67 (m, 4H), 3.64–3.60 (m, 2H), 3.51–3.47 (m, 2H), 2.88–2.77 (m, 1H), 2.57–2.45 (m, 2H), 2.09–2.00 (m, 1H), 1.89–1.79 (m, 1H), 1.36 (d, *J* = 7.1 Hz, 3H) ppm.

^{13}C NMR (125 MHz, $CDCl_3$): δ = 169.7, 122.7, 66.8, 66.5, 45.8, 42.0, 29.9, 29.3, 25.1, 18.2 ppm.

IR (neat): ν = 2967, 2922, 2859, 2237, 1641, 1437, 1231, 1115 cm^{-1}.

HRMS (ESI): calculated for $C_7H_{13}N_2O^+$ = [MH^+]: *m*/*z* = 219.1104, found: *m*/*z* = 219.1106; calculated for $C_7H_{12}N_2NaO^+$ = [MNa^+]: *m*/*z* = 197.1285, found: *m*/*z* = 197.1280.

***N*-methoxy-*N*-methyl-4-cyano-pentanamide (124e)**

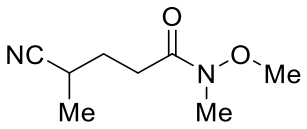

Compound **124e** was prepared according to *GP–XV* from propionitrile (xs reagent as solvent) and acrylamide **118e** (11.5 mg, 0.10 mmol), using CDP (5.2 mg, 0.01 mmol, 10 mol%) as the catalyst, in EtCN (200 µL) at 25 °C for 20 h. **124e** was purified by PTLC on silica gel (EtOAc:PE = 1:1).

Colourless liquid.

Yield: 10.4 mg (61%).

^{1}H NMR (500 MHz, $CDCl_3$): δ = 3.74 (s, 3H), 3.21 (s, 3H), 2.82 (dqd, *J* = 9.5, 7.1, 5.0, 1H), 2.68 (t, *J* = 6.7, 2H), 2.00 (dtd, *J* = 13.2, 6.7, 5.0, 1H), 1.87 (ddt, *J* = 13.2, 9.5, 6.7 Hz, 1H), 1.38 (d, *J* = 7.1 Hz, 3H) ppm.

^{13}C NMR (125 MHz, $CDCl_3$): δ = 168.4, 122.7, 61.3, 29.7, 29.1, 28.8, 25.1, 18.1 ppm.

IR (neat): ν = 2922, 2239, 1655, 1458, 14120, 1387, 993, 735 cm^{-1}.

HRMS (ESI): calculated for $C_8H_{15}N_2O_2^+$ = [MH^+]: *m*/*z* = 171.1128, found: *m*/*z* = 171.1125; calculated for $C_8H_{14}N_2NaO_2^+$ = [MNa^+]: *m*/*z* = 193.0947, found: *m*/*z* = 193.0935.

***N*,*N*-dimethyl-4-cyano-4-phenyl-butanamide (404c)**

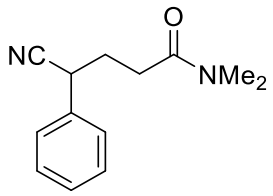

Compound **404c** was prepared according to *GP–XV* from benzylnitrile (14.0 µL, 0.12 mmol, 1.2 equiv) and acrylamide **118c** (9.9 mg, 0.10 mmol), using CDP (5.2 mg, 0.01 mmol, 10 mol%) as the catalyst, in toluene (200 µL) at 25 °C for 20 h. **404c** was purified by PTLC on silica gel (EtOAc:PE = 1:1).

Colourless liquid.

Yield: 17.1 mg (79%).

^{1}H NMR (500 MHz, $CDCl_3$): δ = 7.38 (d, *J* = 4.2 Hz, 4H), 7.33 (d, *J* = 4.2 Hz, 1H), 4.13 (dd, *J* = 9.4, 5.7 Hz, 1H), 2.99 (s, 3H), 2.96 (s, 3H), 2.57 (dt, *J* = 16.6, 7.5 Hz, 1H), 2.44 (dt, *J* = 16.6, 6.2 Hz, 1H), 2.34–2.25 (m, 1H), 2.21–2.11 (m, 1H) ppm.

^{13}C NMR (125 MHz, $CDCl_3$): δ = 170.9, 135.7, 129.1 (2C), 128.1, 127.3 (2C), 120.8, 37.0, 36.4, 35.5, 31.2, 29.8 ppm.

IR (neat): ν = 2932, 2239, 1643, 1495, 1454, 1400, 1142, 700 cm^{-1}.

HRMS (ESI): calculated for $C_{13}H_{17}N_2O^+$ = [MH^+]: *m*/*z* = 217.1335, found: *m*/*z* = 217.1357; calculated for $C_{13}H_{16}N_2NaO^+$ = [MNa^+]: *m*/*z* = 239.1155, found: *m*/*z* = 239.1169.

***N*-methoxy-*N*-methyl-4-cyano-4-phenyl-butanamide (404e)**

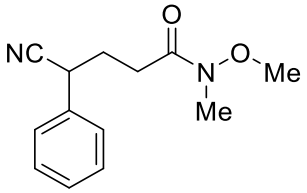

Compound **404e** was prepared according to *GP–XV* from benzylnitrile (14.0 µL, 0.12 mmol, 1.2 equiv) and acrylamide **118e** (11.5 mg, 0.10 mmol), using CDP (5.2 mg, 0.01 mmol, 10 mol%) as the catalyst, in toluene (200 µL) at 25 °C for 20 h. **404e** was purified by PTLC on silica gel (EtOAc:PE = 1:1).

Colourless liquid.

Yield: 20.5 mg (88%).

^{1}H NMR (500 MHz, $CDCl_3$): δ = 7.39–7.36 (m, 4H), 7.35–7.30 (m, 1H), 4.06 (dd, *J* = 9.2, 6.1 Hz, 1H), 3.67 (s, 3H), 3.19 (s, 3H), 2.71 (dt, *J* = 16.9, 7.1 Hz, 1H), 2.58 (dt, *J* = 16.9, 6.1 Hz, 1H), 2.26 (ddt, *J* = 13.9, 7.1, 6.1, 1H), 2.18 (dddd, *J* = 13.9, 9.2, 6.1, 7.1 Hz, 1H) ppm.

^{13}C NMR (125 MHz, $CDCl_3$): δ = 172.6, 135.5, 129.1 (2C), 128.2, 127.3 (2C), 120.6, 61.3, 36.5, 32.2, 30.5, 28.8 ppm.

IR (neat): ν = 2938, 2237, 1655, 1649, 1420, 1389, 995, 700 cm^{-1}.

HRMS (ESI): calculated for $C_{13}H_{17}N_2O_2^+$ = [MH^+]: *m*/*z* = 233.1285, found: *m*/*z* = 233.1281; calculated for $C_{13}H_{16}N_2NaO_2^+$ = [MNa^+]: *m*/*z* = 255.1104, found: *m*/*z* = 255.1102.

5 References

[1] G. Sirasani, R. B. Andrade, *Org. Lett.* **2011**, *13*, 4736-4737.

[2] H. A. Lloyd, E. C. Horning, *J. Org. Chem.* **1960**, *25*, 1959-1962.

[3] J. Clayden, N. Greeves, S. Warren, P. Wothers, *Organic Chemistry (1st ed.)*, Oxford University Press, Oxford, **2001**.

[4] Y. Yamamoto, N. Asao, *Chem. Rev.* **1993**, *93*, 2207-2293.

[5] T. Vilaivan, C. Winotapan, V. Banphavichit, T. Shinada, Y. Ohfune, *J. Org. Chem.* **2005**, *70*, 3464-3471.

[6] G. K. Friestad, C. S. Korapala, H. Ding, *J. Org. Chem.* **2006**, *71*, 281-289.

[7] a) S. Kobayashi, H. Ishitani, *Chem. Rev.* **1999**, *99*, 1069-1094; b) M. Yus, J. C. Gonzalez-Gomez, F. Foubelo, *Chem. Rev.* **2013**, *113*, 5595-5698; c) M. Yus, J. C. Gonzalez-Gomez, F. Foubelo, *Chem. Rev.* **2011**, *111*, 7774-7854; d) H. Ding, G. K. Friestad, *Synthesis* **2005**, 2815-2829.

[8] J. D. Huber, J. L. Leighton, *J. Am. Chem. Soc.* **2007**, *129*, 14552-14553.

[9] M. I. Feske, A. B. Santanilla, J. L. Leighton, *Org. Lett.* **2010**, *12*, 688-691.

[10] H. Nakamura, K. Nakamura, Y. Yamamoto, *J. Am. Chem. Soc.* **1998**, *120*, 4242-4243.

[11] T. Gastner, H. Ishitani, R. Akiyama, S. Kobayashi, *Angew. Chem. Int. Ed.* **2001**, *40*, 1896-1898.

[12] F. Colombo, R. Annunziata, M. Benaglia, *Tetrahedron Lett.* **2007**, *48*, 2687-2690.

[13] R. A. Fernandes, Y. Yamamoto, *J. Org. Chem.* **2004**, *69*, 735-738.

[14] H. Kiyohara, Y. Nakamura, R. Matsubara, S. Kobayashi, *Angew. Chem. Int. Ed.* **2006**, *45*, 1615-1617.

[15] M. Naodovic, M. Wadamoto, H. Yamamoto, *Eur. J. Org. Chem.* **2009**, 5129-5131.

[16] R. Wada, T. Shibuguchi, S. Makino, K. Oisaki, M. Kanai, M. Shibasaki, *J. Am. Chem. Soc.* **2006**, *128*, 7687-7691.

[17] E. M. Vieira, M. L. Snapper, A. H. Hoveyda, *J. Am. Chem. Soc.* **2011**, *133*, 3332-3335.

[18] Y. Luo, H. B. Hepburn, N. Chotsaeng, H. W. Lam, *Angew. Chem. Int. Ed.* **2012**, *51*, 8309-8313.

[19] S. Lou, P. N. Moquist, S. E. Schaus, *J. Am. Chem. Soc.* **2007**, *129*, 15398-15404.

[20] D. L. Silverio, S. Torker, T. Pilyugina, E. M. Vieira, M. L. Snapper, F. Haeffner, A. H. Hoveyda, *Nature* **2013**, *494*, 216-221.

[21] M. B. Shaghafi, B. L. Kohn, E. R. Jarvo, *Org. Lett.* **2008**, *10*, 4743-4746.

[22] P. J. Unsworth, L. E. Löffler, A. Noble, V. K. Aggarwal, *Synlett* **2015**, *26*, 1567-1572.

[23] D. M. Tschaen, S. M. Weinreb, *Tetrahedron Lett.* **1982**, *23*, 3015-3018.

[24] M. K. Pandey, A. Bisai, A. Pandey, V. K. Singh, *Tetrahedron Lett.* **2005**, *46*, 5039-5041.

[25] M. Yamanaka, A. Nishida, M. Nakagawa, *Org. Lett.* **2000**, *2*, 159-161.

[26] W. J. Drury, III, D. Ferraris, C. Cox, B. Young, T. Lectka, *J. Am. Chem. Soc.* **1998**, *120*, 11006-11007.

[27] S. Yao, X. Fang, K. Anker Jorgensen, *Chem. Commun.* **1998**, 2547-2548.

[28] H. Braxmeier, G. Kresze, *Synthesis* **1985**, *1985*, 683-684.

[29] I. Kumadaki, S. Jonoshita, A. Harada, M. Omote, A. Ando, *J. Fluorine Chem.* **1999**, *97*, 61-63.

[30] a) M. S. Chen, M. C. White, *J. Am. Chem. Soc.* **2004**, *126*, 1346-1347; b) M. S. Chen, N. Prabagaran, N. A. Labenz, M. C. White, *J. Am. Chem. Soc.* **2005**, *127*, 6970-6971.

[31] S. A. Reed, A. R. Mazzotti, M. C. White, *J. Am. Chem. Soc.* **2009**, *131*, 11701-11706.

[32] A. J. Young, M. C. White, *J. Am. Chem. Soc.* **2008**, *130*, 14090-14091.

[33] D. J. Covell, M. C. White, *Angew. Chem. Int. Ed.* **2008**, *47*, 6448-6451.

[34] B. M. Trost, D. A. Thaisrivongs, E. J. Donckele, *Angew. Chem. Int. Ed.* **2013**, *52*, 1523-1526.

[35] S. Araki, T. Kamei, T. Hirashita, H. Yamamura, M. Kawai, *Org. Lett.* **2000**, *2*, 847-849.

[36] D. Ferraris, B. Young, C. Cox, T. Dudding, W. J. Drury, III, L. Ryzhkov, A. E. Taggi, T. Lectka, *J. Am. Chem. Soc.* **2002**, *124*, 67-77.

[37] Bordwell pKa Table (Acidity in DMSO), http://www.chem.wisc.edu/areas/reich/pkatable/, 12/06/2016

[38] a) T. Hirashita, Y. Hayashi, K. Mitsui, S. Araki, *J. Org. Chem.* **2003**, *68*, 1309-1313; b) D.-K. Wang, Y.-G. Zhou, Y. Tang, X.-L. Hou, L.-X. Dai, *J. Org. Chem.* **1999**, *64*, 4233-4237.

[39] P.-O. Delaye, J.-L. Vasse, J. Szymoniak, *Org. Lett.* **2012**, *14*, 3004-3007.

[40] M. Giammaruco, M. Taddei, P. Ulivi, *Tetrahedron Lett.* **1993**, *34*, 3635-3638.

[41] A. M. Hafez, A. E. Taggi, T. Dudding, T. Lectka, *J. Am. Chem. Soc.* **2001**, *123*, 10853-10859.

[42] G. Martelli, S. Morri, D. Savoia, *Tetrahedron* **2000**, *56*, 8367-8374.

[43] H. J. Bestmann, G. Wölfel, *Chem. Ber.* **1984**, *117*, 1250-1254.

[44] J. Brüning, *Tetrahedron Lett.* **1997**, *38*, 3187-3188.

[45] C. Krüger, E. G. Rochow, U. Wannagat, *Chem. Ber.* **1963**, *96*, 2132-2137.

[46] E. D. Brady, T. P. Hanusa, M. Pink, V. G. Young, *Inorg. Chem.* **2000**, *39*, 6028-6037.

[47] H. Bürger, W. Sawodny, U. Wannagat, *J. Organomet. Chem.* **1965**, *3*, 113-120.

[48] Y. Yamashita, T. Imaizumi, S. Kobayashi, *Angew. Chem. Int. Ed.* **2011**, *50*, 4893-4896.

[49] Y. Yamashita, T. Imaizumi, X.-X. Guo, S. Kobayashi, *Chem. – Eur. J.* **2011**, *6*, 2550-2559.

[50] W. A. Herrmann, R. Anwander, M. Kleine, W. Scherer, *Chem. Ber.* **1992**, *125*, 1971-1979.

[51] L. R. Avens, S. G. Bott, D. L. Clark, A. P. Sattelberger, J. G. Watkin, B. D. Zwick, *Inorg. Chem.* **1994**, *33*, 2248-2256.

[52] R. E. Mulvey, S. D. Robertson, *Angew. Chem. Int. Ed.* **2013**, *52*, 11470-11487.

[53] M. Westerhausen, *Inorg. Chem.* **1991**, *30*, 96-101.

[54] Z. Yu, S. Yan, G. Zhang, W. He, L. Wang, Y. Li, F. Zeng, *Adv. Synth. Catal.* **2006**, *348*, 111-117.

[55] a) R. Schwesinger, H. Schlemper, *Angew. Chem. Int. Ed.* **1987**, *26*, 1167-1169; b) B. Kovacevic, D. Baric, Z. B. Maksic, *New J. Chem.* **2004**, *28*, 284-288.

[56] a) C. Liu, Y. Zhang, Q. Qian, D. Yuan, Y. Yao, *Org. Lett.* **2014**, *16*, 6172-6175; b) W.-X. Zhang, M. Nishiura, Z. Hou, *Chem. Commun.* **2006**, 3812-3814; c) M. Itoh, K. Inoue, J.-i. Ishikawa, K. Iwata, *J. Organomet. Chem.* **2001**, *629*, 1-6.

[57] a) J. Seayad, A. Tillack, C. G. Hartung, M. Beller, *Adv. Synth. Catal.* **2002**, *344*, 795-813; b) T. E. Mueller, K. C. Hultzsch, M. Yus, F. Foubelo, M. Tada, *Chem. Rev.* **2008**, *108*, 3795-3892; c) R. Wegler, G. Pieper, *Chem. Ber.* **1950**, *83*, 1-6; d) B. W. Howk, E. L. Little, S. L. Scott, G. M. Whitman, *J. Am. Chem. Soc.* **1954**, *76*, 1899-1902; e) R. D. Closson, J. P. Napolitano, G. G. Ecke, A. J. Kolka, *J. Org. Chem.* **1957**, *22*, 646-649.

[58] T.-G. Ong, J. S. O'Brien, I. Korobkov, D. S. Richeson, *Organometallics* **2006**, *25*, 4728-4730.

[59] C. Kourra, F. Klotter, F. Sladojevich, D. J. Dixon, *Org. Lett.* **2012**, *14*, 1016-1019.

[60] H. Suzuki, I. Sato, Y. Yamashita, S. Kobayashi, *J. Am. Chem. Soc.* **2015**, *137*, 4336-4339.

[61] Y. Yamashita, I. Sato, H. Suzuki, S. Kobayashi, *Chem. – Eur. J.* **2015**, *10*, 2143-2146.

[62] G. C. Lloyd-Jones, R. W. Alder, G. J. J. Owen-Smith, *Chem. – Eur. J.* **2006**, *12*, 5361-5375.

[63] J. J. A. Celaje, Z. Lu, E. A. Kedzie, N. J. Terrile, J. N. Lo, T. J. Williams, *Nat. Commun.* **2016**, *7*, 11308.

[64] K. D. Collins, F. Glorius, *Nat. Chem.* **2013**, *5*, 597-601.

[65] M. W. Rathke, D. Sullivan, *Tetrahedron Lett.* **1972**, *13*, 4249-4252.

[66] a) D. Barr, W. Clegg, L. Cowton, L. Horsburgh, F. M. Mackenzie, R. E. Mulvey, *J. Chem. Soc., Chem. Commun.* **1995**, 891-892; b) D. Reed, D. Barr, R. E. Mulvey, R. Snaith, *J. Chem. Soc., Dalton Trans.* **1986**, 557-564.

[67] C. Glock, F. M. Younis, S. Ziemann, H. Görls, W. Imhof, S. Krieck, M. Westerhausen, *Organometallics* **2013**, *32*, 2649-2660.

[68] M. Hassam, A. Taher, G. E. Arnott, I. R. Green, W. A. L. van Otterlo, *Chem. Rev.* **2015**, *115*, 5462-5569.

[69] a) G. V. Salmoria, E. L. Dall'Oglio, C. Zucco, *Synth. Commun.* **2006**, *27*, 4335-4340; b) H. F. Herbrandson, D. S. Mooney, *J. Am. Chem. Soc.* **1957**, *79*, 5809-5814.

[70] a) R. Neumann, Y. Sasson, *J. Org. Chem.* **1984**, *49*, 3448-3451; b) R. Neumann, Y. Sasson, *J. Mol. Catal.* **1985**, *33*, 201-208.

[71] M. Halpern, M. Yonowich-Weiss, Y. Sasson, M. Rabinovitz, *Tetrahedron Lett.* **1981**, *22*, 703-704.

[72] Z. Yu, S. Yan, G. Zhang, W. He, L. Wang, Y. Li, F. Zeng, *Adv. Synth. Catal.* **2006**, *348*, 111-117.

[73] a) N. Nishiwaki, R. Kamimura, K. Shono, T. Kawakami, K. Nakayama, K. Nishino, T. Nakayama, K. Takahashi, A. Nakamura, T. Hosokawa, *Tetrahedron Lett.* **2010**, *51*, 3590-3592; b) D. Gauthier, A. T. Lindhardt, E. P. K. Olsen, J. Overgaard, T. Skrydstrup, *J. Am. Chem. Soc.* **2010**, *132*, 7998-8009; c) B. Cruikshank, N. R. Davies, *Aust. J. Chem.* **1966**, *19*, 815-824.

[74] a) L. Cerveny, A. Krejcikova, A. Marhoul, V. Ruzicka, *React. Kinet. Catal. Lett.* **1987**, *33*, 471-476; b) D. L. Clive, M. Sannigrahi, S. Hisaindee, *J. Org. Chem.* **2001**, *66*, 954-961.

[75] a) A. Scarso, M. Colladon, P. Sgarbossa, C. Santo, R. A. Michelin, G. Strukul, *Organometallics* **2010**, *29*, 1487-1497; b) H. Zhao, G. E. Brandt, L. Galam, R. L. Matts, B. S. J. Blagg, *Bioorg. Med. Chem. Lett.* **2011**, *21*, 2659-2664.

[76] a) B. Lastra-Barreira, A. E. Díaz-Álvarez, L. Menéndez-Rodríguez, P. Crochet, *RSC Advances* **2013**, *3*, 19985; b) T. J. Donohoe, T. J. C. O'Riordan, C. P. Rosa, *Angew. Chem. Int. Ed.* **2009**, *48*, 1014-1017; c) C. R. Larsen, G. Erdogan, D. B. Grotjahn, *J. Am. Chem. Soc.* **2014**, *136*, 1226-1229; d) H. Suzuki, T. Takao, Wiley-VCH Verlag GmbH & Co. KGaA, **2004**, pp. 309-331; e) T. Naota, H. Takaya, S.-I. Murahashi, *Chem. Rev.* **1998**, *98*, 2599-2660.

[77] a) M. Mayer, A. Welther, A. Jacobi von Wangelin, *ChemCatChem* **2011**, *3*, 1567-1571; b) I. Bauer, H.-J. Knölker, *Chem. Rev.* **2015**, *115*, 3170-3387; c) C. Bolm, J. Legros, J. Le Paih, L. Zani, *Chem. Rev.* **2004**, *104*, 6217-6254.

[78] a) W. Rauf, J. M. Brown, *Angew. Chem. Int. Ed.* **2008**, *47*, 4228-4230; b) S.-i. Ikeda, H. Miyashita, Y. Sato, *Organometallics* **1998**, *17*, 4316-4318; c) P. Batsomboon, W. Phakhodee, S. Ruchirawat, P. Ploypradith, *J. Org. Chem.* **2009**, *74*, 4009-4012; d) L. Schwink, P. Knochel, *Chem. – Eur. J.* **1998**, *4*, 950-968.

[79] a) F. C. Whitmore, L. H. Sommer, P. A. D. Giorgio, W. A. Strong, R. E. v. Strien, D. L. Bailey, H. K. Hall, E. W. Pietrusza, G. T. Kerr, *J. Am. Chem. Soc.* **1946**, *68*, 475-481; b) F. C. Whitmore, L. H. Sommer, *J. Am. Chem. Soc.* **1946**, *68*, 481-484.

[80] R. F. Horvath, T. H. Chan, *J. Org. Chem.* **1989**, *54*, 317-327.

[81] a) S. Manzini, D. J. Nelson, S. P. Nolan, *ChemCatChem* **2013**, *5*, 2848-2851; b) G. Occhipinti, F. R. Hansen, K. W. Törnroos, V. R. Jensen, *J. Am. Chem. Soc.* **2013**, *135*, 3331-3334; c) G. Chahboun, C. E. Petrisor, E. Gómez-Bengoa, E. Royo, T. Cuenca, *Eur. J. Inorg. Chem.* **2009**, *2009*, 1514-1520.

[82] a) F. Weber, A. Schmidt, P. Röse, M. Fischer, O. Burghaus, G. Hilt, *Org. Lett.* **2015**, *17*, 2952-2955; b) K. H. Nilsson, Anders, *Acta Chem. Scand.* **1987**, *B41*, 569-576.

[83] a) K. Hong, X. Liu, J. P. Morken, *J. Am. Chem. Soc.* **2014**, *136*, 10581-10584; b) M. W. Rathke, R. Kow, *J. Am. Chem. Soc.* **1972**, *94*, 6854-6856.

[84] a) J. A. Soderquist, S.-J. H. Lee, *Tetrahedron* **1988**, *44*, 4033-4042; b) D. Seyferth, L. G. Vaughan, *J. Organomet. Chem.* **1963**, *1*, 138-152.

[85] S. P. Hopper, M. J. Tremelling, E. W. Goldman, *J. Organomet. Chem.* **1980**, *191*, 363-369.

[86] B. J. Dunne, R. B. Morris, A. G. Orpen, *J. Chem. Soc., Dalton Trans.* **1991**, 653-661.

[87] D. G. Gilheany, *Chem. Rev.* **1994**, *94*, 1339-1374.

[88] a) P. Caramella, T. Bandiera, P. Grünanger, F. Marinone Albini, *Tetrahedron* **1984**, *40*, 441-453; b) S. Krompiec, P. Bujak, J. Malarz, M. Krompiec, Ł. Skórka, T. Pluta, W. Danikiewicz, M. Kania, J. Kusz, *Tetrahedron* **2012**, *68*, 6018-6031; c) E. Block, M. Thiruvazhi, P. J. Toscano, T. Bayer, S. Grisoni, S.-H. Zhao, *J. Am. Chem. Soc.* **1996**, *118*, 2790-2798.

[89] P. Bujak, S. Krompiec, J. Malarz, M. Krompiec, M. Filapek, W. Danikiewicz, M. Kania, K. Gębarowska, I. Grudzka, *Tetrahedron* **2010**, *66*, 5972-5981.

[90] a) S. Krompiec, J. Suwinski, J. Grobelny, *Pol. J. Chem.* **1996**, *70*, 813-818; b) R. Hua, H. Takeda, S.-y. Onozawa, Y. Abe, M. Tanaka, *Org. Lett.* **2007**, *9*, 263-266.

[91] a) A. J. Hubert, H. Reimlinger, *Synthesis* **1969**, *1969*, 97-112; b) J. Sauer, H. Prahl, *Chem. Ber.* **1969**, *102*, 1917-1927; c) S. Escoubet, S. Gastaldi, M. Bertrand, *Eur. J. Org. Chem.* **2005**, *2005*, 3855-3873.

[92] a) S. Krompiec, M. Krompiec, R. Penczek, H. Ignasiak, *Coord. Chem. Rev.* **2008**, *252*, 1819-1841; b) N. Kuznik, S. Krompiec, *Coord. Chem. Rev.* **2007**, *251*, 222-233; c) M. Igarashi, T. Matsumoto, T. Kobayashi, K. Sato, W. Ando, S. Shimada, M. Hara, H. Uchida, *J. Organomet. Chem.* **2014**, *749*, 421-427.

[93] a) S. O. Grim, R. P. Molenda, J. D. Mitchell, *J. Org. Chem.* **1980**, *45*, 250-252; b) L. Horner, I. Ertel, H.-D. Ruprecht, O. Bêlovský, *Chem. Ber.* **1970**, *103*, 1582-1588; c) M. Duncan, M. J. Gallagher, *Org. Magn. Reson.* **1981**, *15*, 37-42.

[94] S. Krompiec, M. Pigulla, M. Krompiec, B. Marciniec, D. Chadyniak, *J. Mol. Catal. A: Chem.* **2005**, *237*, 17-25.

[95] P. Atkins, *Inorganic Chemistry*, 4th ed., Oxford University Press, Oxford, **2006**.

[96] P. Mamone, M. F. Grünberg, A. Fromm, B. A. Khan, L. J. Gooßen, *Org. Lett.* **2012**, *14*, 3716-3719.

[97] a) J. E. Gready, P. M. Hatton, S. Sternhell, *J. Heterocycl. Chem.* **1992**, *29*, 935-946; b) A. C. Rojas, J. K. Crandall, *J. Org. Chem.* **1975**, *40*, 2225-2229.

[98] C. Agami, S. Comesse, C. Kadouri-Puchot, *J. Org. Chem.* **2002**, *67*, 1496-1500.

[99] N. Miyaura, K. Yamada, A. Suzuki, *Tetrahedron Lett.* **1979**, *20*, 3437-3440.

[100] T. Hiyama, M. Obayashi, I. Mori, H. Nozaki, *J. Org. Chem.* **1983**, *48*, 912-914.

[101] D. Milstein, J. K. Stille, *J. Am. Chem. Soc.* **1978**, *100*, 3636-3638.

[102] Y. Cui, Y. Yamashita, S. Kobayashi, *Chem. Commun.* **2012**, *48*, 10319-10321.

[103] Y. Cui, Y. Yamashita, S. Kobayashi, *Chem. Commun.* **2012**, *48*, 10319-10321.

[104] Y. Yamamoto, T. Komatsu, K. Maruyama, *J. Am. Chem. Soc.* **1984**, *106*, 5031-5033.

[105] U. Burckhardt, M. Baumann, A. Togni, *Tetrahedron: Asymmetry* **1997**, *8*, 155-159.

[106] J. W. Faller, M. E. Thomsen, M. J. Mattina, *J. Am. Chem. Soc.* **1971**, *93*, 2642-2653.

[107] P. Beak, K. D. Wilson, *J. Org. Chem.* **1987**, *52*, 218-225.

[108] Z. Pakulski, R. Kwiatosz, K. Michał Pietrusiewicz, *Tetrahedron* **2005**, *61*, 1481-1492.

[109] A. G. M. Barrett, M. A. Seefeld, *Tetrahedron* **1993**, *49*, 7857-7870.

[110] a) D. A. Evans, G. C. Andrews, B. Buckwalter, *J. Am. Chem. Soc.* **1974**, *96*, 5560-5561; b) J. Alladoum, S. Roland, E. Vrancken, C. Kadouri-Puchot, P. Mangeney, *Synlett* **2006**, *2006*, 1855-1858.

[111] J. J. Eisch, J. H. Shah, *J. Org. Chem.* **1991**, *56*, 2955-2957.

[112] M. Schlosser, *Angew. Chem. Int. Ed.* **2005**, *44*, 376-393.

[113] J. Gatignol, C. Alayrac, J.-F. Lohier, J. Ballester, M. Taillefer, A.-C. Gaumont, *Adv. Synth. Catal.* **2013**, *355*, 2822-2826.

[114] DBSWeb National Institute of Advanced Industrial Science and Technology, http://sdbs.db.aist.go.jp/sdbs/cgi-bin/cre_index.cgi, 15/07/2016

[115] F. Ramirez, B. Hansen, N. B. Desai, N. McKelvie, *J. Am. Chem. Soc.* **1961**, *83*, 3539-&.

[116] a) R. Appel, K. Waid, *Angew. Chem. Int. Ed.* **1979**, *18*, 169-169; b) R. Appel, H. D. Wihler, *Chem. Ber. Recl.* **1978**, *111*, 2054-2055.

[117] W. Petz, S. Heimann, F. Oexler, B. Neumueller, *Z. Anorg. Allg. Chem.* **2007**, *633*, 365-367.

[118] a) R. Tonner, F. Oexler, B. Neumueller, W. Petz, G. Frenking, *Angew. Chem. Int. Ed.* **2006**, *45*, 8038-8042; b) R. Tonner, G. Frenking, *Chem. – Eur. J.* **2008**, *14*, 3260-3272.

[119] a) R. Tonner, G. Frenking, *Chem. – Eur. J.* **2008**, *14*, 3260-3272; b) W. Petz, G. Frenking, in *Transition Metal Complexes of Neutral eta1-Carbon Ligands* (Eds.: R. Chauvin, Y. Canac), Springer Berlin Heidelberg, Berlin, Heidelberg, **2010**, pp. 49-92.

[120] R. Tonner, G. Heydenrych, G. Frenking, *ChemPhysChem* **2008**, *9*, 1474-1481.

[121] J. S. Driscoll, D. W. Grisley, J. V. Pustinger, J. E. Harris, C. N. Matthews, *J. Org. Chem.* **1964**, *29*, 2427-2431.

[122] C. Zybill, G. Mueller, *Organometallics* **1987**, *6*, 2489-2494.

[123] a) R. Appel, J. G. Morse, in *Inorg. Synth.*, John Wiley & Sons, Inc., **1986**, pp. 113-117; b) R. Appel, F. Knoll, H. Schöler, H.-D. Wihler, *Angew. Chem.* **1976**, *88*, 769-770.

[124] H. S. Oswald Gasser, *J. Am. Chem. Soc.* **1975**, *97*, 6281-6282.

[125] H. Schmidbaur, O. Gasser, M. S. Hussain, *Chem. Ber. Recl.* **1977**, *110*, 3501-3507.

[126] R. Appel, U. Baumeister, F. Knoch, *Chem. Ber. Recl.* **1983**, *116*, 2275-2284.

[127] M. Alcarazo, K. Radkowski, G. Mehler, R. Goddard, A. Fuerstner, *Chem. Commun.* **2013**, *49*, 3140-3142.

[128] S. Marrot, T. Kato, H. Gornitzka, A. Baceiredo, *Angew. Chem. Int. Ed.* **2006**, *45*, 2598-2601.

[129] U. Schubert, C. Kappenstein, B. Milewskimahrla, H. Schmidbaur, *Chem. Ber. Recl.* **1981**, *114*, 3070-3078.

[130] R. Corberan, S. Marrot, N. Dellus, N. Merceron-Saffon, T. Kato, E. Peris, A. Baceiredo, *Organometallics* **2009**, *28*, 326-330.

[131] a) L. Orzechowski, S. Harder, *Organometallics* **2007**, *26*, 2144-2148; b) S. Harder, *Coord. Chem. Rev.* **2011**, *255*, 1252-1267; c) T. K. Panda, P. W. Roesky, *Chem. Soc. Rev.* **2009**, *38*, 2782-2804.

[132] W. Petz, G. Frenking, *Top. Organomet. Chem.* **2010**, *30*, 49-92.

[133] S. S. Maigali, M. A. Abd-El-Maksoud, F. M. Soliman, *Arch. Pharm.* **2011**, *344*, 442-450.

[134] H. J. Bestmann, W. Kloeters, *Tetrahedron Lett.* **1977**, 79-80.

[135] S. S. Maigali, M. M. Said, M. A. Abd-El-Maksoud, F. M. Soliman, *Monatsh. Chem.* **2008**, *139*, 495-501.

[136] M. M. Said, S. S. Maigali, M. A. Abd-El-Maksoud, F. M. Soliman, *Monatsh. Chem.* **2008**, *139*, 1299-1306.

[137] a) H. Schmidbaur, C. E. Zybill, G. Muller, C. Kruger, *Angew. Chem. Int. Ed.* **1983**, *22*, 729-730; b) G. Muller, C. Kruger, C. Zybill, H. Schmidbaur, *Acta Crystallogr. Sect. C: Cryst. Struct. Commun.* **1986**, *42*, 1141-1144; c) J. Vicente, A. R. Singhal, P. G. Jones, *Organometallics* **2002**, *21*, 5887-5900.

[138] W. Petz, B. Neumüller, *Eur. J. Inorg. Chem.* **2011**, *2011*, 4889-4895.

[139] W. Petz, F. Oexler, B. Neumueller, *J. Organomet. Chem.* **2009**, *694*, 4094-4099.

[140] a) W. C. Kaska, D. K. Mitchell, Reicheld.Rf, *J. Organomet. Chem.* **1973**, *47*, 391-402; b) W. C. Kaska, D. K. Mitchell, Reicheld.Rf, W. D. Korte, *J. Am. Chem. Soc.* **1974**, *96*, 2847-2854; c) J. Sundermeyer, K. Weber, K. Peters, H. G. Vonschnering, *Organometallics* **1994**, *13*, 2560-2562.

[141] W. Petz, K. Dehnicke, N. Holzmann, G. Frenking, B. Neumüller, *Z. Anorg. Allg. Chem.* **2011**, *637*, 1702-1710.

[142] H. Schmidbaur, O. Gasser, *Angew. Chem. Int. Ed.* **1976**, *15*, 502-503.

[143] M. Alcarazo, K. Radkowski, G. Mehler, R. Goddard, A. Fürstner, *Chem. Commun.* **2013**, *49*, 3140.

[144] W. Petz, F. Öxler, B. Neumüller, R. Tonner, G. Frenking, *Eur. J. Inorg. Chem.* **2009**, *2009*, 4507-4517.

[145] S. Khan, G. Gopakumar, W. Thiel, M. Alcarazo, *Angew. Chem. Int. Ed.* **2013**, *52*, 5644-5647.

[146] W. Petz, C. Kutschera, S. Tschan, F. Weller, B. Neumuller, *Z. Anorg. Allg. Chem.* **2003**, *629*, 1235-1244.

[147] I. Kuzu, N.-J. H. Kneusels, M. Bauer, B. Neumüller, R. Tonner, *Z. Anorg. Allg. Chem.* **2014**, *640*, 417-422.

[148] M. Q. Y. Tay, Y. Lu, R. Ganguly, D. Vidović, *Angew. Chem. Int. Ed.* **2013**, *52*, 3132-3135.

[149] M. Q. Y. Tay, G. Ilić, U. Werner-Zwanziger, Y. Lu, R. Ganguly, L. Ricard, G. Frison, D. Carmichael, D. Vidović, *Organometallics* **2016**, *35*, 439-449.

[150] C. N. Matthews, J. S. Driscoll, G. H. Birum, *Chem. Commun.* **1966**, 736-737.

[151] F. P. Ramirez, J; Desai N; Smith, C; Hansen, B; McKelvie, N, *J. Am. Chem. Soc.* **1967**, *89*, 6273-6276.

[152] M. Alcarazo, C. Gomez, S. Holle, R. Goddard, *Angew. Chem. Int. Ed.* **2010**, *49*, 5788-5791.

[153] B. Inés, M. Patil, J. Carreras, R. Goddard, W. Thiel, M. Alcarazo, *Angew. Chem. Int. Ed.* **2011**, *50*, 8400-8403.

[154] R. Dobrovetsky, D. W. Stephan, *Angew. Chem. Int. Ed.* **2013**, *52*, 2516-2519.

[155] H. Schmidbaur, O. Gasser, M. S. Hussain, *Chem. Ber.* **1977**, *110*, 3501-3507.

[156] W.-C. Chen, J.-S. Shen, T. Jurca, C.-J. Peng, Y.-H. Lin, Y.-P. Wang, W.-C. Shih, G. P. A. Yap, T.-G. Ong, *Angew. Chem. Int. Ed.* **2015**, *54*, 15207-15212.

[157] R. Tonner, G. Frenking, *Angew. Chem. Int. Ed.* **2007**, *46*, 8695-8698.

[158] a) C. A. Dyker, V. Lavallo, B. Donnadieu, G. Bertrand, *Angew. Chem. Int. Ed.* **2008**, *47*, 3206-3209; b) A. Fürstner, M. Alcarazo, R. Goddard, C. W. Lehmann, *Angew. Chem. Int. Ed.* **2008**, *47*, 3210-3214.

[159] a) R. Appel, J. G. Morse, in *Inorg. Synth.*, John Wiley & Sons, Inc., **2007**, pp. 113-117; b) R. Appel, F. Knoll, W. Miche, W. Morbach, H.-D. Wihler, H. Veltmann, *Chem. Ber.* **1976**, *109*, 58-70.

[160] I. B. Adilina, T. Hara, N. Ichikuni, S. Shimazu, *J. Mol. Catal. A: Chem.* **2012**, *361-362*, 72-79.

[161] W. Petz, C. Kutschera, M. Heitbaum, G. Frenking, R. Tonner, B. Neumüller, *Inorg. Chem.* **2005**, *44*, 1263-1274.

[162] a) W. Petz, F. Öxler, B. Neumüller, *J. Organomet. Chem.* **2009**, *694*, 4094-4099; b) W. Petz, B. Neumüller, S. Klein, G. Frenking, *Organometallics* **2011**, *30*, 3330-3339.

[163] C. Zybill, G. Muller, *Organometallics* **1987**, *6*, 2489-2494.

[164] a) S. Tang, J. Monot, A. El-Hellani, B. Michelet, R. Guillot, C. Bour, V. Gandon, *Chem. – Eur. J.* **2012**, *18*, 10239-10243; b) A. El-Hellani, J. Monot, R. Guillot, C. Bour, V. Gandon, *Inorg. Chem.* **2012**, *52*, 506-514.

[165] A. El-Hellani, J. Monot, S. Tang, R. Guillot, C. Bour, V. Gandon, *Inorg. Chem.* **2013**, *52*, 11493-11502.

[166] H.-J. Li, R. Guillot, V. Gandon, *J. Org. Chem.* **2010**, *75*, 8435-8449.

[167] a) M. Yamaguchi, T. Sotokawa, M. Hirama, *Chem. Commun.* **1997**, 743-744; b) J.-F. Zhao, Y.-J. Zhao, T.-P. Loh, *Chem. Commun.* **2008**, 1353-1355.

[168] H. Zhou, W.-Z. Zhang, C.-H. Liu, J.-P. Qu, X.-B. Lu, *J. Org. Chem.* **2008**, *73*, 8039-8044.

[169] a) D. W. Stephan, G. Erker, *Angew. Chem. Int. Ed.* **2015**, *54*, 6400-6441; b) G. C. Welch, R. R. S. Juan, J. D. Masuda, D. W. Stephan, *Science* **2006**, *314*, 1124-1126.

[170] B. M. Trost, C. S. Brindle, *Chem. Soc. Rev.* **2010**, *39*, 1600-1632.

[171] J. M. M. Verkade, L. J. C. v. Hemert, P. J. L. M. Quaedflieg, F. P. J. T. Rutjes, *Chem. Soc. Rev.* **2008**, *37*, 29-41.

[172] B. List, *J. Am. Chem. Soc.* **2000**, *122*, 9336-9337.

[173] a) S. Lou, B. M. Taoka, A. Ting, S. E. Schaus, *J. Am. Chem. Soc.* **2005**, *127*, 11256-11257; b) A. L. Tillman, J. Ye, D. J. Dixon, *Chem. Commun.* **2006**, 1191-1193.

[174] M. Hatano, T. Horibe, K. Ishihara, *J. Am. Chem. Soc.* **2010**, *132*, 56-57.

[175] T. Punirun, D. Soorukram, C. Kuhakarn, V. Reutrakul, M. Pohmakotr, *Eur. J. Org. Chem.* **2014**, *2014*, 4162-4169.

[176] R. Appel, H. Mayr, *J. Am. Chem. Soc.* **2011**, *133*, 8240-8251.

[177] J. S. Driscoll, J. E. Harris, D. W. Grisley, J. V. Pustinger, C. N. Matthews, *J. Org. Chem.* **1964**, *29*, 2427-&.

[178] a) M. Horn, H. Mayr, E. Lacôte, E. Merling, J. Deaner, S. Wells, T. McFadden, D. P. Curran, *Org. Lett.* **2011**, *14*, 82-85; b) T. Taniguchi, D. P. Curran, *Org. Lett.* **2012**, *14*, 4540-4543; c) D. M. Lindsay, D. McArthur, *Chem. Commun.* **2010**, *46*, 2474-2476.

[179] X. Hong, H. Wang, B. Liu, B. Xu, *Chem. Commun.* **2014**, *50*, 14129-14132.

[180] V. Pirovano, D. Facoetti, M. Dell'Acqua, E. Della Fontana, G. Abbiati, E. Rossi, *Org. Lett.* **2013**, *15*, 3812-3815.

[181] Y. S. Angelis, M. Orfanopoulos, *J. Org. Chem.* **1997**, *62*, 6083-6085.

[182] P. C. Too, G. H. Chan, Y. L. Tnay, H. Hirao, S. Chiba, *Angew. Chem. Int. Ed.* **2016**, *55*, 3719-3723.

[183] K.-i. Yamada, T. Konishi, M. Nakano, S. Fujii, R. Cadou, Y. Yamamoto, K. Tomioka, *J. Org. Chem.* **2012**, *77*, 1547-1553.

[184] A. M. Seayad, B. Ramalingam, K. Yoshinaga, T. Nagata, C. L. L. Chai, *Org. Lett.* **2010**, *12*, 264-267.

[185] R. E. Grote, E. R. Jarvo, *Org. Lett.* **2009**, *11*, 485-488.

[186] L. Wang, C. Cao, C. Cao, *J. Phys. Org. Chem.* **2014**, *27*, 818-822.

[187] R. Suresh, D. Kamalakkannan, K. Ranganathan, R. Arulkumaran, R. Sundararajan, S. P. Sakthinathan, S. Vijayakumar, K. Sathiyamoorthi, V. Mala, G. Vanangamudi, K. Thirumurthy, P. Mayavel, G. Thirunarayanan, *Spectrochim. Acta, Part A* **2013**, *101*, 239-248.

[188] S. E. Denmark, N. Nakajima, C. M. Stiff, O. J. C. Nicaise, M. Kranz, *Adv. Synth. Catal.* **2008**, *350*, 1023-1045.

[189] A. Jarrahpour, E. Ebrahimi, *Molecules* **2010**, *15*, 515.

[190] R. Pagadala, J. S. Meshram, H. N. Chopde, V. Jetti, V. Udayini, *J. Heterocycl. Chem.* **2011**, *48*, 1067-1072.

[191] J. C. Anderson, G. P. Howell, R. M. Lawrence, C. S. Wilson, *J. Org. Chem.* **2005**, *70*, 5665-5670.

[192] H.-J. Knölker, G. Baum, N. Foitzik, H. Goesmann, P. Gonser, P. G. Jones, H. Röttele, *Eur. J. Inorg. Chem.* **1998**, *1998*, 993-1007.

[193] R. C. Simon, E. Busto, J. H. Schrittwieser, J. H. Sattler, J. Pietruszka, K. Faber, W. Kroutil, *Chem. Commun.* **2014**, *50*, 15669-15672.

[194] N. Mungwe, A. J. Swarts, S. F. Mapolie, G. Westman, *J. Organomet. Chem.* **2011**, *696*, 3527-3535.

[195] R. He, X. Jin, H. Chen, Z.-T. Huang, Q.-Y. Zheng, C. Wang, *J. Am. Chem. Soc.* **2014**, *136*, 6558-6561.

[196] M. Patel, M. Chhasatia, B. Bhatt, *Med. Chem. Res.* **2011**, *20*, 220-230.

[197] Q. Jiang, J.-Y. Wang, C. Guo, *J. Org. Chem.* **2014**, *79*, 8768-8773.

[198] Z. Bengharez, Z. El Bahri, A. Mesli, *Int. J. Chem. Kinet.* **2013**, *45*, 404-414.

[199] D. C. Rogness, N. A. Markina, J. P. Waldo, R. C. Larock, *J. Org. Chem.* **2012**, *77*, 2743-2755.

[200] M. Tomaszewski, J. Warkentin, N. Werstiuk, *Aust. J. Chem.* **1995**, *48*, 291-321.

[201] W.-Y. Wong, W.-T. Wong, *J. Organomet. Chem.* **1999**, *584*, 48-57.

[202] Y. Vara, T. Bello, E. Aldaba, A. Arrieta, J. L. Pizarro, M. I. Arriortua, X. Lopez, F. P. Cossío, *Org. Lett.* **2008**, *10*, 4759-4762.

[203] J. Waser, B. Gaspar, H. Nambu, E. M. Carreira, *J. Am. Chem. Soc.* **2006**, *128*, 11693-11712.

[204] N. Netz, T. Opatz, *J. Org. Chem.* **2016**, *81*, 1723-1730.

[205] P.-S. Lee, N. Yoshikai, *Org. Lett.* **2015**, *17*, 22-25.

[206] N. Iranpoor, F. Panahi, S. Erfan, F. Roozbin, *J. Heterocycl. Chem.* **2016**, early view.

[207] M. Tobisu, S. Yamaguchi, N. Chatani, *Org. Lett.* **2007**, *9*, 3351-3353.

[208] L. Han, P. Xing, B. Jiang, *Org. Lett.* **2014**, *16*, 3428-3431.

[209] S. J. Dickson, M. J. Paterson, C. E. Willans, K. M. Anderson, J. W. Steed, *Chem. – Eur. J.* **2008**, *14*, 7296-7305.

[210] J. H. Wynne, S. E. Price, J. R. Rorer, W. M. Stalick, *Synth. Commun.* **2003**, *33*, 341-352.

[211] O. W. S. Abdulraman O.C.Aliyu, P.K.Onoja, *J. Chem. Pharm. Res.* **2013**, *5*, 129-131.

[212] M. Blümel, P. Chauhan, R. Hahn, G. Raabe, D. Enders, *Org. Lett.* **2014**, *16*, 6012-6015.

[213] Y. Wei, I. Deb, N. Yoshikai, *J. Am. Chem. Soc.* **2012**, *134*, 9098-9101.

[214] A. Henseler, M. Kato, K. Mori, T. Akiyama, *Angew. Chem. Int. Ed.* **2011**, *50*, 8180-8183.

[215] R. J. Lundgren, A. Sappong-Kumankumah, M. Stradiotto, *Chem. – Eur. J.* **2010**, *16*, 1983-1991.

[216] J. Wu, N. Yoshikai, *Angew. Chem. Int. Ed.* **2015**, *54*, 11107-11111.

[217] D. Enders, A. Rembiak, B. A. Stöckel, *Adv. Synth. Catal.* **2013**, *355*, 1937-1942.

[218] A. González, J. Quirante, J. Nieto, M. R. Almeida, M. J. Saraiva, A. Planas, G. Arsequell, G. Valencia, *Bioorg. Med. Chem. Lett.* **2009**, *19*, 5270-5273.

[219] M. Mayer, W. M. Czaplik, A. Jacobi von Wangelin, *Adv. Synth. Catal.* **2010**, *352*, 2147-2152.

[220] R. B. Bedford, P. B. Brenner, E. Carter, J. Clifton, P. M. Cogswell, N. J. Gower, M. F. Haddow, J. N. Harvey, J. A. Kehl, D. M. Murphy, E. C. Neeve, M. L. Neidig, J. Nunn, B. E. R. Snyder, J. Taylor, *Organometallics* **2014**, *33*, 5767-5780.

[221] M. Mayer, W. M. Czaplik, A. J. von Wangelin, *Adv. Synth. Catal.* **2010**, *352*, 2147-2152.

[222] A. B. Weinstein, S. S. Stahl, *Angew. Chem. Int. Ed.* **2012**, *51*, 11505-11509.

[223] R. Frlan, M. Sova, S. Gobec, G. Stavber, Z. Časar, *J. Org. Chem.* **2015**, *80*, 7803-7809.

[224] R. J. Lundgren, B. N. Thomas, *Chem. Commun.* **2016**, *52*, 958-961.

[225] Z. Jiang, A. Sen, *Organometallics* **1993**, *12*, 1406-1415.

[226] V. L. Blair, M. A. Stevens, C. D. Thompson, *Chem. Commun.* **2016**, *52*, 8111-8114.

[227] I. Chatterjee, M. Oestreich, *Org. Lett.* **2016**, *18*, 2463-2466.

[228] B. T. Cho, S. K. Kang, *Tetrahedron* **2005**, *61*, 5725-5734.

[229] T. Hirashita, Y. Hayashi, K. Mitsui, S. Araki, *J. Org. Chem.* **2003**, *68*, 1309-1313.

[230] a) D. S. Matteson, D. Majumdar, *Organometallics* **1983**, *2*, 230-236; b) M. Althaus, A. Mahmood, J. R. Suárez, S. P. Thomas, V. K. Aggarwal, *J. Am. Chem. Soc.* **2010**, *132*, 4025-4028.

[231] E. Block, M. Thiruvazhi, P. J. Toscano, T. Bayer, S. Grisoni, S.-H. Zhao, *J. Am. Chem. Soc.* **1996**, *118*, 2790-2798.

[232] Y.-L. Zhao, G.-J. Wu, Y. Li, L.-X. Gao, F.-S. Han, *Chem. – Eur. J.* **2012**, *18*, 9622-9627.

[233] A. E. Pasqua, J. J. Crawford, D.-L. Long, R. Marquez, *J. Org. Chem.* **2012**, *77*, 2149-2158.

[234] M. Nambo, M. Yar, J. D. Smith, C. M. Crudden, *Org. Lett.* **2015**, *17*, 50-53.

[235] R. Metzner, S. Okazaki, Y. Asano, H. Gröger, *ChemCatChem* **2014**, *6*, 3105-3109.

[236] Q. Liu, F.-P. Zhu, X.-L. Jin, X.-J. Wang, H. Chen, L.-Z. Wu, *Chem. – Eur. J.* **2015**, *21*, 10326-10329.

[237] O. Corminboeuf, P. Renaud, *Org. Lett.* **2002**, *4*, 1735-1738.

[238] L. Zheng, H. Huang, C. Yang, W. Xia, *Org. Lett.* **2015**, *17*, 1034-1037.

[239] S. B. Nimse, D. Pal, A. Mazumder, R. Mazumder, *J. Chem.* **2015**, *2015*, 5.